Scuola Internazionale Superiore di Studi Avanzati - (SISSA)

Identification of the optimal parameters for electrical stimulation to generate locomotor patterns in the rat isolated spinal cord.

Thesis submitted for the degree of "Doctor Philosophiae"

Academic Year 2015 - 2016

Candidate

Francesco Dose

Supervisor

Dr.Giuliano Taccola

Co-supervisor

Prof.Andrea Nistri

SISSA - Via Bonomea 265 - 34136 Trieste - Italy

Table of Contents

Declaration

The data reported in the present thesis have been published in the articles listed below in chronological order of publication. In all cases the candidate personally performed the experimental work, including data acquisition, analysis and contributed to paper writing.

Dose F, Taccola G. (2012) Coapplication of noisy patterned electrical stimuli and NMDA plus serotonin facilitates fictive locomotion in the rat spinal cord. J Neurophysiol 108(11):2977-90.

Dose F, Menosso R, Taccola G. (2013) Rat locomotor spinal circuits in vitro are activated by electrical stimulation with noisy waveforms sampled from human gait. Physiol Rep 1(2):e00025.

Dose F, Zanon P, Coslovich T, Taccola G. (2014) Nanomolar oxytocin synergizes with weak electrical afferent stimulation to activate the locomotor CpG of the rat spinal cord in vitro. PLoS One 9(3):e92967.

Dose F, Deumens R, Forget P, Taccola G. (2016) Staggered multi-site low-frequency electrostimulation effectively induces locomotor patterns in the isolated rat spinal cord. Spinal Cord 54(2):93-101.

Dose F, Taccola G. (2016) Two distinct stimulus frequencies delivered simultaneously at low intensity generate robust locomotor patterns. Neuromodulation 19(6):563-75.

Abstract

Recently, an innovative protocol of electrical stimulation, named “fictive locomotion *induced* stimulation” (FL*i*stim), which consists of an intrinsically variable noisy waveform, has been obtained from a segment of chemically-induced fictive locomotion (FL) sampled from the ventral root (VR) of an *in vitro* preparation of neonatal rat spinal cord. FL*i*stim delivered at sub-threshold intensities to a dorsal root (DR) has been shown to optimally activate the central pattern generators (CPGs) for locomotion (Taccola, 2011).

In an attempt to introduce novel and improved protocols of stimulation in combination with neurochemicals, the current PhD project aims to identify the features that make sub-threshold noisy waveforms effective in activating locomotor patterns.

To reach this aim, locomotor-like patterns in response to different noisy waveforms were compared. In order to obtain a wide palette of noisy protocols electromyographic (EMG) recordings were performed from leg muscles of adult volunteers during walking. These recordings were then delivered as stimulating patterns called real locomotion-*induced* stimulation (ReaL*i*stim).

ReaL*i*stim protocols, sampled during different motor behaviours, are equally able to induce an epoch of locomotor-like oscillations. Conversely, smooth kinematic profiles and non-phasic noisy patterns such as standing and isometric contraction, are unable to activate the locomotor CPGs. The complexity of noisy waveforms was then reduced at motoneuronal level, by recording electrical activity of a single

motoneuron during FL. Long-lasting episode of FL, were evoked in response to intracellular patterns delivered at sub-threshold intensities. The analysis of motoneuronal firing during FL was used to identify four recurrent frequency values that optimally activated the locomotor CPGs when applied simultaneously in a multifrequency protocol. Different permutations were tried to further simplify the multifrequency protocol while isolating the most effective components of the four identified frequencies. The simplest asynchronous paradigm that can induce locomotor-like episodes consists of a train of rectangular pulses that contain two frequencies: 35 and 172 Hz. This protocol resulted already effective at sub-threshold intensity even when delivered for a very short time (500 ms).

The role of oxytocin in the modulation of neuronal networks is explored here on spinal networks. Intracellular recordings demonstrate that oxytocin dose-dependently depolarizes single motoneurons with the appearance of sporadic bursts with superimposed firing. By applying the selective blocker of sodium channels, tetrodotoxin (TTX), the effects of oxytocin can be completely abolished, which suggest a premotoneuronal-level origin.

The neuropeptide is capable to induce VRs depolarization with superimposed synchronous bursts of activity, while reflex responses induced by single pulses are depressed depending on the stimulus strength and peptide-concentration. The disinhibited bursting evoked by the pharmacological blockade of glycine and $GABA_A$ receptors blockers, strychnine and bicuculline, respectively, is accelerated by oxytocin, an effect that is suppressed by the selective oxytocin receptor antagonist atosiban.

On spinal locomotor networks oxytocin facilitates the emergence of FL episodes in response either to weak noisy waveforms protocols or to the conjoint application of NMDA and 5HT at sub-threshold concentrations, even if the periodicity of a stable FL is not significantly affected by the neuropeptide. Interestingly, the facilitation of the locomotor CPGs by oxytocin is dependent on the endogenous release of 5HT, as is demonstrated by incubation with the inhibitor of 5HT synthesis, p-chlorophenilalanine (PCPA).

Low-frequency trains of stereotyped pulses (0.33 and 0.67Hz) delivered with a controlled time interval (delays 0.5 to 2 s) to multiple DRs converged on spinal locomotor circuits to generate locomotor rhythm. The same finding is confirmed by the phase resetting that is induced by single afferent stimuli during a simultaneous train of pulses delivered to another DR. Staggered protocols fail to elicit FL when simultaneously applied to multiple DRs, while a multi-site randomized pulse train is still effective in eliciting locomotor-like patterns.

This thesis outlines new strategies for optimizing the reactivation of spinal locomotor networks after spinal damage. Though the technology that is currently available in clinics does not allow for the delivery of highly-variable stimulating patterns, experiments reported here indicate a way to overcome these limitations.
Indeed, protocols that contain few distinct frequencies that are isolated from the spectrum of noisy waves can activate the CPGs even when delivered with a multi-site approach. This suggests that it may be possible to separately supply multiple trains of pulses to several cord sites using different electrostimulators. The yield of

stimulation in activating locomotor circuits will be further improved by the association with the neuropeptide oxytocin.

Introduction

Locomotion is a parsimonious rhythmic motor behaviour.

Locomotion is a stereotyped rhythmic motor behaviour that allows animals and humans to move through the environment. It involves the coordination of several joints and muscles in the limbs and trunk to attain forward progression while simultaneously maintaining body balance and limiting loss of energy (Grasso et al., 1999).

Over the years, many approaches have been introduced to study the characteristics of locomotion. Among them, biomechanics is a science that studies the internal and external forces acting on the human body and the effects produced by these forces. It consists in the application of Newtonian mechanics to the study of the musculoskeletal system.

During the last century, many hypotheses have been suggested to describe the biomechanics of locomotion. In the early sixties, the **inverted-pendulum model** was introduced (Cavagna et al., 1963). This hypothesis states that the **centre of mass** (**COM**) of the body vaults over the stance leg in an arc (Cavagna et al., 1963). Considering the energy balance, the model suggests that, during the first half of the stance phase, the kinetic energy is converted into potential energy, which is partially recovered through the second half of the stance phase as the COM falls forward and downward. In theory, if an inverted pendulum acted in a purely conservative way during walking, any shift in kinetic energy would be counterbalanced by an opposing variation in potential energy, with no necessity for further mechanical work performed by muscles. Actual walking tends to fit this

theoretical model, though energy is also dispersed in friction and ground resistance.

On the other hand, running patterns have an energy balance very different from that observed during walking. In running, the inverted pendulum mechanism is less dominant (Kuo and Donelan, 2010; Cavagna et al., 1964; Cavagna et al., 1977), and energy is conserved through a mechanism known as **elastic body bounce**. In elastic body bounce, the exchange of mechanical energy that is stored in the elastic elements of muscles is recovered as both kinetic and potential energy, as in a bouncing ball (Cavagna et al., 1977). The two mechanisms that describe the different patterns of forces during walking and running are schematically depicted in Figure 1.

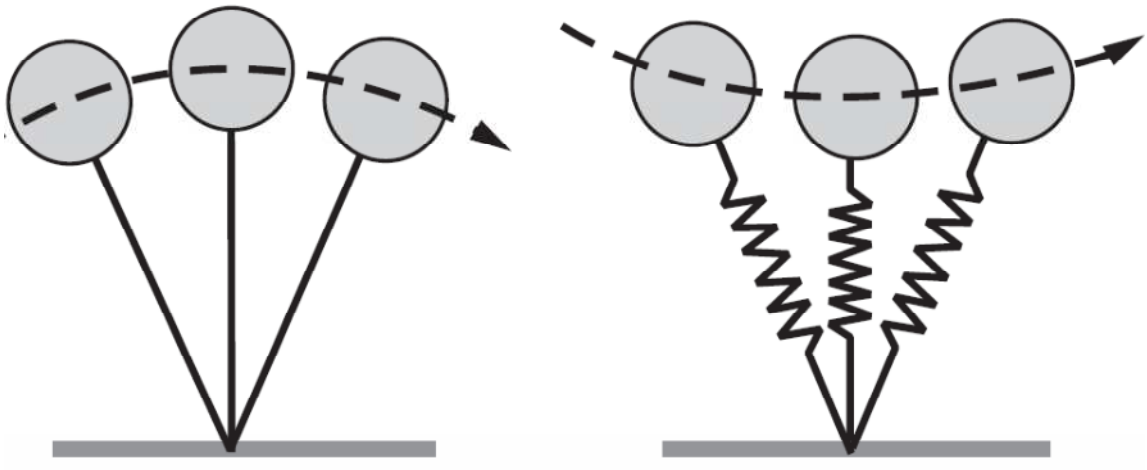

Figure 1. Motor behaviours can be schematized in simplified models. *Walking behaviour is represented on the left. The COM (centre of mass) vaults over a rigid leg, like an inverted pendulum. The COM reaches its highest point in correspondence with the mid stance. Kinetic and gravitational potential energies are exchanged cyclically. The model on the right depicts running behaviour by showing the leg acting as a spring, with the COM reaching its lowest point at mid-*

stance. During running, in the braking phase, the kinetic and gravitational potential energies are stored as elastic energy and are recovered during the propulsive phase (Dickinson et al., 2000).

According to the principle of **dynamic similarity** (Alexander, 1989), geometrically similar bodies that depend on pendulum-like biomechanics of movement show similar gait dynamics. This principle has been demonstrated in humans (Ivanenko, 2004), but also in several animal species which differ in terms of size, mass, posture or skeleton type, including dogs (Goslow et al., 1981), rodents, birds (Heglund et al., 1982), salamanders (Frolich and Biewener, 1992), lizards (Farley and Ko, 1997) and frogs (Ahn et al., 2004).

Biomechanics finds its greatest use in physical medicine and rehabilitation where it is employed for the characterization of musculoskeletal function and dysfunction (Zajac et al., 2002; 2003). Indeed, injuries to the central nervous system (CNS) and other motor disturbances can alter the biomechanical features of a gait to produce walking deficits. At the same time, detailed biomechanics descriptors support the assessment of spontaneous recoveries and the benefits of new neurorehabilitative interventions (Kuo and Donelan, 2010).

Kinematic analysis is a branch of biomechanics that describes the geometric features of movements by tracing positions, angles, velocities and accelerations of body segments and joints during motion. From a kinematic perspective, the gait cycle starts when one foot makes contact with the ground and ends when the same foot contacts the ground again. Each gait cycle has two main phases: the first is the phase during which the foot remains in contact with the ground (*stance*, 60% of the cycle); the second is the phase during which the foot is swinging in the air (*swing*, 40 % of cycle; Perry and Burnfield, 1992). Kinematic analysis suggests that

locomotion is not a perfectly stereotyped behaviour. Indeed, although fluctuations from the main scheme are quite small in moving subjects (Gabel and Najak, 1984; Terrier and Schutz, 2003), highlighting the accuracy and reliability of the finely-tuned systems that regulate gait (Hausdorff, 2005); however, a certain inherent variability is reported at each step (Courtine et al., 2005).

As mentioned above, the kinematic analysis of gait shows a certain inherent variability. Similarly, muscular activation also turns out to be complex and variable, since it requires the concerted activation of a large number of limb and trunk muscles. In addition, it has been shown that, in lower limbs, there are more degrees of freedom (**DOFs**) in the joints and muscles than motor patterns (Aoi and Funato, 2015), thus demonstrating the existence of a discrete **kinematic redundancy**. The prevalent hypothesis is that complex movements such as the gait may be controlled through the flexible combination of **motor primitives** (Giszter et al., 1989)**,** which are defined as set of fixed-duration motor-unit bursts that are assembled by the motor system to compose voluntary or reflexive actions (Bizzi et al. 1991, Mussa-Ivaldi and Giszter, 1992, Mussa-Ivaldi, 1999, Hart and Giszter 2004) and which allow the construction of motor issues (Dominici et al., 2011). Similar patterns of activation have been identified in humans and in various quadrupedal mammals (Grillner, 2011), which suggests that locomotion in vertebrates shares common basic rules.

Central Pattern Generators (CPGs)

Rhythmic motor behaviours are generated by neuronal networks wholly located in the CNS.

In the central nervous system (CNS) neurons are functionally organized in networks with the ability to produce complex, rhythmic motor behaviours such as walking, swimming, chewing, and breathing. A network can produce rhythmic activities mainly through two mechanisms. The first is based on the existence of **peacemaker neurons** that can generate membrane-potential oscillations when isolated from the rest of the network (Harris-Warrick and Flamm, 1987). The second mechanism depends on a phenomenon called **network-driven rhythmicity**, in which the rhythm emerges as a consequence of synaptic connections among neurons that are not themselves intrinsically rhythmic (Marder and Bucher, 2001). These mechanisms are not necessarily in dichotomy, but they may be present concurrently in the same network, as happens for instance in the crustacean stomatogastric ganglion (Harris-Warrick, 2010).

Along the neuraxis there are several interneuronal circuits that can generate rhythmic behaviours that are denominated **central pattern generators** (**CPGs**; Grillner, 2006). As for locomotion, a locomotor CPGs that is entirely localized in the spinal cord (locomotor CPGs; Kjaerulff and Kiehn, 1996) produces the basic locomotor program. It consists in the sequential activation of ipsilateral flexor and extensor muscles in the same limb and in the left / right coordination between limbs (Grillner and El Manira, 2015) independent of both sensory feedback and supraspinal inputs. Although CPGs operate without external commands, the

locomotor circuits in the spinal cord continuously receive and integrate afferent information that helps to refine the motor output according to external demands.

The generation of rhythmic bursts of activity in the locomotor CPGs seems to rely on a core of excitatory interneurons that are coordinated to express an alternating activity by a mechanism of reciprocal inhibition (Grillner and El Manira, 2015).

The first insight into the locomotor CPG organization is dated back to the past century when Thomas Graham Brown demonstrated that rhythmic hind-limb flexor–extensor movements can be induced in a decerebrate cat in the absence of any sensory input from the periphery (Graham Brown, 1911). These results suggest that the locomotor program may be produced by networks of neurons located entirely in the spinal cord. From this pioneering work, CPGs have been extensively studied in several animal models, thereby unveiling noteworthy details about the organization and function of the elements that constitute locomotor circuits (Buschges et al., 2008). For a better understanding of the general principles of locomotor-circuit organization, simplified experimental preparations with relatively few neurons have been adopted that use, for instance, invertebrates such as leeches and crustaceans and vertebrates as lamprey and zebrafish (Selverston and Moulins, 1985; Grillner et al., 1998a, b; Kyriakatos et al., 2011).

The achievements in electrophysiological, pharmacological and genetic properties of the elements that comprise the CPG for locomotion that have been obtained from the above-mentioned models may be then translated to mammals, as the basic mechanisms that generate alternating patterns are generally preserved among species (Grillner, 2011).

CPGs generate rhythmic activity depending on their circuit architecture.

One of the most challenging problems in neuroscience is to understand the operation underlying CPGs networks. Studying the function of a circuit implies the characterization of a high number of neurons and synaptic connections. Since the anatomical and cellular architecture of spinal networks is not yet known, theoretical models of CPGs may facilitate the production of a quantitative description of circuit mechanisms, thereby filling the gap between circuit operation and basic behaviours. The first model proposed to explain the functional organization of CPGs for locomotion is the half-centre. This model states that centres that control the locomotor program are composed of two groups of spinal neurons that are organized reciprocally and are able to mutually inhibit each other (Brown, 1914). However, such a model represents only a simplified CPG organization and cannot explain many features of the real locomotor pattern generated in the mammalian spinal cord. An implementation of the half-centre hypothesis has come from the study of turtles (Lennard, 1985) and adult decerebrate cats. It indicates the existence of separate networks for rhythm generation and pattern formation (Kriellaars et al., 1994; Lafreniere-Roula and McCrea, 2005). Figure 2 depicts the monolateral two-layer organization of the CPGs for locomotion.

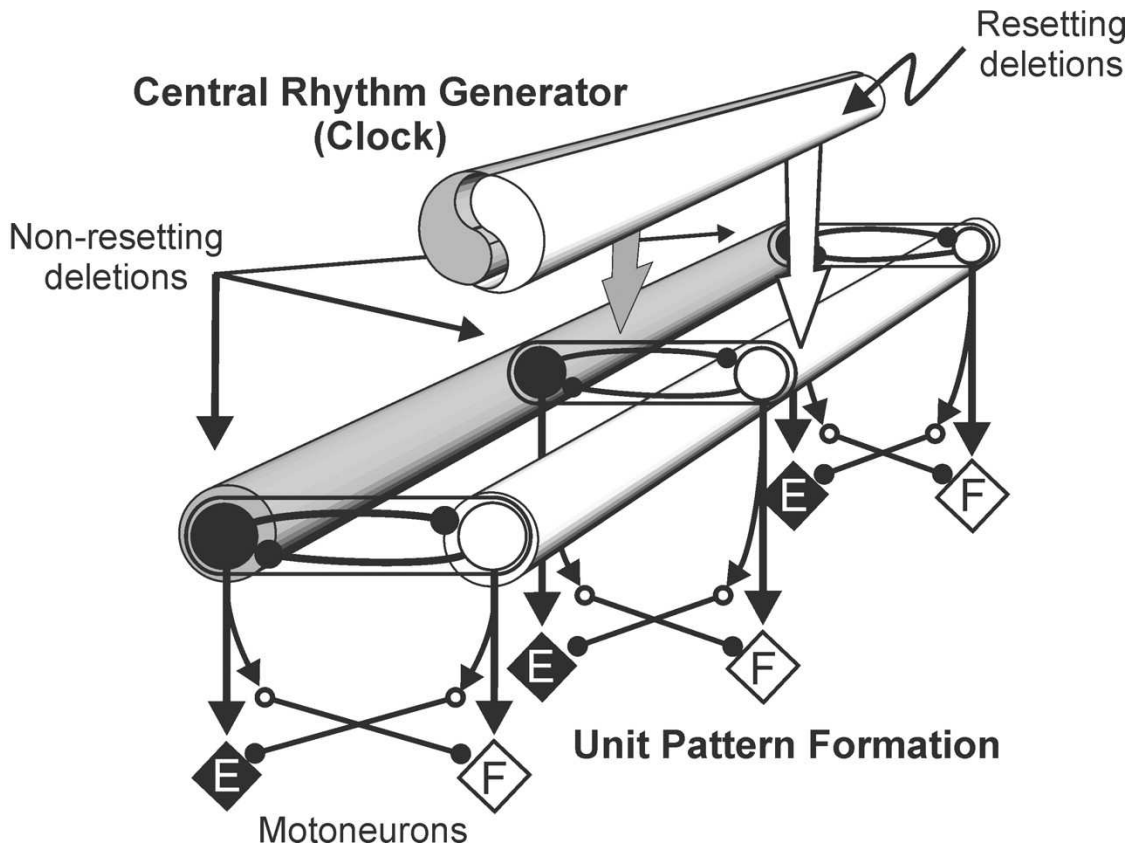

Figure 2. The central pattern generators (CPGs) have a two-layer organization. *The architecture consists of two separate networks: a half-centre rhythm generator (RG or clock) and a pattern-formation network (PF). Spontaneous pause of the rhythmic output (deletions) may occur at the level of the RG or PF (from Lafreniere-Roula and McCrea, 2005).*

The major weakness of the above mentioned models is represented by the difficulty in modelling different sources of variability, since their impact is still matter of debate. To better understand the effect of such variability, stochastic neural networks have been introduced.

Recently, in agreement with stochastic neural networks, Berg and colleagues (2007) have shown that, during the scratch-like behaviour induced by the mechanical stimulation of the carapace in adult turtles, motoneurons enter in a high

conductance state due to intense synaptic activity. By measuring the total excitatory and inhibitory conductance of motoneurons, they propose that synaptic inhibition and excitation alternate in phase (balanced model) instead of out of phase (reciprocal model). In this model, motoneuronal firing is stochastically determined by synaptically-induced fluctuations in membrane potential rather than by intrinsic membrane properties (Berg et al., 2007).

CPGs undergo finely timed developmental changes.

The development of locomotor spinal circuits is linked to both modifications in intrinsic properties of their constituent elements and to changes in the wiring properties of locomotor networks.

Five days prior to birth (E14.5-E16.5), only a spontaneous synchronous motor pattern can be observed (Iizuka et al., 1997; Nishimaru and Kudo, 2000; Nakayama et al., 2004). This type of embryonic network-bursting activity can also be evoked in new-born rodents through the pharmacological blockage of synaptic inhibition. Indeed, developmental studies indicate that, during the embryonic period, the transition from a synchronous to an alternate pattern may depend on the maturation of inhibitory connections between the two sides and on the shift of E_{Cl^-} towards hyperpolarized values. This latter event converts γ-Aminobutyric acid (GABA) and glycine-evoked potentials from excitatory to inhibitory, as they are in the mature state (O`Donovan et al., 1998; Nishimaru and Kudo, 2000; Vinay et al., 2002).

Another fundamental feature of the transition from embryonic to postnatal age is the change in motoneuron morphology and membrane properties that lead to important modifications in excitability, including a decrease in input resistance, an increase in rheobase and a maturation of repetitive firing properties. Furthermore, motoneuronal pools do not maturate simultaneously, as the motoneurons that innervate rat hind-limb extensor muscles are usually less mature than flexors at birth in terms of electrical properties (Vinay et al., 2000; Carrascal et al., 2005).

Finally, the development of descending pathways, especially of monoaminergic projections, represents a further stage in the maturation of lumbar networks. Serotoninergic fibres reach the lumbar enlargement at E17 and from this moment they keep on their maturation process until the end of the first postnatal week. During this period, the growth of serotoninergic axons allows the maturation of electrical properties in mature motoneurons (Vinay et al., 2002). Neuropeptides such as oxytocin also exert trophic and differentiating roles in the maturation of the spinal cord. Oxytocin is produced in the paraventricular hypothalamic nucleus (PVN) (Swanson and McKellar, 1979) and carried to the spinal cord principally through descending pathways. These fibres arrive before birth at the thoracic level and reach the lumbar spinal cord at the second postnatal day (Leong et al., 1984), thereby modulating CPGs activity and its maturation (Pearson et al., 2003). Rodents cannot walk at birth because they lack postural control (Clarac et al., 1998). But when suspended, they show an air-stepping behaviour that lasts a few cycles (Fady et al., 1998). Moreover, once the spinal cord is isolated from newborns by keeping hindlimbs attached, in response to appropriate stimulation, real stepping and a coordinate pattern of muscular activity emerges that is similar

to the adult electromyographic activity recorded during locomotion (Gordon and Whelan, 2006).

In conclusion, since CPG circuits express locomotor patterns similar to those of adults already at birth (Kiehn and Kjaerulff, 1996), results collected from the spinal cord of new-borns may suggest important findings to describe adult locomotor circuits.

The spinal cord isolated from new-born rodents is a very useful model for understanding the CPGs operation.

The most common type of vertebrate model employed in the functional studies of locomotor CPGs is the in-vitro isolated spinal cord of the new-born rat (Smith et al, 1988), which, though deprived of supraspinal and peripheral inputs, retains the ability to generate a coordinated locomotor-like activity if opportunely stimulated (Kudo and Yamada 1987; Cazalets et al. 1992).

This preparation provides several advantages, such as the easy manipulation of the perfusion-medium composition, the possibility to apply drugs that do not cross the blood-brain barrier by simply adding them to the recording chamber, and the ability to reversibly manipulate the excitability of networks within discrete segments of the spinal cord (Beato and Nistri, 1999; Taccola et al., 2010). Furthermore, in new-borns, the CNS is not yet fully myelinated; thus, it is possible to keep the tissue alive for quite a long period through an adequate perfusion system. Indeed, this preparation can be used for several hours when it is maintained in an appropriate oxygenated physiological medium, and it is still able to generate locomotor patterns 24 hours after dissection (Taccola et al., 2008). In a preliminary

test even after 48, hours the preparation was optimally functional in generating a locomotor output (Dose and Taccola, unpublished observations).

The locomotor CPGs output recorded from the isolated spinal cord consists of a pattern of electrical discharges that alternate among the second and fifth lumbar VRs (VRL2-L5) on the same side of the cord, which correspond to flexor and extensor commands, respectively (Kiehn and Kjaerulff, 1996), and between the left and right sides of the spinal cord (Juvin et al., 2007). This phenomenon is called **fictive locomotion** (**FL**) because the alternated neural oscillations recorded from isolated spinal cords resemble the electromyographic patterns recorded in walking animals *in vivo* (Gordon and Whelan, 2006), as depicted in Figure 3. FL is not exclusive of *in vitro* preparations, but it can be recorded also from peripheral nerves in decerebrated and curarized *in vivo* cats (Grillner and Zangger, 1979; Pearson and Rossignol, 1991).

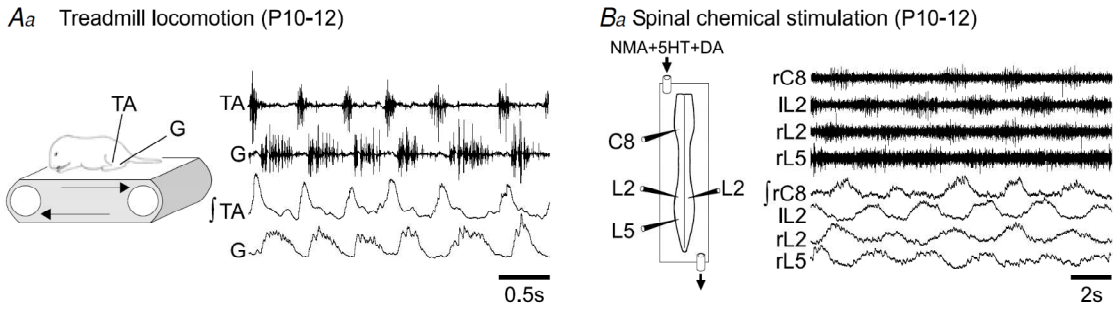

Figure 3. Locomotor activity recorded *in vivo* from adult animals during real stepping is comparable to FL patterns induced *in vitro*. *A depicts the activity of flexor and extensor muscles derived from an adult rodent walking on a treadmill. In B, a chemically induced FL is recorded from the ventral roots of a neonatal isolated spinal cord. As depicted by the figure, the flexor-extensor pattern obtained from the* in-vitro *preparation is similar to that recorded from a rodent during real stepping on a treadmill (Juvin et al., 2007).*

FL may be induced chemically in isolated spinal cords through the bath application of several types of neurotransmitter agonists, such as N-methyl-D-aspartate (NMDA) and serotonin (5-hydroxytryptamine, 5-HT).

The exact mechanism and the site of action of these substances is not known; they might, however, act by increasing neuronal excitability to recruit a sufficient number of CPG neurons (Kiehn et al., 1999a, Madriaga et al., 2004, Christie and Whelan, 2005, Liu and Jordan, 2005). At present, the best way to elicit the locomotor rhythm results to be via the co-application of NMDA and 5-HT (Sqalli-Houssaini et al. 1993; Kiehn and Kjaerulff, 1996; Cazalets and Bertrand, 2000), since in these conditions, FL is regular and stable until neurochemicals are applied (Dose and Taccola, 2012). However, when separately applied, the two neurotransmitters are both able to activate the CPGs.

Excitatory amino acids have a pivotal role in CPG activity (Kudo and Yamada, 1987); they act on both NMDA and non-NMDA glutamate receptors, as is demonstrated by the disappearance of FL in experiments in which both receptors are simultaneously blocked (Smith et al, 1988; Cazalets et al.1992). On the other hand, exogenous 5HT increases FL-cycle duration and period (Harris-Warrick and Cohen 1985), thereby improving left / right and flexor / extensor alternation (Beato et al., 1997; Pearlstein et al., 2005). Indeed, it has been demonstrated that 5-HT reduces the Ca^{2+}-dependent K^+ channel (K_{Ca}) current, thereby reducing the slow afterhyperpolarization (sAHP) and therefore prolonging bursts duration (Hill et al., 1992). Indeed, the summation of the sAHP is an important factor in controlling burst termination and thereby in regulating the frequency of FL (Hill et al., 1992).

Moreover, 5HT increases motorneuron excitability by inhibiting certain channels that are involved in leak conductance—namely, the TASK-1 potassium channels—thereby inducing a more depolarized membrane potential and an increase in input resistance (Perrier et al., 2003). Besides the induction of FL episodes when applied alone (Cazalets et al., 1992), 5HT affects locomotor-related oscillations previously induced by the sole NMDA (Pearlstein et al., 2005). Moreover, inhibition of the endogenous synthesis of 5HT through the p-chloro-phenylalanine (PCPA) leads to a disorganization of the locomotor rhythm that is induced by the activation of NMDA receptors (Pearlstein et al., 2005).

Circuits controlling the locomotor program are located in the ventral lumbar spinal cord.

Pharmacological, electrophysiological and lesion studies in the isolated spinal cord demonstrate that rostral lumbar segments are more rhythmogenic than caudal ones, thus indicating a rostro-caudal distribution of the locomotor network in the lumbar cord with the greatest rhythmogenic potential at L1-L2 segments (Kjaerulff and Kiehn, 1996; Cowley and Schmidt, 1997; Kremer and Lev-Tov, 1997; Grillner et al., 1998; Beato and Nistri, 1999; Lev-Tov et al., 2000, Kiehn and Butt, 2003; Nistri et al., 2006; Kiehn, 2006). Besides the rostro-caudal distribution of the locomotor CPG, its ventral distribution in the spinal cord has been confirmed with dorsal horn-ablation studies (Kjaerulff and Kiehn, 1996; Taccola and Nistri, 2006). Indeed, after the removal of the dorsal region, the locomotor rhythm persists (albeit with reduced cycle frequency), which is probably due to a decreased drive from the CPG onto the motoneuron pools (Kjaerulff and Kiehn, 1996). Precisely, activity-

dependent neuronal labelling indicates that the area around the central canal and the medial part of the intermediate grey matter (Rexed laminae VII-VIII-X) are important for rhythm-generation during locomotion (Viala et al., 1991; Kjaerulff and Kiehn, 1994; Butt and Kiehn, 2003; Miles et al., 2005). Furthermore, it has been demonstrated that left-right coordination is provided by commissural interneurons (CINs), which axons cross the midline and form synapses with motoneurons and / or interneurons located in the contralateral hemicord. Conversely, the coordination of flexor and extensor motoneurons on the same side involves ipsilateral inhibitory networks, as demonstrated by the synchronous activation of flexor and extensor motoneurons in response to the pharmacological blockade of glycinergic inhibition (Cazalets et al. 1998; Beato & Nistri 1999).

The cartoon in Figure 4 shows that the locomotor CPG is located mainly in the ventral lumbar cord and that it has a rostro-caudal distribution.

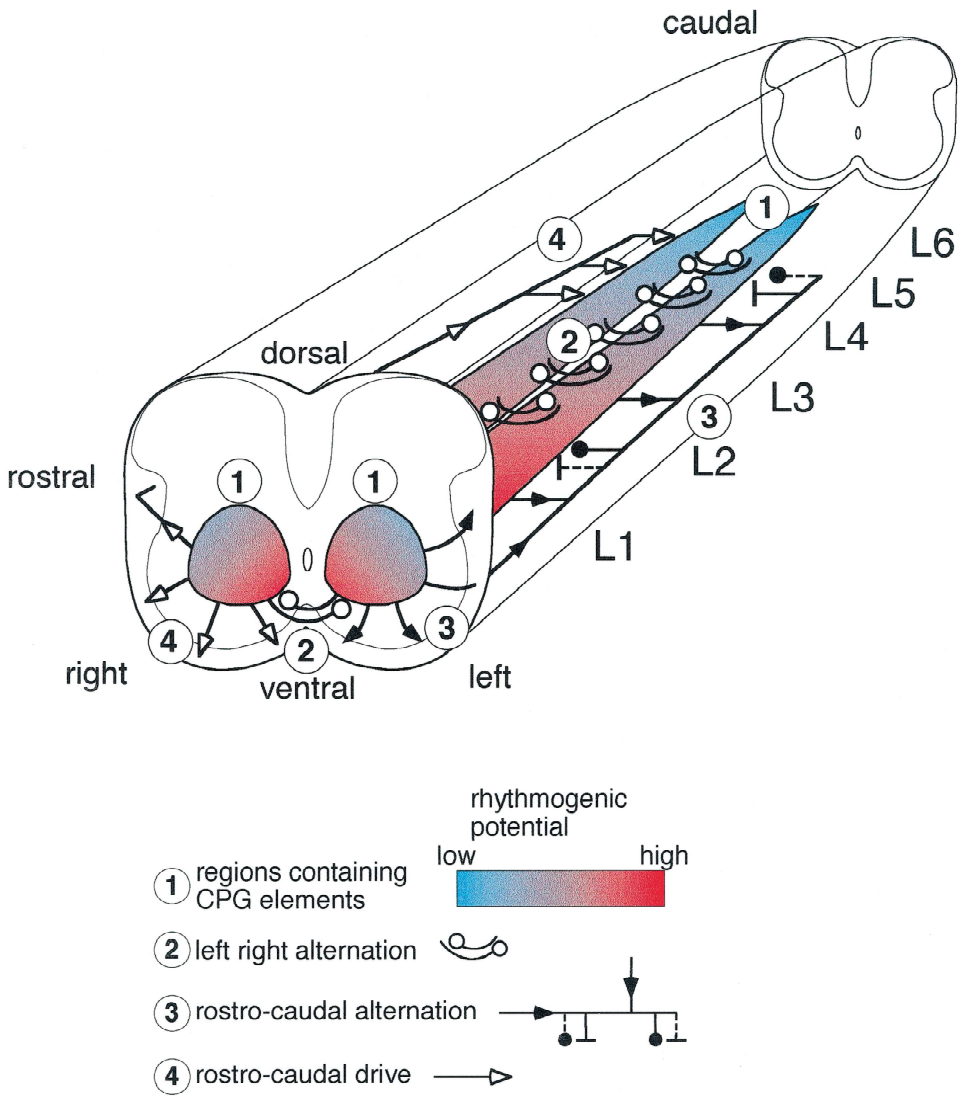

Figure 4. Spinal locomotor networks are localized in the ventral spinal cord. *The locomotor circuit is distributed along the cord from L1 to L6 in two medial columns. The colour gradient points out the higher rostral (red) and lower caudal (blue) capability to generate rhythmic activity. In the ventral commissure is indicated the pathway mediating left-right coordination, while the pathways involved in the flexor and extensor alternation are depicted in figure in the lateral and ventral funiculus (from Kjaerulff and Kiehn, 1996).*

Distinct excitatory and inhibitory interneuronal populations have been identified using genetically-modified animals.

Detailed knowledge of the individual components of the locomotor CPG is still lacking. To relate the locomotor function to the molecular identity of CPGs neurons, many efforts have been made in the last few years to adopt a broad spectrum of genetic manipulations on spinal interneurons and to thereby examine potential consequences on locomotor output. This research, based on molecular biology and genetics techniques, has employed animal models such as mouse, lamprey, tadpole and zebrafish. Many of these techniques, like knockout and knockin technologies, are unavailable in rat studies because it is hard to culture and maintain rat embryonic stem cells (ES). Nevertheless, since rats and mice are phylogenetically very closely related, results collected in mice may be extended to rats.

In mice, four classes of CPG interneurons (V0, V1, V2 and V3) have been identified in the ventral part of the neural tube (Jessel, 2000).

V0 interneurons (mostly inhibitory) are associated with left-right alternation (Lanuza et al., 2004). The V1 inhibitory interneurons are required for the generation of fast motor bursting during locomotion, thus highlighting the important regulatory role on the frequency of the locomotor rhythm (Gosgnach et al., 2006). V2 interneurons are divided into two subpopulations, genetically identified by the expression of specific cell markers. V2a interneurons are glutamatergic, while V2b are GABAergic interneurons (Lundfald et al., 2007). Mice that lack these neurons show alterations in frequency, amplitude and bilateral coordination compared to wild type FL characteristics (Crone et al., 2008). V3 interneurons participate in the

generation of a stable and balanced rhythm (Zhang et al., 2008). Moreover, dI6 cells, which originate from progenitors located immediately dorsally to the V0 interneurons, seem to be involved in the generation of the locomotor rhythm (Gosgnach, 2011). Another class of interneurons that express the Hox gene Hb9 seems to take part in locomotor rhythm generation (Brownstone and Wilson, 2007). In these knockout models for specific interneuronal subpopulations, the locomotor output is not completely abolished. Thus, other, not-yet-identified interneurons should be part of the locomotor CPGs. Another explanation for the persistence of rhythmic activity in knockout animals might consider the presence of redundant circuits that act as ancillary networks. These could be compensatory networks that come into play following selective alterations in circuit membership.

In conclusion, new techniques allow for the identification of single network elements, thereby confirming that the locomotor CPGs has a remarkable cellular heterogeneity and complexity.

The pharmacological blockade of fast synaptic inhibition unveils the intrinsic rhythmicity of the spinal cord.

Spinal circuits possess an intrinsic source of excitability that participates in generating the locomotor program (Eklöf-Ljunggren et al., 2012). Indeed, the blockade of inhibitory transmission uncovers a glutamatergic network that remains capable of producing rhythmic activity. This rhythmic activity comes from a basic excitatory network, which may be seen as a locomotor network deprived of the contribution of inhibitory connections (Clarac et al., 2004). *In vivo* experiments on cats demonstrate that, when the glycinergic inhibition is blocked, the spinal cord

evokes paroxysmal activity (Schwindt and Crill, 1981). Moreover, in cultured spinal neurons, the application of glycine and GABA receptor blockers, strychnine and bicuculline respectively, induces rhythmic and self-sustained bursting activity (Streit, 1993). Also, in the isolated spinal cord from neonatal rat, bursting activity can be elicited through the co-application of strychnine and bicuculline, as depicted in Figure 5 (Bracci et al., 1996a; Beato and Nistri 1999). Discharges are synchronous along the cord and between the left and right VRs, and they are blocked by the conjoint application of the NMDA receptors antagonist, d-(-)-2-amino-5-phosphonopentanoic acid (**APV**), and the (AMPA)/kainate receptors blocker, 6-cyano-7-nitroquinoxaline-2,3-dione (**CNQX**), (Legrand et al., 2004). Since these agents block the excitatory synaptic transmission, their effect highlights the well-defined network origin of the synchronous bursting activity. The rhythm originating from the pharmacological blockage of fast synaptic inhibition is for this reason called disinhibited. It resembles the early types of network bursting activity present at early stages of development (E14.5-E16.5; Iizuka et al., 1998; Nakayama et al., 1999).

However, it has been suggested that bicuculline may distort the real contribution of $GABA_A$ receptors at a network level since bicuculline has two opposite effects on the burst rate (Pflieger et al., 2002). On one hand, it increases burst frequency through the blockade of $GABA_A$ receptors similarly to picrotoxin; on the other hand, like apamin, it decreases the burst rate of disinhibited rhythm through calcium-activated potassium channels (Pflieger et al., 2002).

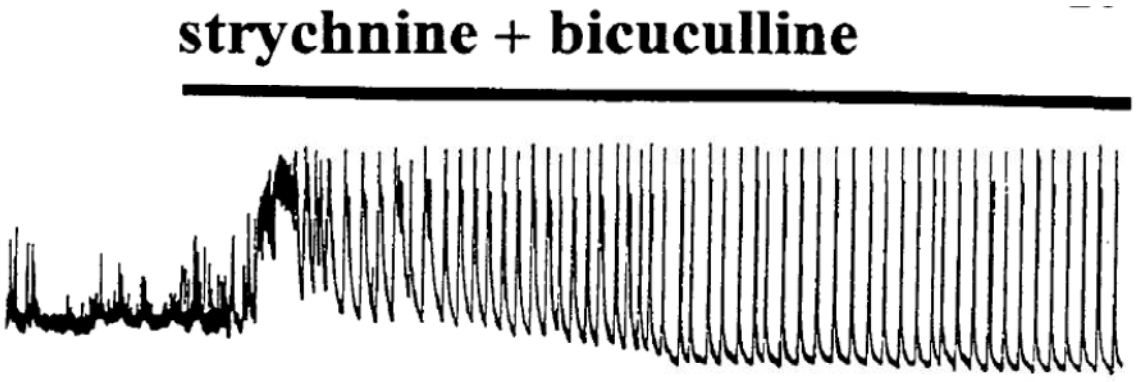

Figure 5. Intracellular recordings from motoneurons show that strychnine and bicuculline induce a disinhibited rhythm when simultaneously applied. *The co-application of strychnine and bicuculline first elicits a strong depolarization of a single motoneuron with the emergence of sporadic bursting activity (synchronous among all motor pools, not shown) that becomes a regular disinhibited rhythm as soon as the cell repolarizes to its resting baseline. The trace depicted in the figure is from a neuron at a resting potential of - 73 mV (modified from Bracci et al., 1996a).*

An interesting question raised by Bracci and colleagues concerns whether this synchronous rhythmic activity is generated by the same network involved in the origin of the rhythmic locomotor-like activity (Bracci et al., 1996b). In favour of the hypothesis of a common source of rhythmicity, there is evidence that some pharmacological agents can modulate the fictive locomotion frequency in a dose-dependent manner (Cazalets et al., 1992) and similarly affect periodicity of the disinhibited rhythm (Bracci et al., 1996a). Moreover, the alternating pattern induced by NMDA and 5-HT may also be transiently converted into a synchronous one as soon as bicuculline and strychnine are applied during fictive locomotion (Kremer and Lev-Tov, 1997). In optogenetic studies, Kiehn and colleagues demonstrate that excitatory neurons are sufficient and necessary for the generation of the locomotor

rhythm and that this function cannot be replaced by the light-mediated activation of inhibitory neurons *(*Hägglund et al., 2013).

In conclusion, disinhibited rhythm induced by bicuculline and strychnine could be used as a valuable tool to reduce the complexity of the network and to study the modulation of rhythmic activity in the spinal cord.

Neuromodulation finely tunes the CPG output.

The operation of the locomotor CPGs depends on both the biophysical properties of its constituent neurons and the connections between them. Both features are continuously modified by neuromodulatory substances, which allow circuits producing an assortment of different motor patterns to better adapt the locomotor program to environmental changes (Marder and Bucher, 2001). Neuromodulators may be differentiated with regard to their sites of synthesis into **extrinsic** and **intrinsic** types (Katz, 1995). While **extrinsic** modulators are produced far from locomotor spinal networks, **intrinsic** modulators are released by spinal interneurons (Katz and Frost, 1996). Furthermore, extrinsic and intrinsic modulators may be further subdivided on the basis of their chemical structure into biogenic amines (5-HT, noradrenaline, dopamine, histamine and trace amines), amino acids (GABA, Glu, Gly) and peptides such as oxytocin. Other molecules that do not fall into these categories have also been shown to modulate the locomotor response, such as ATP, adenosine, endocannabinoids and nitric oxide (NO) (Miles and Sillar, 2011).

Once released, these agents reach their targets in two principal ways that depend on the distance of the release terminal from the postsynaptic site of action. In **wiring transmission**, intercellular communication occurs among well-defined connected structures (synapses). In **volume transmission**, a long-range diffusion of signals within blood, cerebrospinal fluid or extracellular space connects remote targets from the site of release (Agnati and Fuxe, 2000). Wiring transmission includes synaptic transmission and gap junctions (Fuxe et al., 2007). On the other hand, volume transmission also activates extrasynaptic receptors that can be found at various locations in neurons, including the cell body, the dendritic shafts and dendritic spines. These receptors can also be found adjacent to the postsynaptic density zone (PSD) (Petralia et al., 2010; Hardingham and Bading, 2010) and in glial cells (Fuxe et al., 2010).

Therefore, wiring and volume-transmitted signals are continuously integrated by neurons in the CNS.

Furthermore, neuromodulators may be tonically or phasically released. Phasic release produces transient alterations in neuronal circuits; tonic release maintains a low, basal modulatory action over the network.

Since the locomotor CPGs need to rapidly adapt to continuous environmental changes, activity-dependent changes may play a main role in modulating motor outputs (Bertrand and Cazalets, 2013). For instance, during FL, the accumulation of neuromodulators can play a role in the self-termination of this behaviour, as occurs in Xenopus embryos in which ATP and adenosine exert control in the duration of swimming episodes (Dale and Gilday, 1996). Moreover, as seen in lamprey spinal cords, NO released from active neurons induces an amplification of

the network output by decreasing inhibition and increasing excitation in the network (Kyriakatos and El Manira, 2007; Kyriakatos et al., 2009).

Neurotransmitter release is affected after spinal cord injury (SCI), though the expression and functionality of receptors can withstand great changes. For example, in the weeks after SCI, 5-HT_2 become constitutively active because these brain stem-derived neurotransmitters are lacking as a result of the injury (Harvey et al. 2006; Murray et al. 2010).

Furthermore, motoneurons develop supersensitivity to 5-HT, and very small residual amounts of 5HT are able to facilitate sodium-persistent inward currents (Na PICs; Harvey et al., 2006) and calcium PICs mainly through the 5-HT_2 receptor (Li et al., 2007). Therefore, one of the aims of pharmacotherapy after SCI is to restore the physiological levels of neuromodulators and to limit the imbalance created after tissue damage.

The locomotor CPG can be activated more physiologically using electrical stimuli.

Drug applications to the whole spinal cord aimed at inducing FL represent a non-physiological approach, because receptors are continuously stimulated in this way and because substances added to the whole tissue act on all spinal neurons. Contrariwise, the electrical stimulation of primary afferents promotes the release of endogenous neurotransmitters at more specific sites. However, a brief electrical single pulse is not able to trigger an episode of FL. Only a repetitive stimulation can cause persistent neuronal depolarization due to glutamate release from primary afferent (Kangrga and Randic, 1990) and can enrol a larger population of cells of

the circuit up to the threshold for the generation of locomotor pattern (Marchetti et al., 2001a).

Furthermore, it has been shown that extracellular potassium concentration increases during electrically-induced locomotor-like episodes. This phenomenon could influence the excitability of CPGs (Marchetti et al., 2001b). Indeed, by increasing the extracellular potassium concentration in a very narrow range, the isolated spinal cord generates a stable pattern of FL (Bracci et al, 1998).

During the electrical activation of CPGs, despite continuous stimulation, electrically-induced FL decays, even when the intensity of stimulation is augmented (Marchetti et al., 2001a). Probably the termination of FL is due to synaptic fatigue (Lev Tov and Pinco, 1992), the release of inhibitory neurotransmitters or buffering of potassium (Marchetti et al., 2001a).

Interestingly, despite changes in the frequency and amplitude of the stimulating protocols, electrically-induced FL remains relatively stereotyped, preserving a typical periodicity (1-2 seconds) (Marchetti et al., 2001a; Taccola, 2011) consistent with the rhythmic oscillation frequency induced by the bath-application of neurochemicals (Cazalets et al., 1992). This indicates the existence of an intrinsic control in the CPG circuits, with non-linear properties between incoming and outgoing inputs (Marchetti et al., 2001a; Taccola, 2011).

Sensory inputs have a direct access to the CPGs.

Despite the automaticity of the locomotor program (Grillner and Zangger, 1984; Giuliani and Smith, 1987), the operation of CPGs during real locomotion is finely

regulated by afferent feedback which plays a pivotal role in adapting and modulating the output. Indeed, sensory inputs are an important source of feedback during locomotion that reinforce rhythmic patterns (Frigon and Rossignol, 2006). Sensory inputs that originate from the periphery are conveyed to the spinal cord by primary afferent fibres (Figure 6). These signals are generated from different types of receptors located peripherally: namely, **cutaneous receptors**, **muscle spindles**, **Golgi tendon organs** (**GTOs**).

Early studies have shown that proprioceptive afferents possess the ability to initiate or block locomotor movements (Sherrington, 1910b). The stimulation of proprioceptors at the hip level may induce an air-stepping behaviour in spinalized cats (Sherrington, 1910a). Conversely, during locomotion on a treadmill, the flexion of one hip joint prevents the step on ipsilateral side while the other limb continues walking (Grillner and Rossignol, 1978). Moreover, afferents participate in the modulation of locomotor speed, shaping the gait cycle structure (Forssberg et al., 1980a). In fact, an increase in treadmill speed shortens the stance phase, while the swing phase remains constant within a wide range of selected velocities (Barbeau and Rossignol, 1987). In addition, when a cat is placed on a split belt and the two limbs are subjected to different speeds, each limb adapts to the corresponding speed (Forssberg et al., 1980b).

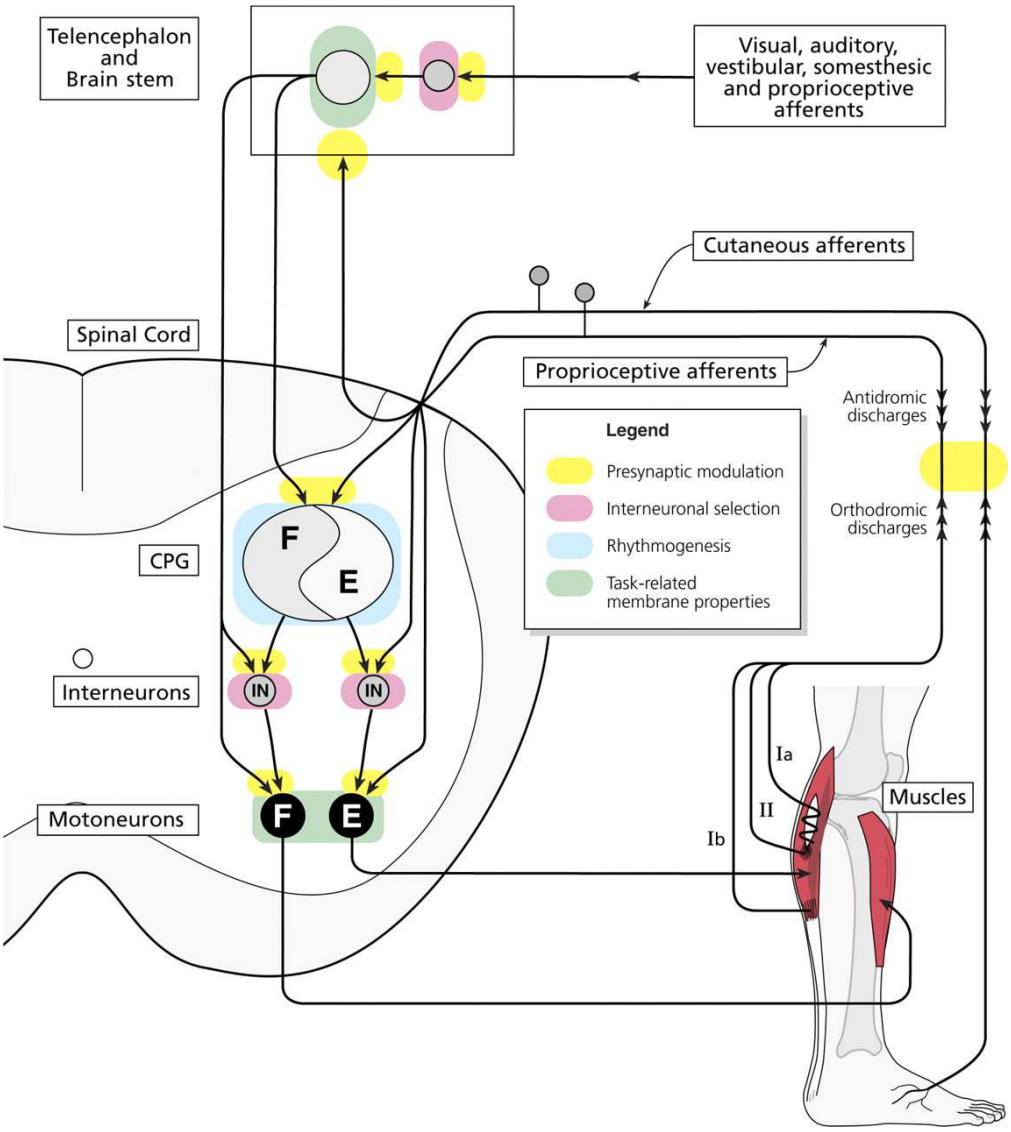

Figure 6. The locomotor CPG receives projections from periphery. *In figure are depicted afferent pathways (Ia, Ib, II, and cutaneous afferents) that from lower limb reach the spinal cord and higher centres, conveying information for adjusting the locomotor output to environmental changes. These inputs (in yellow) are generally subjected to a presynaptic inhibitory control (from Rossignol et al., 2006).*

The important role of sensory feedback in CPG operation has been highlighted by studies conducted during an ongoing locomotor activity recorded in neonatal

rodents from spinal-cord leg-attached preparations. These investigation demonstrated that the removal of sensory feedback from the hind limbs disrupts FL (Acevedo and Diaz-Rioz, 2013).

Afferent inputs are also involved in the regulation of muscle activity levels through different reflex pathways, as highlighted in experiments in which a reduction in sensory feedback from the ankle extensor that becomes less stretchable causes a consequent reduction in the extent of the ongoing activity derived from contracting muscles (Gorassini et al., 1994).

The evidence that afferent inputs have direct access to the CPGs comes from experiments conducted in decerebrated spinal cats. After induction of FL through the administration of L-dopa and nialamide, the conjoint delivery of brief electrical pulses of stimulation to the afferents is able to reset the step cycle in a phase-dependent manner (Conway et al., 1987; Perreault et al., 1995; Iizuka et al., 1997; Pearson et al., 1998). This effect is mediated by polysynaptic pathways (Lam and Pearson, 2002). Studies conducted on rodent (Lizuka et al., 1997) and lamprey (Vogelstein et al., 2006) *in vitro* spinal cord preparations show that, during a chemically-induced FL, electrical stimulation of afferents can reset the rhythm on a cycle-by-cycle basis.

In addition, afferent inputs such those evoked by the stimulation of paw and perianal region receptors are able to trigger episodes of locomotion (Pearson and Rossignol 1991).

In the isolated spinal cord of neonatal rats, inputs evoked by the electrical stimulation of sacrocaudal afferents activate CPG networks through the excitation of sacral neurons, which, in turn, possess crossed and uncrossed ascending

projections through the ventral (VF) and lateral white matter *funiculi* (Lev-Tov et al., 2010; Etlin et al., 2013).

In conclusion, afferent feedback plays an essential role in regulating the operation of the locomotor CPGs in function of the biomechanical characteristics of the limbs and their interactions with the environment. Moreover, because of the favoured access to locomotor circuits and the ability to trigger locomotor episodes, primary afferent fibres could be used to facilitate locomotor recovery to some extent even when the supraspinal drive is compromised.

Posture is a motor behaviour partially controlled by spinal circuits.

Body movement throughout space depends not only on the rhythmic and alternated contraction of flexor and extensor muscles on both lower limbs but also on the maintenance of a correct standing posture.

Postural-control mechanisms have been developed in ground-living animals that allow them to adjust their posture against the force of gravity and equilibrium changes. The mechanisms involved in the regulation of postural muscle tone and in the generation of a locomotor rhythm are closely integrated, thereby allowing the generation of appropriate movements during locomotion (Zelenin et al., 2003; Deliagina et al., 2008). The integrity of reticulospinal and vestibulospinal pathways is crucial for postural control (Takakusaki et al., 2016). Indeed, the postural activity is regulated in two ways: a feedback mode, which is mainly involved in postural corrections, and a feed-forward mode, which is aimed at anticipating and counteracting the destabilizing effects of movement.

Regarding the localization of the postural mechanism, hind-limb posture is controlled by two closed-loop mechanisms: a short one in the spinal cord and a long one involving supraspinal centres (Boulenguez and Vinay, 2009; Deliagina et al., 2008). Under certain conditions in quadrupeds, the system may be dissociated into two independent sub-systems that stabilize the orientation of the anterior and posterior parts of the trunk. These are driven by somato-sensory inputs from limb mechanoreceptors (Deliagina et al., 2007).

Studies conducted in rabbits show that all four limbs are involved in supporting the body in standing animals. If posture is perturbed, each limb participates in the generation of corrective motor responses (Beloozerova et al., 2003). Thus, the spinal cord not only responds to supraspinal commands for postural corrections; it is also able to generate postural corrections in response to local somato-sensory inputs (Deliagina and Orlovsky, 2002).

Following a SCI, the resulting loss of posture is attributable to the great importance of supraspinal centres over spinal mechanisms. Nevertheless, some elements concerning postural control remain at the spinal level. Moreover, after spinal cord transection, the CPG for standing, which is mainly localized at the spinal level, is deprived of the tonic supraspinal drive, thereby reducing its activity.

From a rehabilitative perspective, a prerequisite for the recovery of the locomotor behaviour after SCI is the restoration of postural control. Therefore, it is intriguing to consider the possibility of reactivating standing CPG using the same interventions aimed to modulate the locomotor CPGs: namely, pharmacological and electrical stimulation. Experiments conducted on spinalized rabbits show that epidural stimulation of the spinal cord can partly substitute the supraspinal

excitatory drive and activate the standing CPG to a certain extent (Musienko et al., 2010).

In conclusion, the optimal neurorehabilitation that aims to restore locomotion should also provide a functional return of standing ability. Indeed, even though it is possible to step with an appropriate weight-bearing system, this does not correspond to the movement of the body throughout a real environment.

Functional recovery after spinal-cord injury can be promoted by electrostimulation.

SCI consists in a temporary or permanent impairment in sensory, motor and autonomic functions (Hulsebosch, 2002). In addition, it can lead to the onset of chronic pain and spasticity (Sjölund, 2002; Saulino, 2014). Regarding aetiology, a SCI can be subdivided into traumatic and non-traumatic. Furthermore, depending on the degree of damage to the descending and ascending pathways that pass through the damage site, the injury is considered complete or incomplete (Harkey, 2003).

According to the National Spinal Cord Injury Statistical Center (NSCISC), there are about 54 new traumatic spinal-cord injuries per million persons every year in the U.S. (National Spinal Cord Injury Statistical Center, 2016). Data collected in 2014 in Friuli Venezia Giulia indicates a much lower incidence of SCIs than that in the U.S.: namely, about 14 new cases per million (personal communication by Zampa, M.D, IMFR, Udine, Italy, 2014). The majority of traumatic injuries (55%) affect the cervical and thoracic levels (De Vivo, 2012) and are due to motor-vehicle accidents or falls. From a pathophysiological point of view, SCI shows a biphasic trend,

presenting a first phase or **primary injury** that is consequent to the mechanical injury that disrupts axons, blood vessels, and cell membranes. In a following stage, it manifests a **secondary injury**, which is characterized by vascular dysfunction edema and ischemia, excitotoxicity, production of free radicals, inflammation and apoptosis (Rowland et al., 2008). While the primary injury phase lasts from 1 to 2 hours, the secondary phase may continue for 2 weeks. During this period, the effects produced by the primary injury are amplified and extended.

Since the vast majority of SCIs involve the cervico-thoracic cord (National Spinal Cord Injury Statistical Center, 2016), lumbar spinal circuits that underlie the locomotor program are potentially still able to perform complex motor tasks in the absence of supra-spinal control and can be modulated by activity-dependent neuro-rehabilitative approaches (Edgerton et al., 2004). Although therapy for SCI is currently still lacking, one of the most common rehabilitation strategies involves the use of functional electrical stimulation (FES). This technique applies electric current to the neuromuscular junction to induce externally driven muscle contractions that supplement or replace lost functions in people with SCI (Peckham and Knutson, 2005). However, FES is far from restoring locomotor behaviour in SCI persons; therefore, more targeted approaches need to be developed. Thus, epidural stimulation has been introduced to activate spinal CPGs for locomotion.

The first use of epidural electrical stimulation comes from the treatment of chronic pain (Shealy et al., 1967; Broggi et al., 1994; Lang, 1997; Moreno-Duarte et al., 2014) or spasticity (Barolat-Romana et al., 1985). Recently, several studies carried out in preclinical models of complete SCI show that epidural electrical stimulation can induce stepping movements in adult cats (Kazennikov et al., 1983; Iwahara et

al., 1992; Gerasimenko et al., 2003; Musienko et al., 2012) and rats (Ichiyama et al., 2005).

Also, clinical studies in humans with SCI have demonstrated the efficacy of epidural stimulation in temporally-activating locomotor circuits, as is shown in Figure 7 (Dimitrijevic et al., 1998a, Dietz and Harkema, 2004; Minassian et al., 2007, Gerasimenko et al., 2008).

More recently, it has been demonstrated that epidural stimulation applied to the lumbosacral region in combination with intense training can aid the recovery of volitional control in humans with SCI (Edgerton and Harkema, 2011; Harkema et al., 2011; Angeli et al., 2014).

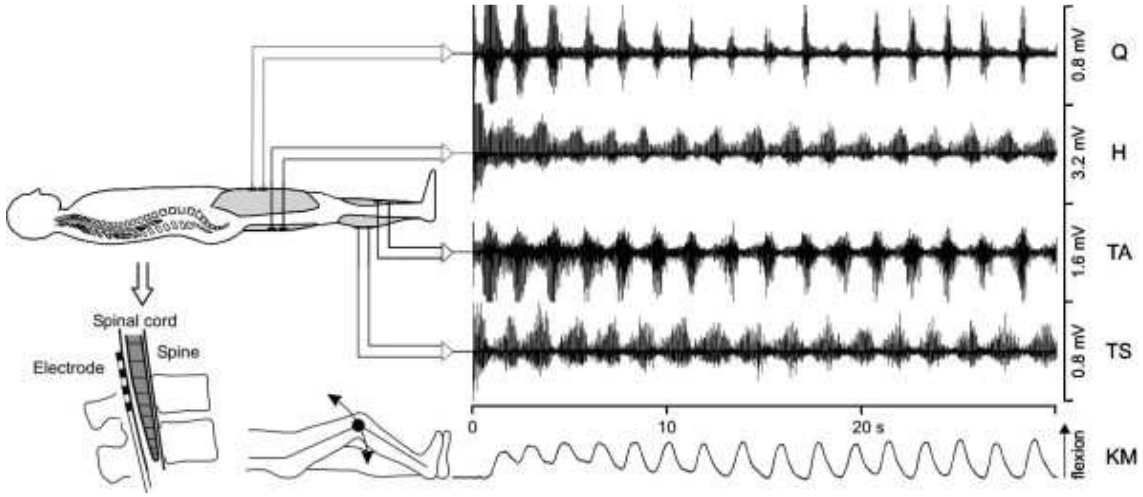

Figure 7. Epidural stimulation triggers the locomotor CPG in spinal-cord injured persons. *A spinal-cord injured subject is lying in supine position while an epidural electrode, placed at the lumbar level, delivers a train of electrical pulses at 25Hz (left). As a consequence of the stimulation, surface EMG electrodes positioned at flexor and extensor muscles in the lower limbs produce a rhythmic, alternated activity (right). Real stepping-like movements are recorded by the position sensor located on the knee (bottom cartoon and trace; Minassian et al., 2007).*

Some characteristics of electrical stimulation have been designed by experimental and clinical studies. In particular, it has been shown that the best site of stimulation is the lumbar enlargement, which is very effective in facilitating CPG activation in cats, rats and humans (Gerasimenko et al, 2001; Ichiyama et al., 2005; Lavrov et al., 2006; Dimitrijevic et al., 1998). The optimal frequency of stimulation for inducing stepping-like movements in decerebrated cats is between 5 and 10 Hz (Iwahara et al., 1992), in chronic spinal rats between 40 and 60 Hz (Ichiyama et al., 2005) while in man between 30 and 40 Hz (Dimitrijevic et al., 1998).

The mechanism by which epidural stimulation improves motor function is not well understood. One hypothesis involves Hebbian mechanisms of synaptic facilitation (Young, 2015). Indeed, the widespread activation of ascending and descending pathways in the spinal cord, which occurs during electric stimulation, could strengthen synaptic activity (Young, 2015). Another hypothesis suggests that epidural stimulation acts through the activation of DRs (Tator et al., 2012).

Epidural stimulation is an invasive practice that requires the surgical implant of epidural electrodes, but it has been recently demonstrated that non-invasive transcutaneous stimulation can activate locomotor circuits and also alleviate spasticity in people with incomplete SCI (Minassian et al., 2012; Hofstoetter et al., 2014, Hofstoetter et al., 2015). Transcutaneous stimulation of non-injured persons effectively induces robust locomotor behaviour when applied in a multi-site approach (Gerasimenko et al., 2015). It may be used to selectively activate specific motor pools to produce modulatory effects that depend on the characteristics of the stimulation protocol (Sayenko et al., 2015). For instance, it seems that a way to

fine-tune locomotor networks is to control timing of stimulation onset among multiple spinal electrodes (Shah et al., 2016).

In conclusion, electrical stimulation of the lumbar spinal cord may be a valid tool for improving ambulation in SCI persons. Despite advancements in the hardware technology, the current protocols have been slightly changed since their introduction and consist of stereotyped trains of rectangular pulses.

Consequently, there is an urgent need to focus on innovative and more effective stimulating protocols to better facilitate spinal CPGs post lesion.

Combined strategies help to facilitate the CPG circuits.

In the last few years, much evidence has spread the firm conviction that therapy for the recovery of locomotion after SCI requires a combined neurorehabilitative approach (Edgerton et al., 2006).

Although electrical stimulation can induce stepping movements in the absence of supraspinal control, it is difficult to attain a weight-bearing step using only electrical stimulation. Pharmacological substances can provide a modulatory drive to the locomotor CPG.

In this regard, different types of chemicals—such as the 5HT receptor agonist, quipazine (Gerasimenko et al., 2007); the dopamine precursor, L-DOPA (Guertin, 2004b); and the alpha-2 agonists, clonidine (Côté et al., 2003)—facilitate the recovery of locomotion in spinalized animals.

The combination of electrical stimulation and pharmacology induces a certain degree of locomotor recovery in rodents (Chau et al., 1998b; Gerasimenko et al.,

2007; Courtine et al., 2009; Van den Brand et al., 2012), putatively by replacing the excitatory drive lost after SCI, mimicking the action of neuromodulators on spinal locomotor circuits.

Among these, an important role in the facilitation of locomotion in the presence of epidural stimulation is played by the serotonergic system (Gerasimenko et al., 2009). Recently, a new drug combination (Guertin et al., 2010) has been tested for its safety in humans (Guertin and Brochu, 2009; Rouleau and Guertin, 2011). However, this drug combination has not been used conjointly with electrical stimulation and further investigation is required. Besides the few therapeutics now under investigation, it is compelling to find new and more specific substances that selectively target distinct elements of the CPG to sustain the locomotor program when triggered by the best protocols of spinal-cord electrical stimulation.

Aims

In the attempt to improve the efficiency of stimulating protocols for the recovery of locomotion, an innovative protocol of electrical stimulation has recently been suggested that is called fictive locomotion *induced* stimulation (FL*i*stim). It consists in an intrinsically variable noisy waveform that is sampled from VRs during fictive locomotion (Taccola, 2011). FL*i*stim has been shown to be able to produce a longer-lasting episode of rhythmically alternated oscillations than that produced by the classical train of rectangular pulses (Taccola, 2011).

a) This thesis aims to determine the features that make the noisy waveforms optimally effective in activating the CPG. To answer this question, I have employed two approaches:

- The first approach is to compare the appearance of FL patterns in response to different noisy stimulating waveforms. To this purpose, EMG recordings from different limb muscles of neurologically intact volunteers, obtained during the execution of different rhythmic motor tasks, have provided a wide palette of noisy waveforms to be tested on *in vitro* spinal cords.
- The second approach is to reduce the complexity of the noisy waveform at the single motoneuronal level. To this end, I determined whether distinct groups of frequencies besides those contained in motoneuronal firing during FL can selectively activate locomotor CPG when simultaneously delivered as a multifrequency protocol.

b) Furthermore, to reach a better activation of the locomotor CPGs, I investigated whether new neurochemicals might be co-applied with the electrical stimulation of

DRs. In particular, the neuropeptide oxytocin, which has been proven to modulate neuronal networks, might further increase the efficacy of noisy waveforms in evoking locomotor patterns.

c) Lastly, I focused my research project on the multi-site electrical stimulation of the spinal cord. Thus, in an effort to develop more effective stimulating protocols, I explored the following issues:

- Whether staggered trains of pulses, delivered simultaneously to different DRs at the same frequency of stimulation, elicit episodes of FL.
- Whether multifrequency protocols are effective even if simultaneously delivered to two different DRs.

Materials, methods and results

See enclosed papers.

J Neurophysiol 108: 2977–2990, 2012.
First published September 5, 2012; doi:10.1152/jn.00554.2012.

Coapplication of noisy patterned electrical stimuli and NMDA plus serotonin facilitates fictive locomotion in the rat spinal cord

Francesco Dose[1,2] and Giuliano Taccola[1,2]

[1]*Neuroscience Area International School for Advanced Studies, Trieste, Italy; and* [2]*Spinal Person Injury Neurorehabilitation Applied Laboratory, Istituto di Medicina Fisica e Riabilitazione, Udine, Italy*

Submitted 25 June 2012; accepted in final form 3 September 2012

Dose F, Taccola G. Coapplication of noisy patterned electrical stimuli and NMDA plus serotonin facilitates fictive locomotion in the rat spinal cord. *J Neurophysiol* 108: 2977–2990, 2012. First published September 5, 2012; doi:10.1152/jn.00554.2012.—A new stimulating protocol [fictive locomotion-induced stimulation (FL*i*stim)], consisting of intrinsically variable weak waveforms applied to a single dorsal root is very effective (though not optimal as it eventually wanes away) in activating the locomotor program of the isolated rat spinal cord. The present study explored whether combination of FL*i*stim with low doses of pharmacological agents that raise network excitability might further improve the functional outcome, using this in vitro model. FL*i*stim was applied together with *N*-methyl-D-aspartate (NMDA) + serotonin, while fictive locomotion (FL) was electrophysiologically recorded from lumbar ventral roots. Superimposing FL*i*stim on FL evoked by these neurochemicals persistently accelerated locomotor-like cycles to a set periodicity and modulated cycle amplitude depending on FL*i*stim rate. Trains of stereotyped rectangular pulses failed to replicate this phenomenon. The $GABA_B$ agonist baclofen dose dependently inhibited, in a reversible fashion, FL evoked by either FL*i*stim or square pulses. Sustained episodes of FL emerged when FL*i*stim was delivered, at an intensity subthreshold for FL, in conjunction with subthreshold pharmacological stimulation. Such an effect was, however, not found when high potassium solution instead of NMDA + serotonin was used. These results suggest that the combined action of subthreshold FL*i*stim (e.g., via epidural stimulation) and neurochemicals should be tested in vivo to improve locomotor rehabilitation after injury. In fact, reactivation of spinal locomotor circuits by conventional electrical stimulation of afferent fibers is difficult, while pharmacological activation of spinal networks is clinically impracticable due to concurrent unwanted effects. We speculate that associating subthreshold chemical and electrical inputs might decrease side effects when attempting to evoke human locomotor patterns.

fictive locomotion; central pattern generator; dorsal root train; FL*i*stim

IN THE ISOLATED SPINAL CORD of the neonatal rat, episodes of locomotor-like oscillations can be recorded from lumbar (L) 2 and L5 ventral roots (VRs), alternating between the left and right sides of the cord, due to rhythmic activation of flexor and extensor motor pools, respectively (Kiehn and Kjaerulff 1996). This phenomenon is ascribed to the existence of a neuronal spinal network, named central pattern generator (CPG) that, following diverse stimuli (Cazalets et al. 1992; Lev-Tov et al. 2000), automatically triggers the locomotor program that can be recorded extracellularly from VRs and intracellularly from motoneurons and premotoneurons (Kiehn 2006).

Although experimental studies have indicated the possibility to activate the CPG using trains of square pulses applied to dorsal afferents (Marchetti et al. 2001a) or to the cauda equina (Blivis et al. 2007), to date it is impossible to evoke stable locomotion in humans by electrical stimulation of sensory afferents (Selinov et al. 2009). Epidural electrical stimulation associated with intense neurorehabilitation has recently produced encouraging clinical benefits in reactivating, albeit transiently, standing in persons with incomplete traumatic lesions of the spinal cord (Harkema et al. 2011). The lack of effectiveness of electrical stimulation can be attributed to the filtering effect of CPG interneurons receiving synaptic inputs from the spinal rhythm generator to gate the flow of sensory information in the spinal cord (Sillar 1991). Interestingly, a better outcome is observed when stimuli are applied close to the spinal cord region, which putatively contains the CPG (Kiehn and Butt 2003), using epidural (Lavrov et al. 2008a, 2008b) or intraspinal (Gaunt et al. 2006) electrodes.

In the attempt to better activate spinal locomotor circuits, studies on spinalized animals have proposed the association of electrical stimulation of the lumbo-sacral spinal cord to the systemic administration of substances that can activate CPG neurons (Musienko et al. 2011). Using just pharmacological agents to activate the CPG in humans requires, however, doses that are associated to strong collateral effects (Hollenberg 1988; Moreau et al. 1989). From this perspective, it would be more practical to refine the parameters of electrical stimulation, rather than to titrate the concentrations of pharmacological drugs, which possess complex pharmacokinetics and pharmacodynamics. Thus the design of new stimulating protocols, in parallel with a better understanding of the pharmacology of locomotor spinal circuits, might open up a broader repertoire of neurorehabilitative treatments to specifically restore motor functions following a severe spinal cord injury (Musienko et al. 2012).

An innovative protocol of electrical stimulation, named FL*i*stim (fictive locomotion-induced stimulation; Taccola 2011), has recently been shown to evoke locomotor-like activity in vitro. FL*i*stim is obtained by sampling, from one VR, noisy waveforms that previously appeared during fictive locomotion [FL; in the presence of *N*-methyl-D-aspartate (NMDA) plus serotonin] and delivering the recorded trace to one lumbar dorsal root (DR) or to the cauda equina of the in vitro spinal cord. The clear advantage of FL*i*stim relies on the stimulation strength that is much lower than the minimum one required to induce a reflex response. Compared with the classic protocols of electrical stimulation, which use trains of stereotyped rectangular impulses (Marchetti et al. 2001a), FL*i*stim, regardless of the main frequency of waveforms composing it, induces locomotor-like oscillations of longer duration and with a

Address for reprint requests and other correspondence: G. Taccola, IMFR, via Gervasutta 48, 33100 Udine, Italy (e-mail: taccola@sissa.it).

greater number of cycles (Taccola 2011). This makes of FL*i*stim a novel tool for the electrical activation of the locomotor CPG.

The present study aims at optimizing the effect of the new FL*i*stim protocol, through the joint application of pharmacological drugs, capable of activating the neurons of the locomotor CPG. Moreover, we have assessed whether a low-amplitude FL*i*stim could facilitate subthreshold concentrations of neurochemicals to trigger the emergence of a locomotor rhythm.

METHODS

Electrophysiological recordings. In accordance with the guidelines of the National Institutes of Health and the Italian Act Decreto Legislativo 27/1/92 n. 116 (implementing the European Community directives n. 86/609 and 93/88) and under the authorization of the Italian Ministry of Health, experiments were performed on spinal cord preparations after isolation from neonatal rats as previously reported (Taccola 2011). Although, in the first days after birth, maturation of locomotor networks occurs (Jamon and Clarac 1998; Clarac et al. 2004), for this study were used animals in the range of P0–P4, since, at this stage, the alternating pattern is characterized by stable timing (Kiehn and Kjaerulff 1996; Juvin et al. 2007) and, when electrically stimulating dorsal afferents, comparable effectiveness in activating the CPG is reported (Kiehn et al. 1992; Marchetti et al. 2001a). Since data from P0 and P4 did not differ in terms of FL*i*stim effects, results were pooled together.

All efforts were made to reduce the number of animals and their suffering. Each spinal cord (sectioned from the mid-thoracic region to the cauda equina) was mounted in a small recording chamber (maintained at constant room temperature, 22° C), which was continuously superfused (5 ml/min) with oxygenated (95%-O_2 5%-CO_2) Krebs solution of the following composition (in mM): 113 NaCl, 4.5 KCl, 1 $MgCl_2 7H_2O$, 2 $CaCl_2$, 1 $NaH_2PO_4^{3-}$, 25 $NaHCO_3$, and 11 glucose, pH 7.4. AC-coupled recordings (range 0.1–10,000 Hz) from lumbar VRs were obtained by using tight-fitting suction electrodes (Taccola 2011). In a few experiments, DC-coupled records were also acquired. As a routine, recordings were taken from L2 VRs, which primarily consist of axons from flexor motoneurons to hindlimb muscles, and from L5 VRs, which are primarily composed of axons driving extensor motoneurons of the same limbs (Kiehn and Kjaerulff 1996). The alternation of discharges between flexor and extensor motor pools and between left (l) and right (r) sides of the cord represents the hallmark of FL (Juvin et al. 2007).

Parameters of spinal network activities. FL rhythm (Cazalets et al. 1992) was induced by the continuous bath-application of NMDA (Tocris, Bristol, UK) plus serotonin [5-hydroxytryptamine (5-HT); Sigma, Milan, Italy].

In accordance with previous studies, the concentration of NMDA was selected in each experiment to produce a stable FL with typical periodicity (2–4 s; Bracci et al. 1998; Beato and Nistri 1999; Bertrand and Cazalets 1999; Pearlstein et al. 2005; Juvin et al. 2007). Usually, the concentration of NMDA was 3–6 μM with the expected acceleration of FL period for the larger dose (Kudo and Yamada 1987; Smith and Feldman 1988; Atsuta et al. 1991; Cazalets et al. 1992). This approach allowed us to select the most appropriate period of FL to be tested in experiments with FL*i*stim application as the goal was to explore how these electrical stimuli (of varying frequency) could modulate either slow or fast ongoing patterns. The same approach was used for the concentration of 5-HT (3–10 μM) that is typically added to the NMDA solution to stabilize the rhythm (Pearlstein et al. 2005). In this study, we considered as subthreshold a pharmacological stimulation based on half of the lowest concentration of NMDA + 5-HT capable of evoking a stable FL rhythm.

For each preparation, a VR recording was randomly chosen and, from it, at least 20 cycles of FL activity were analyzed for periodicity (defined as the time between the onset of two cycles of oscillatory activity) and amplitude (calculated as the voltage difference expressed in μV between the baseline at the beginning of each cycle and its peak). Variations in period and amplitude occurring during electrical stimulation are indicated as a percentage of prestimulus control conditions.

FL activity was also assessed based on its regularity, expressed by the coefficient of period variation (CV; displayed as standard deviation [SD] mean^{-1}). Correlation among signals arising from pairs of VRs was expressed by the cross-correlation function (CCF), obtained with Clampfit 10.1 software (Molecular Devices). While a CCF greater than +0.5 indicates that two roots are synchronous, a CCF less than −0.5 shows full alternation (Ryckebusch and Laurent 1994; Taccola et al. 2008).

Designing the FListim. FL*i*stim was always elicited by applying a reconstructed series of electrical pulses to a single DR as previously detailed (Taccola 2011). In our experiments, this type of stimulation was ineffective to evoke FL when applied to a VR, either L1 or from L4 to L7 of both sides ($n = 7$). The method of constructing the protocol for FL*i*stim started with AC-coupled recordings of FL induced by NMDA (4–6 μM) and 5-HT (10 μM) acquired (range 0.1 Hz - 10 000 Hz; sampling rate = 500 Hz) from VRs. Epochs (60 s or 30 s) of FL were promptly processed for off-line analysis (Clampfit 10.1 software; Molecular Devices) and randomly selected for use. Sampled traces were imported into an Origin 7.5 spreadsheet (OriginLab), where the *x*-axis comprised each sampling time for every epoch duration and the *y*-axis was used for the corresponding current amplitude. Through Origin software the amplitude of FL*i*stim was optimized to evoke a FL in each preparation. The optimal amplitude of FL*i*stim was in the range of 0.2–0.6 times the threshold, while larger intensities only induced a synchronous rhythm on all four VRs, which was time locked with the stimulating pattern (Taccola 2011).

The two columns of values were then exported (as an ASCII text file) to a multichannel stimulation device STG 4004 (Multi Channel Systems).

The stimulating protocol resulting from this procedure was termed FL*i*stim and was applied to one DR through a bipolar suction electrode, after the neurochemicals were washed off, to allow the preparation to return to baseline conditions.

In accordance with the previously described method (Taccola 2011), the experimental protocol used to generate FL with distinct electrical stimuli applied to a single DR is illustrated in Fig. 1*A*. In detail, AC-coupled recordings were first obtained from a stable FL rhythm induced by the coapplication of NMDA (5 μM) and 5-HT (10 μM; mean period of oscillations was 2.54 ± 0.36 s; CV = 0.14) and stored. After extensive washout (30 min) and return to control (Ctrl) conditions, a 60-s epoch from VRlL2 (shaded box) was digitized and converted into the electrical stimulation protocol FL*i*stim (see above), delivered to the DRrL5 of the same preparation. FL*i*stim, delivered at an amplitude of 0.53 times the threshold (Th, defined as the minimum intensity required to induce a reflex response using a single square pulse of duration = 0.1 ms), evoked a sustained episode of locomotor oscillations of 58.17 s duration with 25 oscillations (mean period of 2.43 ± 0.24 s; CV = 0.10; Fig. 1 *B*). In a random sample of 15 spinal cords, delivery of 60 s FL*i*stim (amplitude = 0.51 ± 0.31 Th) generated locomotor episodes with alternating oscillations of 2.59 ± 0.72 s mean period, i.e., faster than the ones induced in the same preparations by the application of NMDA (4–5 μM) + 5-HT (10 μM; 3.91 ± 0.90 s; $P < 0.001$, paired *t*-test).

To minimize the potential bias of conditioning network excitability by the initial application of NMDA and 5-HT so that effects induced by FL*i*stim would be greatly facilitated, alternating VR discharges elicited by the same dose of NMDA and 5-HT were recorded from one preparation and converted to FL*i*stim applied to a naïve preparation. This approach has demonstrated (see Taccola 2011) that the locomotor-like response elicited by FL*i*stim in the two experimental protocols was comparable in terms of number oscillations (15 ± 4 vs.

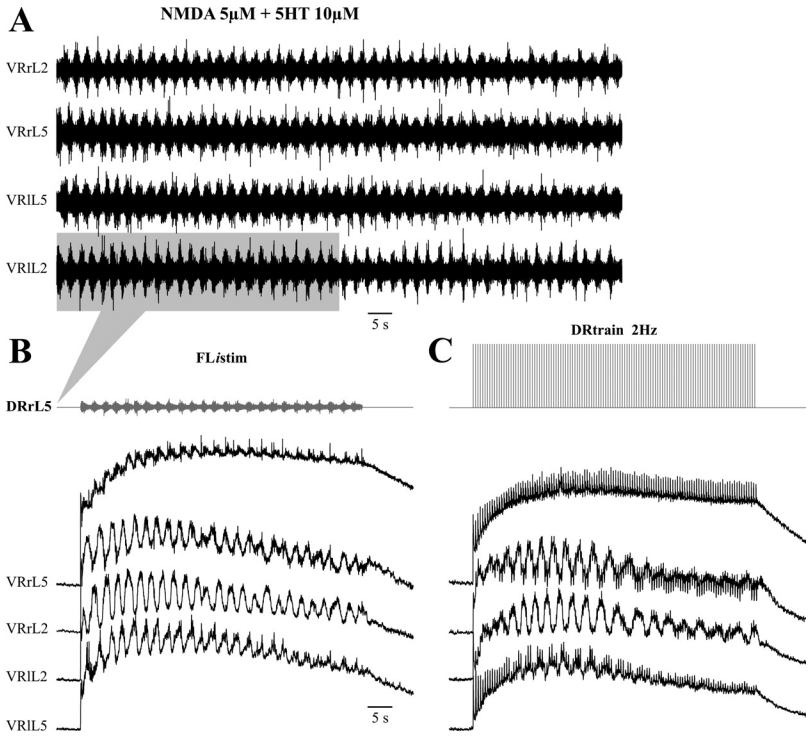

Fig. 1. *A*: stable fictive locomotion (FL) rhythm is recorded in AC mode in response to the application of *N*-methyl-D-aspartate (NMDA; 5 μM) and serotonin [5-hydroxytryptamine (5-HT); 10 μM]. A 60-s segment sampled from the trace recorded from the ventral root (VR)lL2 (shaded box) is imported in the programmable stimulator and delivered, at an intensity of 0.53 times the threshold (Th), to the right L5 dorsal root of the same preparation perfused in physiological solution (*B*). The episode of locomotor oscillations induced by fictive locomotion-induced stimulation (FL*i*stim) is compared in *C* to the one evoked by a traditional train of 2 Hz rectangular stimuli (DRtrain) at an amplitude of 1.5 times the Th. Note greater number of cycles in response to FL*i*stim.

19 ± 3; $P = 0.018$, Mann-Whitney rank sum test; $n = 7$); mean cycle period (2.44 ± 0.35 s vs. 2.73 ± 0.60 s; $P = 0.262$, Mann-Whitney rank sum test; $n = 7$); and regularity of oscillations (0.18 ± 0.03 vs. 0.21 ± 0.08; $P = 0.262$, Mann-Whitney rank sum test; $n = 7$).

The protocol of FL*i*stim is, therefore, different from the standard train of square pulses applied to a single DR as exemplified in Fig. 1*C* (Etlin et al. 2010; Dunbar et al. 2010; Marchetti et al. 2001a). In the latter case, the stimulus intensity was chosen to be slightly above Th as this is typically sufficient to induce FL (Etlin et al. 2010; Dunbar et al. 2010; Marchetti et al. 2001a). Figure 1*C* indicates that, on the same preparation, the response induced by a rectangular pulse train (DRtrain) at 2 Hz (amplitude = 1.5 Th) elicited a shorter episode of alternating oscillations, that lasted for 36.81 s, with only 13 cycles whose period and regularity (2.93 ± 0.54 s and CV = 0.19, respectively) were not different from those seen in response to FL*i*stim. Previous studies have demonstrated that even stronger DR square stimuli did not improve the length of FL (Atsuta et al. 1990; Delvolvé et al. 2001; Marchetti et al. 2001a).

Statistical analysis. Data are expressed as means (±SD), while *n* indicates the number of spinal cord preparations. After distinguishing between parametric or nonparametric data using a normality test, all parametric values were analyzed with Student's *t*-test (paired or unpaired) to compare two groups of data or ANOVA for more than two groups. For nonparametric values, Mann-Whitney test was used for two groups, while, for multiple comparisons, ANOVA on Ranks was first applied, followed by a post hoc test (Dunnett's method). Statistical analysis was performed using SigmaStat 3.5 software (Systat Software). Results were considered significant when $P < 0.05$.

RESULTS

Continuous delivery of FListim induced reproducible bouts of locomotor-like oscillations. To assess the reproducibility of the locomotor-like response elicited by FL*i*stim, in 10 experiments, FL*i*stims (average amplitude 0.39 ± 0.14 Th) were repetitively delivered to the same preparations at 5-min interval for a total of 175 min. As indicated in Fig. 2, *A* and *B*, in response to stimulation with FL*i*stim, stable episodes of FL were observed even after 175 min, preserving a similar number of cycles (93.6 ± 7.5% of Ctrl; $P = 0.630$, Kruskal-Wallis one way ANOVA on Ranks on raw data; $n = 10$), thus demonstrating that FL*i*stim could be used as a long-term routine protocol for activating the spinal CPG in a reproducible manner. On a set of preparations ($n = 7$), FL*i*stim that successfully evoked locomotor-like patterns when applied to a single DR, was then delivered to a lumbar VR and failed to produce any sustained epoch of FL.

Unlike standard trains of stimuli, FListim could modulate pharmacologically induced locomotor cycles. Figure 3*A* shows an example of FL induced by NMDA (5 μM) + 5-HT (10 μM) with oscillation period of 3.97 ± 0.27 s (CV = 0.07), during which the concurrent application of FL*i*stim (applied at 5 min intervals for a total of 175 min) increased rhythm frequency (mean period 2.78 ± 0.18 s) and cycle amplitude (averaged value 116.74% of Ctrl) with similar regularity (mean period CV = 0.07). This pattern was typically stable because the rhythm period at the start and after 110 min of uninterrupted FL was 2.94 ± 1.02 and 3.83 ± 0.49 s, respectively (paired *t*-test on raw data, $P = 0.117$; $n = 4$). Similarly, cycle amplitude remained unmodified (0.29 ± 0.15 and 0.25 ± 0.12 mV, respectively; paired *t*-test on raw data, $P = 0.217$; $n = 4$).

When delivering FL*i*stim in the presence of neurochemicals, the double alternation pattern (typical of locomotor-like oscillations as clearly shown on faster time-base in Fig. 3*B*) was accelerated (Fig. 3*A*). However, in the 60-s epoch following termination of each FL*i*stim, despite the continuous application of neurochemicals, the rhythm was transiently (30.94 ± 8.85 s) reduced in amplitude (averaged value 91.34% of Ctrl). Correspondingly, the rhythm was slowed down (mean period = 3.46 ± 0.28 s) towards preFL*i*stim values, while regularity remained similar (mean period CV = 0.08).

Histograms of Fig. 3*C* show that, on average taken from four VRs of either side of four spinal cords, FL*i*stim delivery

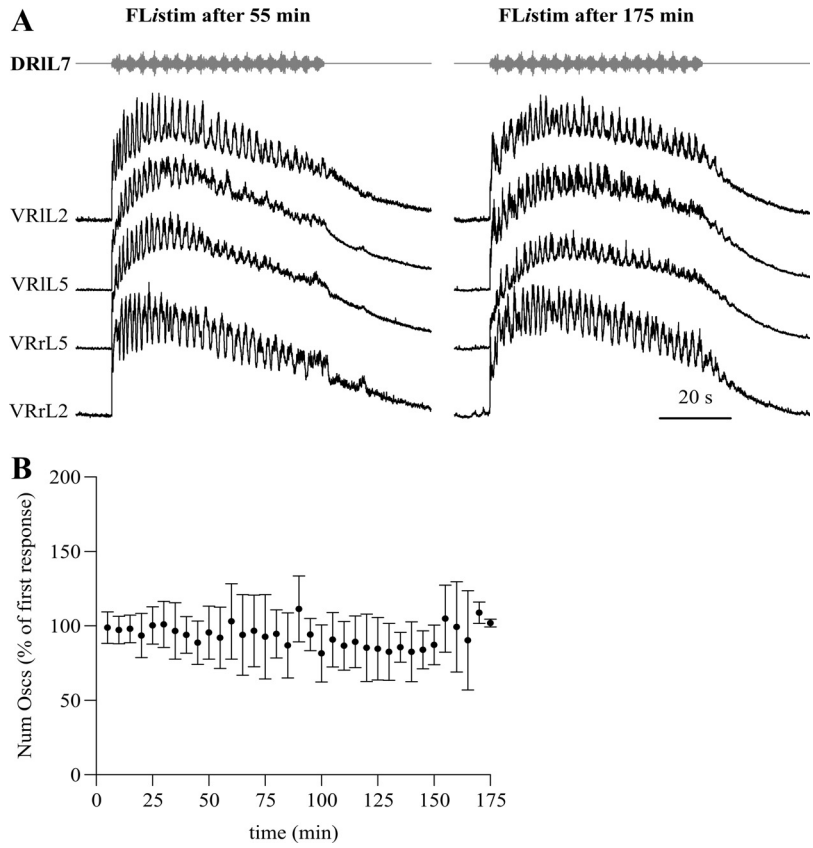

Fig. 2. *A*: series of FL*i*stims of an intensity of 0.2 times the Th are repeatedly delivered at 5-min intervals for a total time of 175 min. Motor responses induced after 55 min (*left*) are similar (in terms of duration of locomotor-like episode, number of cycles and cumulative depolarization) to the ones recorded in response to the same stimulus and in the same preparation at the 175th min (*right*). *B*: time course of mean number of oscillations elicited by delivery of FL*i*stims (expressed as percentage of the response evoked by the first FL*i*stim applied) is obtained from similar experiments ($n = 10$).

accelerated FL rhythm ($P = 0.005$, one-way ANOVA followed by Dunnett's method; $n = 4$), which returned to control when stimulation ceased, with unvaried regularity throughout all the different experimental phases (mean period CV in Ctrl = 0.17 ± 0.06, mean period CV during FL*i*stim = 0.12 ± 0.04, and mean period CV after FL*i*stim = 0.15 ± 0.05; $P = 0.630$, Kruskal-Wallis one-way ANOVA on ranks; $n = 4$). The average amplitude of oscillations regularly increased during each stimulation episode and returned to control after the end of stimulation, as indicated in Fig. 3*D* ($P = 0.029$, Mann-Whitney rank sum test; $n = 4$). Lack of FL fatigue was also confirmed by the observation that (in the continuous presence of NMDA and 5-HT) the period of FL oscillations evoked by the first FL*i*stim was similar to the value recorded at 110 min (3.41 ± 1.30 s vs. 3.01 ± 0.52 s, respectively; paired *t*-test on raw data, $P = 0.775$; $n = 4$). Likewise, cycle amplitude (0.28 ± 0.19 vs. 0.30 ± 0.14 mV; paired *t*-test on raw data, $P = 0.537$; $n = 4$) remained constant.

FL induced by NMDA plus 5-HT was modulated by FL*i*stim even when records had been sampled in DC mode (data not shown). Out of 10 preparations, delivery of FL*i*stim cycles sampled in DC-mode (Taccola 2011) with an average period of 4.09 ± 0.84 s evoked an increase in frequency and amplitude of locomotor oscillations induced by neurochemicals (period = 3.41 ± 0.92 s; amplitude = 132.89 ± 19.78% compared with Ctrl) similar to the one reported in response to stimulation with AC FL*i*stim. At the end of DC FL*i*stim, it was again observed a temporary reduction in period (4.13 ± 1.06 s; $P = 0.038$ vs. stimulation without FL*i*stim, Mann-Whitney rank sum test) and amplitude (94.12 ± 9.70% compared with Ctrl; $P < 0.001$ vs. stimulation with FL*i*stim, Mann-Whitney rank sum test on raw data).

Table 1 summarizes the average value of FL oscillation period by FL*i*stim (intensity of 0.4 Th) in standard solution, by NMDA (5 μM) + 5-HT (10 μM), and by the combination of electrical and chemical stimulation ($n = 17$). The period of oscillations induced by NMDA and 5-HT alone was significantly greater than the one obtained from the alternating oscillations evoked in standard solution by FL*i*stim or the one calculated from alternating cycles during the combined stimulation (respectively $P < 0.001$ and $P = 0.004$, one-way ANOVA followed by Tukey's test).

Comparing the effect of FListim or DRtrain on chemically induced FL. In another set of experiments, similar to the ones shown in Fig. 4*A*, during a stable pharmacologically evoked FL (period = 4.37 ± 0.31 s), DRtrain (frequency = 2 Hz, amplitude = 1.5 Th), or FL*i*stim (intensity of stimulation = 0.6 Th) were alternatively delivered to compare their differential effects. Figure 4*A* (and Fig. 4*B*, *inset*) shows that the DRtrain did not interfere with average FL cycle period (3.91 ± 0.21 s) induced by NMDA and 5-HT. Thus, even if a similar train of weak DR pulses could evoke per se FL, it could not modify the ongoing pattern elicited by neurochemicals. This observation accords with previous data demonstrating that electrical stimuli of an intensity at least double than the one used in the present experiments are necessary to modulate the FL (Kiehn et al. 1992; Taccola et al. 2010).

On the other hand, FL*i*stim of rather weak intensity sped up average FL cycles calculated for the whole stimulation epoch (period decreased to 2.93 ± 0.34 s).

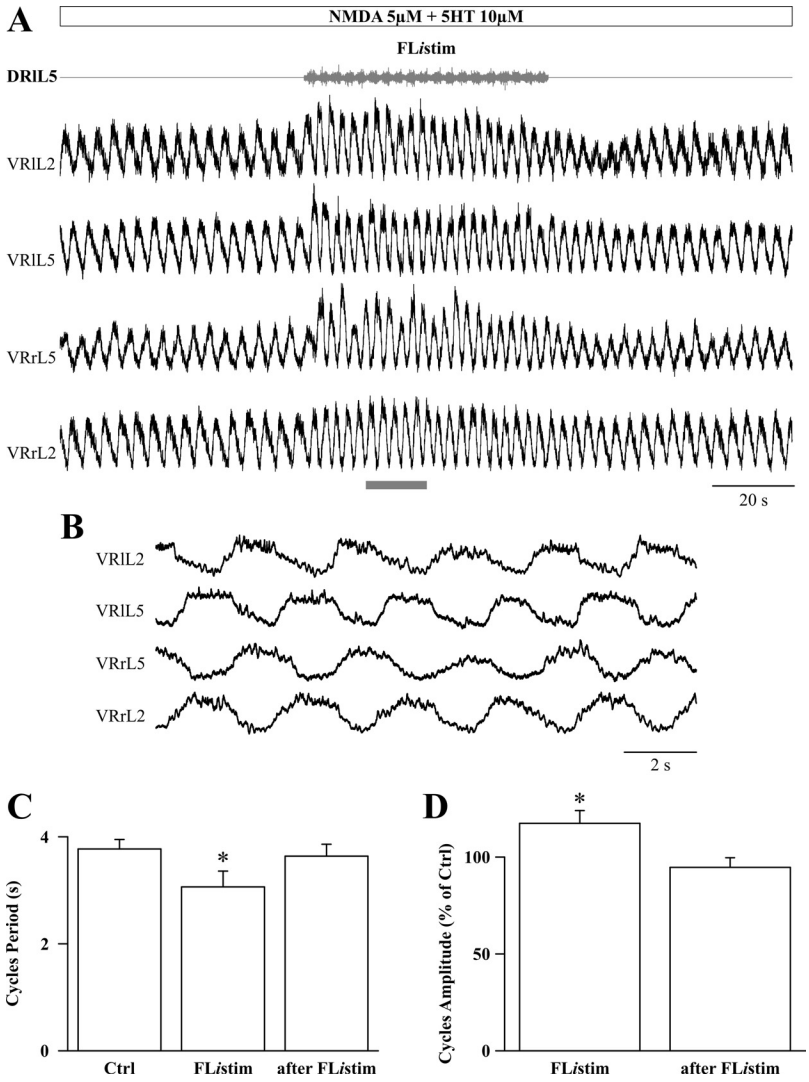

Fig. 3. *A*: during a stable FL rhythm induced by NMDA (5 μM) and 5-HT (10 μM), the corresponding delivery of FL*i*stim to DRlL5 at an intensity of 0.23 times the Th increases frequency and amplitude of cycles. *B*: a segment corresponding to the gray bar in *A* illustrates, on higher time base, the double alternation of locomotor oscillations recorded from the L2 and L5 ventral roots on both sides of the cord. Histograms in *C* and *D* report average values from the three stages of the experimental protocol, obtained from 4 experiments, in which period is expressed in s (*$P = 0.005$) and amplitude as a percentage value of control (Ctrl; *$P = 0.029$).

We also investigated if, during the continuous application of FL*i*stim, the coincidence of a stimulus with the peak or trough of the FL cycle could reset the periodicity of the subsequent oscillation: this is exemplified in Fig. 4*C* in which FL*i*stim pulses are shown in correspondence to FL cycles (indicated by circles) from three VRs. Thus, for an average of 6 preparations, the cycle period was 3.22 ± 1.30 or 3.08 ± 0.88 s when a FL*i*stim pulse coincided with either a trough or a peak ($P = 0.56$, Wilcoxon signed rank test). These data show that, on average, FL oscillations were accelerated by FL*i*stim but were not reset during persistent stimulation.

Table 1. *Summary of effects produced by neurochemicals, FListim, or their combination*

	Period (means ± SD)	*n*	Statistics
A: NMDA (5 μM) + 5-HT (10 μM)	4.01 ± 0.81 s	17	$P < 0.001$ for *A* vs. *B* $P = 0.004$ for *A* vs. *C*
B: FL*i*stim 0.4 Th	2.62 ± 0.93 s	17	$P < 0.001$ for *A* vs. *B* $P = 0.469$ for *B* vs. *C*
C: cumulative effect	2.98 ± 0.90 s	17	$P = 0.004$ for *A* vs. *C* $P = 0.469$ for *B* vs. *C*

NMDA, *N*-methyl-D-aspartate; 5-HT, 5-hydroxytryptamine; FL*i*stim, fictive locomotion-induced stimulation; Th, threshold. All 3 experimental conditions were tested on the same preparation. Statistic was performed by applying one-way ANOVA followed by all pairwise multiple comparison procedures (Tukey's test) for group pairs as indicated by *A*–*C*.

Histograms in Fig. 4*D* summarize the mean values collected from five spinal cords, demonstrating that the application of FL*i*stim (intensity of stimulation = 0.51 ± 0.12 Th) during chemically induced FL (unlike DRtrains) could significantly improve periodicity and amplitude of FL ($P = 0.008$, Mann-Whitney rank sum test).

Comparing the effect of FListim or DRtrain in the presence of baclofen. The $GABA_B$ receptor agonist baclofen is a potent inhibitor of excitatory synaptic transmission in the spinal cord by reducing release of glutamate from primary afferents and depressing network excitability (Nistri 1975; Curtis et al. 1981; Bertrand and Cazalets 1998, 1999). Thus we wondered whether baclofen might differentially affect FL evoked by FL*i*stim or square pulse trains applied to activate afferent fibers impinging upon the locomotor CPG. In fact, it has been demonstrated that baclofen slows down the chemically induced FL in the rat spinal cord (Bertrand and Cazalets 1998, 1999).

As depicted in Fig. 5, *A–D*, *left*, and *E*, baclofen (0.2–1 μM) dose dependently and reversibly disrupted FL induced by FL*i*stim (0.2 Th intensity) as cycle period increased with

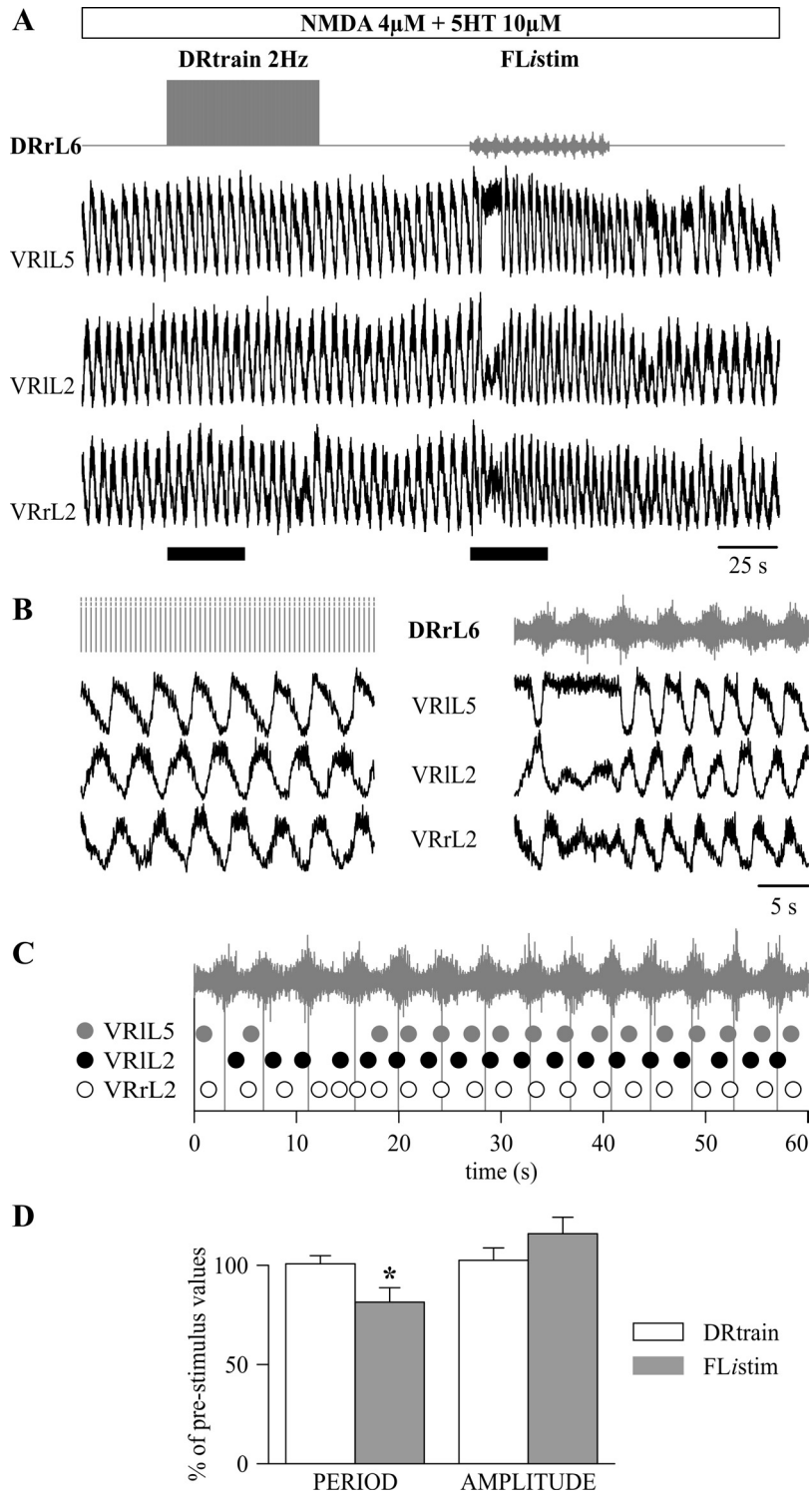

Fig. 4. *A*: during FL rhythm evoked by NMDA (5 μM) and 5-HT (10 μM), a standard train of 2 Hz rectangular stimuli at an intensity of 1.5 times the Th (DRtrain) or a FL*i*stim of an amplitude of 0.6 times the threshold are delivered to the right L6 dorsal root. Effect elicited by the two protocols on locomotor oscillations is depicted at a higher temporal resolution in the *insets* in *B*, corresponding to the black bars reported in the section above. In *C* is reported a schematic representation of the effect of FL*i*stim, as shown in *A* and *B*, *right*. No stable coincidence appears among the peaks of the stimulating noisy waveforms (vertical gray lines) and the peaks of FL oscillations recorded from the three VRs (gray, black and empty circles), demonstrating that FL*i*stim could not entrain the periodicity of FL cycles. Note the lack of gray circles occurring at the beginning of FL*i*stim delivery, corresponding to the deletions experienced by VRlL5. Histograms in *D* report the average percentage values (compared to prestimulus control, Ctrl) for period and amplitude obtained for each of the two different protocols delivered in sequence to the same preparations. It is noteworthy that FL*i*stim, as opposed to DRtrains, significantly reduces period of FL cycles (*P = 0.008; n = 5).

augmenting concentrations of baclofen (Fig. 5*D*), while the CV was unvaried (0.22 ± 0.07; n = 8). At the concentration of 5 μM (not shown), the locomotor-like response induced by FL*i*stim was replaced by synchronous discharges that reproduced the stimulating pattern.

The locomotor-like response induced by a square pulse DRtrain (Fig. 5, *A–D*, *right*) was also strongly (yet reversibly) inhibited with loss of alternating VR cycles at 1 μM baclofen (Fig. 5*D*, *right*). Figure 5*F* summarizes the mean period of oscillations for DRtrains applied at 1.5 Th intensity (n = 8).

Figure 5, *B–D*, shows that augmenting concentrations of baclofen delayed rhythm onset in a dose-dependent manner and that this effect was stronger during the DRtrain-triggered FL. In particular, for 0.2 μM baclofen, the initial pause was 7.14 ± 1.46 s with DRtrain and 3.85 ± 0.76 s with FL*i*stim. For 0.5 μM baclofen, the pause was 12.38 ± 0.13 s with DRtrain and 6.36 ± 1.59 s with FL*i*stim.

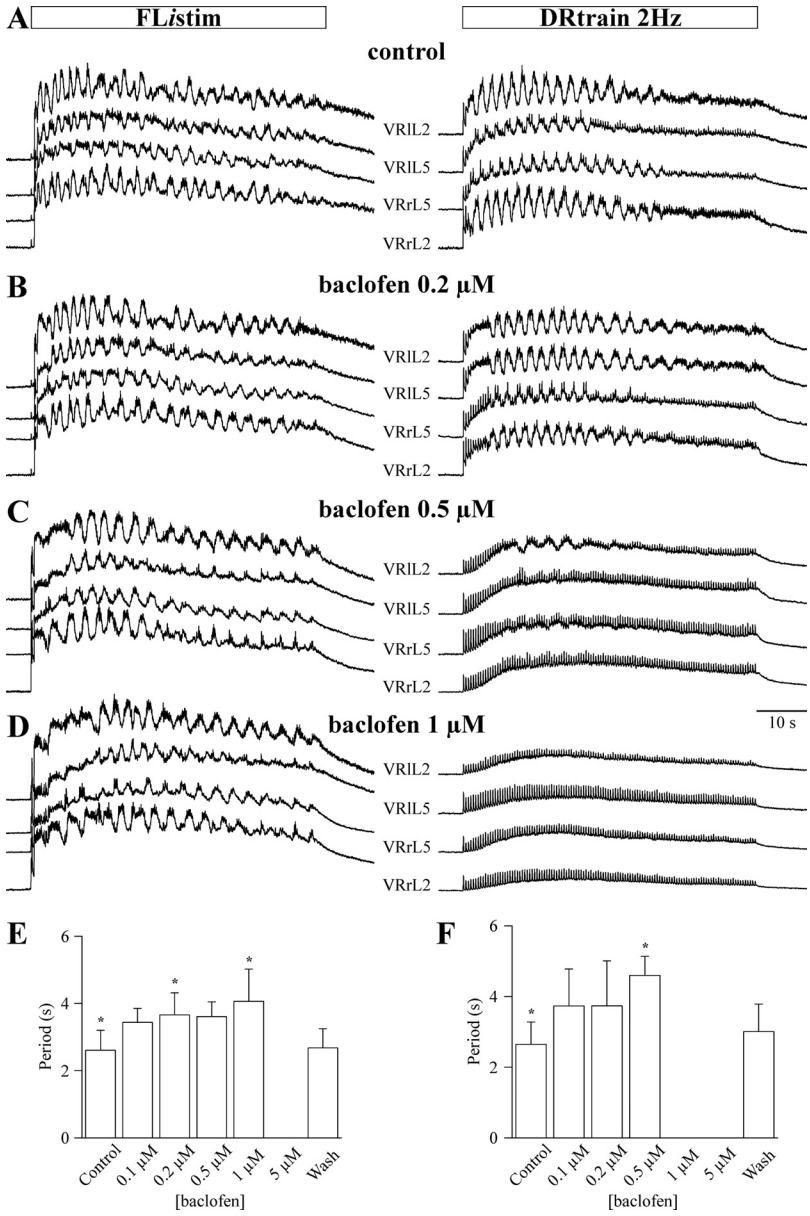

Fig. 5. Alternating oscillations, induced in control by the delivery of FL*i*stim (intensity = 0.2 Th; *A*, *left*) or DRtrain (intensity = 1.5 Th; *A*, *right*) to one DR, are reduced in number and appear to slow down at increasing concentrations of baclofen (0.2–1 μM; *B–D*). Nevertheless, while oscillations evoked by FListim persist even at a concentration of baclofen of 1 μM (*D*, *left*), the DRtrain induced cycles, at the same concentration, are completely abolished (*D*, *right*). Histograms represent the significant slow down in the average period of oscillations, evoked by FL*i*stim (*E*) and DRtrain (*F*) respectively, when increasing concentrations of baclofen until suppression of cycles (*left*: *P = 0,010; *right*: *P = 0,030, one-way ANOVA followed by Dunnett's method, n = 8). Note that the two protocols were delivered in sequence to the same DR on the same preparations.

Stereotypic acceleration of FL. To verify whether the accelerated average periodicity of FL oscillations observed during the combined pharmacological and FL*i*stim stimulation was related to the main periodicity of stimulating waveforms, experiments were performed in which FL*i*stims of different frequencies were repeatedly delivered to a stable FL, induced by application of NMDA (5 μM) + 5-HT (10 μM). FL*i*stims were obtained from a separate group of experiments by sampling FL traces in the presence of 10 μM of 5-HT plus increasing concentrations of NMDA (from 4 μM to 6 μM), thus providing stimulating protocols of different periodicity (5.10 ± 0.33 s for slow rate FL*i*stim; 4.14 ± 0.33 s for medium rate FL*i*stim; 3.33 ± 0.39 s for fast rate FL*i*stim).

Figure 6*A* shows an example in which, during FL induced by NMDA + 5-HT (period = 3.98 ± 0.30 s), all three different FL*i*stims decreased cycle period to a similar degree. In fact, in five preparations, the mean FL period induced by neurochemicals alone (4.27 ± 0.75 s) became 3.48 ± 0.79 s for slow rate FL*i*stim, 3.42 ± 0.75 s for medium rate FL*i*stim, and 3.69 ± 1.10 s for fast rate FL*i*stim (P = 0.946, Kruskal-Wallis one way ANOVA on Ranks on raw data; n = 5). Thus period acceleration evoked by FL*i*stim was apparently independent from stimulation periodicity.

Did the FL cycle amplitude depend upon the frequency of stimulation? It is known that neuronal output increases in response to stimulation with sinusoidal inputs close to the oscillation frequency of the networks (Leung and Yu 1998; van Brederode and Berger 2008; Haas et al. 2010). We wanted to clarify whether a resonance phenomenon might have occurred to account for the enhancement of cycle amplitude observed during the joint application of FL*i*stim plus NMDA + 5-HT.

Figure 7*A* depicts a FL induced by 3 μM NMDA + 10 μM 5-HT (period = 6.22 ± 0.63 s; period CV = 0.10) upon which fast rate FL*i*stim was superimposed. For the whole duration of application (60 s), cycle period dropped to 4.06 ± 0.43 s (CV = 0.11), while, compared with prestimulus values, cycle amplitude increased to 170%. On the same preparation, after wash-

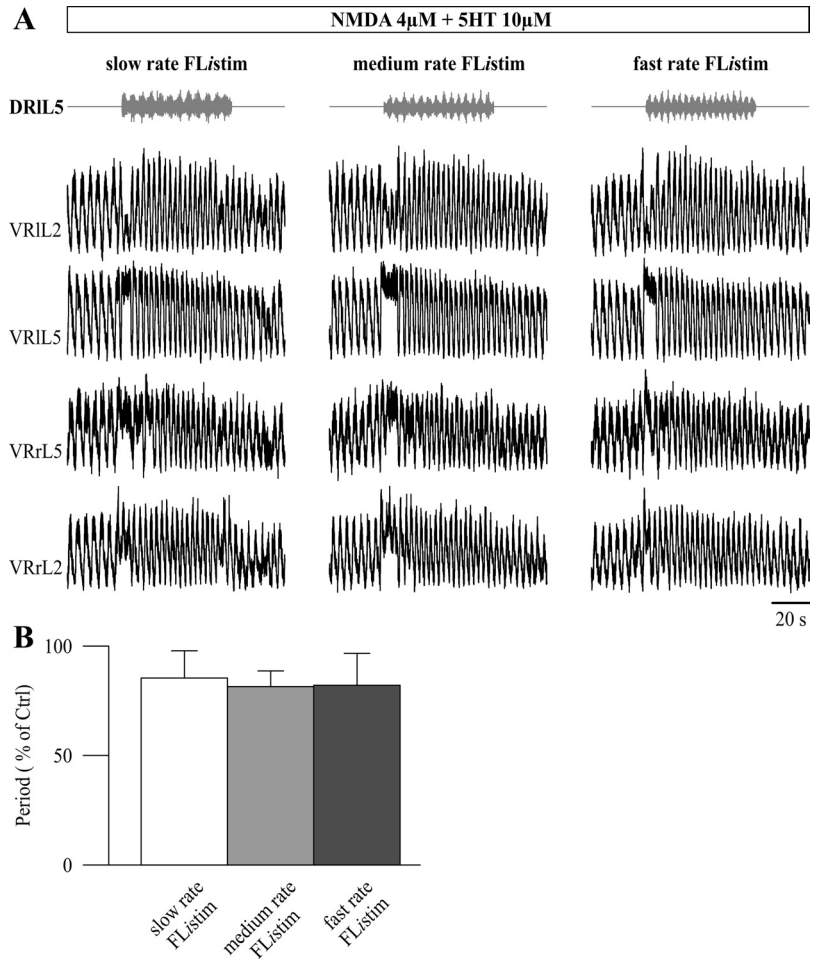

Fig. 6. Three FL*i*stims of equal intensity (0.5 times Th), but with different frequency (slow, medium, and fast rates), are obtained from a preparation perfused with increasing concentrations of NMDA (from 4 to 6 μM) and stable 5-HT (10 μM). In another experiment, the effect of the three protocols on FL oscillations induced by 5 μM NMDA and 10 μM 5-HT is demonstrated in *A* for the same spinal cord. The histogram in *B* summarizes the average percentage value of period with respect to the prestimulus interval (1 min, Ctrl) for each of the three FL*i*stims ($n = 5$).

out, concentration of NMDA was raised to 6 μM (keeping the 5-HT concentration at 10 μM) to induce a faster FL (period = 1.51 ± 0.13 s; CV 0.09). By stimulating with a slow rate FL*i*stim, locomotor oscillations were accelerated (period of 1.38 ± 0.19 s; CV 0.14), while cycle amplitude was reduced to a 61%.

In the graph of Fig. 7*C*, the percentage of locomotor cycle amplitude during delivery of FL*i*stim (compared with the prestimulus control phase) is plotted against the phase shift between locomotor output and stimulating input, calculated as the difference between the period of FL oscillations before stimulus and the main period of stimulating oscillations. The linear regression analysis obtained from the values collected from 21 spinal cords ($y = 8.93x + 116.51$; Pearson's $r = 0.57$; $n = 92$) showed that there exists a linear relationship, with a biphasic trend, between the increasing positive values of phase displacement of the two waveforms and the variations in cycle amplitude.

In fact, for positive phase shift values between the two waveforms (Fig. 7, *A* and *C*), which correspond to the situation in which the frequency of the afferent stimulating pattern is higher than the frequency of the rhythmic motor output recorded from VRs before FL*i*stim, a strengthened amplitude of locomotor-like cycles appears. Vice versa, for FL*i*stims slower than the frequency of prestimulus FL cycles (Fig. 7, *B* and *C*), a reduction in amplitude of oscillations was observed.

FListim and neurochemicals cooperate to bring locomotor CPG to threshold. We explored whether combined subthreshold stimuli of different nature, namely low concentrations of neurochemicals and weak FL*i*stim, could contribute to bring the CPG to threshold for triggering the locomotor program.

For this purpose, we first delivered a FL*i*stim of strength = 0.2 Th to elicit a long lasting locomotor episode (duration = 55.10 s) composed of 32 cycles of 1.78 ± 0.38 s period (data not shown). Thereafter, as shown in Fig. 8*A*, the same FL*i*stim was halved (0.1 Th) and evoked only sporadic events instead of stable alternating oscillations. Then, we applied NMDA + 5-HT at subthreshold concentrations (respectively, 2.5 and 5 μM), which induced noisier baseline activity unable to trigger FL (Fig. 8*B*, *left*). When the weak FL*i*stim was superimposed (but not so when using weak 2 Hz DRtrains; data not shown), FL emerged with period = 3.25 ± 0.09 s and CV period = 0.14 ± 0.06 (Fig. 8*B*, *right*, and traces on faster time scale in Fig. 8*C*). Correlograms (Fig. 8*D*) confirmed the double alternation among pairs of homolateral (upper; CCF = −0.755) and homosegmental (lower; CCF = −0.814) VRs.

This observation was replicated on nine spinal cords. In all tested cases, in the presence of subthreshold concentrations of neurochemicals, weak FL*i*stim (0.31 ± 0.18 Th), evoked locomotor-like oscillations (3.24 ± 1.05 s period) comparable to those detected in the same preparation in the presence of 5 μM NMDA and 10 μM 5-HT (2.80 ± 0.75 s; $P = 0.299$, paired *t*-test). In four of these preparations, low intensity (Th)

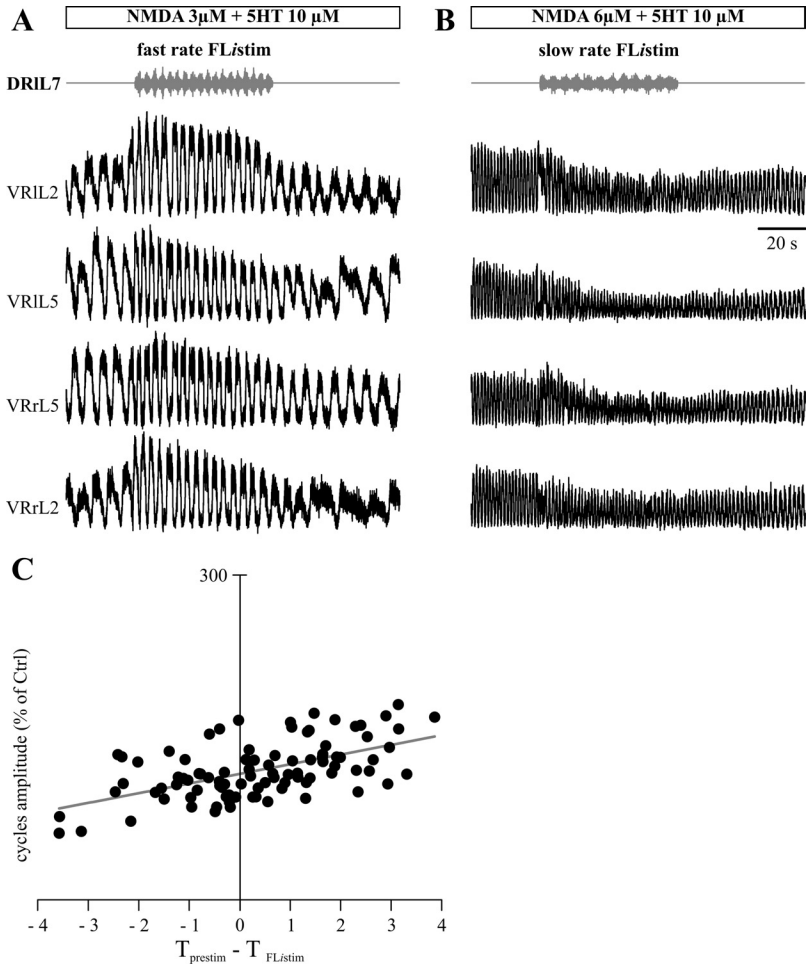

Fig. 7. *A*: during a slow FL induced by low concentrations of NMDA (3 μM) and standard concentrations of 5-HT (10 μM) in response to stimulation with a fast rate FL*i*stim (amplitude = 0.45 times the threshold), FL cycles are accelerated and increased in amplitude. On the contrary, in *B* is shown that during a fast FL induced by higher concentrations of NMDA (6 μM, while 5-HT concentrations remained at 10 μM), stimulation with a slow rate FL*i*stim of an amplitude identical to the FL*i*stim in *A*, reduces amplitude of oscillations. This biphasic trend, for different experiments, is represented by the slope of the regression line depicted in the plot in *C*, which represents on the *y*-axis the percentage amplitude of cycles during FL*i*stim, with respect to prestimulus values (Ctrl), and on the *x*-axis the phase displacement defined as the difference between FL period before stimulation ($T_{prestim}$) and the one owned by the stimulation wave ($T_{FListim}$).

DRtrains were also delivered, which, unlike FL*i*stim, did not facilitate emergence of FL.

Low intensity FListim delivered in the presence of higher extracellular potassium. We wondered whether increasing network excitability, by elevating extracellular potassium without reaching threshold for FL, could synergize with weak FL*i*stim to evoke a locomotor pattern. In control conditions, weak FL*i*stim (0.08 times Th) induced irregular discharges with no alternating oscillations (Fig. 9*A*), as indicated by the cross-correlation values reported in Fig. 9A_2 for a pair of L2 and L5 homolateral (CCF = −0.110) and homosegmental (CCF = −0.092) VRs. Subthreshold concentrations of NMDA (2 μM) and 5-HT (3 μM), together with the same weak FL*i*stim, elicited a stable FL with 16 ± 1 oscillations (period and CV were 3.49 ± 0.26 s and 0.07, respectively; Fig. 9*B*), alternating among pairs of L2 and L5 homolateral (CCF = −0.654) and homosegmental (CCF = −0.655) VRs (Fig. 9B_2).

While an increased K^+ concentration (6 mM) evoked only sporadic discharges (not shown), superimposed weak FL*i*stim elicited a short FL episode with 23 ± 8 cycles, of period and regularity of 1.85 ± 0.04 s and 0.02, respectively (Fig. 9*C*). These oscillations showed a modest alternating trend among pairs of L2 and L5 homolateral (CCF = −0.408) and homosegmental (CCF = −0.420) VRs, as indicated by the cross-correlogram in Fig. 9C_2. When the concentration of potassium was raised stepwise up to 11 mM, no alternating oscillations appeared in the presence of FL*i*stims of subthreshold intensity (n = 4).

DISCUSSION

The main outcome of this study is the demonstration that a new stimulation protocol, which uses a noisy waveform sampled from the motor output during FL (as opposed to a classic train of rectangular pulses), could potentiate the pharmacological stimulation of the CPG to facilitate FL. FL*i*stim regulated the oscillation amplitude in a biphasic manner, as the slowest noisy waveforms decreased the amplitude of VR cycles, while the higher frequency ones enhanced the oscillation size. FL*i*stim in association with subthreshold concentrations of NMDA and serotonin facilitated the emergence and duration of a locomotor rhythm. A similar effect was not observed in case of a generalized increase in spinal cord neuronal excitability, suggesting that, to optimally activate spinal locomotor circuits, it is necessary to combine a selective pharmacological stimulation of CPG elements with an electrical stimulation using a noisy waveform that corresponds to the locomotor pattern.

Delivery of FListim during FL rhythm modulates the properties of locomotor cycles. The fast periodicity of FL discharges has been traditionally ascribed to the variable number of neurons activated through the gradual recruitment of usually silent premotoneurons (Sillar and Roberts 1993; Grillner 2003). More recently, it has been proposed that the frequency

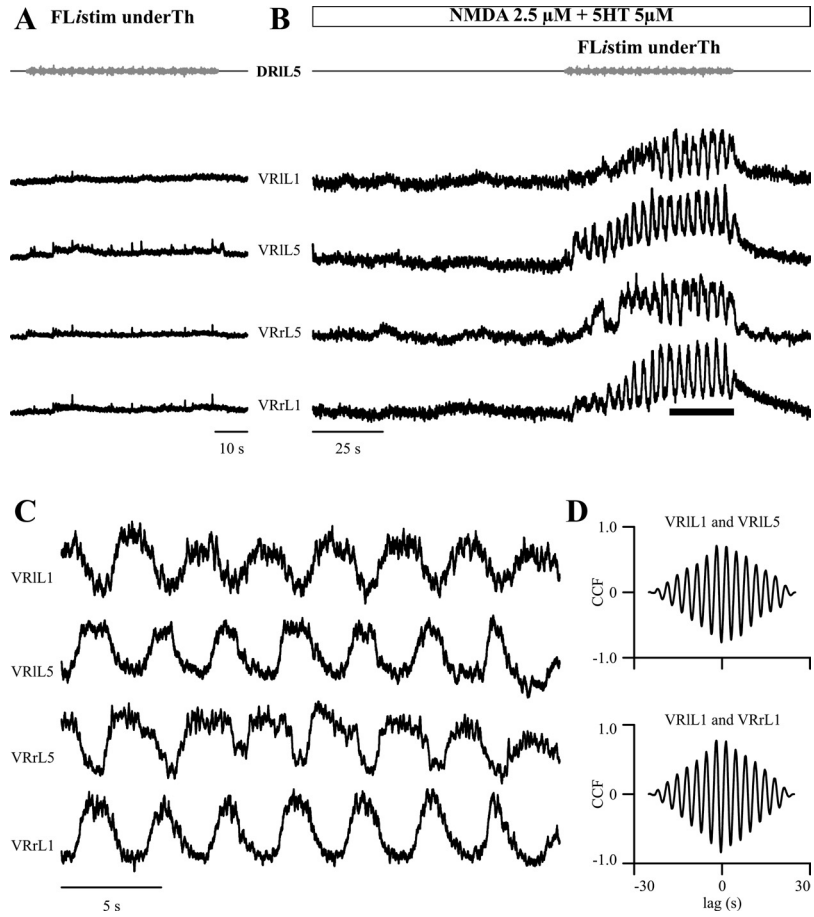

Fig. 8. *A*: in the presence of weak FL*i*stim (amplitude = 0.1 times the Th), alternating oscillations are replaced by a series of synchronous discharges. *B*: subsequent application of subthreshold concentrations of NMDA (2.5 μM) plus 5-HT (5 μM) generates only an increase in tonic activity. In the continuous presence of subthreshold concentrations of neurochemicals, the delivery of a weak FL*i*stim generates now a prolonged episode of locomotor-like oscillations, as highlighted, on a higher time scale, in *C*, *inset*, which corresponds to the gray bar in *B*. Cross-correlogram analysis (CCF) illustrated in *D* confirms the characteristic alternation of locomotor-like oscillations, derived from pairs of ventral roots.

of rhythmic oscillations is related to a selective switch from an interneuronal population activated at low speed to another group of interneurons that respond only to higher speeds and that seem to be anatomically and genetically distinct from the first ones (Crone et al. 2009; Fetcho and McLean 2010). During locomotor performance, recruitment of V2a interneurons, essential for the alternation between right and left limbs, has been suggested to be dependent on the frequency of the rhythmic synaptic drive from the CPG. At high frequencies, a neuronal subpopulation (normally silent at rest) is selectively added to maintain coordination between the left and right sides during accelerations (Zhong et al. 2011).

Notwithstanding the fact that the detailed topography of neurons recruited during stimulation with FL*i*stim remains to be explored, the increase in cycle amplitude due to stimulation with higher frequencies may correspond to the involvement of a larger number of motoneurons, as a previous study has reported a relation between number of motoneurons and cycle amplitude (Mazzone et al. 2010). On the other hand, the larger cycle amplitude due to stimulation with high frequency waveforms might also be determined by the recruitment of an additional pool of motoneurons within the same segment. In fact, homologous motoneurons possessing distinct intrinsic membrane properties and synaptic drive can contribute to stronger oscillations (Gabriel et al. 2011). We can also suppose that the involvement of a wider population of premotoneurons, selectively recruited by FL*i*stim, could better synchronize motoneurons, with the result of increasing the amplitude of each cycle. It is noteworthy that pharmacological block of spinal inhibition elicits synchronous discharges recorded from all VRs and, at the same time, determines an increase in amplitude of single rhythmic events (Beato and Nistri 1999).

FListim compared with standard protocols of electrical stimulation. In the present study, by comparing the effect of classic stimulation and FL*i*stim, both of them sequentially applied to the same DR, it emerged as clearly shown in Fig. 4 that only this latter one could modify the properties of alternated cycles. This fact suggests that the mechanisms that render FL*i*stim capable of generating locomotor oscillations may be different from those induced by stereotyped rectangular stimuli. One possibility comes from the high intrinsic signal variability contained in FL*i*stim, which corresponds to the high sampling frequency of a FL trace (500 Hz) and may determine a profile of transmitter release to CPG elements that is different from the one induced by a traditional train of 2-Hz impulses.

FL epochs evoked by either electrical stimulation protocols inevitably decayed, although they lasted longer with FL*i*stim. By associating FL*i*stim with subthreshold concentrations of neurochemicals, it was possible to significantly prolong the episode of locomotor oscillations. Conversely, in the presence of the same subthreshold concentration of neurochemicals, a classical DRtrain was far less effective in evoking FL cycles. These results suggest that the causes of termination of FL induced by FL*i*stim in control conditions could be compensated, at least in part, by the pharmacological activation of the CPG.

Previous studies have reported that repeated VR stimuli can trigger FL in the mouse spinal cord (O'Donovan et al. 2010).

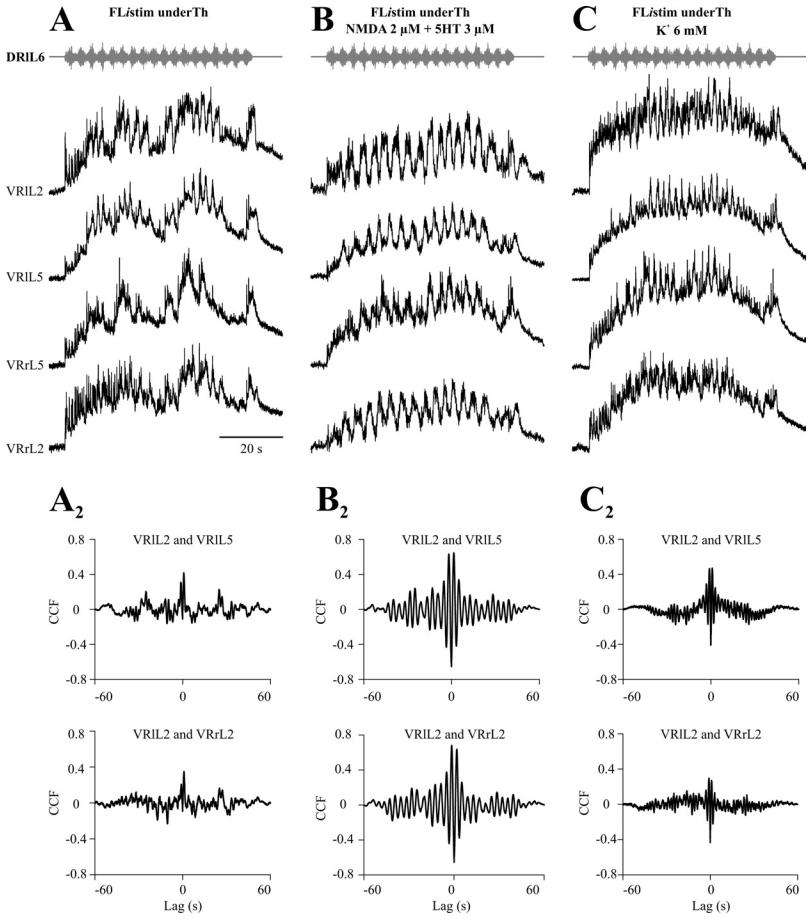

Fig. 9. *A*: FL*i*stim of low intensity (0.08 times to threshold, Th) induces cumulative depolarization with superimposed sporadic discharges, predominantly synchronous on all VRs. *B*: when weak FL*i*stim is applied in the presence of subthreshold concentration of NMDA (2 μM) and 5-HT (3 μM), a stable episode of locomotor-like oscillations appears. The same stimulating protocol, when delivered in high K^+ (6 mM; *C*) solution, elicits stronger cumulative depolarization, with uncorrelated discharges mingled with brief episodes of alternating fast oscillations. A_2–C_2: values of the correlation analysis among pairs of homolateral (*top*) and homosegmental (*bottom*) VRs during the delivery of FL*i*stim each one of the experimental conditions indicated in *A*–*C*, *bottom*.

When FL*i*stim was applied to a single VR, no FL was observed. This result suggests that the antidromic pathways activated by FL*i*stim could not readily access the locomotor CPG that needs to be stimulated by stronger electrical pulses (Mentis et al. 2005) than the ones used in the present investigation. This notion accords with the demonstration that inhibitory Renshaw cells activate different postsynaptic receptors on motoneurons, depending on the stimulation frequency (McCrea et al. 1980; Lamotte d'Incamps and Ascher 2008). As one aim of the current report was to identify patterns of stimulation with minimal deleterious effects and with sustained efficiency on the locomotor CPG, it seemed desirable to carry further experiments with weak intensity FL*i*stim applied to a single DR.

Baclofen differently affects alternating rhythms evoked by FListim or DRtrain. Baclofen, by acting on pre- and postsynaptic metabotropic $GABA_B$ receptors, depresses synaptic transmission (Nistri 1975; Curtis et al. 1981) and neuronal network activity (Brockhaus and Ballanyi 1998; Brown et al. 2007). In this study we demonstrated that increasing concentrations of baclofen augmented, in a dose-dependent manner, the period of electrically-induced locomotor cycles and reduced the number of oscillations up to a complete suppression for higher concentrations of this drug. An analogous depressing effect of baclofen on the locomotor patterns evoked through direct activation of CPG by neurochemicals has been reported (Bertrand and Cazalets 1998, 1999). The effect of baclofen has been ascribed to the activation of $GABA_B$ receptors that slow down the timing of the motor pattern (due to their direct action on the network) and also inhibit presynaptically the CPG output, with a minor direct effect on motoneurons (Cazalets et al. 1998). In our experiments, the electrically induced locomotor rhythm appeared sensitive to even lower concentrations of baclofen than the ones reported to suppress the chemical FL (Bertrand and Cazalets 1998, 1999). In fact, when the CPG was activated through electrical stimulation of a DR, the well-known reduction of glutamate release from primary afferents (Nistri 1975; Curtis et al. 1981) was likely additive to the effects of baclofen listed above.

The present data showed a differential sensitivity of FL to baclofen depending on the protocol of electrical stimulation. In fact, although significantly slower, the locomotor-like oscillations elicited by FL*i*stim could still be recorded at concentrations of baclofen that, conversely, abolished FL elicited by stimulation with standard square pulse trains. It should be noted that the different stimulus strength used in the two protocols presumably recruited a different set of afferent fibers (Koga et al. 2005) with distinct sensitivity to baclofen (Ataka et al. 2000; Yang et al. 2001) due to dishomogeneity of $GABA_B$ receptor expression (Price et al. 1984) or subunit composition (Bonanno and Raiteri 1993).

Conjoint pharmacological and electrical stimulation facilitates CPG activity. The contrasting ability of FL*i*stim applied to a single DR to modulate FL evoked by NMDA and 5-HT, whereas standard square pulses delivered to the same DR could not do so, clearly indicated that FL*i*stim was the protocol of choice to influence the activity of the locomotor CPG. Thus it

was important to consider how pharmacological agents and FL*i*stim could summate to facilitate locomotor-like patterns.

Previous studies have demonstrated that catecholamines prolong the locomotor response induced by tonic epidural electrical stimulation in the spinalized rat (Musienko et al. 2011). This in vivo effect is proposed (Musienko et al. 2012) to arise from the combination of the direct electrical stimulation of spinal circuits, to replace the lost excitatory drive, with the pharmacological agents that would mimic the modulatory action of monoaminergic systems on spinal networks (Conway et al. 1988). In the present experiments, FL*i*stim, in combination with agonists of the glutamatergic and serotoninergic systems, cooperated in facilitating FL rhythm, further validating the close analogy between in vivo observations and in vitro data. In fact, FL*i*stim increased the frequency of stable locomotor oscillations induced by NMDA + 5-HT, a result reminiscent of the better functional outcome of the association of pharmacological and electrical stimuli in the spinal rat (Ichiyama et al. 2008).

The role of neuromodulators may consist in the activation of extrasynaptic serotoninergic receptors (Smeets and González 2000) that positively modulate synaptic inputs (triggered by electrical stimulation) to crucial CPG elements (Hinckley et al. 2010). In support of this notion, it has been shown that epidural spinal cord stimulation recruits the serotoninergic system (Song et al. 2009, 2011) that plays a pivotal role in modulating the activity of locomotor networks (Zhong et al. 2006; Dunbar et al. 2010).

The present data provide the demonstration that stimulation with combined subthreshold electrical and pharmacological stimuli cooperated in activating the in vitro locomotor pattern. Widespread activation of spinal neurons with a high potassium solution did not produce a comparable effect. Although discrete increases in extracellular potassium are likely to trigger FL episodes induced by dorsal afferent stimulation (Marchetti et al. 2001b), it is difficult to activate the CPG by increasing extracellular potassium, as the effective concentration window is very narrow (Bracci et al. 1998). Thus a broad increase in spinal cord excitability evoked by high potassium was not per se sufficient to synergize the effect of a weak FL*i*stim.

The neurochemicals employed in this experimental study to activate the CPG evoke severe central and systemic collateral effects (Hollenberg 1988; Moreau et al. 1989). Nevertheless, the discovery of new drug combinations that can selectively act on the CPG (Guertin et al. 2010), along with the development of innovative systems for a more localized drug delivery (Kang et al. 2009) or with new substrates for the controlled release of neuroactive chemicals directly at the level of the spinal subarachnoid space (Cobacho et al. 2009), may help targeting pharmacological agents to modulate the activity of spinal circuits. Hence, the present study suggests that conjoint electrical stimulation using weak noisy waves with even subthreshold concentrations of neurochemicals may actually be a desirable process to pharmacologically manipulate CPG excitability to restore functional benefits to persons with a spinal cord injury.

ACKNOWLEDGMENTS

We are grateful to Andrea Nistri and Dr. Elisa Ius for the excellent assistance in preparing the manuscript.

GRANTS

This work was supported by a grant from the Friuli Venezia Giulia Region, VERTICAL foundation (Rome), FAIP Federazione delle Associazioni Italiane Para-Tetraplegici (Rome), Messina Line (Genova), and Associazione Tetra-Paraplegici FVG (Udine).

DISCLOSURES

No conflicts of interest, financial or otherwise, are declared by the author(s).

AUTHOR CONTRIBUTIONS

Author contributions: F.D. and G.T. performed experiments; F.D. and G.T. analyzed data; F.D. and G.T. interpreted results of experiments; F.D. and G.T. approved final version of manuscript; G.T. conception and design of research; G.T. prepared figures; G.T. drafted manuscript; G.T. edited and revised manuscript.

REFERENCES

Ataka T, Kumamoto E, Shimoji K, Yoshimura M. Baclofen inhibits more effectively C-afferent than δ-afferent glutamatergic transmission in substantia gelatinosa neurons of adult rat spinal cord slices. *Pain* 86: 273–282, 2000.

Atsuta Y, Garcia-Rill E, Skinner RD. Characteristics of electrically induced locomotion in rat in vitro brain stem-spinal cord preparation. *J Neurophysiol* 64: 727–735, 1990.

Atsuta Y, Abraham P, Iwahara T, Garcia-Rill E, Skinner RD. Control of locomotion in vitro: II. Chemical stimulation. *Somatosens Mot Res* 8: 55–63, 1991.

Beato M, Nistri A. Interaction between disinhibited bursting and fictive locomotor patterns in the rat isolated spinal cord. *J Neurophysiol* 82: 2029–2038, 1999.

Bertrand S, Cazalets JR. $GABA_A$ and $GABA_B$ modulations of synaptic transmission between L1–L2 locomotor network and the motoneurons in the newborn rat isolated spinal cord. *Ann NY Acad Sci* 860: 470–471, 1998.

Bertrand S, Cazalets JR. Presynaptic GABAergic control of the locomotor drive in the isolated spinal cord of neonatal rats. *Eur J Neurosci* 11: 583–592, 1999.

Blivis D, Mentis GZ, O'Donovan MJ, Lev-Tov A. Differential effects of opioids on sacrocaudal afferent pathways and central pattern generators in the neonatal rat spinal cord. *J Neurophysiol* 97: 2875–2886, 2007.

Bonanno G, Raiteri M. Multiple $GABA_B$ receptors. *Trends Pharmacol Sci* 14: 259–261, 1993.

Bracci E, Beato M, Nistri A. Extracellular K^+ induces locomotor-like patterns in the rat spinal cord in vitro: comparison with NMDA or 5-HT induced activity. *J Neurophysiol* 79: 2643–2652, 1998.

Brockhaus J, Ballanyi K. Synaptic inhibition in the isolated respiratory network of neonatal rats. *Eur J Neurosci* 10: 3823–3839, 1998.

Brown JT, Davies CH, Randall AD. Synaptic activation of $GABA_B$ receptors regulates neuronal network activity and entrainment. *Eur J Neurosci* 25: 2982–2990, 2007.

Cazalets JR, Sqalli-Houssaini Y, Clarac F. Activation of the central pattern generators for locomotion by serotonin and excitatory amino acids in neonatal rat. *J Physiol* 455: 187–204, 1992.

Cazalets JR, Bertrand S, Sqalli-Houssaini Y, Clarac F. GABAergic control of spinal locomotor networks in the neonatal rat. *Ann NY Acad Sci* 860: 168–180, 1998.

Clarac F, Brocard F, Vinay L. The maturation of locomotor networks. *Prog Brain Res* 143: 57–66, 2004.

Cobacho N, Serano AB, Casarejos MJ, Mena MA, Paíno CL. Use of transduced adipose tissue stromal cells as biologic minipumps to deliver levodopa for the treatment of neuropathic pain: possibilities and limitations. *Cell Transplant* 18: 1341–1358, 2009.

Conway BA, Hultborn H, Kiehn O, Mintz I. Plateau potentials in alpha-motoneurones induced by intravenous injection of L-dopa and clonidine in the spinal cat. *J Physiol* 405: 369–384, 1988.

Crone SA, Zhong G, Harris-Warrick R, Sharma K. In mice lacking V2a interneurons, gait depends on speed of locomotion. *J Neurosci* 29: 7098–7109, 2009.

Curtis DR, Lodge D, Bornstein JC, Peet MJ. Selective effects of (–)-baclofen on spinal synaptic transmission in the cat. *Exp Brain Res* 42: 158–170, 1981.

Delvolvé I, Gabbay H, Lev-Tov A. The motor output and behavior produced by rhythmogenic sacrocaudal networks in spinal cords of neonatal rats. *J Neurophysiol* 85: 2100–2110, 2001.

Dunbar MJ, Tran MA, Whelan PJ. Endogenous extracellular serotonin modulates the spinal locomotor network of the neonatal mouse. *J Physiol* 588: 139–156, 2010.

Etlin A, Blivis D, Ben-Zwi M, Lev-Tov A. Long and short multifunicular projections of sacral neurons are activated by sensory input to produce locomotor activity in the absence of supraspinal control. *J Neurosci* 30: 10324–10336, 2010.

Fetcho JR, McLean DL. Some principles of organization of spinal neurons underlying locomotion in zebrafish and their implications. *Ann NY Acad Sci* 1198: 94–104, 2010.

Gabriel JP, Ausborn J, Ampatzis K, Mahmood R, Eklöf-Ljunggren E, El Manira A. Principles governing recruitment of motoneurons during swimming in zebrafish. *Nat Neurosci* 14: 93–99, 2011.

Gaunt RA, Prochazka A, Mushahwar VK, Guevremont L, Ellaway PH. Intraspinal microstimulation excites multisegmental sensory afferents at lower stimulus levels than local alpha-motoneuron responses. *J Neurophysiol* 96: 2995–3005, 2006.

Grillner S. The motor infrastructure: from ion channels to neuronal networks. *Nat Rev Neurosci* 4: 573–586, 2003.

Guertin PA, Ung RV, Rouleau P. Oral administration of a tri-therapy for central pattern generator activation in paraplegic mice: proof-of-concept of efficacy. *Biotechnol J* 5: 421–426, 2010.

Haas JS, Kreuz T, Torcini A, Politi A, Abarbanel HD. Rate maintenance and resonance in the entorhinal cortex. *Eur J Neurosci* 32: 1930–1939, 2010.

Harkema S, Gerasimenko Y, Hodes J, Burdick J, Angeli C, Chen Y, Ferreira C, Willhite A, Rejc E, Grossman RG, Edgerton VR. Effect of epidural stimulation of the lumbosacral spinal cord on voluntary movement, standing, and assisted stepping after motor complete paraplegia: a case study. *Lancet* 377: 1938–1947, 2011.

Hinckley CA, Wiesner EP, Mentis GZ, Titus DJ, Ziskind-Conhaim L. Sensory modulation of locomotor-like membrane oscillations in Hb9-expressing interneurons. *J Neurophysiol* 103: 3407–3423, 2010.

Hollenberg N. Serotonin, atherosclerosis, and collateral vessel spasm. *Am J Hypertens* 1: 312S–316S, 1988.

Ichiyama RM, Gerasimenko Y, Jindrich DL, Zhong H, Roy RR, Edgerton VR. Dose dependence of the 5-HT agonist quipazine in facilitating spinal stepping in the rat with epidural stimulation. *Neurosci Lett* 438: 281–285, 2008.

Jamon M, Clarac F. Early walking in the neonatal rat: a kinematic study. *Behav Neurosci* 112: 1218–1228, 1998.

Juvin L, Simmers J, Morin D. Locomotor rhythmogenesis in the isolated rat spinal cord: a phase-coupled set of symmetrical flexion extension oscillators. *J Physiol* 583: 115–128, 2007.

Kang CE, Poon PC, Tator CH, Shoichet MS. A new paradigm for local and sustained release of therapeutic molecules to the injured spinal cord for neuroprotection and tissue repair. *Tissue Eng Part A* 15: 595–604, 2009.

Kiehn O, Iizuka M, Kudo N. Resetting from low threshold afferents of N-methyl-D-aspartate-induced locomotor rhythm in the isolated spinal cord-hindlimb preparation from newborn rats. *Neurosci Lett* 148: 43–46, 1992.

Kiehn O, Kjaerulff O. Spatiotemporal characteristics of 5-HT and dopamine-induced rhythmic hindlimb activity in the in vitro neonatal rat. *J Neurophysiol* 75: 1472–1482, 1996.

Kiehn O, Butt SJ. Physiological, anatomical and genetic identification of CPG neurons in the developing mammalian spinal cord. *Prog Neurobiol* 70: 347–361, 2003.

Kiehn O. Locomotor circuits in the mammalian spinal cord. *Annu Rev Neurosci* 29: 279–306, 2006.

Koga K, Furue H, Rashid MH, Takaki A, Katafuchi T, Yoshimura M. Selective activation of primary afferent fibers evaluated by sine-wave electrical stimulation. *Mol Pain* 1–13, 2005.

Kudo N, Yamada T. N-methyl-D,L-aspartate-induced locomotor activity in a spinal cord-hindlimb muscles preparation of the newborn rat studied in vitro. *Neurosci Lett* 75: 43–48, 1987.

Lamotte d'Incamps B, Ascher P. Four excitatory postsynaptic ionotropic receptors coactivated at the motoneuron-Renshaw cell synapse. *J Neurosci* 28: 14121–14131, 2008.

Lavrov I, Courtine G, Dy CJ, van den Brand R, Fong AJ, Gerasimenko Y, Zhong H, Roy RR, Edgerton VR. Facilitation of stepping with epidural stimulation in spinal rats: role of sensory input. *J Neurosci* 28: 7774–7780, 2008a.

Lavrov I, Dy CJ, Fong AJ, Gerasimenko Y, Courtine G, Zhong H, Roy RR, EdgertonVR. Epidural stimulation induced modulation of spinal locomotor networks in adult spinal rats. *J Neurosci* 28: 6022–6029, 2008b.

Leung LS, Yu HW. Theta-frequency resonance in hippocampal CA1 neurons in vitro demonstrated by sinusoidal current injection. *J Neurophysiol* 79: 1592–1596, 1998.

Lev-Tov A, Delvolve I, Kremer E. Sacrocaudal afferents induce rhythmic efferent bursting in isolated spinal cords of neonatal rats. *J Neurophysiol* 83: 888–895, 2000.

Marchetti C, Beato M, Nistri A. Alternating rhythmic activity induced by dorsal root stimulation in the neonatal rat spinal cord in vitro. *J Physiol* 530: 105–112, 2001a.

Marchetti C, Beato M, Nistri A. Evidence for increased extracellular K(+) as an important mechanism for dorsal root induced alternating rhythmic activity in the neonatal rat spinal cord in vitro. *Neurosci Lett* 304: 77–80, 2001b.

Mazzone GL, Margaryan G, Kuzhandaivel A, Nasrabady SE, Mladinic M, Nistri A. Kainate-induced delayed onset of excitotoxicity with functional loss unrelated to the extent of neuronal damage in the in vitro spinal cord. *Neuroscience* 168: 451–462, 2010.

McCrea DA, Pratt CA, Jordan LM. Renshaw cell activity and recurrent effects on motoneurons during fictive locomotion. *J Neurophysiol* 44: 475–488, 1980.

Mentis GZ, Alvarez FJ, Bonnot A, Richards DS, Gonzalez-Forero D, Zerda R, O'Donovan MJ. Noncholinergic excitatory actions of motoneurons in the neonatal mammalian spinal cord. *Proc Natl Acad Sci USA* 102: 7344–7349, 2005.

Moreau JL, Pieri L, Prud'hon B. Convulsions induced by centrally administered NMDA in mice: effects of NMDA antagonists, benzodiazepines, minor tranquilizers and anticonvulsants. *Br J Pharmacol* 98: 1050–1054, 1989.

Musienko P, van den Brand R, Märzendorfer O, Roy RR, Gerasimenko Y, Edgerton VR, Courtine G. Controlling specific locomotor behaviors through multidimensional monoaminergic modulation of spinal circuitries. *J Neurosci* 31: 9264–9278, 2011.

Musienko P, Heutschi J, Friedli L, van den Brand R, Courtine G. Multi-system neurorehabilitative strategies to restore motor functions following severe spinal cord injury. *Exp Neurol* 235: 100–109, 2012.

Nistri A. Further investigations into the effects of baclofen (Lioresal) on the isolated spinal cord. *Experientia* 31: 1066–1068, 1975.

O'Donovan MJ, Bonnot A, Mentis GZ, Chub N, Pujala A, Alvarez FJ. Mechanisms of excitation of spinal networks by stimulation of the ventral roots. *Ann NY Acad Sci* 1198: 63–71, 2010.

Pearlstein E, Ben Mabrouk F, Pflieger JF, Vinay L. Serotonin refines the locomotor-related alternations in the in vitro neonatal rat spinal cord. *Eur J Neurosci* 21: 1338–1346, 2005.

Price GW, Wilkin GP, Turnbull MJ, Bowery NG. Are baclofen-sensitive $GABA_B$ receptors present on primary afferent terminals of the spinal cord? *Nature* 307: 71–74, 1984.

Ryckebusch S, Laurent G. Interactions between segmental leg central pattern generators during fictive rhythms in the locust. *J Neurophysiol* 72: 2771–2785, 1994.

Selionov VA, Ivanenko YP, Solopova IA, Gurfinkel VS. Tonic central and sensory stimuli facilitate involuntary air-stepping in humans. *J Neurophysiol* 101: 2847–2858, 2009.

Sillar KT. Spinal pattern generation and sensory gating mechanisms. *Curr Opin Neurobiol* 1: 583–589, 1991.

Sillar KT, Roberts A. Control of frequency during swimming in Xenopus embryos: a study on interneuronal recruitment in a spinal rhythm generator. *J Physiol* 472: 557–572, 1993.

Smeets WJ, González A. Catecholamine systems in the brain of vertebrates: new perspectives through a comparative approach. *Brain Res Brain Res Rev* 33: 308–379, 2000.

Smith JC, Feldman JL, Schmidt BJ. Neural mechanisms generating locomotion studied in mammalian brain stem-spinal cord in vitro. *FASEB J* 2: 2283–2288, 1988.

Song Z, Ultenius C, Meyerson BA, Linderoth B. Pain relief by spinal cord stimulation involves serotonergic mechanisms: an experimental study in a rat model of mononeuropathy. *Pain* 147: 241–248, 2009.

Song Z, Meyerson BA, Linderoth B. Spinal 5-HT receptors that contribute to the pain-relieving effects of spinal cord stimulation in a rat model of neuropathy. *Pain* 152: 1666–1673, 2011.

Taccola G, Margaryan G, Mladinic M, Nistri A. Kainate and metabolic perturbation mimicking spinal injury differentially contribute to early damage of locomotor networks in the in vitro neonatal rat spinal cord. *Neuroscience* 155: 538–555, 2008.

Taccola G, Mladinic M, Nistri A. Dynamics of early locomotor network dysfunction following a focal lesion in an in vitro model of spinal injury. *Eur J Neurosci* 31: 60–78, 2010.

Taccola G. The locomotor central pattern generator of the rat spinal cord in vitro is optimally activated by noisy dorsal root waveforms. *J Neurophysiol* 106: 872–884, 2011.

van Brederode JF, Berger AJ. Spike-firing resonance in hypoglossal motoneurons. *J Neurophysiol* 99: 2916–2928, 2008.

Yang K, Wang D, Li YQ. Distribution and depression of the $GABA_B$ receptor in the spinal dorsal horn of adult rat. *Brain Res Bull* 55: 479–485, 2001.

Zhong G, Díaz-Ríos M, Harris-Warrick RM. Serotonin modulates the properties of ascending commissural interneurons in the neonatal mouse spinal cord. *J Neurophysiol* 95: 1545–1555, 2006.

Zhong G, Sharma K, Harris-Warrick RM. Frequency-dependent recruitment of V2a interneurons during fictive locomotion in the mouse spinal cord. *Nat Commun* 2: 274, 2011.

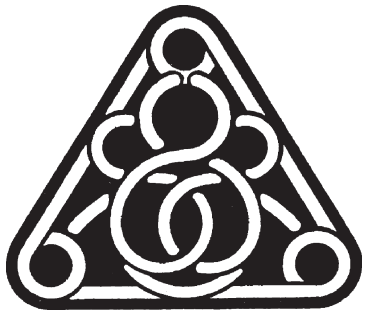

Physiological Reports

Open Access

Physiological Reports ISSN 2051-817X

ORIGINAL RESEARCH

Rat locomotor spinal circuits in vitro are activated by electrical stimulation with noisy waveforms sampled from human gait

Francesco Dose[1,2], Rachele Menosso[3] & Giuliano Taccola[1,2]

1 Neuroscience Department, International School for Advanced Studies (SISSA), via Bonomea 265, Trieste, Italy
2 SPINAL (Spinal Person Injury Neurorehabilitation Applied Laboratory), Istituto di Medicina Fisica e Riabilitazione (IMFR), via Gervasutta 48, Udine, Italy
3 IMFR, ASS4 Medio Friuli, via Gervasutta 48, Udine, Italy

Keywords
CPG, EMGs, spinal cord.

Correspondence
Giuliano Taccola, via Gervasutta 48, 33100 Udine, Italy.
Tel: +39 040 3787 725
Fax: +39 040 3787 702
E-mail: taccola@sissa.it

Funding Information
This work was supported by a grant from the Friuli Venezia Giulia Region, Azienda per i Servizi Sanitari 4 Medio Friuli, VERTICAL Foundation (Rome) and Associazione Tetra - Paraplegici FVG (Udine).

Received: 17 April 2013; Revised: 8 June 2013; Accepted: 11 June 2013

doi: 10.1002/phy2.25

Physiol Rep, 1 (2), 2013, e00025, doi: 10.1002/phy2.25

Abstract

Noisy waveforms, sampled from an episode of fictive locomotion (FL) and delivered to a dorsal root (DR), are a novel electrical stimulating protocol demonstrated as the most effective for generating the locomotor rhythm in the rat isolated spinal cord. The present study explored if stimulating protocols constructed by sampling real human locomotion could be equally efficient to activate these locomotor networks in vitro. This approach may extend the range of usable stimulation protocols and provide a wide *palette* of noisy waveforms for this purpose. To this end, recorded electromyogram (EMG) from leg muscles of walking adult volunteers provided a protocol named ReaL*i*stim (Real Locomotion-*induced* stimulation) that applied to a single DR successfully activated FL. The smoothed kinematic profile of the same gait failed to do so like nonphasic noisy patterns derived from standing and isometric contraction. Power spectrum analysis showed distinctive low-frequency domains in ReaL*i*stim, along with the high-frequency background noise. The current study indicates that limb EMG signals (recorded during human locomotion) applied to DR of the rat spinal cord are more effective than EMG traces taken during standing or isometric contraction of the same muscles to activate locomotor networks. Finally, EMGs recorded during various human motor tasks demonstrated that noisy waves of the same periodicity as ReaL*i*stim, could efficiently activate the in vitro central pattern generator (CPG), regardless of the motor task from which they had been sampled. These data outline new strategies to optimize functional stimulation of spinal networks after injury.

Introduction

One important goal for spinal network rehabilitation is the possibility to activate locomotor patterns with electrical stimuli applied to afferent inputs (Harkema et al. 2011). This is particularly attractive as a tool to recover, at least in part, locomotor activity after spinal cord injury. In the attempt to optimize the parameters for such a stimulation using as a test model the in vitro spinal cord preparation, we recently discovered a new stimulating protocol, named FL*i*stim (Fictive Locomotion-*induced* stimulation) based on high-frequency sampling of FL records from a ventral root (VR) of an isolated neonatal rat spinal cord and delivering it to a single dorsal root (DR) of the same preparation (Taccola 2011; Dose and Taccola 2012). This special stimulation pattern, even when applied at amplitude lower than the one required by standard square pulses, was able to induce locomotor-like oscillations of longer duration and with a greater number of cycles than hitherto described (Taccola 2011). The specific recruitment of the locomotor central pattern generator (CPG) made by FL*i*stim is confirmed by its ability to synergize the FL induced by NMDA (N-Methyl-D-aspartate) + 5-HT (5-hydroxytryptamine; Dose and

Taccola 2012). Although the precise mechanisms through which FL*i*stim can activate locomotor CPG remain unclear, its intrinsic noise turns out to be a crucial feature (Taccola 2011). The results so far were exclusively obtained using FL patterns sampled from neonatal rat spinal cords. We wondered if collecting records of limb muscle activity during real locomotion from healthy human volunteers might also have the ability to induce FL in the isolated rat spinal cord. This seems to be a desirable goal because the characteristics of human and rodent locomotor patterns, although similar, are not identical. Furthermore, using human electromyogram (EMG) data also allows DR stimulation with noisy, non-phasic traces (obtained during isometric or postural contraction of antigravity muscles) to assess the relative role of noise in the CPG activation.

Furthermore, detailed analysis of the EMG recorded from human leg muscles has allowed identifying distinct activation profiles during the execution of a specific motor task (Raasch and Zajac 1999; Bizzi et al. 2008; Wakeling and Horn 2009). Thus, we can hypothesize that stimulating protocols obtained from EMGs sampled during several motor tasks may activate, more or less efficiently, the in vitro CPG. To this aim, EMGs referred to distinct rhythmic movements, such as pedaling, hopping, or jumping, were recorded from volunteers, digitized and applied to a single DR to assess their impact on the locomotor CPG in vitro. Finally, stimulating patterns obtained from the EMG captured from repetitive flexions of the ankle joint were used to evaluate whether noisy waves sampled from monoarticular rhythmic oscillations were per se sufficient to activate the in vitro CPG.

Methods

Electrophysiological recordings

All procedures were conducted in accordance with the guidelines of the National Institutes of Health and the Italian Act Decreto Legislativo 27/1/92 n. 116 (implementing the European Community directives n. 86/609 and 93/88) and under the authorization of the Italian Ministry of Health. All efforts were made to reduce the number of animals and their suffering.

Experiments were performed on spinal cord preparations after isolation from neonatal rats (P0-P4), as previously reported (Taccola et al. 2004). Briefly, spinal cords were sectioned from the midthoracic region to the *cauda equina*, maintained at a constant room temperature of 22°C and continuously superfused (5 mL/min) with oxygenated (95% O_2; 5% CO_2) Krebs solution of the following composition (in mmol/L): 113 NaCl, 4.5 KCl, 1 $MgCl_27H_2O$, 2 $CaCl_2$, 1 NaH_2PO_4, 25 $NaHCO_3$, and 11 glucose, pH 7.4. VR recordings in DC mode were taken from L2 VRs, which contain axons from motoneurons that innervate mainly hindlimb flexor muscles, and from L5 VRs containing axons which drive primarily hindlimb extensor muscles (Kiehn and Kjaerulff 1996). The alternation of discharges between flexor and extensor motor pools and between left (l) and right (r) sides of the cord represents the hallmark of FL (Juvin et al. 2007).

Parameters of spinal network activity

Electrical stimuli were delivered, using bipolar suction electrodes, in order to evoke single VR responses. Stimuli were considered as threshold (Th) according to their ability to elicit fast synaptic responses from the homologous VR (see Marchetti et al. 2001). In response to DR stimulation with repetitive stimulating patterns, epochs of FL arise over a background of cumulative depolarization. FL cycles were analyzed for their periodicity (time between the onset of two consecutive cycles of oscillatory activity) and regularity, expressed by the coefficient of period variation (CV; displayed as standard deviation [SD] mean^{-1}). The correlation among signals arising from pairs of VRs was expressed by the cross-correlogram function (CCF), obtained using Clampfit® 10.3 software (Molecular Devices LLC, CA). While a CCF greater than −0.5 indicated that two VRs were synchronous, a CCF less than −0.5 showed full alternation (Ryckebusch and Laurent 1994; Taccola et al. 2010).

The power spectrum for stimulating patterns was obtained through Clampfit® 10.3 software (Molecular Devices, LLC, CA).

Designing the ReaL*i*stim

EMG recordings from several muscles were obtained during various motor tasks carried out by two healthy volunteers. Epochs (60 sec) of EMG traces were promptly processed for off-line analysis (Clampfit® 10.3 software; Molecular Devices) and records from one muscle were randomly selected for use. The sampled trace was imported into a spreadsheet of Origin® 9 (OriginLab, North Hampton, MA), where the *x*-axis considered each sampling time for the epoch duration and the *y*-axis was used for the corresponding current amplitude. The two columns of values were then exported (as an ASCII text file) to a programmable stimulation device (STG® 2004; Multi Channel Systems, Reutlingen, Germany). The stimulating protocol resulting from this procedure was termed ReaL*i*stim (Real Locomotion-*induced* stimulation) and was applied to a DR.

Subjects

Two healthy right leg dominant subjects (female, 31 years old, 62 kg, 1.74 m; male, 43 years old, 76 kg, 1.77 m) volunteered for the experiments. Human recordings were performed by specialized health care professionals in the SPINAL Clinical lab at Istituto di Medicina Fisica e Riabilitazione (Udine, Italia) and in the Gait & Motion Analysis Laboratory at Sol et salus hospital (Torre Pedrera, Rimini, Italy). The study conformed to the Declaration of Helsinki and the written informed consent was obtained from participants according to the clinical protocols established by the Istituto di Medicina Fisica e Riabilitazione (Udine, Italia).

EMG recordings

Spectrum profiles of EMG intensities were continuously obtained for 60 sec during different motor tasks, namely standing, overground walking at a self selected speed, incremental squats at 30°, 60°, and 90° of knee flexion, hopping, two legged or one legged jumping, and pedaling on an Ergoselect® 100K bicycle ergometer (Ergoline GmbH, Deutschland) at the frequency of 60 rpm and power output of 120 W.

EMG recordings from rhythmic oscillations of the right ankle joint, featuring a cycle period approximating that for walking and cycling, were also taken from a subject lying supine with one foot supported by a researcher.

During the performance of these exercises, subjects were instructed to generate stepping, jumping, or ankle flexions at the same frequency using an auditory metronome.

Briefly, EMG Ag/AgCl surface electrodes (10 mm diameter, 21 mm interelectrode distance) were positioned on the right leg and connected to TELEMG® system (BTS, Milano, Italia). Guidelines provided by the European Project SENIAM (Surface EMG for Non Invasive Assessment of Muscles, 1996–1999; Hermens et al. 2000) were followed in positioning electrodes. EMG signals were simultaneously recorded from the tibialis anterior (TA), medial gastrocnemius (GM), vastus medialis (VM), rectus femoris (RF), and vastus lateralis (VL). The EMG signals were band-pass filtered, with cut-off frequencies from 5 to 200 Hz, amplified 1000× and then sampled at 500 Hz.

Analysis of EMG signals and gait

As a control to define the role of intrinsic variability of the stimulating pattern in effectively activating the CPG, we compared alternating oscillations induced by noisy waves recorded from limb muscles with the effects elicited by simultaneously derived kinematic patterns (from limb markers) that were smooth sinusoids. Kinematic profiles were obtained with the Elite® 2000 system (BTS, Milano, Italia) consisting of six infrared cameras (positioned 4.5 m along the progression line of the subjects) operating at a sampling frequency of 50 Hz (Ferrigno and Pedotti 1985). After three-dimensional calibration, the spatial accuracy of the system was greater than 1.5 mm. Infrared reflective marks were positioned in correspondence to the lateral condyle of the knee (knee), the lateral malleolus (mall), between the lateral condyle of the knee and the lateral malleolus in the midpoint (bar), the heel, and the 5th metatarsal (met; Davis et al. 1991). Subjects were asked to walk barefoot as naturally as possible, looking straightforward. During the acquisition of kinematic data, the activity of soleus muscle was simultaneously recorded as described above.

Statistical analysis

All data are reported as mean ± SD, where n indicates the number of spinal cord preparations. After distinguishing between parametric or nonparametric data, using a normality test, all parametric values were analyzed with Student's *t*-test (paired or unpaired) to compare two groups of data or with analysis of variance (ANOVA) for more than two groups. For nonparametric values, Mann–Whitney test was used for two groups, while, for multiple comparisons, ANOVA on Ranks was first applied, followed by a post hoc test (Dunnett's method). Statistical analysis was performed using SigmaStat 3.5 software (Systat Software Inc, IL). Results were considered significant when $P < 0.05$.

Results

Noisy waves obtained from EMG recordings of the lower limb during human locomotion activate the in vitro CPG

We aimed at assessing whether electrical stimulation with noisy waveforms corresponding to locomotor patterns of an adult volunteer was able to trigger the CPG of the in vitro neonatal rat spinal cord. Thus, we first recorded EMGs from five muscles in the lower limb (RF, VM, TA, GM, and VL; Fig. 1A) of a volunteer walking at a freely chosen stride frequency (average speed = 1.01 m/sec). For each EMG trace, a 60 sec segment was randomly sampled in order to design the stimulation protocol, that we named ReaListim, which, in this example, was characterized by noisy waves with average 1.25 sec period. Figure 1A exemplifies how the noisy traces obtained from the VL muscle (shaded box), when delivered (intensity = 0.54 Th) to rL6 DR of the isolated rat spinal

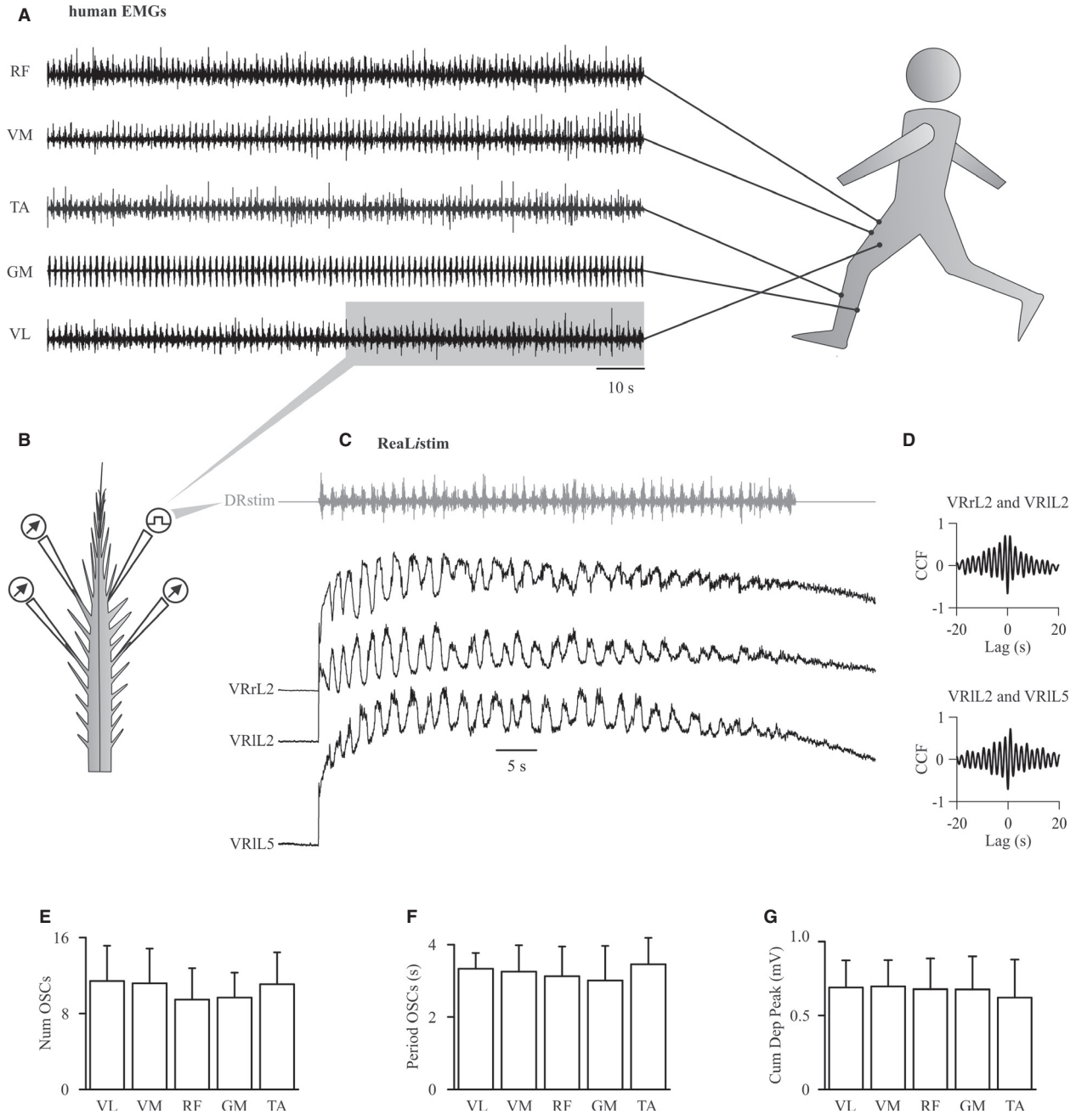

Figure 1. EMG recordings during human locomotion provide noisy waveforms able to activate the in vitro CPG. In A, EMGs are simultaneously recorded from five muscles of the right leg during real locomotion in an adult volunteer walking overground at normal speed. The superficial electrodes are positioned as indicated by the black lines in the cartoon (right). A segment of 60 sec duration is extracted through offset analysis from the VL EMG (shaded box) and used for designing the Rea*Li*stim protocol, later delivered to the DRrL6 of a neonatal rat isolated spinal cord (intensity = 0.54 Th), while the motor response is continuously monitored through recording suction electrodes from VRs L2 and L5 (B). During electrical stimulation with Rea*Li*stim, VRs are depolarized with a superimposed episode of locomotor-like oscillations (C), as confirmed by the negative peaks centered at zero lag value in the cross-correlogram functions in D. In E, F, and G, histograms show, respectively, that the mean number and the mean period of FL oscillations, as well as the mean cumulative depolarization amplitude, do not statistically change, even in response to delivery of noisy waveforms obtained from different leg muscles (n = 7; P = 0.723 for E; P = 0.740 for F; P = 0.967 for G).

cord (Fig. 1B), evoked cumulative VR depolarization (1.17 mV) with superimposed 28 oscillating cycles (2.06 ± 0.41 sec period and 0.20 CV; Fig. 1C). Oscillations between L2 and L5 VRs on the two sides of the spinal cord were alternated, as confirmed by the value of the cross-correlograms illustrated in Figure 1D (CCF homolateral = −0.71; CCF homosegmental = −0.66), indicating, therefore, their characteristic FL property.

EMG recordings obtained in three sessions of locomotion (average speed of 1.11 ± 0.07 m/sec) provided ReaListims (period = 1.12 ± 0.11 sec for 60 sec epoch), which induced, in 11 preparations, cumulative VR depolarization of 0.71 ± 0.33 mV with a superimposed episode of FL (52.15 ± 7.08 sec long, 21 ± 4 locomotor cycles of 2.73 ± 0.65 sec period and 0.28 ± 0.11 CV). In six experiments, ReaListims, simultaneously sampled from flexor and extensor muscles of leg and calf, and delivered in sequence to a single DR of the isolated rat spinal cord, were equally capable of evoking locomotor-like responses of similar duration, period, and cumulative depolarization (Fig. 1E–G).

Different responses of the in vitro CPG to electrical stimulation with EMGs or kinematic profiles

Stimulating patterns composed of noisy or smooth sinusoidal waves of identical main frequency were obtained by simultaneously recording, during the same session of human locomotion, the activity of the soleus muscle, and the variations in the joint profile of the heel, on the *y*-axis. The two traces were imported into the programmable stimulator and corrected to obtain waveform traces of the same maximal amplitude. Hence, the two stimulating patterns (ReaListims and kinematic profiles) provided either a noisy baseline or a smooth baseline.

Figure 2A shows that stimulation of the DRrS1 of the isolated spinal cord with ReaListim (intensity = 0.33 Th) induced cumulative depolarization (0.46 mV) with FL of 57.31 sec duration with 22 cycles (period and CV of 2.73 ± 1.03 sec and 0.38, respectively). Conversely, on the same preparation, electrical stimulation of the same DR with the protocol obtained from the kinematic profile of the heel (intensity = 0.33 Th) induced very small cumulative depolarization (0.08 mV), with a series of synchronous discharges among the four VRs. The cross-correlogram analysis (Fig. 2C and E) confirms that ReaListim evoked FL with alternating oscillations among homosegmental (lL2 and rL2, CCF = −0.88) and homolateral (lL2 and lL5, CCF = −0.66) VRs, while a sinusoidal stimulation obtained from the heel kinematic profile evoked only synchronous oscillations both at homosegmental (VRlL2 and VRrL2, CCF = 0.65) and homolateral (VRlL2 and VRlL5, CCF = 0.75) levels.

These results were confirmed in five preparations (Fig. 2D) with mean CCF of −0.68 ± 0.12 for homosegmental VRs and of −0.38 ± 0.14 for homolateral VRs during ReaListim. In the same preparations, delivery of waves obtained from the kinematic analysis of the heel evoked synchronous discharges (homosegmental CCF = 0.60 ± 0.16 and homolateral CCF = 0.70 ± 0.07) only.

We tested whether the inability to activate the in vitro FL with Kstim was due to the absence of noise in kinematic profiles. For this reason, numerous kinematic patterns were simultaneously sampled, on the *y*-axis, from different track positions in the lower limb during the same locomotor session. As schematized in Figure 3A, in correspondence to gait phases exemplified as a stick diagram, kinematic traces from different tracks of the lower limb were recorded for the first two steps of a locomotor session. These traces were synchronized with the EMG recorded from the right soleus (bottom record in Fig. 3A). The metatarsal trace presented the most different profile from the one from the heel as it comprises a second peak in coincidence with ankle flexion. Fourier analysis (Fig. $3B_1$–C_1) confirms that both traces had a main peak at 0.9 Hz and a second component at 1.8 Hz, while the metatarsal trace shows a further component at 2.9 Hz (Fig. 3C).

As illustrated in Figure $3B_2$ and C_2, we subsequently delivered, to the same DR in the same preparation, first, a smoothed wave obtained from the heel trace and, then, the one recorded from the metatarsus, both at the same maximum amplitude. Responses from VRs (see Fig. $3B_2$– and C_2) indicate that, in both cases, the stimulation induced similar cumulative depolarization (0.35 μV for the heel and 0.41 μV for the metatarsus), followed by baseline repolarization despite continuous stimulation. Reflex discharges were observed during each stimulating cycle plus sporadic, slow bursts. The cross-correlogram analysis (Fig. 3D and E) confirms events synchronicity among homosegmental (heel CCF = 0.66; met CCF = 0.83) and homolateral (heel CCF = 0.88; met CCF = 0.96) VRs. The same observations were obtained from three spinal cords. These results indicate that, unlike ReaListim, Kstim could not evoke FL, suggesting that the noise contained in the stimulating traces sampled from the motor output of a human individual was a crucial characteristic for activating the in vitro CPG.

Noisy traces obtained during isometric contractions or static posture do not induce FL

To further clarify the characteristics of ReaListim responsible for the activation of the in vitro CPG, we have

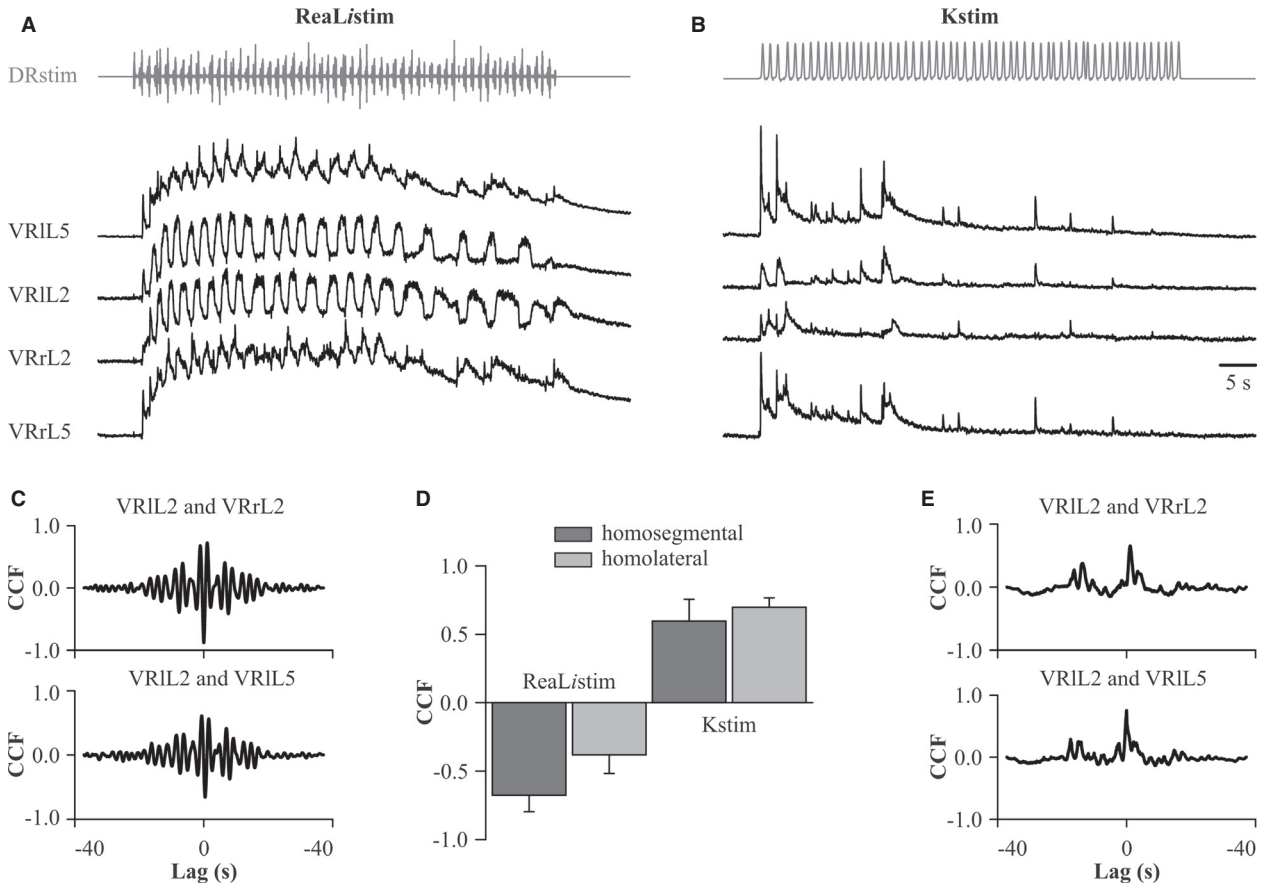

Figure 2. Kstim, unlike ReaL*i*stim, does not trigger FL. In A, ReaL*i*stim, designed from right soleus EMG (intensity = 0.33 Th), when applied to DRrS1, evokes an episode of FL from VRs L2 and L5 on both side of the spinal cord. In the same experiment, delivery of Kstim, sampled from the kinematic profile of right heel (intensity = 0.33 Th), generates only a slight cumulative depolarization with sporadic electrical discharges (B). In C, the cross-correlogram analysis performed for the traces shown in A reports negative values, representing the double alternation among pairs of homosegmental L2 (top) and homolateral L2 and L5 (bottom) VRs. Conversely, in E, the cross-correlogram analysis for traces in B shows positive peaks, describing full synchrony among discharges recorded from homosegmental (top) and homolateral (bottom) VRs. In D, histograms summarize the mean CCF values obtained for homosegmental (dark gray) and homolateral (light gray) VRs in response to stimulation of the same cords with ReaL*i*stim (right) and Kstim (left), respectively. While ReaL*i*stim always evokes alternating oscillations, Kstim generates only synchronous events (n = 5).

explored whether the EMG phasic patterns, used to design ReaL*i*stim, were a crucial characteristic. Thus, we compared stimulation using ReaL*i*stim (see top record in Fig. 4A) with noisy traces derived from the tonic activation of the same muscle, either during the antigravity contraction for standing (top trace in Fig. 4B) or during an isometric contraction task (top record in Fig. 4C and D).

As demonstrated by Figure 4A, 60 sec stimulation with ReaL*i*stim (VM muscle) evoked (intensity = 0.15 Th) cumulative depolarization (0.80 mV) with a longlasting episode of FL (57.77 sec, 23 oscillations, period and CV of 2.62 ± 0.51 sec and 0.20, respectively). Oscillations alternated among homosegmental VRs, as confirmed by the cross-correlogram analysis (homosegmental CCF = −0.50; not shown).

On the other hand, stimulation with EMG traces sampled during static posture or isometric contraction did not evoke cumulative depolarization, but only sporadic tonic discharges (Fig. 4B and C). Even when increasing the amplitude of the EMG trace from the isometric contraction to that of the ReaL*i*stim one, no alternating oscillations appeared, although the stimulating protocol was able to induce cumulative VR depolarization (0.31 mV; Fig. 4D).

Analogous observations were replicated with six preparations, in which ReaL*i*stim induced an average cumulative depolarization of 0.66 ± 0.29 mV, superimposed by

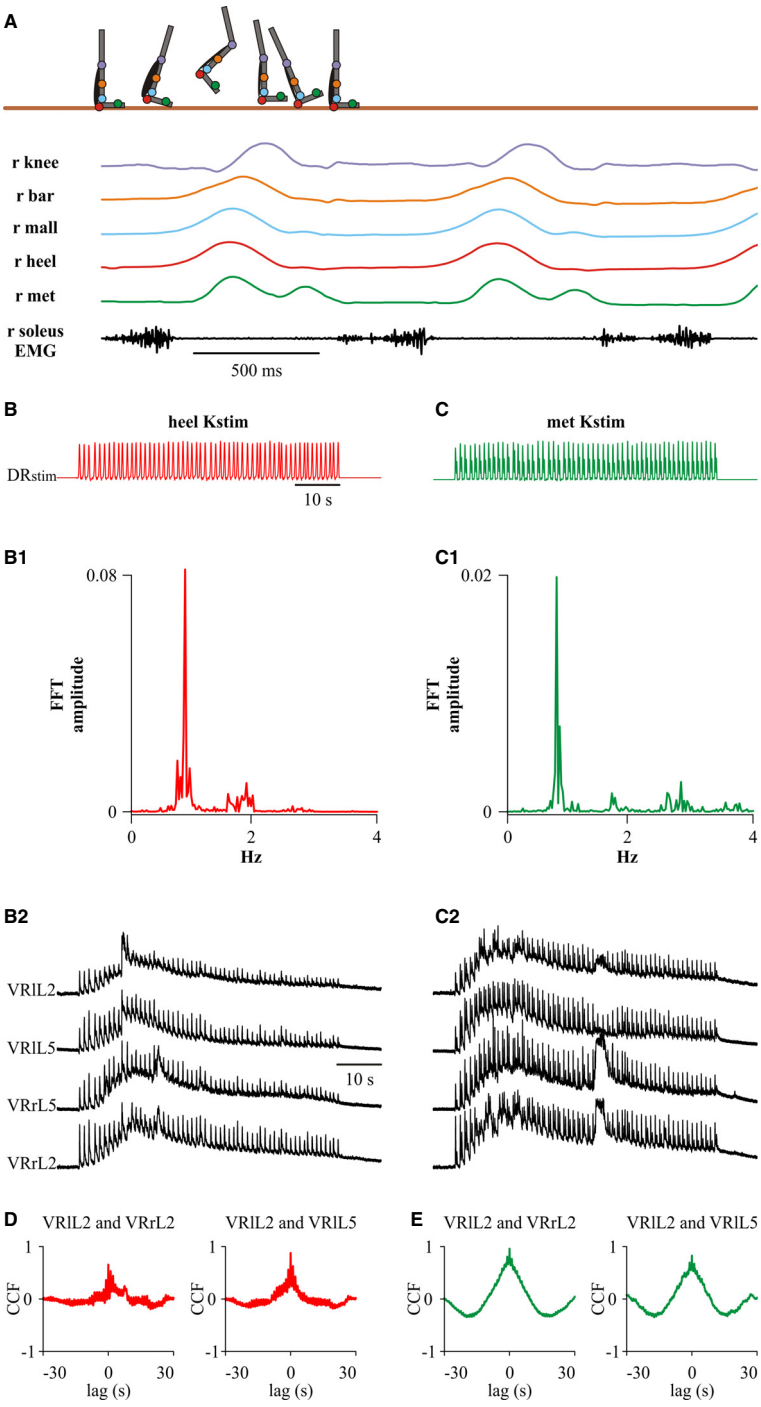

Figure 3. Kstims sampled from different tracks of the lower limb are ineffective in eliciting FL. The kinematic analysis of locomotion is performed on several tracks of the right leg (knee, bar, mall, heel, and met), as reconstructed for consecutive phases of the first step in A. The kinematic profiles are indicated in gray scale and synchronized with the soleus muscle EMG. Segments of 60 sec duration are sampled from heel and met profiles to produce the stimulating protocols heel Kstim (B) and met Kstim (C), for which power spectra are obtained (B_1 and C_1, respectively). Heel Kstim applied to DRrS4 (intensity = 0.33 Th) evokes a small cumulative depolarization accompanied by single reflex responses, corresponding to stimulating pattern peaks, and by the sporadic appearance of bursts (B_2). Analogously, met Kstim (intensity = 0.33 Th) depolarizes VRs, with single reflex responses and sporadic bursts that are synchronous among all VRs (C_2). The cross-correlogram analysis from pairs of homosegmental (left) and homolateral (right) VRs quantifies the synchrony among discharges elicited by Kstims (D for heel Kstim and E for met Kstim).

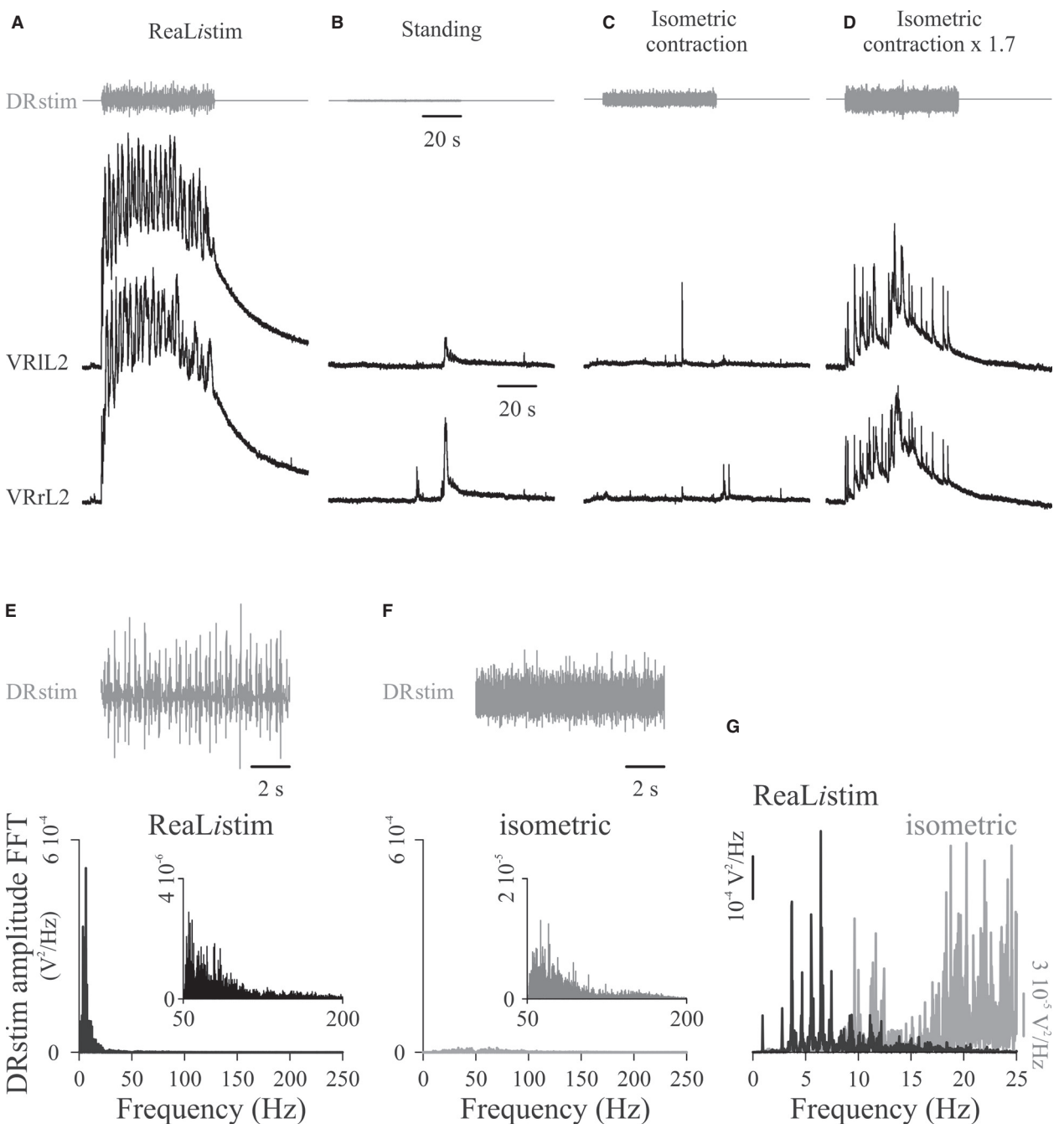

Figure 4. Human EMGs sampled during standing and isometric contraction fail in inducing FL. In A, ReaL*i*stim is designed from rVM EMG recording and applied to DRlL7 (intensity = 0.15 Th) to elicit an epoch of alternating oscillations from L2 VRs. In the same experiments, delivery of the EMGs recorded from rVM during standing static posture (B, intensity = 0.01 Th) or isometric muscle contraction (C, intensity = 0.09 Th) does not depolarize VRs, although elicits few uncorrelated discharges. Finally, when the peaks of the EMG in C are artificially adjusted to the same maximum amplitude of ReaL*i*stim in A, the resulting stimulating protocol can generate a small cumulative depolarization with synchronous events (D). In E, a segment of the same ReaL*i*stim shown in A is displayed at a faster time base scale, while the power spectrum of the entire stimulating pattern (60 sec) is reported below. An analogous Fourier analysis is performed also for isometric EMGs (F, in top panel see a sample episode of the DRstim in C, at a faster time base scale). Note in the inserts the magnification of spectra in the high-frequency regions. The power spectra of the two protocols are superimposed in G (black trace, ReaL*i*stim; gray trace, isometric contraction), emphasizing that, among the noisy waveforms sampled from EMGs, only ReaL*i*stim presented a series of components in the low-frequency domain.

FL of 53.65 ± 3.98 sec duration with 20 ± 2 alternating cycles of period and CV 2.90 ± 0.36 sec and 0.29 ± 0.11, respectively. In the same spinal cords, in response to stimulation with EMGs recorded during standing posture or isometric contractions, we did not observe any depolarization or appearance of locomotor oscillations. Even stimulation with the EMG traces of an isometric contraction with amplitude brought to ReaL*i*stim values, did not induce any locomotor cycles, despite an average cumulative depolarization of 0.36 ± 0.13 mV. These findings suggest that the basic intrinsic noise of the human EMG was unable to elicit FL.

To look for discrete frequency domains within the noisy waveforms necessary for activate FL, we analyzed the power spectra of the ReaL*i*stim record (see, in Fig. 4E, example at high gain and faster time base taken from the record shown in A) and isometric contraction trace (see, in Fig. 4F, example at high gain and faster time base taken from the record shown in C). While the power spectrum of ReaL*i*stim (Fig. 4E, bottom) revealed principal components clustered at the low frequency, on the other hand, the spectrum of isometric contraction lacked these peaks and contained only small components at higher frequency (Fig. 4F, bottom). The insets to Figure 4E and F show that, in the high-frequency domain, a similar pattern for both protocols (albeit smaller in amplitude for ReaL*i*stim) was present. Figure 4G indicates that, after alignment of both traces in the frequency range below 25 Hz, ReaL*i*stim (black trace) was characterized by a series of components between 0 to 10 Hz, whereas the isometric contraction stimulus (gray trace) lacked any elements. On the contrary, from 15 to 25 Hz, only the isometric contraction profile was observed (Fig. 4G).

Effect of stimuli sampled from human EMGs during nonlocomotor rhythmic activity

We next tested whether stimulation with noisy waveforms from EMG recordings of the right GM during the execution of nonlocomotor rhythmic activities could activate the in vitro CPG. Thus, we sampled 60 sec EMG records taken while one volunteer was pedaling or hopping.

Figure 5A shows that ReaL*i*stim (period = 1.07 ± 0.10 sec and intensity of stimulation peak = 0.5 Th; top row shows pattern at fast time base) depolarized VRs by 0.22 mV and evoked FL of 53.04 sec duration, with 22 locomotor cycles (period = 2.51 ± 0.55 sec; CV = 0.22). Figure 5B indicates that, on the same in vitro preparation, the EMG pattern obtained during pedaling (period = 1.07 ± 0.11 sec; intensity of stimulation peak = 0.4 Th; top row shows pattern at fast time base) delivered to the same DR induced cumulative depolarization (0.23 mV) with FL (lasting 41.09 sec with 18 locomotor-like oscillations; period = 2.42 ± 0.44 sec; CV = 0.18). Finally, stimulation with a pattern corresponding to the repeated hopping (Fig. 5C; period = 0.58 ± 0.02 and amplitude of stimulation peak = 0.5 Th; top row shows pattern at fast time base) generated a cumulative depolarization (0.20 mV) with short FL (13 oscillations for 28.96 sec; cycle period = 2.41 ± 0.34 sec; CV = 0.14).

FL episodes have been quantified with respect to the number of oscillations (Fig. 5D), cycle period (Fig. 5E) and peak of cumulative depolarization (Fig. 5F), for the three different stimulating protocols delivered to the same five preparations. The ReaL*i*stim appeared to activate the in vitro CPG more efficiently than the EMG pattern recorded during hopping, as shown by the significantly greater number of alternating cycles evoked.

We next designed another stimulating pattern that requires the synchronous activation of limbs, like hopping, carried out at a periodicity approximating the one of ReaL*i*stim. To this aim, EMGs of right VM, TA, and GM during both two legged and one legged jumping were sampled. Figure 6A–C compares the EMG records used for ReaL*i*stim (see example of a single burst in the gray box; period of 1.00 ± 0.01 sec), with two legged or one legged jumping. It is noteworthy that despite the EMG similar periodicity, namely of 1.25 ± 0.04 and 1.20 ± 0.03 sec, respectively, bursts for EMGs referred to the two legged or one legged jumping (see examples in the gray boxes of Fig. 6B and C), show the characteristic biphasic component due to, first, contraction of the muscle for the spring phase and, second, the contraction during the return phase.

In Figure 6A, ReaL*i*stim sampled from the rGM induced, at the peak of a cumulative depolarization of 0.49 mV, an episode of 60.58 sec with 30 oscillations, of 2.08 sec period (CV = 0.30). In the same spinal cord, a stimulus of an amplitude approximating that of ReaL*i*stim, sampled from the rGM during jumping, depolarized VRs by 0.51 mV and induced a locomotor episode of 31.591 sec duration and 18 oscillations (period = 1.87 sec and CV = 0.20; Fig. 6B). Similarly, the subsequent delivery to the same DR of EMGs provided of equal intensity and sampled during one legged jumping, determined a depolarization of 0.46 mV and an episode of FL comparable to the ones obtained with the other two patterns of stimulation (duration = 38.30, number of oscillations = 21; period = 1.91 sec, CV = 0.22; Fig. 6C).

The histograms of Figure 6D–F quantify FL episodes evoked by these stimulating patterns (average of six preparations) in terms of the number of oscillations (Fig. 6D), cycle period (Fig. 6E), and peak of cumulative depolarization (Fig. 6F): thus, noisy patterns with a periodicity similar to that of ReaL*i*stim, but sampled during tasks

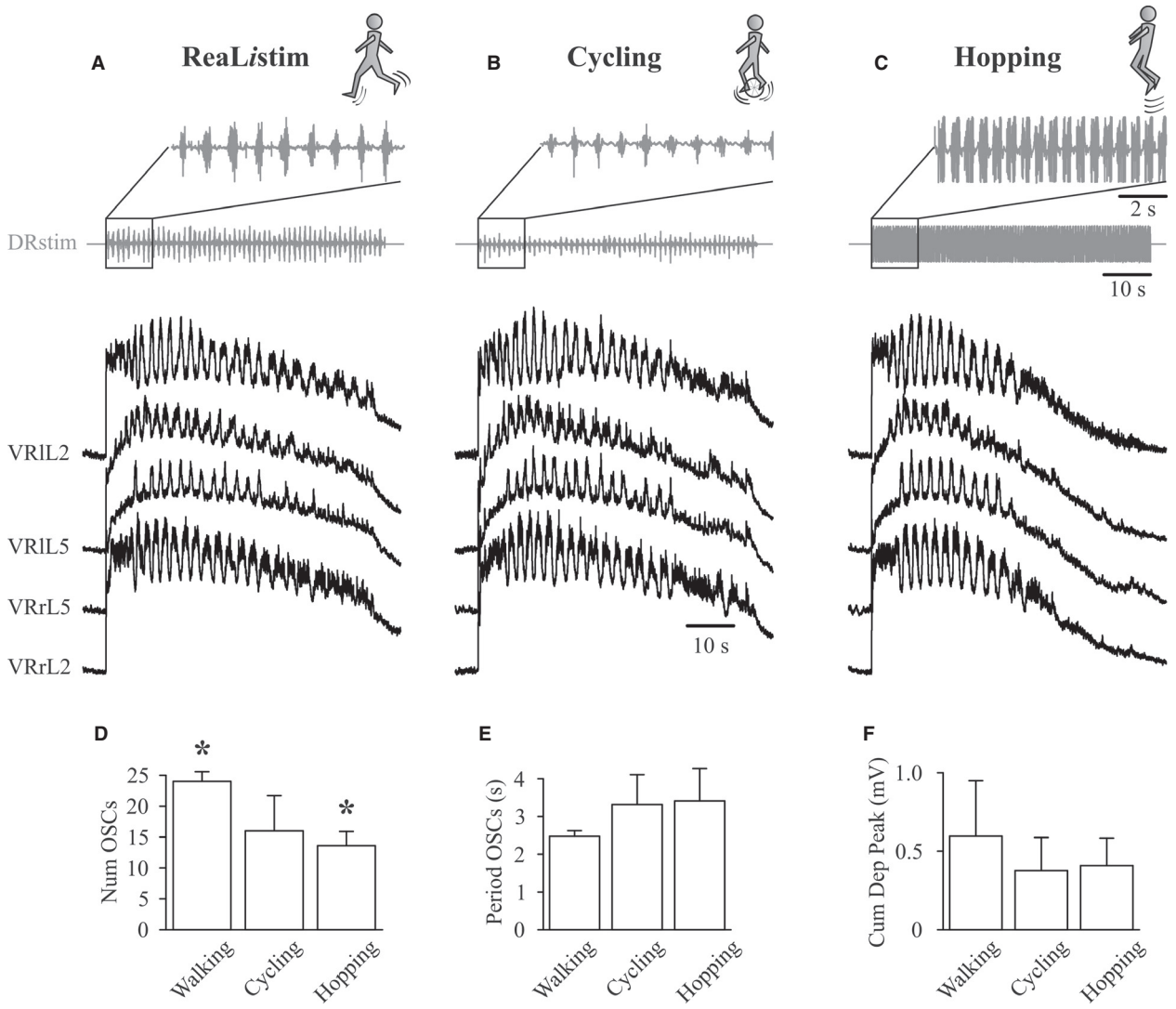

Figure 5. Stimulating protocols obtained from human EMGs during walking, cycling, and hopping induce a different number of FL cycles. In A, ReaL*i*stim is designed from the EMG recording (duration 60 sec; in top panel is reported a faster sample trace) of rGM during locomotion. The stimulating pattern is applied to DRlL6 (intensity = 0.50 Th), evoking an episode of FL from L2 and L5 VRs on both side of the cord. A FL episode of duration similar is generated by a stimulating protocol (duration = 60 sec; intensity = 0.40 Th), sampled from the rGM EMG recording while the volunteer is pedaling (B, in top panel is reported a faster sample trace). Contrarily, by applying a rGM EMG trace (duration = 60 sec; intensity = 0.50 Th; in top panel is reported a faster sample trace) recorded during hopping a shorter episode of FL is obtained. Note that A, B, and C are referred to the same preparation. Histograms in D, E, and F summarize the mean value for number and period of oscillations and for cumulative depolarization amplitude. Note that the number of locomotor-like oscillations using the hopping pattern is significantly reduced with respect to ReaL*i*stim (n = 5; P = 0.011).

involving the synchronous activation of lower limbs, were equally able to activate the in vitro CPG.

Stimulating patterns sampled from human EMGs during rhythmic single joint flexions can activate FL

We wanted to assess whether phasic EMGs, with the same periodicity as ReaL*i*stim and obtained in the absence of multisegmental movement of lower limbs, were appropriate to generate FL. For this reason, the activity from TA and GM muscles was recorded during rhythmic oscillations of the ankle joint under weight-bearing conditions, with a cycle period (1.09 ± 0.01 sec) approximating that for walking, cycling, and jumping (gray trace in Fig. 7B). Stimulation with a ReaL*i*stim sampled from the rGM induced a depolarization of 1.20 mV with a superimposed episode of 60.37 sec duration with 26 locomotor oscilla-

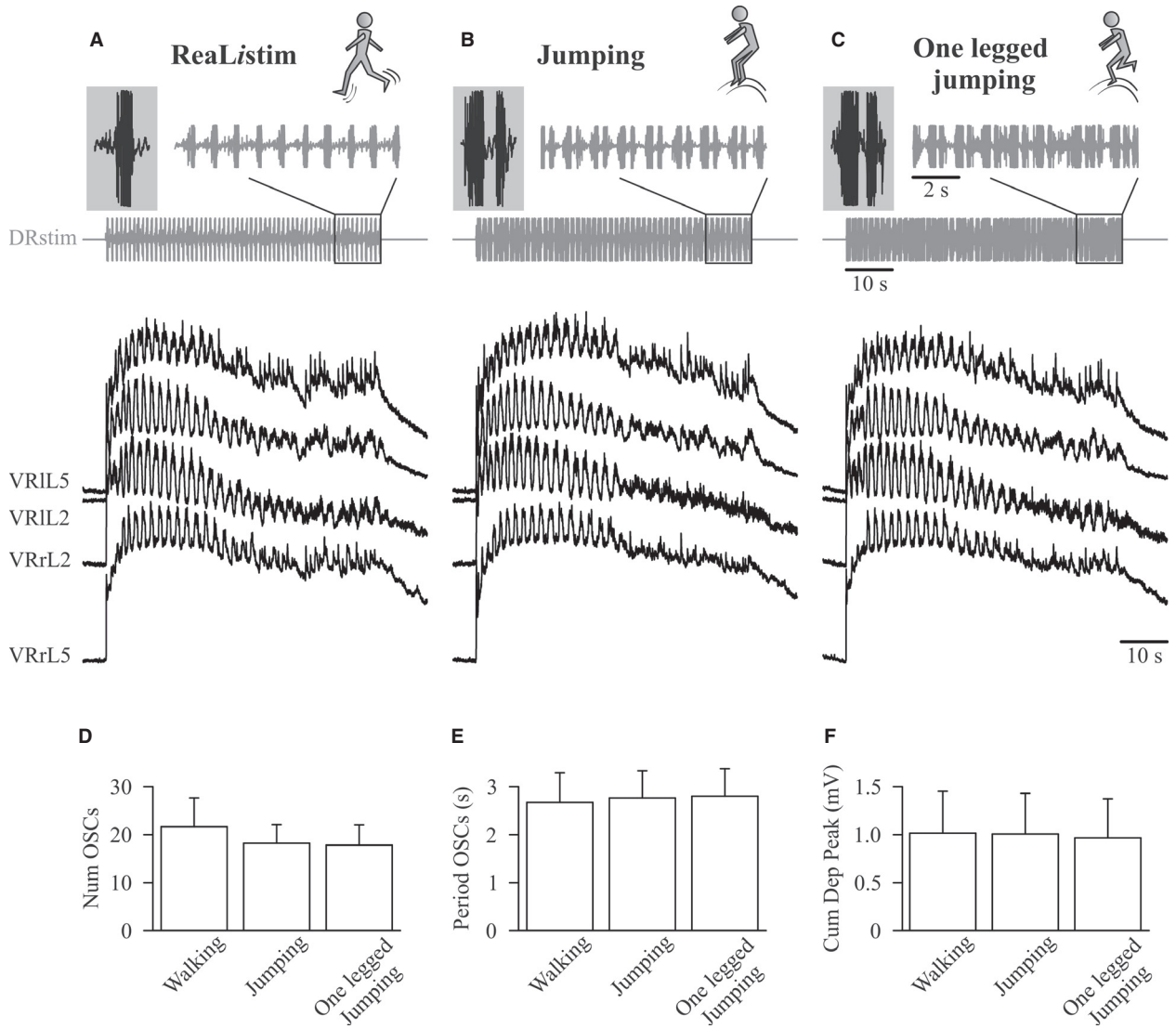

Figure 6. Human EMGs sampled during walking, two legged jumping and one legged jumping provide stimulating waveforms that similarly activate the in vitro CPG. A, ReaL*i*stim is designed from the EMG recordings of the rGM during locomotion (duration 60 sec; top panel shows faster sample trace). The gray box on the left (1 sec width) shows a typical single burst of an EMG during a gait cycle. The stimulating pattern applied to DRrL7 (intensity = 0.1 Th) elicited an epoch of FL from the controlateral L2 and L5 VRs. A similar locomotor-like response was generated by EMGs obtained from rGM muscle (duration = 60 sec; intensity = 0.1 Th) and sampled while the volunteer was jumping on two legs (B). B, top panel on the left shows a single burst, while a sample of the stimulating pattern is illustrated on a faster time base scale. Applying a rGM EMG trace (duration = 60 sec; intensity = 0.1 Th) recorded during one legged jumping generated a comparable episode of FL (C). Top panels in C show one single burst, and 10 sec stimulating pattern (faster time scale). Note that all data depicted in A, B, and C were obtained from the same preparation. Histograms in D, E, and F indicate that no statistical difference appeared in response to the three stimulating protocols, as far as number and period of oscillations, and cumulative depolarization amplitude were concerned (n = 6).

tions of a period of 2.41 sec (CV = 0.38; Fig. 7A). A pattern of similar amplitude to the one of ReaL*i*stim, but obtained from the rTA during repetitive ankle flexions, generated an episode of FL with similar features (cumulative depolarization = 1.14 mV; duration = 58.50 sec; number of oscillations = 23; period of oscillations = 2.67 sec with CV = 0.39; Fig. 7B). Average values obtained from six spinal cords are quantified in terms of number of oscillations, cycle period, and cumulative depolarization in Figure 7D–F.

In conclusion, in the present study, all stimulating patterns obtained from noisy and phasic EMGs, characterized by a periodicity approximating that of ReaL*i*stim, were able to activate the in vitro CPG, regardless

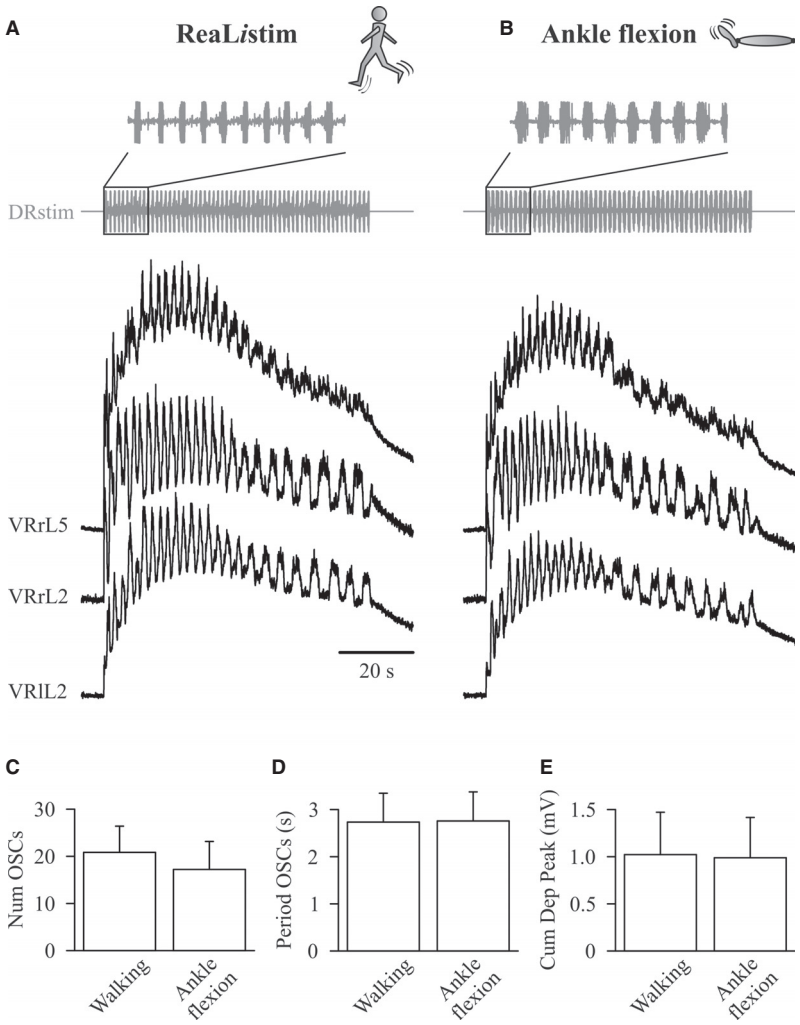

Figure 7. Stimulating patterns obtained from human EMGs from the rhythmic oscillations of ankle joint generate locomotor-like responses similar to the ones induced by ReaL*i*stim. A, ReaL*i*stim (60 sec duration, 0.2 Th intensity), sampled from rGM and delivered to DRrS4, induced a series of alternating oscillations among VRs. At the top, a segment of the trace comprised in the open box is displayed at faster time scale. An analogous response is recorded in B from the same preparation when stimulated with the EMG (60 sec duration, 0.2 Th intensity) captured from rTA during rhythmic oscillations of the ankle joint. A segment of the stimulating pattern (open box) is displayed at the top on a faster time scale. The mean values of pooled data from six experiments are summarized in the histograms below, as for number of oscillations (C), cycle period (D), and peak of cumulative depolarization (E), demonstrating that these two stimulating patterns were similarly effective in inducing an episode of FL with similar characteristics.

of the type of rhythmic task from which they were obtained.

Discussion

The present study shows that using the EMG records obtained from human leg muscles during normal gait (ReaL*i*stim) and applying them to a single DR of the rat isolated spinal cord was very effective in eliciting a long-lasting series of FL cycles. This novel observation demonstrates that the type of DR stimulus (containing locomotor-related signals) was important rather than its origin (in vitro rat spinal cord or human muscle activity) and that, whether recorded from an in vitro preparation or a healthy volunteer, the rat locomotor networks reacted with similar responses.

Characteristics of the ReaL*i*stim protocol to activate FL

A protocol of undulatory, noisy stimuli from the human leg EMG during real locomotion (named ReaL*i*stim) activated locomotor-like oscillations in the isolated spinal cord even when the stimulus amplitude was subthreshold

to induce a VR reflex. Interestingly, EMG records sampled from flexor or extensor leg muscles were equally effective to evoke FL.

Nevertheless, reconstructing the DR stimulation protocols from the kinematic records of the same human walking activity (Kstim) was not able to induce FL despite collecting stimulus data from either the heel or the metatarsal joint. Thus, the information of simple stimulus alternation contained in the kinematic profile at walking speed could not be sufficient for FL. Likewise, sustained EMG discharge sampled during standing posture or during the execution of isometric squat exercises failed to activate FL. These results are reminiscent of previous data when a broad range of DR stimulation patterns was used to elicit sustained FL in vitro with poor success (Taccola 2011). Thus, we reasoned that the original FL record obtained from the spinal cord in vitro or the ReaL*i*stim obtained from human gait must contain certain properties that confer them the ability to activate the locomotor CPG.

In fact, an epoch of FL analogous for duration and number of oscillations to the one evoked by ReaL*i*stim has been previously observed with FL*i*stim elicited by NMDA + 5-HT (Taccola 2011; Dose and Taccola 2012).

The importance of noise for electrical stimuli eliciting FL

If the smooth kinematic stimulus pattern as well as the high-frequency firing during isometric contraction were unable to produce FL, we suspected that the intrinsic variability of the stimulating traces used in this study was a crucial element for an optimal CPG activation. This notion is in accordance with previous observations that the efficacy of stimulation with noisy waves was lost when the stimulating pattern was smoothed (Taccola 2011). This result reaffirms the importance of variability for spinal CPG function (Ziegler et al. 2010; Lee et al. 2011), in line with error-based motor learning paradigms (Huang et al. 2011).

As EMG records cannot provide detailed information on the nature of these electrical signals, we have indicated such traces as "noisy", based on the sole macroscopic observation of the ragged baseline. In line with this point of view, the ReaL*i*stim protocol apparently possesses the same level of noise as FL*i*stim. However, intrinsic variability of FL*i*stim mainly corresponds to the firing profile of motoneurons within the same pool during FL (Berg et al. 2007), while for the EMG of real locomotion in a volunteer, additional nonlinear sources of variability need to be considered. For instance, stiffness, viscoelastic properties of muscles, coupling among limb segments and biomechanical constrains, anticipatory adjustments from supraspinal centers, and reflex responses to external perturbations are likely contributors to the noise within in vivo EMGs (Thrasher et al. 2011). Other forms of variability in human EMG signals are attributable to specific muscle pennation and fiber composition (Johnson et al. 1973) or to the proximity of EMG electrodes to the muscle innervation (De Luca 1997). These sources of EMG variability seemed negligible in activating the CPG because EMGs from either different leg muscles or the same muscle in different recording sessions appeared to have the same ability to elicit FL.

Thus, baseline noise associated with a certain waveform with main frequency within the real or fictive locomotion rhythms was the crucial requirement for activating the locomotor network in vitro. Another possibility is that the noise sampled from the EMG or from the FL contains distinctive information that codifies the state of network activity and the type of motor task undertaken. In support of this notion is the report that in the cerebral cortex the noise fluctuations in neuronal network output rely on the frequency of sensory stimuli in a state-dependent manner (White et al. 2012).

Comparison of power spectra of noisy waveforms shows low-frequency domain components, which seem to distinguish ReaL*i*stim from the isometric contraction protocol (ineffective in recruiting the CPG). Future work will be necessary to explore whether low-frequency components are sufficient per se in activating FL or if they also need the high-frequency background that characterizes all noisy stimulating patterns from EMG recordings.

Phasic EMGs of frequency similar to ReaL*i*stim equally activated the CPG regardless of their task specificity

The first part of the study reported the optimal locomotor-like response evoked by stimulating waves, sampled from limb muscles during the execution of rhythmic tasks, such as walking and cycling, that both involve an alternated pattern. On the other hand, EMGs obtained during synchronous rhythmic activation of lower limbs (e.g., hopping) appeared less effective. This difference may be attributed to certain intrinsic characteristics of the various EMGs. In fact, although the stimulating pattern was always recorded from one single leg, the EMG of even one muscle during alternated activation of lower limbs (running or pedaling) may contain distinct information for the activation of the in vitro CPG. The same does not seem to occur, though, with the EMG sampled during the execution of tasks that require the synchronous activation of limbs, like hopping (Bizzi et al. 2008). Examples of task specificity in network output have already been reported and attributed to the modulation

provided by the differential afferent feedback that characterizes different motor tasks (Brooke et al. 1992).

In the present experiments, comparing the stimulating effectiveness of EMGs from hopping or walking is misleading, as their cycle period was clearly different. Despite repeated attempts, volunteers failed to hop and to walk at identical frequency. Hence, to compare ReaL*i*stim with the one obtained with EMGs from two legged synchronous movements, we recorded EMGs from different muscles during jumping with both legs at the same main frequency as gait. Stimulation with EMGs obtained from one legged jumping was also tested to evaluate the influence of the proprioceptive information coming from the rhythmic movement of the controlateral limb (Savin et al. 2010). In fact, it has been demonstrated the existence of a movement-related afferent feedback originating from network interaction of inputs arising from the two limbs (McIlroy et al. 1992; Peper and Carson 1999) and this modulation seems to be accounted by presynaptic inhibitory mechanisms (Stein 1995). In particular, passive movement of one limb can drive phase and frequency of the controlateral one (Gunkel 1962; deGuzman and Kelso 1991).

In our experiments, stimulation with EMGs obtained from both two legged and one legged jumping did not appear to be statistically different from ReaL*i*stim in inducing FL. Thus, most noisy patterns recorded during limb movement, as long as they possess a main frequency similar to the one of ReaL*i*stim, appeared to be equally effective in activating the CPG, regardless of the motor task under which they were taken.

Furthermore, to confirm the scarce task specificity of EMG traces to induce a FL, we stimulated the isolated spinal cord with noisy and phasic patterns of a main frequency equal to that of locomotor patterns, but recorded during a nonpropulsive action of lower limbs, such as rhythmic flexions of the ankle in weight-bearing conditions and observed little task specificity of the stimulating patterns.

Future perspectives

Although stimulation of a dorsal or sacral afferent with a noisy wave represents the most powerful tool to electrically generate the locomotor rhythm in the isolated neonatal rat spinal cord (Taccola 2011), to date there is no clinical experience in the use of a similar protocol for epidural or peripheral stimulation.

Solving the complexity of the undulatory asynchronous stimulus used in our experiments may facilitate the introduction of new parameters for clinical electrostimulators. For this purpose, the isolated spinal cord, thanks to its well defined dorsal input and ventral motor output, represents a very useful model to assess the degree of recruitment of locomotor network through afferent electrical inputs.

Acknowledgments

I am grateful to Andrea Nistri and Elisa Ius for the excellent assistance in preparing the manuscript. A special thanks to M. Saccavini for providing the kinematic traces, in collaboration with P. Prati and D. Mazzoli from the Sol et Salus Hospital, Torre Pedrera, Rimini. We are also grateful to R. Blanco and to C. Pinzini and G. De Maio for the assistance during EMG recordings and to M. Delle Vedove for the helpful share of opinion. This work was supported by a grant from the Friuli Venezia Giulia Region, Azienda per i Servizi Sanitari no. 4 Medio Friuli, VERTICAL Foundation (Rome) and Associazione Tetra - Paraplegici FVG (Udine).

Conflict of Interest

None declared.

References

Berg, R. W., A. Alaburda, and J. Hounsgaard. 2007. Balanced inhibition and excitation drive spike activity in spinal half-centers. Science 315:390–393.

Bizzi, E., V. C. Cheung, A. d'Avella, P. Saltiel, and M. Tresch. 2008. Combining modules for movement. Brain Res. Rev. 57:125–133.

Brooke, J. D., W. E. McIlroy, and D. F. Collins. 1992. Movement features and H-reflex modulation. I. Pedalling versus matched controls. Brain Res. 582:78–84.

Davis, R. B., S. Õunpuu, D. Tyburski, and J. R. Gage. 1991. A gait analysis data collection and reduction technique. Hum. Mov. Sci. 10:575–587.

De Luca, C. J. 1997. The use of surface electromyography in biomechanics. J. Appl. Biomech. 13:135–163.

Dose, F., and G. Taccola. 2012. Coapplication of noisy patterned electrical stimuli and NMDA plus serotonin facilitates fictive locomotion in the rat spinal cord. J. Neurophysiol. 108:2977–2990.

Ferrigno, G., and A. Pedotti. 1985. ELITE: a digital dedicated hardware system for movement analysis via real-time TV signal processing. IEEE Trans. Biomed. Eng. 32: 943–950.

Gunkel, M. 1962. Relative coordination in voluntary limb movements in man. Pflügers Arch. 275:427–477.

deGuzman, C. G., and J. A. S. Kelso. 1991. Multifrequency behavioral patterns and the phase attractive circle map. Biol. Cybern. 64:485–495.

Harkema, S., Y. Gerasimenko, J. Hodes, J. Burdick, C. Angeli, Y. Chen, et al. 2011. Effect of epidural stimulation of the

lumbosacral spinal cord on voluntary movement, standing, and assisted stepping after motor complete paraplegia: a case study. Lancet 377:1938–1947.

Hermens, H. J., B. Freriks, C. Disselhorst-Klug, and G. Rau. 2000. Development of recommendations for SEMG sensors and sensor placement procedures. J. Electromyogr. Kinesiol. 10:361–374.

Huang, V. S., A. Haith, P. Mazzoni, and J. W. Krakauer. 2011. Rethinking motor learning and savings in adaptation paradigms: model-free memory for successful actions combines with internal models. Neuron 70:787–801.

Johnson, M. A., J. Polgar, D. Weightman, and D. Appleton. 1973. Data on the distribution of fibre types in thirty-six human muscles. An autopsy study. J. Neurol. Sci. 18:111–129.

Juvin, L., J. Simmers, and D. Morin. 2007. Locomotor rhythmogenesis in the isolated rat spinal cord: a phase-coupled set of symmetrical flexion extension oscillators. J. Physiol. 583:115–128.

Kiehn, O., and O. Kjaerulff. 1996. Spatiotemporal characteristics of 5-HT and dopamine-induced rhythmic hindlimb activity in the in vitro neonatal rat. J. Neurophysiol. 75:1472–1482.

Lee, C., D. Won, M. J. Cantoria, M. Hamlin, and R. D. de Leon. 2011. Robotic assistance that encourages the generation of stepping rather than fully assisting movements is best for learning to step in spinally contused rats. J. Neurophysiol. 105:2764–2771.

Marchetti, C., M. Beato, and A. Nistri. 2001. Alternating rhythmic activity induced by dorsal root stimulation in the neonatal rat spinal cord in vitro. J. Physiol. 530:105–112.

McIlroy, W. E., D. F. Collins, and J. D. Brooks. 1992. Movement features and H-reflex modulation. II. Passive rotation, movement velocity and single leg movements. Brain Res. 582:85–93.

Peper, C. E., and R. G. Carson. 1999. Bimanual coordination between isometric contractions and rhythmic movements: an asymmetric coupling. Exp. Brain Res. 129:417–432.

Raasch, C. C., and F. E. Zajac. 1999. Locomotor strategy for pedaling: muscle groups and biomechanical functions. J. Neurophysiol. 82:515–525.

Ryckebusch, S., and G. Laurent. 1994. Interactions between segmental leg central pattern generators during fictive rhythms in the locust. J. Neurophysiol. 72:2771–2785.

Savin, D. N., S. C. Tseng, and S. M. Morton. 2010. Bilateral adaptation during locomotion following a unilaterally applied resistance to swing in nondisabled adults. J. Neurophysiol. 104:3600–3611.

Stein, R. B. 1995. Presynaptic inhibition in humans. Prog. Neurobiol. 47:533–544.

Taccola, G. 2011. The locomotor central pattern generator of the rat spinal cord in vitro is optimally activated by noisy dorsal root waveforms. J. Neurophysiol. 106:872–884.

Taccola, G., C. Marchetti, and A. Nistri. 2004. Role of group II and III metabotropic glutamate receptors in rhythmic patterns of the neonatal rat spinal cord in vitro. Exp. Brain Res. 156:495–504.

Taccola, G., M. Mladinic, and A. Nistri. 2010. Dynamics of early locomotor network dysfunction following a focal lesion in an in vitro model of spinal injury. Eur. J. Neurosci. 31:60–78.

Thrasher, T. A., J. S. Ward, and S. Fisher. 2011. Classification of rhythmic locomotor patterns in electromyographic signals using fuzzy sets. J. Neuroeng. Rehabil. 8:65.

Wakeling, J. M., and T. Horn. 2009. Neuromechanics of muscle synergies during cycling. J. Neurophysiol. 101: 843–854.

White, B., L. F. Abbott, and J. Fiser. 2012. Suppression of cortical neural variability is stimulus- and state-dependent. J. Neurophysiol. 108:2383–2392.

Ziegler, M. D., H. Zhong, R. R. Roy, and V. R. Edgerton. 2010. Why variability facilitates spinal learning. J. Neurosci. 30:10720–10726.

OPEN ACCESS Freely available online

PLOS ONE

Nanomolar Oxytocin Synergizes with Weak Electrical Afferent Stimulation to Activate the Locomotor CPG of the Rat Spinal Cord *In Vitro*

Francesco Dose[1,2], Patrizia Zanon[1,2], Tamara Coslovich[1,2], Giuliano Taccola[1,2]*

1 Neuroscience Department, International School for Advanced Studies (S.I.S.S.A.), Trieste, Italy, **2** Spinal Person Injury Neurorehabilitation Applied Laboratory (S.P.I.N.A.L.), Istituto di Medicina Fisica e Riabilitazione (IMFR), Udine, Italy

Abstract

Synergizing the effect of afferent fibre stimulation with pharmacological interventions is a desirable goal to trigger spinal locomotor activity, especially after injury. Thus, to better understand the mechanisms to optimize this process, we studied the role of the neuropeptide oxytocin (previously shown to stimulate locomotor networks) on network and motoneuron properties using the isolated neonatal rat spinal cord. On motoneurons oxytocin (1 nM–1 μM) generated sporadic bursts with superimposed firing and dose-dependent depolarization. No desensitization was observed despite repeated applications. Tetrodotoxin completely blocked the effects of oxytocin, demonstrating the network origin of the responses. Recording motoneuron pool activity from lumbar ventral roots showed oxytocin mediated depolarization with synchronous bursts, and depression of reflex responses in a stimulus and peptide-concentration dependent fashion. Disinhibited bursting caused by strychnine and bicuculline was accelerated by oxytocin whose action was blocked by the oxytocin antagonist atosiban. Fictive locomotion appeared when subthreshold concentrations of NMDA plus 5HT were coapplied with oxytocin, an effect prevented after 24 h incubation with the inhibitor of 5HT synthesis, PCPA. When fictive locomotion was fully manifested, oxytocin did not change periodicity, although cycle amplitude became smaller. A novel protocol of electrical stimulation based on noisy waveforms and applied to one dorsal root evoked stereotypic fictive locomotion. Whenever the stimulus intensity was subthreshold, low doses of oxytocin triggered fictive locomotion although oxytocin *per se* did not affect primary afferent depolarization evoked by dorsal root pulses. Among the several functional targets for the action of oxytocin at lumbar spinal cord level, the present results highlight how small concentrations of this peptide could bring spinal networks to threshold for fictive locomotion in combination with other protocols, and delineate the use of oxytocin to strengthen the efficiency of electrical stimulation to activate locomotor circuits.

Citation: Dose F, Zanon P, Coslovich T, Taccola G (2014) Nanomolar Oxytocin Synergizes with Weak Electrical Afferent Stimulation to Activate the Locomotor CPG of the Rat Spinal Cord *In Vitro*. PLoS ONE 9(3): e92967. doi:10.1371/journal.pone.0092967

Editor: Michael Fehlings, University of Toronto, Canada

Received November 6, 2013; **Accepted** February 27, 2014; **Published** March 21, 2014

Funding: This work was supported by Vertical Foundation, Rome, Italy (http://www.fondazione-vertical.it). The funders had no role in study design, data collection and analysis, decision to publish, or preparation of the manuscript.

Competing Interests: The authors have declared that no competing interests exist.

* E-mail: taccola@sissa.it

Introduction

It is well known that the thoraco-lumbar spinal cord of mammals contains the neuronal hardware, indicated as central pattern generator (CPG), required to express the basic program that drives the alternated activation of flexor and extensor limb muscles during gait [1,2]. The locomotor output is already present at birth and depends on the biophysical properties of motoneurons and interneurons composing the CPG, as well as on the connectivity among the elements of the network [3].

Neuromodulatory substances sculpt the rhythmic CPG pattern and confer the necessary flexibility to the network in response to demands from the external environment and afferent inputs [4]. Among the wide family of neuromodulators, certain agents can trigger locomotion, while others can speed it up or facilitate it in concomitance with suitable stimuli [4]. Drugs in the latter category are the most interesting, as they might be used to synergize rehabilitation techniques that exploit the proprioceptive physiological feedback [5,6] to restore post-lesion locomotor patterns [7,8,9,10,11,12]. Unfortunately, the drugs tested so far have shown contrasting results, underpinning the need for more efficient conjoint strategies, using both afferent and pharmacological stimulations [13]. However, *in vitro* studies have shown that neuromodulators can differently affect the chemically and electrically evoked fictive locomotion (FL) [14,15,16], indicating the complexity of network targets.

The neuropeptide oxytocin is a nona-peptide endogenously synthesized in the central nervous system, at the level of hypothalamic nuclei, medial amygdale, locus coeruleus and olfactory bulb [17]. In the spinal cord, oxytocin is exclusively localized within axons [18] and the majority of oxytocin-containing fibers originate from the hypothalamic paraventricular nucleus (PVN) [19], as confirmed, in the rat, by the complete disappearance of oxytocin after lesioning the PVN [20,21]. Moderate presence of oxytocin-containing fibers (but not cell bodies) was confirmed in all laminae of the rat spinal cord, with clear predominance in laminae I, II, VII and X [22,23] especially at lumbar level [18].

Oxytocin, which during neonatal life plays a role as trophic or differentiating factor during spinal cord maturation [23,24], serves

as a neurotransmitter on receptors coupled to different G proteins to mobilize intracellular Ca^{2+} and either open a non-specific cationic channel or close a K^+ channel [25]. The neuronal distribution of oxytocin receptors (OTRs) parallels the distribution of its fibers [26,27]. Oxytocin, on par with other neuropeptides, does not seem to work directly on its target, but rather it appears to have a neuromodulatory action in making it more responsive to any incoming inputs [28]. Endogenous oxytocin concentrations in the rodent cerebrospinal fluid (CSF) range from 15 to 80 pg/mL [29], that is similar to values of the human neonatal CSF (20–30 pg/mL) [30]. In the spinal cord, the overall content of oxytocin is rather homogeneous (< 70 pg/mm of tissue), although three times more oxytocin has been found in the first lumbar segments [31], where the locomotor CPG is mainly localized [2]. Nonetheless, there are only few studies about oxytocin role in the chemically-evoked locomotor network activity in vitro [32,33]. Thus, there are no data on the effects of oxytocin in integrating afferent inputs into the CPG. The role of primary afferents in modulating the locomotor pattern is linked to the existence of sensory feedbacks evoked during gait to physiologically control, at a pre-synaptic level, incoming inputs to the spinal cord [34], and to convey facilitatory signals to the CPG via multisegmental sacrocaudal afferents [35], even with nociceptive content [36].

An innovative protocol of electrical stimulation, characterized by noisy waveforms and named FL*i*stim (Fictive Locomotion-induced stimulation) [37], has recently demonstrated to generate locomotor-like oscillations when delivered to a dorsal root (DR) or to sacrocaudal afferents of the isolated spinal cord.

Compared to classic protocols of electrical stimulation, which use trains of standard rectangular impulses [38], FL*i*stim requires a much lower stimulation strength and induces locomotor-like oscillations of longer duration [37]. Furthermore, FL*i*stim, as opposed to trains of pulses traditionally delivered to dorsal afferents, synergizes with sub-threshold concentrations of N-methyl-D-aspartate (NMDA) and serotonin (5-hydroxytryptamine, 5HT) to activate the CPG [39]. Using the *in vitro* rat spinal cord, the present study aims at exploring whether the neuropeptide could facilitate the effects of FL*i*stims, comparing it with chemically-evoked FL, and relating to its actions of synaptic transmission, network rhythmicity induced by pharmacological disinhibition [40] and motoneuron properties.

Methods

Spinal cord preparation and electrophysiological recordings

All experiments involving the use of rats and the procedures followed therein were approved by the Scuola Internazionale Superiore di Studi Avanzati (SISSA) ethics committee and are in accordance with the European Union guidelines. Animals were maintained in accordance with the guidelines of the Italian Animal Welfare Act. Spinal cords of neonatal Wistar rats (0 – 5 days old) were isolated from the mid-thoracic segments to the *cauda equine*, as previously described [41]. All efforts were made to minimize number and suffering of animals used for the experiments.

After surgical dissection, each spinal cord was mounted in a small recording chamber maintained at a constant room temperature of 22°C and continuously superfused (5 mL/min) with oxygenated (95% O_2 and 5% CO_2) Krebs solution, composed as follows (in mM): 113 NaCl, 4.5 KCl, 1 $MgCl_2$ $7H_2O$, 2 $CaCl_2$, 1 NaH_2PO_4, 25 $NaHCO_3$, and 11 glucose, pH 7.4.

For intracellular recordings, antidromically identified lumbar (L4 or L5) motoneurons [42] were impaled using microelectrodes filled with 3 M-KCl (30 – 40 MΩ resistance), in current-clamp conditions. The input resistance of motoneurons was obtained by delivering steps of current (amplitude from −0.8 to 0.8 nA, duration = 80 ms). Current/voltage plots were linear within the voltage range recorded and their slope indicates cell input resistance. In control conditions, baseline input resistance and membrane potential of motoneurons were, on average, 47.73±19.50 MΩ (from 24.30 MΩ to 72.03 MΩ) and −65.72±6.15 (n = 16), respectively.

Nerve recordings were performed in DC mode, using tight-fitting suction electrodes, from the lumbar (L) ventral roots (VRs). As a routine, recordings were obtained from the left (l) and right (r) L2 VRs, which mainly convey flexor motor-pool signals to hindlimb muscles, and from the l and r L5 VRs, principally expressing extensor commands to the same hindlimbs [43].

Therefore, the characteristic alternation among the discharges recorded from the flexor and extensor motor pools and between the left and right sides of the cord proves activation of the locomotor CPG. Signals were recorded, digitized and analyzed adopting pClamp software (version 10.3; Molecular Devices, PA, USA).

FL rhythm is elicited by the continuous bath application of NMDA (1,5–5 μM; Tocris, Bristol, UK) plus 5HT (4–10 μM; Sigma, Milan, Italy). Subthreshold pharmacological stimulation is obtained by reducing the concentration of NMDA + 5HT to the minimum required to induce a stable FL rhythm. To reduce the synthesis of endogenous 5HT, several experiments were performed where spinal cords were maintained overnight in Krebs solution containing the tryptophan hydroxylase inhibitor, p-chlorophenylalanine (PCPA, 10 μM; Sigma, Milan, Italy) in accordance with Branchereau et al. [44]. On the following day we recorded, in the continuous presence of PCPA, FL evoked by NMDA (5 μM) plus 5HT (10 μM). Afterwards, oxytocin (100 nM or 1 μM) was added to subthreshold concentrations of neurochemicals as indicated earlier. Control sham preparations were kept for the same period in Krebs solution, to confirm that maintaining the spinal cord for 1 day in vitro does not change the characteristics of chemically induced FL [45]. Longer in vitro maintenance was not viable, since after 2 days in vitro, only 1 out of 4 cords could express a brief episode of FL induced by NMDA (5 μM) and 5HT (10 μM).

Out of a series of 19 experiments, we considered for analysis only those which expressed stable FL after 10 min of continuous superfusion with NMDA (5 μM) + 5HT (10 μM): that is, 6 cords in Krebs solution and 9 in the group treated with PCPA (10 μM), respectively.

A disinhibited bursting, that was synchronous among all VRs, was produced by the pharmacological blockage of spinal inhibition, mediated by $GABA_A$ and glycine receptors, with a continuous bath-application of strychnine (1 μM; Tocris, Milano, Italia) and bicuculline methiodide (20 μM; Abcam PLC, Cambridge, UK). To validate the specificity of OTR activation, atosiban was used at the same concentration that showed a selective antagonism on *in vitro* experimental preparations of neonatal rat central nervous system (5 μM) [46]. To reduce synaptic input on motoneurons, the broad sodium channels blocker, TTX (Abcam PLC, Cambridge, UK), was applied at the concentration of 1 μM until electrically evoked antidromic spikes fully disappeared (5 min). Afterwards, TTX was continuously perfused at lower concentration (250 nM) to maintain sodium current block throughout the experiment [47].

Single or repetitive electrical stimulation of dorsal or ventral roots

Single electrical pulses were applied to either DRs or VRs via a bipolar suction electrode, in order to evoke either DR-DR potentials (DR-DRPs) [48], DR-VR potentials from the homologous VR (DR-VRPs) or antidromic action potentials from single motoneuron, respectively. Stimulus intensity was then calculated in terms of threshold (Th = 11.37±5.63 μA), which is defined as the minimum intensity required to elicit a detectable response from the homologous VR.

The stimulating protocol FL*i*stim (Fictive Locomotion-*induced* stimulation) used corresponds to a 60 s segment of a chemically induced FL recorded in AC mode from a VR, that was randomly selected (range 0.1 Hz – 10 000 Hz; sampling rate = 500 Hz). Through off-line analysis with Origin 9.0 software (OriginLab, North Hampton, MA), the maximum current amplitude was adjusted to pre-selected values, then the trace was exported (as an ASCII text file) to a programmable stimulator (STG 4002; Multi Channel Systems, Reutlingen, Germany). At last, FL*i*stim was delivered to one DR, using a bipolar suction electrode, at an optimal amplitude comprised within the range of 0.144±0.077×Th. On the other hand, adopted intensities for electrical subthreshold stimulation were considered equal to 0.095±0.069×Th.

Analysis of rhythmic activity

Each FL rhythm was analyzed in terms of periodicity (considered as the time between the onset of two consecutive cycles) and amplitude (defined as the height of signals, expressed in μV, calculated from the baseline at the beginning of each cycle to its peak). Furthermore, regularity of rhythmic patterns was expressed by the period coefficient of variation (CV; displayed as standard deviation [SD] mean^{-1}). The strength of coupling among pairs of VRs signals was defined by the cross-correlation function (CCF) analysis. A CCF greater than + 0.5 indicates that two roots are synchronous, while a CCF smaller than − 0.5 shows full alternation [49].

All parameters used for the definition of disinhibited bursting and its measures (duration, cycle period, number and frequency of intraburst oscillations) are in accordance with Bracci et al. [40]. Within each preparation and for each test conditions, at least 20 cycles of bursting were analyzed to average data.

All data are expressed as mean ± S.D., where "n" indicates the number of experiments. Before assessing statistical differences among groups, a normality test was performed to select the use of either parametric or non-parametric tests. Different statistical approaches were used to compare sets of data. For parametric values, the Student's t-test (paired or unpaired) was used for comparison between two groups of data and ANOVA (analysis of variance), followed by post hoc analysis with Dunnett's or Tukey method for more than two groups. When referring to non-parametric values, the tests used were Mann-Whitney or Wilcoxon for comparing two groups and Kruskal-Wallis ANOVA on ranks, followed by post hoc analysis with Dunn's method, for a number of groups greater than two. As for parametric data, one way repeated ANOVA measures were used when each one of the cords analyzed was exposed to more than two treatments. To assess the success rates in inducing an episode of alternating oscillations by weak FL*i*stims, plus increasing concentrations of oxytocin, with respect to weak FL*i*stim alone, we applied the chi-squared test. Collected results were considered significant when $P<0.05$.

Results

Nanomolar concentrations of oxytocin excite spinal motoneurons

The example of Fig. 1 A, recorded from a motoneuron under current clamp conditions, shows that, after 5 min application, oxytocin (100 nM) depolarized the cell (plateau amplitude = 8.85 mV), with superimposed firing activity (2.14 Hz). The effects of oxytocin waned after 30 min washout when a second exposure to oxytocin induced similar depolarization (8.76 mV) and firing (2.9 Hz). A longer perfusion (40 min) at a lower concentration (1 nM, Fig. 1B) induced, after 8 min, the appearance of sporadic bursts with superimposed action potentials, associated with minimal change in baseline at steady state (3 mV) that persisted through the entire application.

Two consecutive applications of oxytocin (1 μM, duration = 10 min), alternated with 20 min washout phases, were repeated on the same cell (Fig. 1 C) and induced comparable depolarizations (ΔV first application = 13.34 mV; ΔV last application = 13.12 mV). Thus, in our experiments, even at higher concentrations, no desensitization appeared when applications of oxytocin were spaced out by at least 20 min.

The average cumulative dose-response curve (Fig. 1 D), obtained from different (3–10) motoneurons, had a shallow slope extending over a 0.5–1000 nM range (EC_{50} of 72 nM). Fig. 1 D also shows that, for each concentration of oxytocin, there was no change in input resistance at rest (filled triangles; one way ANOVA on raw data; P = 0.995; n = 3–4). Hence, these results suggested that the depolarizing effect of oxytocin had a mainly indirect origin. We corroborated this hypothesis by performing experiments in the presence of tetrodotoxin (TTX; 250 nM) to block network synaptic transmission, in analogy with our former study [47]: the example in Fig. 1 E indicates absence of motoneuron depolarization under this condition, without any change in the frequency of miniature post synaptic potentials (1.17±0.24 Hz vs 1.08±0.07 in control TTX solution). Thus, the most likely explanation is that the depolarization mediated by oxytocin was not evoked by the direct action on motoneuron membrane, but it arose from the activation of a premotoneuron network.

Network effects of oxytocin

Extracellular recordings from several VRs expressing the discharge of motoneuron pools and their premotoneuron circuitry (as exemplified in Fig. 2 A) showed strong network activity induced by oxytocin (100 nM) consisting in an initial VR depolarization on both sides of the cord, reaching (after 2 min) a maximal peak of 0.50±0.25 mV (average data from the four recorded VRs) versus the control baseline. After 6 min of continuous application, VR depolarization declined to a stable value (0.31±0.19 mV) versus the control baseline before oxytocin application. During the initial depolarization, irregular VR activity emerged together with bursts (synchronous among all VRs; Fig. 2 B), which eventually faded away.

In a series of six preparations, for each spinal cord, the steady state depolarization induced by 100 nM oxytocin on each VR was recorded and averaged among the four roots to provide the datapoints used to construct the histogram shown in Fig. 2C (0.33±0.20 mV).

We next explored whether the network effects induced by oxytocin were associated to any change in reflex activity. One representative experiment is shown in Fig. 3 A, B in which we averaged five consecutive Dorsal Root-evoked Ventral Root Potentials (DR-VRPs) elicited on one lumbar VR by weak (A) or

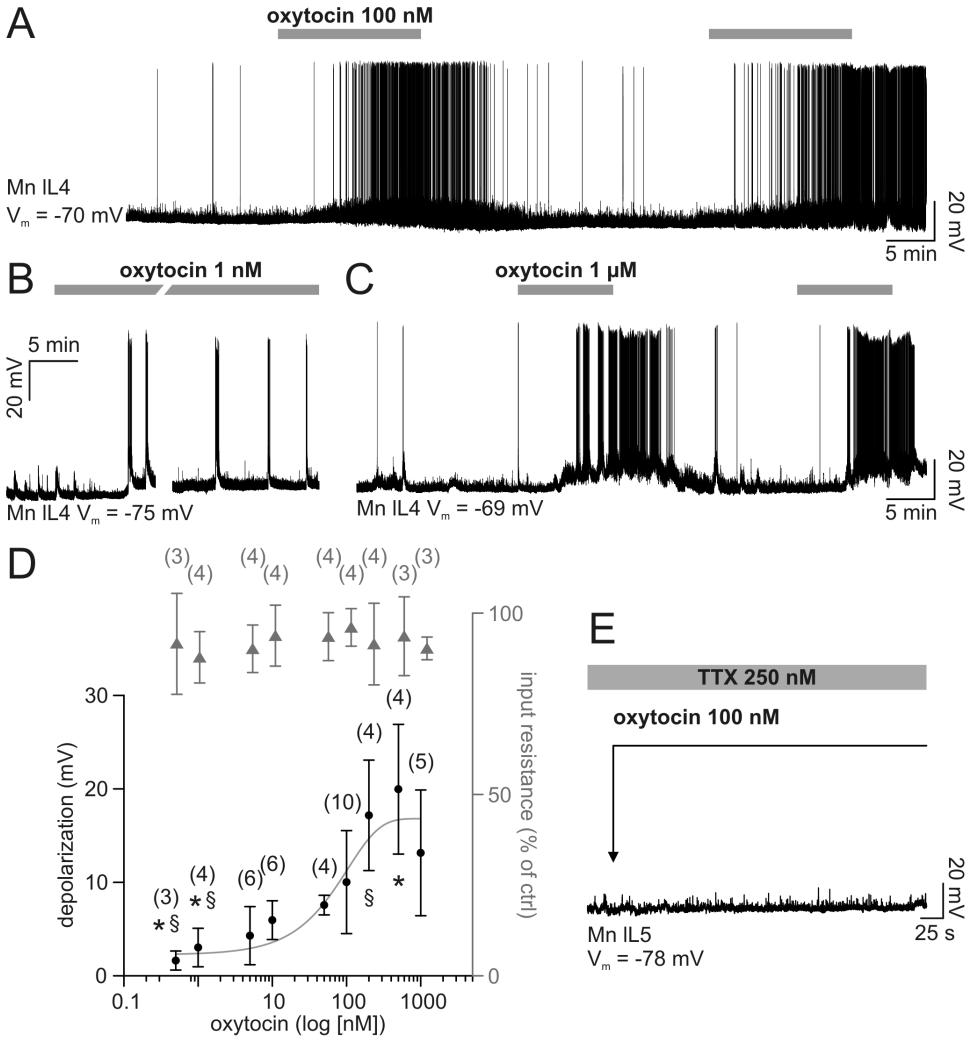

Figure 1. Oxytocin indirectly depolarizes single motoneurons. A, intracellular recording from a single motoneuron (IL4) shows that, after 5 min, oxytocin (100 nM; see gray bars) depolarises membrane potential and evokes high frequency spiking. Initial resting potential (V_m) is −70 mV. B, lower concentration of oxytocin (1 nM; see bar) determines a slower (8 min) onset of bursts with intense firing activity despite minimal baseline depolarization that persists throughout the long neuropeptide perfusion (40 min). Initial resting potential is −75 mV. Note that the 10 min trace break corresponds to the time spent in generating tests for the cell I/V curve. Different cell from A. C, two consecutive applications of oxytocin (1 µM) induce reproducible responses when timed 20 min apart. Initial resting potential is −69 mV. Different cell from A, B. D, dose response plots of membrane potential depolarization (from baseline; fitted with sigmoidal curve; filled circles) and input resistance (as percentage value with respect to control; gray triangles) for cumulative doses of oxytocin (log scale). Symbols *, § indicate significant difference versus the higher concentrations data (Kruskal-Wallis one way ANOVA on ranks followed by all pairwise multiple comparison with Dunn's method; $P<0.001$; the number of preparations used to calculate the mean is shown in parentheses; the error bars indicate SD). E, sample trace from a single motoneuron (IL5) demonstrates that oxytocin (100 nM) fails to depolarize the cell when applied (see arrow) in the presence of network block by TTX (250 nM; gray bar).
doi:10.1371/journal.pone.0092967.g001

strong (B) electrical pulses (gray arrows). When weak DR stimuli (intensity = 10 µA, Th, 1×Th) were used to activate low threshold afferent fibers, 100 nM oxytocin induced a reversible depression of DR-VRPs (Fig. 3 A), as confirmed by the mean values pooled from five spinal cords (Fig. 3 C). On the other hand, at a higher stimulating strength (3×Th), the same oxytocin concentration (100 nM) did not produce any significant change in peak and area of polysynaptic responses (Fig. 3 B middle), while only a 10-fold larger concentration (1 µM) did depress reflexes (Fig. 3 B right). On average, at higher intensities of stimulation, concentrations of oxytocin up to 100 nM did not change DR-VRPs (Fig. 3 D), while a significant decrease (by 20 – 25% vs control) in peak reflex amplitude was detected at 200 nM and 1 µM oxytocin.

Augmenting concentrations of oxytocin speeded up the disinhibited rhythm by acting selectively on oxytocin receptors

The emergence of irregular bursts during oxytocin application suggested that this neuropeptide could trigger, albeit for a short time, the intrinsic rhythmicity manifested as synchronous discharges from VRs. To further explore this issue, we examined how oxytocin could affect the spontaneous bursting of spinal networks, which appears when spinal inhibition mediated by $GABA_A$ and glycine receptors is blocked by strychnine (1 µM) and bicuculline (20 µM) and requires a minimal circuitry restricted to a ventral quadrant of the spinal cord [40].

In the example of Fig. 4 A, a stable disinhibited rhythm (top trace) was speeded up by 5 nM oxytocin, without changing burst

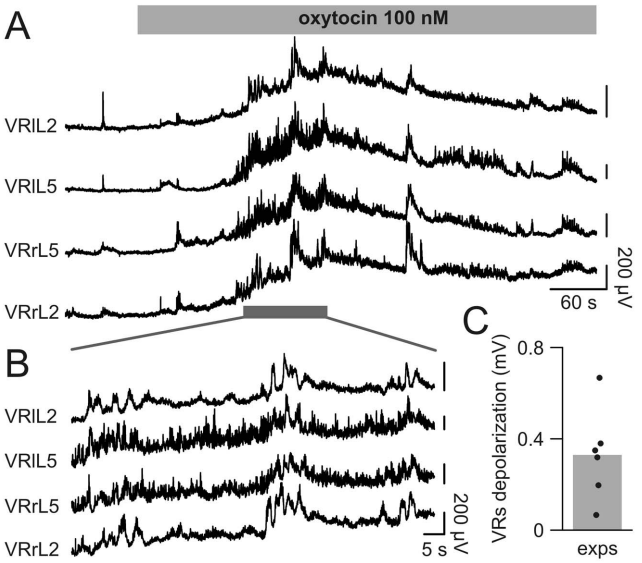

Figure 2. Oxytocin induces VR rhythmic activity. The application of 100 nM of oxytocin (gray bar) depolarizes bilateral VRs at L2 and L5 levels (A). The early phase of VR depolarization is associated with bursts synchronous among all roots, followed by a partial repolarization. B, the rhythmic activity evoked by oxytocin on the four VRs shown in A (gray bar) is displayed, on a faster time scale, to depict synchronous bursts composed of apparently unrelated, fast intraburst oscillations. Histogram (C) illustrates, for each spinal cord, the average depolarization (recorded from 4 VRs) induced by oxytocin 100 nM, while the gray bar shows the mean value of all experiments. All vertical bars are 200 µV.
doi:10.1371/journal.pone.0092967.g002

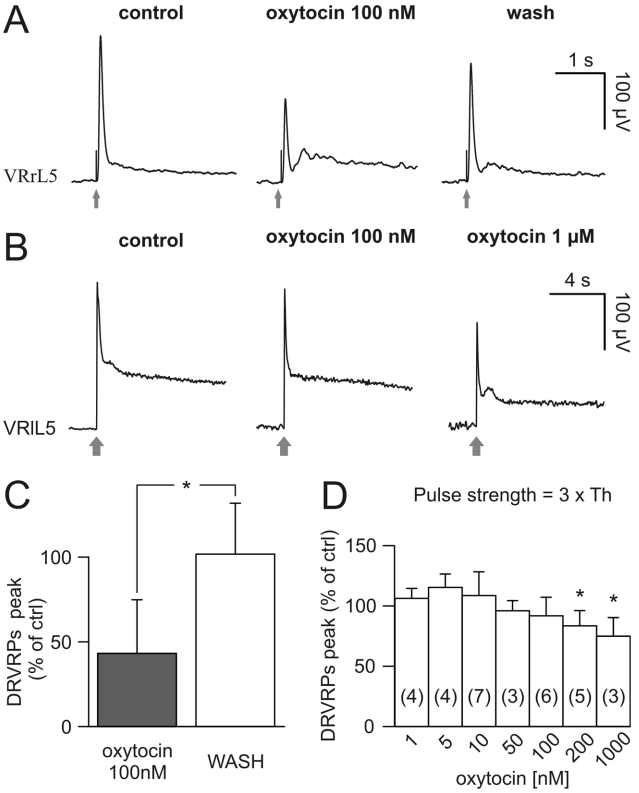

Figure 3. Oxytocin differentially affects DR-VRPs. A, the monosynaptic response elicited by stimulating the homologous DR at just threshold intensity (duration = 0.1 ms; intensity = 15 µA, 1×Th) is significantly depressed by the addition of 100 nM of oxytocin, an effect that partially reversed after 20 min washout. B, DR-VRPs, extracellularly recorded from VRIL5, are evoked by strong electrical stimulation of the homologous DR (duration = 0.1 ms; intensity = 45 µA, 3×Th; arrows) in control (left), or after applying oxytocin 100 nM (middle) and 1 µM (right). Note records in B are shown on a slower time base to display the secondary component of polysynaptic DR-VRP and, therefore, hide the stimulus artifact. Only the highest tested concentration of the neuropeptide is able to reduce the peak of reflex response. Traces in A and B are mean values from five events and are obtained from different spinal cords. Histograms (C) show summary of responses to low strength of stimulation (1×Th) with significant reduction in the percentage peak obtained from 5 experiments (*; Mann-Whitney rank sum test; P = 0.016). D shows the average percentage variation in peak amplitude of DR-VRPs (with respect to control) evoked by strong stimuli (3×Th), against cumulative increase in oxytocin concentrations. Only the higher concentrations (0.2–1 µM) significantly depress responses (*; Kruskal-Wallis one way ANOVA on ranks followed by multiple comparison vs WASH with Dunn's method; P = 0.004, the number of preparations used to calculate the mean is shown in parentheses; the error bars indicate SD).
doi:10.1371/journal.pone.0092967.g003

amplitude. On the same preparation, further increases in rhythm frequency were obtained with 100 nM or 1 µM oxytocin. The cumulative dose-response curve in Fig. 4 B reports a dose-dependent reduction in the mean period (expressed as a percent of control) for increasing concentrations of oxytocin (0.5 nM – 10 µM), with an IC_{50} of 55 nM (n = 3–6) with an effect saturation amounting to circa 60% acceleration. Oxytocin did not significantly modify burst amplitude (gray triangles in Fig. 4 B; Kruskal-Wallis one way ANOVA, P = 0.961, n = 3–6) and bursting regularity (calculated as CV value; one way ANOVA, P = 0.300, n = 3–6).

The structure of single disinhibited bursts was altered by the addition of the neuropeptide. In particular, despite an unchanged first phase of depolarizing plateau (one way ANOVA, P = 0.117, n = 9), the total duration of the single burst was reduced (one way ANOVA, P = 0.021, n = 3–6), along with faster intraburst oscillations (one way ANOVA, P = 0.034, n = 3–6), while their number remained unaffected (one way ANOVA, P = 0.765, n = 3–6).

In the presence of strychnine and bicuculline, oxytocin (100 nM) slowly depolarized VRs with a plateau (10 min) of 0.77±0.10 mV (n = 3), which did not statistically differ from the depolarization elicited by the neuropeptide in control conditions (t-test, P = 0.355).

The effects of oxytocin were mediated by OTRs as demonstrated by applying the selective pharmacological antagonist, atosiban (5 µM) that (as shown in Fig. 4 C), without modifying *per se* rhythm features, fully prevented burst acceleration and VR depolarization by 100 nM oxytocin. This observation suggests that OTRs are not endogenously activated during disinhibited rhythm, yet mediate the action of exogenously-applied oxytocin. The histograms in Fig. 4 D summarize the average values of bursting periodicity obtained from 4–6 experiments. While oxytocin (100 nM) significantly reduced the period (black bar), there was no significant variation with atosiban (5 µM) alone or of atosiban plus oxytocin. These results are consistent with an action by oxytocin on spinal networks accessory to the rhythmic ones and capable of modulating intrinsic rhythmicity.

Neither oxytocin nor atosiban altered frequency and regularity of oscillations of the chemically evoked fictive locomotion

The discrete effects by oxytocin on spontaneous bursting prompted further experiments to find out if the peptide could

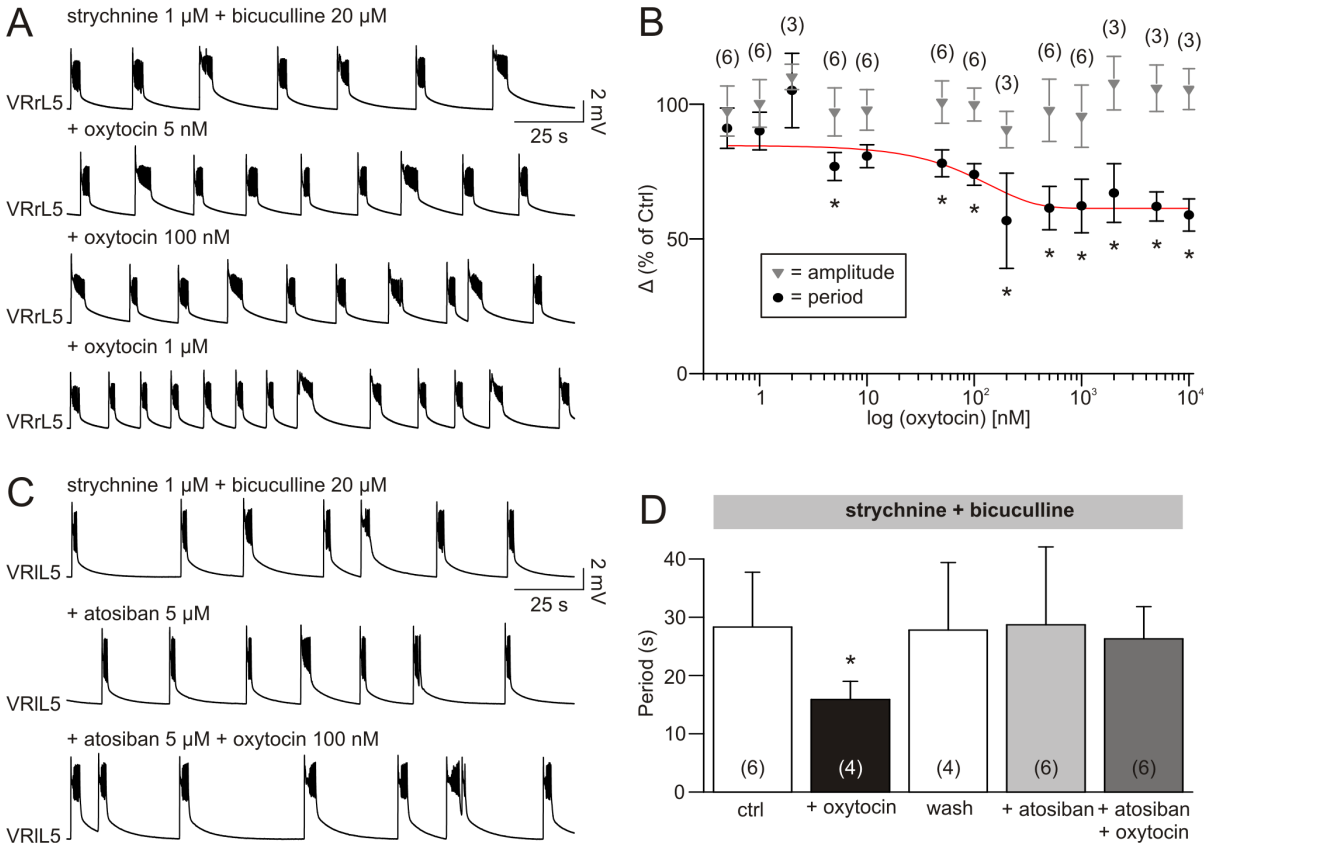

Figure 4. Disinhibited bursting is accelerated by oxytocin, an effect prevented by its selective antagonist. A, regular disinhibited rhythm induced by 1 μM strychnine and 20 μM bicuculline (top trace in A) is stably sped up (with burst length reduction) by the cumulative addition of oxytocin (5, 100 nM and 1 μM), without any further modifications in the characteristics of single bursts. The cumulative dose response curve in B indicates significant reduction in the average period (expressed as a percentage of the mean variation), starting at concentration of 5 nM (*; one way ANOVA followed by multiple comparison vs strychnine + bicuculline only with Dunnett's method; P = <0.001; the number of preparations used to calculate the mean is shown in parentheses; the error bars indicate SD). C, on a different preparation, a stable disinhibited rhythm (top) remains unchanged by the addition of the OTRs antagonist, atosiban (5 μM, middle), which prevents any acceleration during the following addition of oxytocin (100 nM). The histograms in D, which report the average value of period of disinhibited rhythm in correspondence to the different treatments, show significant rhythm acceleration in the presence of oxytocin (100 nM), an effect reverted to control values after washout (30 min), and prevented by the addition of atosiban (5 nM), which does not *per se* vary rhythm periodicity (*; Kruskal-Wallis one way ANOVA on ranks followed by multiple comparison vs strychnine + bicuculline only with Dunn's method; P = 0,038; the number of preparations used to calculate the mean is shown in parentheses; the error bars indicate SD).
doi:10.1371/journal.pone.0092967.g004

modulate locomotor-like oscillations that require a more complex pattern of rhythmic activity including reciprocal inhibition [1]. Fig. 5 A shows (on a slow time base) a stable FL rhythm evoked by 5 μM of NMDA and 10 μM of 5HT (open horizontal bar). On a faster time base, a sample of this record clearly demonstrates the characteristic double alternation of FL cycles recorded from L2 and L5 VRs on both sides of the cord (Fig. 5 B). Addition of 100 nM oxytocin (gray bar in Fig. 5 A) depolarized VRs (0.27±0.06 mV average from four VRs) and reduced the amplitude of locomotor cycles, without modifying frequency or regularity of rhythm (Fig. 5 C). The same observation was repeated with a random sample of 9 experiments, that gave an average depolarization of 0.35±0.22 mV, not statistically different from the depolarization elicited by oxytocin (100 nM) in control conditions (t-test, P = 0.284).

Oxytocin (100 nM) did not modify period (paired t-test, P = 0.054, n = 13) or regularity (Wilcoxon signed rank test, P = 0,094, n = 13) of FL rhythm, while the amplitude of FL oscillations was significantly reduced in each preparation (Fig. 5 D).

Additional experiments were performed in order to verify whether higher doses of oxytocin could vary any of the rhythm parameters unaffected by 100 nM oxytocin. In five spinal cords, on which oxytocin was tested at 100 nM and 1 μM during a stable FL, period or CV values were not statistically different for either concentrations (one way repeated measures ANOVA, P = 0.808 and P = 0.927, respectively), while cycle amplitude was equally reduced by either concentrations with respect to their control (Fig. 5 E; one way repeated measures ANOVA followed by all pairwise multiple comparison procedures with Tukey test, P = 0.004). Finally, as demonstrated with the example of Fig. S1, the oxytocin receptor antagonist atosiban (5 μM) applied together with NMDA (5 μM) and 5HT (10 μM) did not change FL. On average, on 6 spinal cords, the addition of atosiban (5 μM) to a stable FL rhythm induced by NMDA and 5HT did not depolarize VRs (0.20±0.45 mV), nor did it modify period (3.56±1.09 s in ctrl vs. 3.86±0.53 s plus atosiban; paired t-test, P = 0.606), regularity of alternating oscillations (Wilcoxon signed rank test, P = 0.563) or cycle amplitude (Wilcoxon signed rank test, P = 0.688).

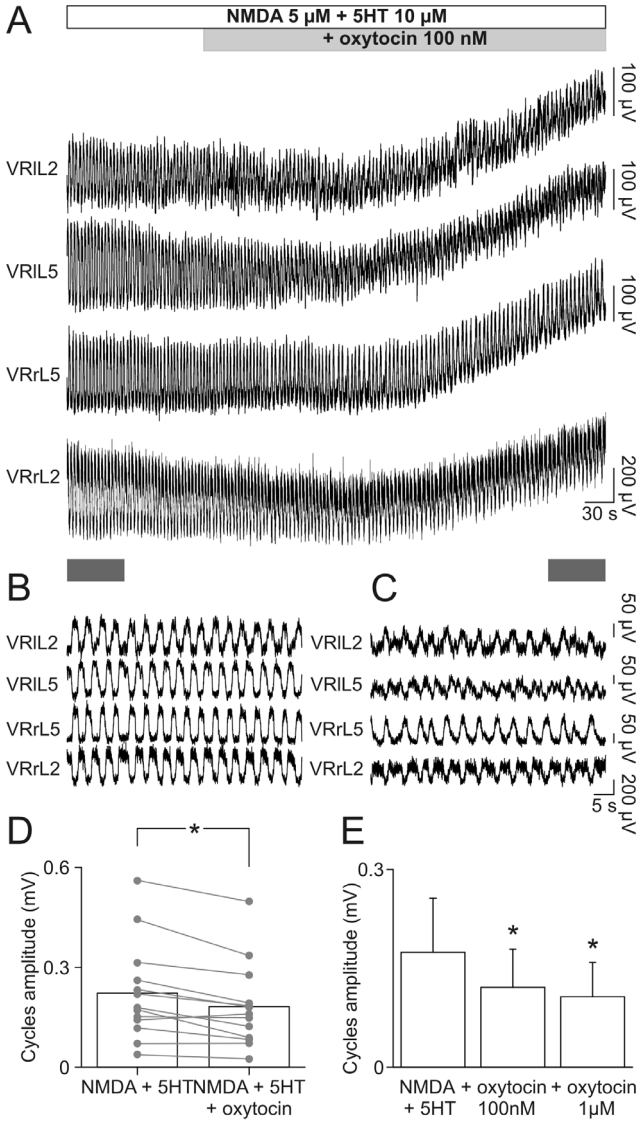

Figure 5. Oxytocin decreases cycle amplitude of FL without changing periodicity. A, a stable FL is induced by the application of 5 μM NMDA and 10 μM 5HT. A sample of traces, corresponding to the gray bar in the bottom-left, shows, on a faster time base, the characteristic double alternation among L2 and L5 homosegmental and homolateral VRs (B). Addition of oxytocin (100 nM; see gray bar in A, top) depolarizes all VRs. As depicted in the insert corresponding to the gray bar in the bottom-right of A, in the presence of oxytocin oscillations maintain their typical double alternation, although with smaller amplitude. The scatter plot in D reports the single values of cycle amplitude for different experiments (gray dots and lines), pointing out the significant reduction in average amplitude of oscillations (open bars) after the addition of oxytocin (0.22±0.15 and 0.18±0.13 mV, respectively; *; paired t-test; P = 0,001; n = 13). Histograms in E depict the reduction in amplitude of FL oscillations in correspondence to cumulative increase in oxytocin concentrations (100 nM and 1 μM) that are equally able to reduce cycle amplitude with respect to control (*, one way repeated measures ANOVA followed by all pairwise multiple comparison procedures with Tukey test, P = 0.004, n = 5).
doi:10.1371/journal.pone.0092967.g005

Synergy between oxytocin and NMDA plus 5HT in eliciting FL

Although OTRs did not physiologically control chemically-induced FL, we explored whether the accelerating property shown by this neuropeptide could be exploited to facilitate the activation of locomotor circuits. For this reason a stable FL was first induced using the lowest effective concentrations of NMDA and 5HT (Fig. 6 A). Afterwards, the concentration of neurochemicals was decreased to slow down rhythm period (Fig. 6 B), and eventually to replace FL with a mere irregular activity (Fig. 6 C). Doses of oxytocin as low as 1 nM were not able to re-establish alternating discharges (Fig. 6 D). However, by combining the application of oxytocin (100 nM) with low concentrations of neurochemicals, stable locomotor oscillations reappeared (Fig. 6 E). A further increase in oxytocin concentrations did not modify the features of the reinstated FL (Fig. 6 F).

Similar experiments were repeated with 12 preparations, in which 100 nM oxytocin in the presence of subthreshold concentrations of neurochemicals induced a FL similar to control for mean period, period CV and cycle amplitude (Table S1 summarizes these data). To explore the possibility that an increase in oxytocin might change any of the parameters related to the rhythm rescued by 100 nM oxytocin, we cumulatively added 1 μM oxytocin to subthreshold concentrations of neurochemicals. On average, neither periodicity (one way repeated measures ANOVA, P = 0.313, n = 3), regularity (one way repeated measures ANOVA, P = 0.232, n = 3) nor cycle amplitude (one way repeated measures ANOVA, P = 0.296, n = 3) were further affected. Finally, in five experiments, oxytocin applied within the concentration of 1–50 nM was unable to activate a subthreshold FL.

Oxytocin facilitation of fictive locomotor patterns requires endogenous 5HT synthesis

Since OTRs are reported to modulate the release of 5HT [50,51] that largely contributes to FL [52], it seemed likely that oxytocin-mediated increase in endogenous 5HT release contributed to bring FL patterns to threshold. To explore this hypothesis, we performed experiments in which the isolated spinal cord was treated overnight with the inhibitor of the tryptophan hydroxylase, p-chlorophenylalanine (PCPA, 10 μM), with the aim of reducing the synthesis of endogenous 5HT. Fig. 7 shows two typical experiments run in parallel, in which two different spinal cords were kept overnight in a Krebs (A) or PCPA (10 μM; B) solution, respectively. On the second day, in the presence of NMDA (5 μM) and 5HT (10 μM), both preparations displayed a stable FL (Fig. 7 A,B, left panels). On average, all cords tested the day after, showed a FL period of 2.98±1.22 s (CV = 0.12±0.04; n = 15), without any significant difference between the sham group and the one treated with PCPA (t-test, P = 0.843, n = 6–9).

After washout (20 min), preparations were first perfused with subthreshold concentrations of neurochemicals (Fig. 7 A,B, second panels) to which 100 nM oxytocin was subsequently added (Fig. 7 A,B) without emergence of any FL. In the example depicted in Fig. 7 A (right), further increase in oxytocin concentration (1 μM) triggered a stable FL similar to control for period (90% of control), CV (0.12 vs 0.15 in control) and amplitude (90% of control) values. This observation was replicated in three out of four sham spinal cords, as 1 μM oxytocin re-established the FL rhythm with regularity (CV period = 0.12), period (paired t-test, P = 0.266, n = 3) and amplitude (paired t-test, P = 0.669, n = 3) comparable to those induced on the same preparations by NMDA (5 μM) and 5HT (10 μM). On the contrary, in all preparations treated with PCPA (10 μM), as exemplified in Fig. 7 B, oxytocin at 100 nM (9/9) or 1 μM (7/7) concentration never triggered FL in the presence of subthreshold NMDA and 5HT, even if these preparations displayed control patterns with NMDA (5 μM) plus 5HT (10 μM).

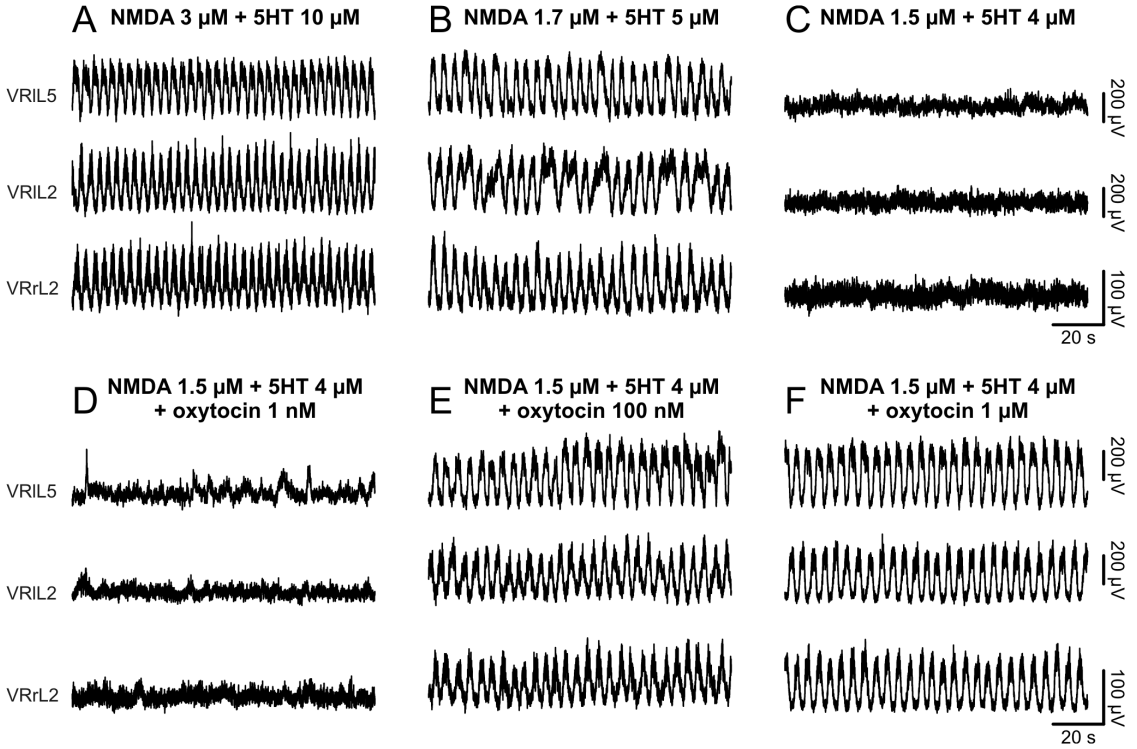

Figure 6. Oxytocin reinstates fictive locomotor oscillations, despite subthreshold concentrations of neurochemicals. Alternating oscillations of a stable FL, evoked by the addition of 3 μM NMDA and 10 μM 5HT (A), slow down once the concentration of neurochemicals is finely titrated down to 1.7 μM NMDA and 5 μM 5HT (B). A further decrease in NMDA (1.5 μM) + 5HT (4 μM) suppresses locomotor-like discharges, which are finally replaced by a tonic activity (C). By adding oxytocin (1 nM) to subthreshold concentrations of NMDA and 5HT, no FL oscillations reappear (D). By augmenting the neuropeptide to 100 nM, locomotor-like oscillations are restored (E). Further increase in oxytocin (1 μM) does not affect periodicity of the reinstated pattern nor its cycle amplitude (F).
doi:10.1371/journal.pone.0092967.g006

Nanomolar concentrations of oxytocin synergize with the delivery of innovative protocols of low intensity electrical stimulation

The novel FL*i*stim protocol of DR electrical stimulation based on capturing the FL cycles and applying them to one DR, has been shown to optimally activate the *in vitro* CPG much more effectively than standard trains of DR pulses: the resulting rhythm shows, however, stereotypic periodicity [37].

The present study investigated whether oxytocin could synergize with a subthreshold FL*i*stim. Fig. 8 shows one example taken from the same preparation tested with various protocols. Thus, the FL*i*stim protocol (duration = 60 s, intensity = 0.2×Th) [37,39] was first applied to a sacral DR, inducing a cumulative depolarization with superimposed an episode of alternating cycles on L2 and L5 VRs (on both sides), lasting throughout the delivery of the stimulating pattern (Fig. 8 A). At the same strength of stimulation, alternating oscillations evoked by FL*i*stim were not statistically modified by the conjoint application of oxytocin (1 – 100 nM; not shown).

By lowering the strength of FL*i*stim (0.1×Th), the resulting cumulative depolarization was smaller with sporadic oscillations, synchronous among all VRs (Fig. 8 B). Nevertheless, applying the lowest tested concentration of oxytocin (1 nM), the weak FL*i*stim was now able to evoke a cumulative depolarization (0.97 mV) with a superimposed episode of FL (Fig. 8 C), comparable to the one recorded in control with FL*i*stim delivered at optimal amplitude (0.2×Th; Fig. 8 A). However, increasing oxytocin up to 100 nM (to induce 0.96 mV cumulative depolarization *per se*) together with FL*i*stim at 0.1×Th failed to elicit a FL (Fig. 8 D).

The cross-correlograms on the pair of homosegmental VRs at L2 level for the three protocols are superimposed in Fig. 8 E to assess cycle alternation. Thus, the negative peak centred around zero lag during the coapplication of 0.1×Th FL*i*stim plus oxytocin 1 nM (red trace) confirms FL pattern comparable to the one evoked by FL*i*stim at 0.2×Th (blue trace), while the plot for 0.1×Th FL*i*stim alone yielded a flat trace (black), indicating uncorrelated activity.

In eight experiments, oxytocin (1 nM) in combination with a weak FL*i*stim, always triggered the onset of FL as much as a stronger FL*i*stim did. Conversely, the probability to induce FL fell with stepwise increase in oxytocin concentrations, while keeping the same weak FL*i*stim (Fig. 8 F) without variation in the amplitude of cumulative depolarization (Kruskal Wallis one way ANOVA on ranks followed by post hoc analysis with Dunn's method, $P = 0.286$; $n = 8$).

One component of the oxytocin complex action on FL*i*stim might have comprised dose-dependent modulation of pre-synaptic inhibition on afferent inputs investigated as reported by Hochman et al. [53]. Thus, experiments were performed in which dorsal root potentials were recorded in response to electrical stimulation of the adjacent dorsal root (DR-DRPs), at both low and high pulse strength (Fig. S2 A, B). In the presence of oxytocin (1 or 100 nM), no differences were observed in the peak amplitude of DR-DRPs, at either low (Fig. S2 C) or high (Fig. S2 D) intensity, or in the area recorded with the high-strength stimulation (Fig. S2 E). These results show that the enhancement in post-synaptic responses

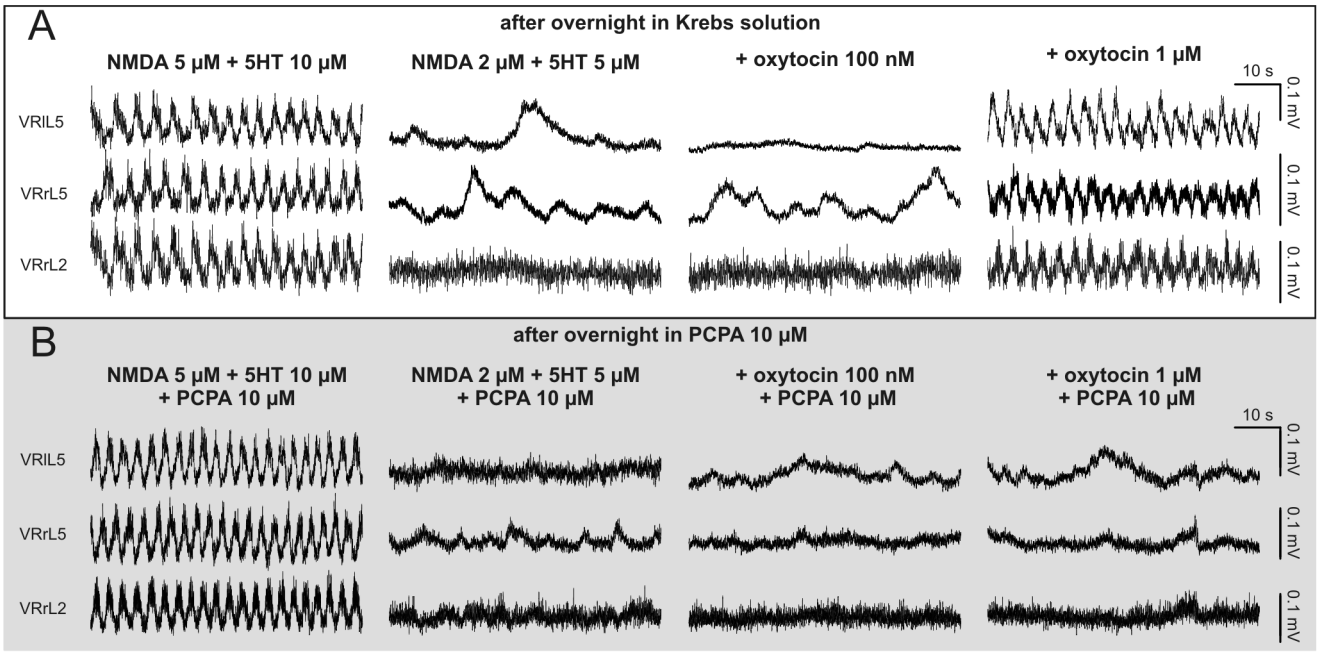

Figure 7. Inhibitor of endogenous 5HT synthesis prevents facilitation by oxytocin of FL. Two different preparations are maintained overnight in Krebs solution, upper traces (A), or in the presence of the inhibitor of 5HT synthesis (PCPA, 10 μM; lower traces, light gray field, B), respectively. On the following day, in both preparations, a stable FL is recorded in the presence of NMDA (5 μM) plus 5HT (10 μM; A, B, left). By decreasing the concentration of neurochemicals, alternating oscillations are replaced by a tonic activity with slow depolarizing events, apparently unrelated among different VRs (A, B, second panels). The addition of oxytocin (100 nM) to subthreshold concentrations of NMDA and 5HT fails to reinstate FL (A, B, third panels). However, further increase in oxytocin to 1 μM induces reappearance of a stable FL only in the preparation maintained in Krebs solution (A, right), while, in the one incubated with PCPA, no alternating oscillations are observed (B, right). Note that PCPA (10 μM) is continuously perfused during all different experimental phases conducted on the spinal cords treated in PCPA overnight (B).
doi:10.1371/journal.pone.0092967.g007

generated by the downstream motor networks after application of oxytocin, was not accompanied by any detectable modulation of pre-synaptic inhibition on primary afferent signals.

Discussion

The present study analyses the complex effects evoked by oxytocin in modulating the basal characteristics of single motoneurons, the synaptic responses induced by afferent stimulation, and two different types of locomotor network activity. Although these data were collected from the *in vitro* mammal spinal cord, they can help to interpret the functional impact of oxytocin targets on spinal circuits and emphasize how even nanomolar concentrations of this neuropeptide could synergize with innovative stimulation protocols to elicit locomotor network activation.

Facilitatory effects by oxytocin

While application of oxytocin *per se* never elicited FL in line with previous observations [32,33], the peptide did evoke a number of responses that ranged from dose-related motoneuron depolarization (lacking change in input resistance) with repetitive or burst firing, VR depolarization associated with synchronous discharges, and acceleration of disinhibited bursting (with burst length reduction). All these effects were persistent and showed no tachyphylaxis. When network activity was blocked by TTX to minimize spike-dependent neurotransmission [54], inhibition of oxytocin responses was observed in accordance with a previous study [55]. In slices of neonatal rat spinal cords, no depolarization of motoneurons is observed, indicating that a substantial multisegmental network is a prerequisite for observing these responses [23,56]. These results suggest that most (if not all) of these actions were likely exerted at premotoneuron level. This notion is consistent with the description of sparse oxytocin-containing fibers contacting motoneurons [57] and lack of evidence supporting the expression of OTRs by motoneurons [23,26,27,58]. Despite the report of a subpopulation of glycinergic dorsal interneurons with OTR [23], the present data obtained with strychnine and bicuculline application suggest that the activation of such interneurons is not mandatory to produce these stimulatory effects. Future studies are necessary to identify the precise premotoneuron elements responsible for the observed effects by oxytocin in analogy with the approach used to dissect out the mechanism of action of dopamine to stabilize FL and excite motoneurons [59].

Oxytocin-mediated modulation of synaptic responses

Unlike the facilitatory effects produced by oxytocin on the basal activity of spinal circuits, oxytocin elicited more complex responses when such spinal networks were electrically or chemically stimulated. Although low nanomolar concentrations of the peptide had no significant action on reflexes, at concentrations $\geq$ 100 nM oxytocin significantly depressed DR-VRPs (see also [60]), especially those evoked by weak stimuli. Since OTRs are not expressed by afferent fibers [61], the observed changes in synaptic transmission were probably generated within spinal networks. Assuming that one important factor determining the size of the DR-VRP is the extent of the activated premotoneuron circuitry in turn related to the electrical pulse strength, the present results suggests that the depressant action of oxytocin was dependent on the activation state of network elements. This suggestion was

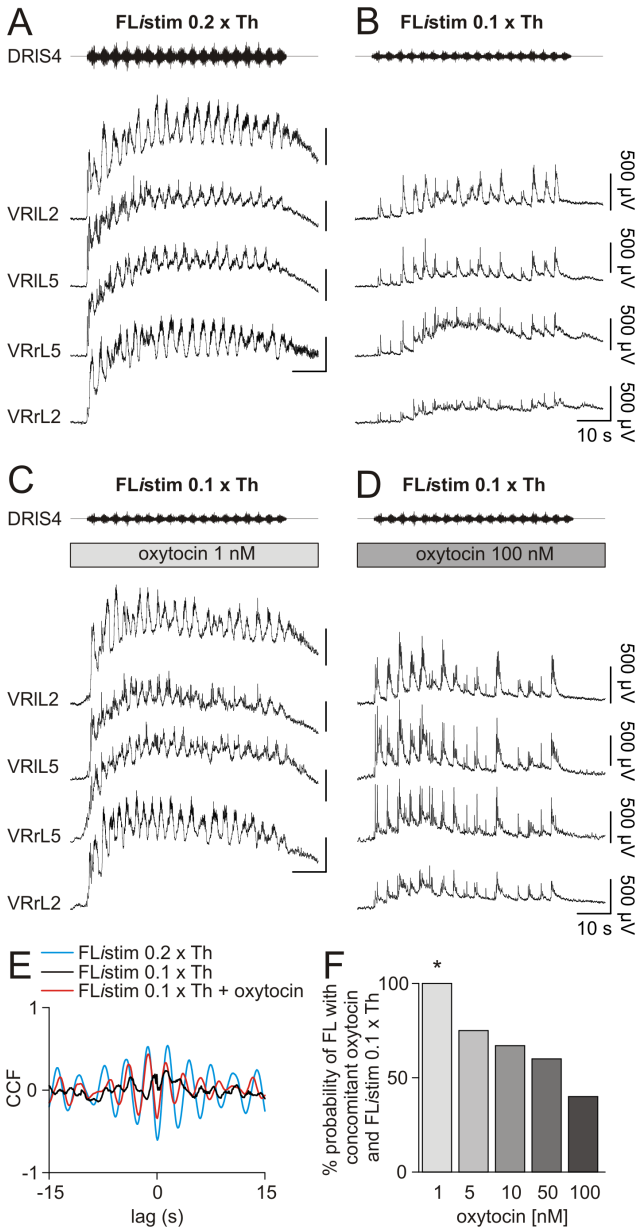

Figure 8. Low nanomolar concentrations of oxytocin synergize with FL*stim* in expressing fictive locomotor patterns. A, FL*stim* (0.2×Th) generates cumulative depolarization with alternating oscillations among homolateral L2 and L5 VRs and among controlateral homosegmental VRs. When stimulus intensity is halved (0.1×Th), a slight cumulative depolarization with synchronous discharges (time locked with the stimulating pattern) appears among all VRs (B). Despite the weak electrical stimulation (FL*stim* 0.1×Th), the addition of low concentration of oxytocin (1 nM) re-establishes cumulative depolarization and FL cycles (C). Increased concentration of oxytocin (100 nM) fails to synergize with the same FL*stim* 0.1×Th (D). Cross correlation analysis for traces related to the pair of L2 VRs in A–C shows a negative peak centered around zero lag for suprathreshold FL*stim* (blue trace) or subthreshold FL*stim* plus 1 nM oxytocin (red trace). The weak FL*stim* alone (black trace) has a CCF value close to zero, corresponding to an uncorrelated activity among the two VRs (E). F, histograms show that, by increasing the concentration of oxytocin, the probability of bringing FL to threshold with a weak FL*stim* diminishes in a dose dependent manner (*; Chi-square vs FL*stim* 0.1×Th alone; P = 0.005; n = 8).
doi:10.1371/journal.pone.0092967.g008

further explored by studying how a function-related network rhythm of the CPG was modulated by the peptide.

Oxytocin facilitates the expression of the locomotor pattern

Despite its inhibitory effects on reflex activity, oxytocin (≥ 100 nM) showed functional synergy with NMDA and 5HT in triggering oscillations when the CPG activity was subthreshold [32,33]. When locomotor networks were fully activated by NMDA and 5HT to express strong neuronal discharges alternating among distributed motor pools [62], 100 nM oxytocin unexpectedly failed to up or downregulate FL, suggesting that either any reflex depression was restricted to certain pathways not essential for FL (albeit impinging on motoneurons), and/or that the degree of neuronal activation by NMDA and 5HT was large enough to overwhelm oxytocin-mediated decrease in synaptic transmission. This view is consistent with the lack of effects by the OTR antagonist atosiban on a stable FL pattern.

The precise mechanism responsible for these divergent effects by oxytocin remains unclear. Nevertheless, similar effects were also observed with extracellular recordings from rat dorsal horn neurons in vivo with half of them being inhibited and the rest being activated by focally applied oxytocin, suggesting activation of inhibitory interneurons upstream of excitatory neurons [63]. While these in vivo results preclude the possibility of in vitro artefacts, various hypotheses might be advanced to account for the action of oxytocin on locomotor networks. In fact, although the spinal locomotor networks include distributed neuronal elements as indicated by functional labelling experiments [64], the expression of OTRs by lamina X neurons [27], that comprise commissural cells suitable to generate adaptable inputs to fine tune locomotor outputs [65], appears to link the effects of oxytocin to the pattern-generating networks.

A potential mechanism for the facilitatory role played by oxytocin might reside in the reported enhancement of endogenous 5HT release [50,51] because this biogenic amine is well-known to potently modulate locomotor-like activity [52]. To test this notion in the present study, 5HT synthesis was inhibited by overnight incubation with PCPA [44] and fully prevented any facilitatory action by oxytocin on the locomotor CPG. Nevertheless, because 5HT receptors include a large family of subtypes [66] with multiple effects and even functionally-distinct targets in the rat spinal cord [67,68,69], it is proposed that the functional outcome of the oxytocin action might be related to where and how extensively endogenous 5HT was concurrently liberated. In addition, as oxytocin positively modulates AMPA receptor-dependent transmission in a subpopulation of neurons only [70], location and synaptic contact topography of such neurons may determine the expression of oxytocin action.

A further possibility to account for the multifarious effects by oxytocin relies on the peculiar characteristics of its G-protein coupled receptors that can be coupled to different G-proteins (activating divergent intracellular signalling pathways). These receptors are often promiscuous, as a single receptor subtype may couple to more than one G-protein, thus activating, in the same cells, multiple responses at the same time [71,72]. Moreover, OTR may cluster together to produce functional oligodimers whose assembly and signalling strength depends on the agonist concentration with differential results in terms of functional responses [71,73]. Through a combination of these properties, oxytocin may show different potency/efficacy via different signalling pathways activated by the same receptor, in analogy with a multistate model of receptor activation [72].

Oxytocin synergizes with stimulation by weak noisy waveforms

There were several analogies in the effects by oxytocin on FL evoked by chemical agents or by FL*i*stim. In the present experiments, oxytocin facilitated the emergence of FL in the presence of a train of weak FL*i*stim *per se* unable to elicit persistent alternating patterns. The probability of triggering FL depended on the oxytocin concentration, i.e. when it was low, a high probability of success emerged, conversely with high concentrations it was more difficult to induce FL. It is noteworthy that the most favourable outcome therefore implied weak FL*i*stim and low oxytocin, a paradigm that, at least in theory if applied in vivo, should be the less prone to evoke unwanted side effects cause by peripheral action of oxytocin or local dysfunction by application of strong current pulses. The only apparent difference of this paradigm against FL caused by NMDA and 5HT was the effective concentration range of oxytocin that was optimal at small doses found to be ineffective on chemically-induced FL. It should be borne in mind that FL*i*stim requires repeated activation of dorsal afferents and that any reflex-depressant action by larger doses of oxytocin would probably have a negative impact on efficient signalling to attain CPG activation. This problem would be circumvented by chemical FL as afferent fibres are not concomitantly stimulated because the locomotor CPG displays a modular organization, whereby different inputs may activate subpopulations of interneurons, that only partially overlap [62,74].

The synergy between weak FL*i*stim and low oxytocin indicated an interesting protocol whereby FL*i*stim, due to the low stimulation intensities used, might represent a signal to activate only a network subpopulation crucial for the expression of FL, unlike the more generalized activation obtained with neurochemicals, which inevitably recruits many other spinal interneurons, some of which even unrelated to locomotion [62]. The most parsimonious hypothesis of the observed synergy is that a discrete distribution of OTRs with intrinsic properties (like affinity or intracellular effector coupling) might be found on certain network elements that selectively contribute to the expression of FL.

Conclusions

Due to the well defined sensory input through DRs and motor output through VRs, the isolated neonatal rodent spinal cord represents a suitable model to investigate innovative protocols of afferent stimulation able to optimally activate the spinal interneuronal network [75]. The combination of intra and extracellular recordings, associated with the direct application of selective pharmacological protocols for inducing different types of rhythmic activity, allowed us to postulate that OTRs are strategically located on locomotor circuit nodes whose activation is necessary to propagate and recruit the CPG operation.

Current interest in the central effects of oxytocin includes clinical trials of this peptide for schizophrenia or learning disorders [25]. The wide gap between these disorders points a broad role of the neuropeptide in modulating central networks and its overall safety in man. Thus, the present data may add a further hint to test low doses of oxytocin in combination with direct electrical stimulation of the spinal cord [5,76] in exploiting the residual locomotor capacities after spinal damage. In conclusion, our results appear interesting when considering ongoing clinical trials targeting oxytocin for spinal cord dysfunction (http://clinicaltrials.gov).

Supporting Information

Figure S1 Endogenous oxytocin does not modulate locomotor patterns. A, a stable FL is recorded in response to the co-application of NMDA (5 μM) and 5HT (10 μM). The addition of the selective antagonist for OTRs (atosiban, 5 μM) does not alter periodicity of FL rhythm or amplitude of oscillations.
(TIF)

Figure S2 DR-DRPs are unaffected by oxytocin. Depolarizing potentials are recorded from DRlL5 following electric stimulation of the controlateral DR by a series of single pulses (duration = 0.1 ms, 0.016 Hz). A, average DR-DRP evoked by low- strength stimulation (1×Th) is unchanged by increasing concentrations of oxytocin (1 nM, middle; 100 nM, right). Note the artefact of stimulation as indicated by arrows. On the same preparation, by augmenting the pulse strength (delivered as indicated by the arrows) to evoke larger and longer DRPs, no significant change is induced by this neuropeptide (B). Traces in A and B are mean of five responses. Histograms for the mean values obtained from four experiments, demonstrate that the addition of oxytocin, at both 100 nM and 1 μM, does not alter peak of DR-DRPs evoked at lower strength (C; one way repeated measures ANOVA, $P = 0.155$, $n = 4$), or peak (D; one way repeated measures ANOVA, $P = 0.392$, $n = 4$) and area (E; one way repeated measures ANOVA, $P = 0.306$, $n = 4$) of responses at the higher strength of stimulation.
(TIF)

Table S1 Characteristics of FL patterns induced by NMDA + 5HT or in the presence of subthreshold concentrations of neurochemicals + oxytocin.
(DOC)

Acknowledgments

We are grateful to Prof. Andrea Nistri for data discussion and to Dr. Elisa Ius for her excellent assistance in preparing the manuscript.

Author Contributions

Conceived and designed the experiments: GT. Performed the experiments: FD PZ TC GT. Analyzed the data: FD PZ TC GT. Wrote the paper: GT.

References

1. Grillner S (2006) Biological pattern generation: the cellular and computational logic of networks in motion. Neuron 52: 751–766.
2. Kiehn O (2006) Locomotor circuits in the mammalian spinal cord. Annu Rev Neurosci 29: 279–306.
3. Harris-Warrick RM (2011) Neuromodulation and flexibility in Central Pattern Generator networks. Curr Opin Neurobiol 21: 685–692.
4. Miles GB, Sillar KT (2011) Neuromodulation of vertebrate locomotor control networks. Physiology (Bethesda) 26: 393–411.
5. Harkema S, Gerasimenko Y, Hodes J, Burdick J, Angeli C, et al. (2011) Effect of epidural stimulation of the lumbosacral spinal cord on voluntary movement, standing, and assisted stepping after motor complete paraplegia: a case study. Lancet 377: 1938–1947.
6. Fong AJ, Roy RR, Ichiyama RM, Lavrov I, Courtine G, et al. (2009) Recovery of control of posture and locomotion after a spinal cord injury: solutions staring us in the face. Prog Brain Res 175: 393–418.
7. Boulenguez P, Vinay L (2009) Strategies to restore motor functions after spinal cord injury. Current Opinion in Neurobiology 19: 587–600.
8. Edgerton VR, Tillakaratne NJ, Bigbee AJ, de Leon RD, Roy RR (2004) Plasticity of the spinal neural circuitry after injury. Annu Rev Neurosci 27: 145–167.
9. Gerasimenko YP, Ichiyama RM, Lavrov IA, Courtine G, Cai L, et al. (2007) Epidural spinal cord stimulation plus quipazine administration enable stepping in complete spinal adult rats. J Neurophysiol 98: 2525–2536.

10. Ichiyama RM, Gerasimenko Y, Jindrich DL, Zhong H, Roy RR, et al. (2008) Dose dependence of the 5-HT agonist quipazine in facilitating spinal stepping in the rat with epidural stimulation. Neurosci Lett 438: 281–285.
11. Musienko P, van den Brand R, Märzendorfer O, Roy RR, Gerasimenko Y, et al. (2011) Controlling specific locomotor behaviors through multidimensional monoaminergic modulation of spinal circuitries. J Neurosci 31: 9264–9278.
12. van den Brand R, Heutschi J, Barraud Q, DiGiovanna J, Bartholdi K, et al. (2012) Restoring voluntary control of locomotion after paralyzing spinal cord injury. Science 336: 1182–1185.
13. Domingo A, Al-Yahya AA, Asiri Y, Eng JJ, Lam T (2012) A systematic review of the effects of pharmacological agents on walking function in people with spinal cord injury. J Neurotrauma 29: 865–879.
14. Jacobs BL, Fornal CA (1993) 5-HT and motor control: a hypothesis. Trends Neurosci 16: 346–352.
15. Strauss I, Lev-Tov A (2003) Neural pathways between sacrocaudal afferents and lumbar pattern generators in neonatal rats. J Neurophysiol 89: 773–784.
16. Taccola G, Olivieri D, D'Angelo G, Blackburn P, Secchia L, et al. (2012) A_1 adenosine receptor modulation of chemically and electrically evoked lumbar locomotor network activity in isolated newborn rat spinal cords. Neuroscience 222: 191–204.
17. Stoop R (2012) Neuromodulation by oxytocin and vasopressin. Neuron 76: 142–159.
18. Jójárt J, Jójárt I, Boda K, Gálfi M, Mihály A, et al. (2009) Distribution of oxytocin-immunoreactive neuronal elements in the rat spinal cord. Acta Biol Hung 60: 333–346.
19. Sawchenko PE, Swanson LW (1982) Immunohistochemical identification of neurons in the paraventricular nucleus of the hypothalamus that project to the medulla or to the spinal cord in the rat. J Comp Neurol 205: 260–272.
20. Lang RE, Heil J, Ganten D, Hermann K, Rascher W, et al. (1983) Effects of lesions in the paraventricular nucleus of the hypothalamus on vasopressin and oxytocin contents in brainstem and spinal cord of rat. Brain Res 260: 326–329.
21. Hawthorn J, Ang VT, Jenkins JS (1985) Effects of lesions in the hypothalamic paraventricular, supraoptic and suprachiasmatic nuclei on vasopressin and oxytocin in rat brain and spinal cord. Brain Res 346: 51–57.
22. Gibson SJ, Polak JM, Bloom SR, Wall PD (1981) The distribution of nine peptides in rat spinal cord with special emphasis on the substantia gelatinosa and on the area around the central canal (lamina X). J Comp Neurol 201: 65–79.
23. Liu X, Tribollet E, Ogier R, Barberis C, Raggenbass M (2003) Presence of functional vasopressin receptors in spinal ventral horn neurons of young rats: a morphological and electrophysiological study. Eur J Neurosci 17: 1833–1846.
24. Tribollet E, Charpak S, Schmidt A, Dubois-Dauphin M, Dreifuss JJ (1989) Appearance and transient expression of oxytocin receptors in fetal, infant, and peripubertal rat brain studied by autoradiography and electrophysiology. J Neurosci 9: 1764–1773.
25. Gimpl G, Fahrenholz F (2001) The oxytocin receptor system: structure, function, and regulation. Physiol Rev 81: 629–683.
26. Reiter MK, Kremarik P, Freund-Mercier MJ, Stoeckel ME, Desaulles E, et al. (1994) Localization of oxytocin binding sites in the thoracic and upper lumbar spinal cord of the adult and postnatal rat: a histoautoradiographic study. Eur J Neurosci 6: 98–104.
27. Wrobel L, Schorscher-Petcu A, Dupré A, Yoshida M, Nishimori K, et al. (2011) Distribution and identity of neurons expressing the oxytocin receptor in the mouse spinal cord. Neurosci Lett 495: 49–54.
28. Kombian SB, Hirasawa M, Mouginot D, Pittman QJ (2002) Modulation of synaptic transmission by oxytocin and vasopressin in the supraoptic nucleus. Prog Brain Res 139: 235–246.
29. Martínez-Lorenzana G, Espinosa-López L, Carranza M, Aramburo C, Paz-Tres C, et al. (2008) PVN electrical stimulation prolongs withdrawal latencies and releases oxytocin in cerebrospinal fluid, plasma, and spinal cord tissue in intact and neuropathic rats. Pain 140: 265–273.
30. Artman HG, Leake RD, Weitzman RE, Sawyer WH, Fisher DA (1984) Radioimmunoassay of vasotocin, vasopressin, and oxytocin in human neonatal cerebrospinal and amniotic fluid. Dev Pharmacol Ther 7: 39–49.
31. Juif PE, Breton JD, Rajalu M, Charlet A, Goumon Y, et al. (2013) Long-Lasting Spinal Oxytocin Analgesia Is Ensured by the Stimulation of Allopregnanolone Synthesis Which Potentiates GABAA Receptor-Mediated Synaptic Inhibition. J Neurosci 33: 16617–16626.
32. Pearson SA, Mouihate A, Pittman QJ, Whelan PJ (2003) Peptidergic activation of locomotor pattern generators in the neonatal spinal cord. J Neurosci 23: 10154–10163.
33. Barrière G, Bertrand S, Cazalets JR (2005) Peptidergic neuromodulation of the lumbar locomotor network in the neonatal rat spinal cord. Peptides 26: 277–286.
34. Hochman S, Hayes HB, Speigel I, Chang YH (2013) Force-sensitive afferents recruited during stance encode sensory depression in the contralateral swinging limb during locomotion. Ann N Y Acad Sci 1279: 103–113.
35. Etlin A, Finkel E, Mor Y, O'Donovan MJ, Anglister L, et al. (2013) Characterization of sacral interneurons that mediate activation of locomotor pattern generators by sacrocaudal afferent input. J Neurosci 33: 734–747.
36. Mandadi S, Hong P, Tran MA, Bráz JM, Colarusso P, et al. (2013) Identification of multisegmental nociceptive afferents that modulate locomotor circuits in the neonatal mouse spinal cord. J Comp Neurol 521: 2870–2887.
37. Taccola G (2011) The locomotor central pattern generator of the rat spinal cord in vitro is optimally activated by noisy dorsal root waveforms. J Neurophysiol 106: 872–884.
38. Marchetti C, Beato M, Nistri A (2001) Alternating rhythmic activity induced by dorsal root stimulation in the neonatal rat spinal cord in vitro. J Physiol 530: 105–112.
39. Dose F, Taccola G (2012) Coapplication of noisy patterned electrical stimuli and NMDA plus serotonin facilitates fictive locomotion in the rat spinal cord. J Neurophysiol 108: 2977–2990.
40. Bracci E, Ballerini L, Nistri A (1996) Spontaneous rhythmic bursts induced by pharmacological block of inhibition in lumbar motoneurons of the neonatal rat spinal cord. J Neurophysiol 75: 640–647.
41. Taccola G, Marchetti C, Nistri A (2004) Role of group II and III metabotropic glutamate receptors in rhythmic patterns of the neonatal rat spinal cord in vitro. Exp Brain Res 156: 495–504.
42. Fulton BP, Walton K (1986) Electrophysiological properties of neonatal rat motoneurones studied in vitro. J Physiol 370: 651–678.
43. Kiehn O, Kjaerulff O (1998) Distribution of central pattern generators for rhythmic motor outputs in the spinal cord of limbed vertebrates. Ann N Y Acad Sci 860: 110–129.
44. Branchereau P, Chapron J, Meyrand P (2002) Descending 5-hydroxytryptamine raphe inputs repress the expression of serotonergic neurons and slow the maturation of inhibitory systems in mouse embryonic spinal cord. J Neurosci 22: 2598–2606.
45. Taccola G, Mladinic M, Nistri A (2010) Dynamics of early locomotor network dysfunction following a focal lesion in an in vitro model of spinal injury. Eur J Neurosci 31: 60–78.
46. Tyzio R, Cossart R, Khalilov I, Minlebaev M, Hübner CA, et al. (2006) Maternal oxytocin triggers a transient inhibitory switch in GABA signaling in the fetal brain during delivery. Science 314: 1788–1792.
47. Taccola G, Nistri A (2006) Fictive locomotor patterns generated by tetraethylammonium application to the neonatal rat spinal cord in vitro. Neuroscience 137: 659–670.
48. Taccola G, Nistri A (2005) Characteristics of the electrical oscillations evoked by 4-aminopyridine on dorsal root fibers and their relation to fictive locomotor patterns in the rat spinal cord in vitro. Neuroscience 132: 1187–1197.
49. Ryckebusch S, Laurent G (1994) Interactions between segmental leg central pattern generators during fictive rhythms in the locust. J Neurophysiol 72: 2771–2785.
50. Eaton JL, Roache L, Nguyen KN, Cushing BS, Troyer E, et al. (2012) Organizational effects of oxytocin on serotonin innervation. Dev Psychobiol 54: 92–97.
51. Marazziti D, Baroni S, Giannaccini G, Betti L, Massimetti G, et al. (2012) A link between oxytocin and serotonin in humans: supporting evidence from peripheral markers. Eur Neuropsychopharmacol 22: 578–583.
52. Dunbar MJ, Tran MA, Whelan PJ (2010) Endogenous extracellular serotonin modulates the spinal locomotor network of the neonatal mouse. J Physiol 588: 139–156.
53. Hochman S, Shreckengost J, Kimura H, Quevedo J (2010) Presynaptic inhibition of primary afferents by depolarization: observations supporting nontraditional mechanisms. Ann N Y Acad Sci 1198: 140–152.
54. Butt SJ, Harris-Warrick RM, Kiehn O (2002) Firing properties of identified interneuron populations in the mammalian hindlimb central pattern generator. J Neurosci 22: 9961–9971.
55. Suzue T, Yanaihara N, Otsuka M (1981) Actions of vasopressin, gastrin releasing peptide and other peptides on neurons on newborn rat spinal cord in vitro. Neurosci Lett 26: 137–142.
56. Oz M, Kolaj M, Renaud LP (2001) Electrophysiological evidence for vasopressin V(1) receptors on neonatal motoneurons, premotor and other ventral horn neurons. J Neurophysiol 86: 1202–1210.
57. Schoenen J, Lotstra F, Vierendeels G, Reznik M, Vanderhaeghen JJ (1985) Substance P, enkephalins, somatostatin, cholecystokinin, oxytocin, and vasopressin in human spinal cord. Neurology 35: 881–890.
58. Véronneau-Longueville F, Rampin O, Freund-Mercier MJ, Tang Y, Calas A, et al. (1999) Oxytocinergic innervation of autonomic nuclei controlling penile erection in the rat. Neuroscience 93: 1437–1447.
59. Han P, Nakanishi ST, Tran MA, Whelan PJ (2007) Dopaminergic modulation of spinal neuronal excitability. J Neurosci 27: 13192–13204.
60. Wilson LA, Wayman CP, Jackson VM (2009) Neuropeptide modulation of a lumbar spinal reflex: potential implications for female sexual function. J Sex Med 6: 947–957.
61. Moreno-López Y, Martínez-Lorenzana G, Condés-Lara M, Rojas-Piloni G (2013) Identification of oxytocin receptor in the dorsal horn and nociceptive dorsal root ganglion neurons. Neuropeptides 47: 117–123.
62. Hägglund M, Dougherty KJ, Borgius L, Itohara S, Iwasato T, et al. (2013) Optogenetic dissection reveals multiple rhythmogenic modules underlying locomotion. Proc Natl Acad Sci USA 110: 11589–11594.
63. Condés-Lara M, González NM, Martínez-Lorenzana G, Delgado OL, Freund-Mercier MJ (2003) Actions of oxytocin and interactions with glutamate on spontaneous and evoked dorsal spinal cord neuronal activities. Brain Res 976: 75–81.
64. Cina C, Hochman S (2000) Diffuse distribution of sulforhodamine-labeled neurons during serotonin-evoked locomotion in the neonatal rat thoracolumbar spinal cord. J Comp Neurol 423: 590–602.
65. Bertrand SS, Cazalets JR (2011) Cholinergic partition cells and lamina x neurons induce a muscarinic-dependent short-term potentiation of commissural glutamatergic inputs in lumbar motoneurons. Front Neural Circuits 5: 15.

66. Barnes NM, Sharp T (1999) A review of central 5-HT receptors and their function. Neuropharmacology 38: 1083–1152.
67. Beato M, Nistri A (1998) Serotonin-induced inhibition of locomotor rhythm of the rat isolated spinal cord is mediated by the 5-HT1 receptor class. Proc Biol Sci 265: 2073–2080.
68. Bracci E, Beato M, Nistri A (1998) Extracellular K+ induces locomotor-like patterns in the rat spinal cord in vitro: comparison with NMDA or 5-HT induced activity. J Neurophysiol 79: 2643–2652.
69. Garraway SM, Hochman S (2001) Pharmacological characterization of serotonin receptor subtypes modulating primary afferent input to deep dorsal horn neurons in the neonatal rat. Br J Pharmacol 132: 1789–1798.
70. Jo YH, Stoeckel ME, Freund-Mercier MJ, Schlichter R (1998) Oxytocin modulates glutamatergic synaptic transmission between cultured neonatal spinal cord dorsal horn neurons. J Neurosci 18: 2377–2386.
71. Chini B, Manning M (2007) Agonist selectivity in the oxytocin/vasopressin receptor family: new insights and challenges. Biochem Soc Trans 35: 737–741.
72. Viero C, Shibuya I, Kitamura N, Verkhratsky A, Fujihara H, et al. (2010) Oxytocin: Crossing the bridge between basic science and pharmacotherapy. CNS Neurosci Ther 16: e138–156.
73. Albizu L, Cottet M, Kralikova M, Stoev S, Seyer R, et al. (2010) Time-resolved FRET between GPCR ligands reveals oligomers in native tissues. Nat Chem Biol 6: 587–594.
74. Frigon A (2012) Central pattern generators of the mammalian spinal cord. Neuroscientist 18: 56–69.
75. Hochman S, Gozal EA, Hayes HB, Anderson JT, DeWeerth SP, et al. (2012) Enabling techniques for in vitro studies on mammalian spinal locomotor mechanisms. Front Biosci 17: 2158–2180.
76. Gad P, Choe J, Shah P, Alias GG, Rath M, et al. (2013) Sub-threshold spinal cord stimulation facilitates spontaneous motor activity in spinal rats. J Neuroeng Rehabil 10: 108.

Supplementary Information

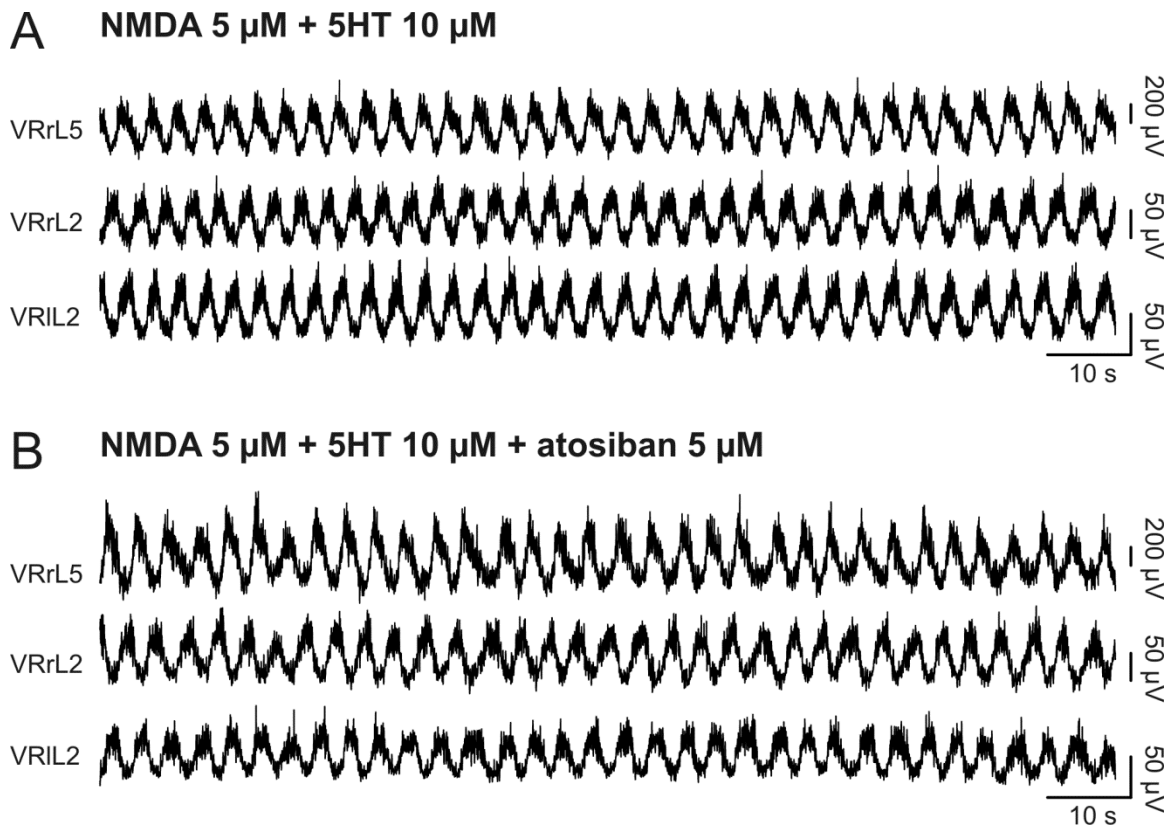

Figure S1. Endogenous oxytocin does not modulate locomotor patterns. *A, a stable FL is recorded in response to the co-application of NMDA (5 µM) and 5HT (10 µM). The addition of the selective antagonist for OTRs (atosiban, 5 µM) does not alter periodicity of FL rhythm or amplitude of oscillations.*

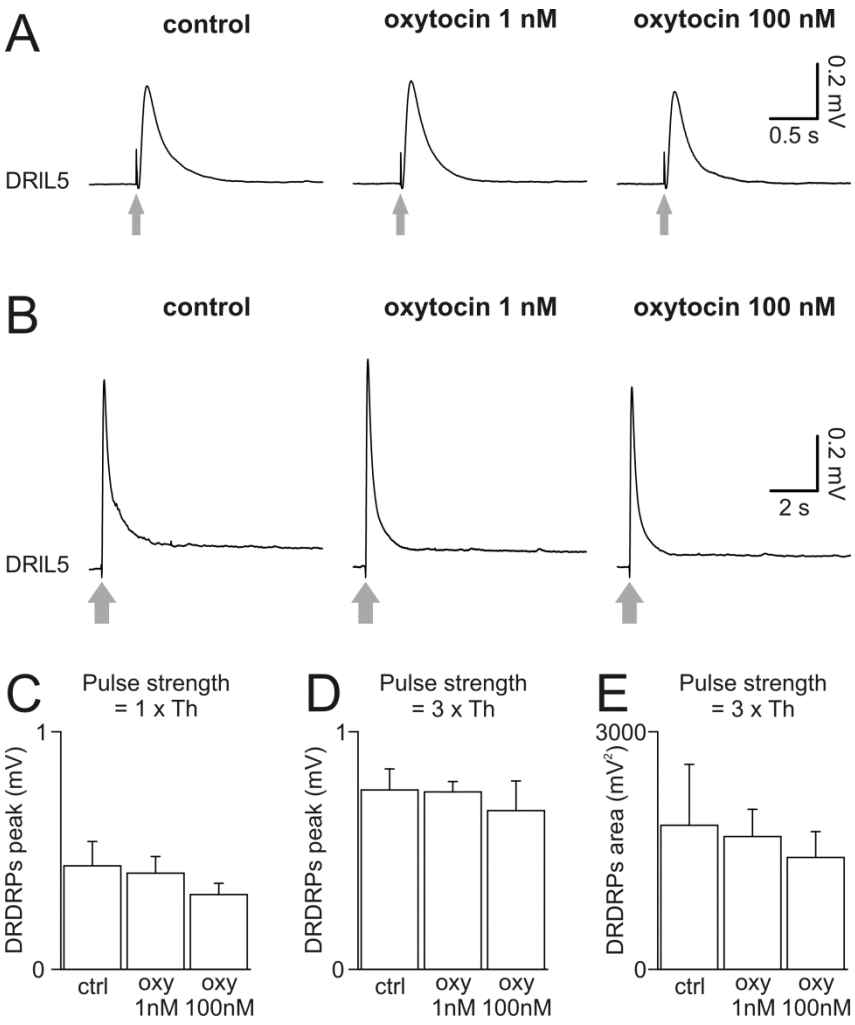

Figure S2. DR-DRPs are unaffected by oxytocin. *Depolarizing potentials are recorded from DRIL5 following electric stimulation of the controlateral DR by a series of single pulses (duration = 0.1 ms, 0.016 Hz). A, average DR-DRP evoked by low- strength stimulation (1×Th) is unchanged by increasing concentrations of oxytocin (1 nM, middle; 100 nM, right). Note the artefact of stimulation as indicated by arrows. On the same preparation, by augmenting the pulse strength (delivered as indicated by the arrows) to evoke larger and longer DRPs, no significant change is induced by this neuropeptide (B). Traces in A and B are mean of five responses. Histograms for the mean values obtained from four experiments, demonstrate that the addition of oxytocin, at both 100 nM and 1 μM, does not alter peak of DR-DRPs evoked at lower strength (C; one way repeated measures ANOVA, P=0.155, n=4), or peak (D; one way repeated measures ANOVA, P=0.392, n=4) and area (E; one way repeated measures ANOVA, P=0.306, n=4) of responses at the higher strength of stimulation.*

	NMDA + 5HT	Subthreshold NMDA and 5HT + oxytocin (100 nM)	Statistical test (n = 12 cords)
Period (s) ± SD	4.26 ± 1.00	5.52 ± 2.23	paired t-test, P = 0.085
CV of Period ± SD	0.13 ± 0.10	0.13 ± 0.08	Wilcoxon signed rank test, P = 0.733
Amplitude (mV) ± SD	0.24 ± 0.15	0.24 ± 0.21	paired t-test, P = 0.339

Table S1. Characteristics of FL patterns induced by NMDA + 5HT or in the presence of subthreshold concentrations of neurochemicals + oxytocin

Spinal Cord (2016) 54, 93–101

www.nature.com/sc

ORIGINAL ARTICLE

Staggered multi-site low-frequency electrostimulation effectively induces locomotor patterns in the isolated rat spinal cord

F Dose[1,2,4], R Deumens[3,4], P Forget[3] and G Taccola[1,2]

Study design: Experimental animal study.
Objectives: Epidural stimulation has been used to activate locomotor patterns after spinal injury and typically employs synchronous trains of high-frequency stimuli delivered directly to the dorsal cord, thereby recruiting multiple afferent nerve roots. Here we investigate how spinal locomotor networks integrate multi-site afferent input and address whether frequency coding is more important than amplitude to activate locomotor patterns.
Setting: Italy and Belgium.
Methods: To investigate the importance of input intensity and frequency in eliciting locomotor activity, we used isolated neonatal rat spinal cords to record episodes of fictive locomotion (FL) induced by electrical stimulation of single and multiple dorsal roots (DRs), employing different stimulating protocols.
Results: FL was efficiently induced through staggered delivery (delays 0.5 to 2 s) of low-frequency pulse trains (0.33 and 0.67 Hz) to three DRs at intensities sufficient to activate ventral root reflexes. Delivery of the same trains to a single DR or synchronously to multiple DRs remained ineffective. Multi-site staggered trains were more efficient than randomized pulse delivery. Weak trains simultaneously delivered to DRs failed to elicit FL. Locomotor rhythm resetting occurred with single pulses applied to various distant DRs.
Conclusion: Electrical stimulation recruited spinal networks that generate locomotor programs when pulses were delivered to multiple sites at low frequency. This finding might help devising new protocols to optimize the increasingly more common use of epidural implantable arrays to treat spinal dysfunctions.
Spinal Cord (2016) **54,** 93–101; doi:10.1038/sc.2015.106; published online 23 June 2015

INTRODUCTION

A promising neurorehabilitative approach to provide functional benefits to persons with a chronic spinal injury is the direct electrostimulation of the dorsal cord via epidural electrodes.[1,2] However, this procedure is invasive, because it requires surgical electrode implantation into the epidural space for the delivery of electrical impulses that can elicit a brief bout of alternating leg movements in paraplegic persons.[3] The appearance of such locomotor-like episodes has been attributed to the reactivation of functionally impaired spinal neuronal circuits by inputs from dorsal root (DR) afferents.[4] Because of recent upgrades in hardware technology, that is, grouping 16 electrodes into an epidural array, such a paradigm together with rehabilitative training is reported to facilitate voluntary motor control plus conferring other functional benefits in complete spinal cord-injured persons.[2] It should be noted that unlike single electrodes, these arrays excite a much wider area in the dorsal cord and may, thus, recruit a greater number of DR fibres establishing synapses with dorsal horn neurons.[4] In previous studies, arrays have been used to activate spinal white matter tracts and to induce locomotor patterns in the isolated neonatal rat spinal cord,[5] as well as to facilitate locomotion through a new flexible implantable electrical epidural array in animal models of spinal lesion.[6]

With the perspective of further improvement in spinal neurorehabilitation, more advanced electrical stimulation paradigms are required to optimize the array construction, location and stimulation protocols. In particular, considering the latter issue, it is noteworthy that stimulation programs have remained unchanged in the past 15 years and still consists in stereotyped high-frequency trains of rectangular electrical pulses (25–40 Hz) simultaneously delivered through all electrodes in the array. Thus, future hardware developments should be associated with more performance-selective stimulating paradigms that are also expected to decrease the total amount of current supplied with decreased occurrence of side effects. The aim of the present work is to construct novel stimulation paradigms based on low-threshold amplitude and/or frequency that selectively activate the locomotor central pattern generator through a patterned stimulation of multiple afferent sites. Thus, we explored how spinal interneuronal circuits impinging on locomotor networks may integrate sensory afferent inputs arising from distinct segments in a concerted or staggered manner. Our data suggest that the delivery of staggered

[1]Neuroscience Department, International School for Advanced Studies (SISSA), Trieste, Italy; [2]SPINAL (Spinal Person Injury Neurorehabilitation Applied Laboratory), Istituto di Medicina Fisica e Riabilitazione (IMFR), Udine, Italy and [3]Institute of Neuroscience, Université catholique de Louvain, Brussels, Belgium
[4]These authors contributed equally to this work.
Correspondence: Dr G Taccola, Neuroscience Department, International School for Advanced Studies (SISSA), IMFR, via Gervasutta 48, Udine 33100, Italy.
E-mail: taccola@sissa.it
Received 30 January 2015; revised 22 May 2015; accepted 27 May 2015; published online 23 June 2015

low-frequency stimuli to multiple sites of the isolated spinal cord could represent a suitable protocol to efficiently activate ventral root (VR) discharges, alternating among pairs of L2 and L5 on either side, defined as fictive locomotion (FL).[7]

MATERIALS AND METHODS

Isolation of spinal cord and rhythm induction

We certify that all applicable institutional and governmental regulations concerning the ethical use of animals were followed during the course of this research. All procedures were approved by the Scuola Internazionale Superiore di Studi Avanzati ethics committee and are in accordance with the European Union directive for animal experiments (86/609/EEC). Every effort was made to reduce the number of rats used for the isolation of spinal cord and to minimize their suffering. All experiments were performed, in line with the guidelines provided by the Italian Animal Welfare Act, on spinal cord preparations isolated from neonatal rats (0–2 days old), as previously described.[7] Spinal cords were dissected from thoracic level 5–6 to the cauda equina and care was taken to leave the DRs and VRs attached, which allows for the study of FL.[8] FL is a locomotor-like rhythm originating in the spinal cord preparation and consisting of an episode of electrical discharges that can be measured from VRs. This FL is characterized by discharges alternating between pairs L2 and L5 VRs. Therefore, FL is considered to provide important information about the function of locomotor spinal circuits that can be observed in isolated neonatal rat spinal cord preparations.[9] In our setting, we induced FL by applying a train of rectangular electrical pulses to a single DR or to sacrocaudal afferents (cauda equina), as described previously.[8,10]

Electrostimulating paradigms

Thirty- or sixty-second trains of pulses (duration 0.1 ms) were delivered to several segmental levels (from L5 to the cauda equina), in a different range of frequencies (0.33–2 Hz) and with a variable strength (9–400 μA). Although previous studies indicated that there was no significant change in FL features due to varying train frequency (1–50 Hz[8]), in this study we considered the 2 Hz protocol as a benchmark for comparing efficacy of the new multi-site stimulation protocols.

Nevertheless, in a subset of experiments, we reduced stimulating frequency to assess the lowest value able to induce an episode of FL, which was 1 Hz. In this case, FL was rarely evoked, but the features of FL episodes were similar to those evoked by the 2 Hz protocol.

Single pulses (duration = 0.1 ms) were delivered at a strong intensity to induce phase resetting during FL.[11] In these experiments, absolute strength of stimulation spanned from 40 to 400 μA at the lumbar level and from 90 to 400 μA at the sacral level. We ascertained that the maximum strength of stimulation applied to a DR did not cause a non-selective activation of nearby DRs through leakage of current from the stimulating electrode. Therefore, we stimulated DRL6 at the maximum intensity used in the study (400 μA), which evoked a reflex response from both the homosegmental VR and the adjacent VRS2. Similarly, stimulation of DRS2 at an intensity of 400 μA induced a synchronous response from S2 and L6 VRs. After the complete horizontal transection of the spinal cord at the level of S1 segment, the stimulation of the same two DRs at the same intensity now only evoked a response from homolateral VRs, without affecting the disconnected portion of the cord (data not shown). This test proved that stimulation of a DR at maximal intensity did not evoke any aspecific activation of the adjacent DR, caused by leakage of current from miniature bipolar stimulating electrodes.

Electrophysiological recordings

Spinal cords were placed in a recording chamber, continuously superfused (5 ml min^{-1}) at room temperature (22 °C–24 °C) with carbogenated (95% O_2, 5% CO_2) Krebs solution of the following composition (in mM): 113 NaCl, 4.5 KCl, 1 $MgCl_2 \times 7H_2O$, 2 $CaCl_2$, 1 NaH_2PO_4, 25 $NaHCO_3$ and 11 glucose, pH 7.4. Traces were obtained from lumbar (L) VRs, by using tight-fitting suction electrodes.[7] DC-coupled recordings were acquired with a differential amplifier (DP-304, Warner Instruments, Hamden, CT, USA) at a sampling rate of 10 KHz, low-pass-filtered 10 Hz and high-pass 0.1 Hz, and digitalized (Digidata 1440, Molecular Devices, Sunnyvale, CA, USA). The alternation of discharges between L2 and L5 VRs and between the left (l) and right (r) L2 VRs were considered distinct features of FL, as previously reported.[12]

Parameters of spinal network activities

Single or repetitive electrical pulses were delivered by a programmable stimulator (STG4004, Multichannel System, Reutlingen, Germany). DR electrical stimuli were adapted to evoke both single VR responses and cumulative depolarization[8] originating from the addition of individual pulses delivered at each segments. Herein, the lowest stimuli able to elicit a detectable short-latency response (usually as long as 10 ms and as high as 3× the width of baseline) from the corresponding VR were defined as threshold stimuli.[8] Out of 31 preparations, the average threshold value of short-latency reflex response was 20.19 ± 22.05 μA. Oscillations of FL were analysed based on their periodicity (time between the onset of two consecutive cycles of oscillatory activity) and regularity, expressed as coefficient of period variation (given by s.d. per mean). The strength of coupling among pairs of signals of VRs was measured using the cross-correlation function (CCF) analysis. When a CCF is higher than +0.5, two roots are synchronous, whereas a CCF smaller than −0.5 corresponds to full alternation.[12]

Data representation and statistics

Data are reported as mean ± s.d. values. Number of samples is indicated as *n* in the results. Normality testing showed a normal Gaussian distribution for all data sets. Accordingly, parametric data were analysed with the Student's *t*-test or one-way analysis of variance (ANOVA), whereas Kruskal–Wallis one–way ANOVA on ranks was used for non-parametric data. Differences were considered statistically significant when $P < 0.05$. Multiple comparisons were corrected for *post-hoc* analysis using pairwise multiple comparisons (Dunn's or Tukey's method).

RESULTS

Specificity of VR responses induced by electrical stimulation of multiple neighbouring DRs

As in this study we investigated the responses to electrical pulses applied to multiple DRs, it was important to exclude that, in our set up, electrical stimulation of a DR aspecifically activated closeby DRs simply by leakage of current through the stimulating electrode. Therefore, strong electrical pulses (intensity = 300 ± 100 μA) were serially delivered to a pair of neighbouring DRs (L6 and S2). Evoked reflex responses were recorded from homosegmental VRs ($peak_{VRlL6} = 0.32 \pm 0.01$ mV, $peak_{VRlS2} = 0.27 \pm 0.03$ mV, $n = 3$; Supplementary Figures 1a and b) and, with a delay of 11.6 ± 2.77 ms, from adjacent VRs ($peak_{VRlS2} = 0.16 \pm 0.01$ mV, $peak_{VRlL6} = 0.14 \pm 0.07$ mV, $n = 3$; Supplementary Figures 1a and b). Next, we performed a complete transection at S1 level to obtain two separate portions of the spinal cord, which were left close to each other. Although distance between DRs was negligible, no spinal cord circuitry between the two tissue portions was preserved. Following electrical stimulation of a DR elicited a homosegmental reflex response ($peak_{VRlL6} = 0.33 \pm 0.03$ mV, $peak_{VRlS2} = 0.19 \pm 0.04$ μV, $n = 3$; Supplementary Figures 1c and d), but failed to induce responses in segments disconnected from the stimulating site (Supplementary Figures 1c and d). This observation demonstrates that intersegmental VR responses are driven by intact spinal circuitries rather than by a generalized electrical activation of closeby afferents.

Low-intensity simultaneous multi-site DR trains fail to elicit FL

Our first aim was to explore how spinal interneuronal circuits for locomotion integrate convergent sensory afferent inputs originating from different sites. The effect of stimulating a single DR, at low lumbar or sacral level, with pulse trains of high intensity was therefore

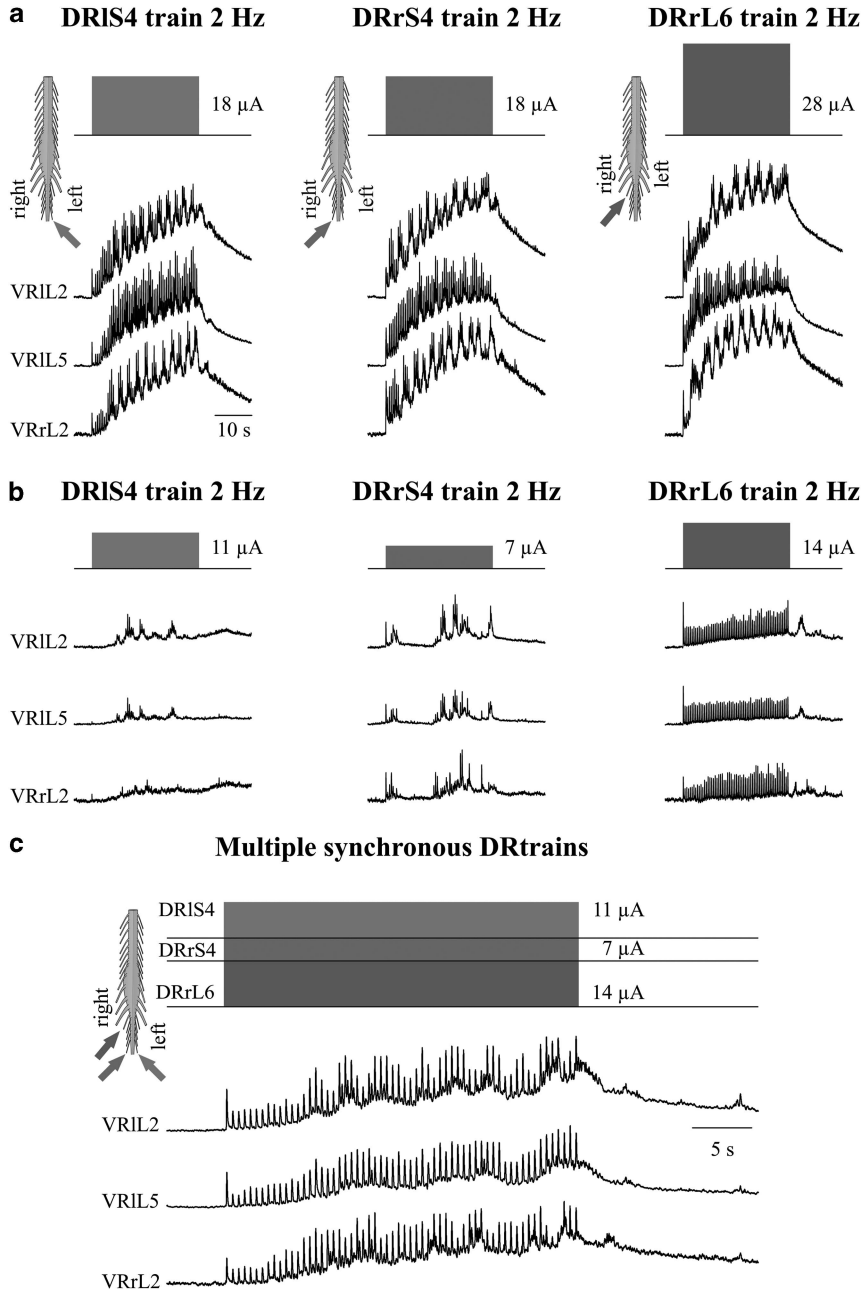

Figure 1 Multiple subthreshold amplitude DR trains do not reach threshold when delivered at once. (**a**, Left) A train of 60 stimuli at 2 Hz applied to DRlS4 (amplitude = 18 µA, 1.5 × threshold) generates a cumulative depolarization and an episode of FL (CCF = – 0.488). In the same preparation, an episode of FL is also evoked when the train at 2 Hz is applied to the contralateral DR (amplitude = 18 µA, 2 × threshold; (**a,** middle) CCF = – 0.570) or to DRrL6 (amplitude = 28 µA, 2 × threshold; (**a**, right) CCF = – 0.569). (**b**) When the amplitude of stimulation of each train is lowered, no cumulative depolarization is evoked and uncorrelated discharges replace locomotor oscillations (CCF = 0.109, 0.434 and 0.930, respectively). (**c**) Three trains of low intensity are now delivered synchronously, each to one of the three afferents of the same spinal cord. Although the sum of amplitudes of single protocols is above the value to trigger FL with individually applied trains, no locomotor response was observed (CCF = 0.647). CCF, cross-correlation function; DRlL, left lumbar dorsal root; DRrL, right lumbar dorsal root; DRrS, right sacral dorsal root; VRlL, left lumbar ventral root; VRrL, right lumbar ventral root.

compared with the stimulation of three DRs at lower intensity (that is, an intensity that was ineffective for inducing FL through a single DR). Initially, an episode of FL was observed as a series of oscillatory cycles recorded from L2 (flexor-related) and L5 (extensor-related) VRs, evoked by a train of 2 Hz stimuli delivered at optimal amplitude to just one DR among the three selected (Figure 1a; 18, 18 and 28 µA, respectively). Notably, these effects were not dependent on the DR selected. Whenever canonical 2 Hz DR trains[8] were applied to various DRs, the main properties of FL episodes (such as periodicity or number of oscillations superimposed on the cumulative depolarization elicited by the stimulus train) remained similar (Table 1). Table 1 also lists other parameters typical of FL such as the CCF, which according to its positive or negative value shows phase synchrony or alternation of cycles.[12] Likewise, when the same protocol was applied for an extended duration (60 s), the number of FL cycles did not increase (data not shown).

Table 1 Main features of FL episodes induced by a train of electrical pulses (2 Hz) delivered to a single DR at different spinal cord levels

Spinal level	*Intensity of stimulation (×threshold)*	*Duration (s)*	*Number of oscillations*	*Period of oscillations (s)*	*CV*	*Cumulative depolarization peak (mV)*	*CCF*	n
L6–S1	1.60±0.62	25.95±2.58	11±2	2.58±0.41	0.16±0.04	0.94±0.46	−0.576±0.433	12
S2–S3	1.57±0.38	26.23±3.12	12±1	2.45±0.32	0.17±0.05	0.96±0.50	−0.747±0.100	6
S4–S5	1.65±0.44	25.54±2.33	11±1	2.45±0.19	0.15±0.03	0.58±0.29	−0.632±0.158	8
Cauda	1.73±0.25	25.71±3.66	12±3	2.38±0.34	0.13±0.02	0.75±0.14	−0.778±0.127	3
Statistics	$P=0.798$	$P=0.970$	$P=0.944$	$P=0.726$	$P=0.523$	$P=0.223$	$P=0.322$	

Abbreviations: CCF, cross-correlation function; CV, coefficient of period variation; DR, dorsal root; FL, fictive locomotion.

Next, we reduced the stimulus intensity down to a value that, per se, no longer generated locomotor-like responses (Figure 1b; 11, 7 and 14 μA, respectively). The resulting low-intensity train was simultaneously applied to three distinct DRs (overall stimulus amplitude = 32 μA). Although the total intensity of the three stimuli was greater than the value needed to activate FL with a single DR train at 2 Hz, it proved ineffective in inducing FL when distributed through three DRs, even though a slight cumulative depolarization with asynchronous slow oscillations appeared (Figure 1c). The same results were confirmed in further three experiments (CCF = 0.446 ± 0.311, $n=4$). Even though the data were obtained on the basis of *in vitro* preparations, they indicate that the spinal locomotor networks process incoming stimuli in a complex manner, which is different from the mere summation of multiple, simultaneous single inputs originating from different afferent fibres.

Phase resetting of electrically induced FL by delivering single pulses to a distant DR

In order to test whether different afferent inputs converge onto common spinal locomotor networks, we used the method of locomotor phase resetting, whereby the regularity of a rhythmic pattern induced by pulses delivered to a range of lumbosacral DRs is perturbed by a single pulse delivered to another DR. This phenomenon has been well-described for both *in vitro* chemically induced[13] and *in vivo* electrically induced FL,[14] to demonstrate how afferent signals of various origins affect the same network. As there are no data on phase resetting of the DR-evoked FL *in vitro*, we first studied its presence in our preparation. FL was induced by a single DR stimulation during which further stimuli were delivered through a distinct DR. In the example of Figure 2a, a series of electrical pulses (60 stimuli, 2 Hz, amplitude = 9 μA) was applied to a sacral DR and induced an episode of locomotor-like oscillations recorded from L2 and L5 VRs. The regularity of FL was perturbed by two single stimuli (amplitude = 130 μA; see vertical lines), delivered to a sacral DR of the opposite side and temporally separated by a 10-s interval. Figure 2b (note faster time base) clearly shows phase resetting: the single impulses delivered to lS2 (occurred in correspondence to the peak in the VRL2) lengthened the cycle ipsilateral to the stimulating site, while prolonging the trough in the contralateral VRL2 and VRL5. In five preparations, phase resetting of FL cycles was induced in 12 out of 24 impulses delivered as single sacral DR stimuli (mean stimulus strength equal to 222.50 ± 116.39 μA). Furthermore, electrical stimulation of lumbar DRs (mean amplitude 187.89 ± 120.95 μA) produced a comparable occurrence of phase resetting (19/34, $n=5$ cords).

Interestingly, the phenomenon was observed more often when single pulses were delivered in correspondence to peaks in FL cycles recorded from flexor-related VRs homolateral to the stimulating DR (16/24), rather than from contralateral flexor-related VRs (8/24). These data show that in our preparations, activity at lumbar or sacral DRs possesses analogous resetting ability and, therefore, is most likely converging onto the spinal locomotor networks.

Multi-site delivery renders subthreshold frequency DR trains effective in triggering FL

So far, our experiments demonstrated that despite convergence onto the same spinal circuits, simultaneous weak stimulus delivery to various DRs was not able to evoke comparable amplitudes. For our next question, we then tested whether the spinal circuits could process stimulating frequencies in a different manner.

Thus, electrical trains were first delivered to one sacral DR as 60 rectangular pulses (2 Hz), to produce cumulative depolarization (0.64 ± 0.26 mV peak; $n=18$) with superimposed oscillations alternating among homosegmental VRs (CCF = −0.667 ± 0.153, $n=18$). FL lasted for the whole duration of the 2-Hz stimulating protocol (26.21 ± 2.36 s, $n=18$; see examples in Figure 3a–c, left panels), with optimal strength amplitude of 1 to 2.5 × threshold for inducing the highest number of alternating oscillations (11 ± 2, $n=18$). This frequency of stimulation was then reduced by a third (0.67 Hz), while maintaining the same stimulation intensity. None of the resulting low-frequency trains was then able to activate the FL pattern when delivered alone, as low cumulative depolarization (0.36 ± 0.17 mV, $n=9$) accompanied by reflex responses (CCF = 0.567 ± 0.280, $n=9$) in correspondence to each impulse was detected (Figures 3a–c, right panels). Afterwards, the protocol of multi-site stimulation was applied as illustrated in Figure 3d. Three trains of low-frequency stimulation (0.67 Hz) were delivered together to three different sacral DRs of the same preparation, with a phase delay of 0.5 and 1 s for the second and third trains, respectively. By graphically superimposing the three single trains, we obtained the resulting multi-site stimulation protocol (Figure 3d, lower panel). This now showed an overall frequency of 2 Hz and was found to trigger FL with a number of cycles similar to single-site higher-frequency stimulation (Figure 3e) of similar amplitude.

We studied the effects of the multiple staggered low-frequency protocols in more detail in three preparations, where trains were applied to three different DRs (from L2 to the cauda equina) to generate a cumulative depolarization of 0.79 ± 0.18 mV, accompanied by 10 ± 1 locomotor-like cycles (CCF = −0.722 ± 0.100). This effect was not significantly different from that evoked in the same preparations by single 2 Hz trains in terms of total duration of FL episodes (*t*-test, $P=0.297$; $n=3, 9$), mean cycle period (*t*-test, $P=0.907$; $n=3, 9$) and regularity, expressed as period coefficient of period variation (*t*-test, $P=0.078$; $n=3, 9$). Responses were not affected by the order in which various afferents were stimulated (data not shown). Delivery of multiple staggered DR trains of low frequency for 60 s did not prevent the spontaneous decay of locomotor response (mean duration of FL episodes = 38.63 ± 7.23 s, $n=8$; Figure 4a), as noted when a single afferent was stimulated with a classical 2-Hz train.[8]

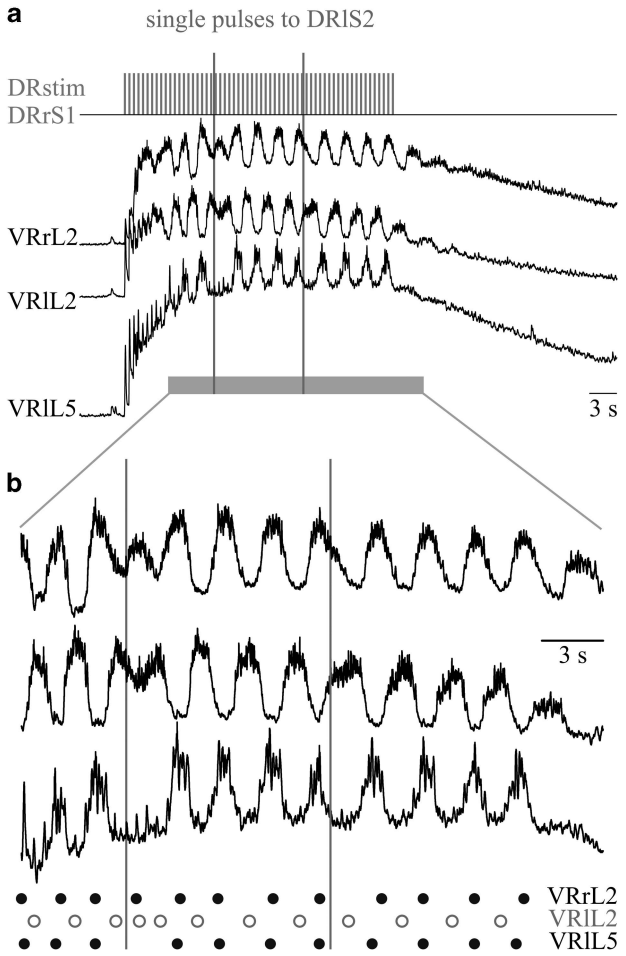

Figure 2 Single DR pulses evoke phase resetting of electrically induced FL cycles. (**a**) A train of 60 stimuli at 2 Hz (amplitude = 9 μA, 1 × threshold) applied to DRIS1 induces an episode of alternating oscillations among right L2 and contralateral L2 and L5 VRs (CCF = − 0.821). During train delivery, two other single impulses are added at a higher intensity (amplitude = 130 μA, 8.7 × threshold) to DRIS2, which disturbed regularity of FL oscillations. (**b**) In correspondence to the first stimulus, delivered at the peak on the VRL2 homolateral to the site of stimulation, an early peak on VRrL2 appears, which is followed by an extra peak that prolongs the burst on VRIL2 and by a protracted pause on VRIL5. Note that traces are a higher magnification of VR recordings referring to the grey bars in **a**. On the other hand, during the first ascending phase of a cycle on the VRL2 homolateral to the stimulation site, the second impulse is delivered and delays the following peak on VRrL2, lengthens the burst of VRIL2 and slightly slows down rhythm on VRIL5. The scattered representation below highlights phase relation among peaks of oscillations in the three VRs. CCF, cross-correlation function; DRstim, dorsal root electrical stimulation; DRrL, right lumbar dorsal root; DRIS, left sacral dorsal root; VRIL, left lumbar ventral root; VRrL, right lumbar ventral root.

The minimum frequency of DR trains to effectively elicit FL was 1 Hz (Supplementary Figure 2a–c). Furthermore, the staggered multiple stimulation of three DRs at 0.33 Hz was still capable to evoke an episode of FL once applied with a phase delay of 1 s (Supplementary Figure 2d).

To verify whether the synchronous delivery of three trains at optimal intensity can evoke an FL notwithstanding low frequency of stimulation, we then simultaneously applied three 0.67 Hz trains to three DRs for 60 s (synchronous onset among three DRs; Figure 4b). Compared with staggered stimulation of three DRs in the same preparation (Figure 4a), this protocol failed to generate FL (Figure 4b), as confirmed by cross-correlation analysis on pairs of VRL2 (mean CCF for staggered DR trains = -0.502 ± 0.138 vs mean CCF for synchronous DR trains = -0.162 ± 0.238; Mann–Whitney rank sum test, $P = 0.005$; $n = 8$). This suggests that efficacy of the staggered protocol does not originate from the sole simultaneous stimulation at optimal amplitude of multiple DRs, but also exploits the controlled time interval for the delivery of the trains.

Multiple delivery of random low-frequency trains still induced FL episodes, but with inferior coupling than canonical protocols

To clarify whether a staggered approach is absolutely necessary for the expression of FL episodes using low-frequency stimulation, multiple trains with the same number of pulses (mean frequency = 0.67 Hz) were delivered randomly to three DRs.

As depicted in Figure 5a–c (left), single DR trains at classical 2 Hz evoked a cumulative depolarization with superimposed, fully alternated locomotor-like cycles. Conversely, FL was not elicited by a randomized delivery of stimuli with a mean frequency of 0.67 Hz to the same DRs, despite the similar amplitude of single pulses (Figure 5a–c, right).

On the other hand, the protocol resulting from the combined delivery of three random trains (Figure 5d) elicited FL cycles similar to the ones induced by staggered low-frequency trains, as exemplified in Figure 5e.

In four cords, 2 Hz DR trains (mean intensity = $1.56 \pm 0.19 \times$ threshold) induced a mean cumulative depolarization of 1.06 ± 0.53 mV, with an episode of 11 ± 1 locomotor-like oscillations for a total mean duration of 25.18 ± 1.59 s. Moreover, multiple random trains of identical amplitude evoked a comparable mean cumulative depolarization (1.00 ± 0.53 mV) with an FL epoch of similar duration (23.85 ± 0.93 s) and number of cycles (10 ± 1). Locomotor-like response evoked by multiple random trains was similar to the one elicited by the staggered protocol (cumulative depolarization = 0.93 ± 0.48 mV; duration = 23.93 ± 4.90 s; cycles = 11 ± 3).

In fact, the three different types of stimulation were not statistically different as for cumulative depolarization (one-way ANOVA, $P = 0.898$; $n = 12, 4, 4$), duration of FL episodes (one-way ANOVA, $P = 0.447$; $n = 12, 4, 4$) and number of oscillations (Kruskall–Wallis one-way ANOVA, $P = 0.173$; $n = 12, 4, 4$).

On the other hand, FL evoked by multiple random trains displayed a mean phase coupling among L2 VRs that was statistically lower than the one triggered by 2 Hz trains, which in turn was not statistically different from staggered protocols (Kruskal–Wallis one-way ANOVA followed by all pairwise multiple comparison with Dunn's method, $P = 0.011$; $n = 12, 4, 4$; Figure 5f).

DISCUSSION

The principal finding of the present study is the experimental demonstration that optimal activation of the spinal locomotor program was achieved by delivering low-frequency trains in a staggered manner to multiple DRs of the rat spinal cord. Thus, locomotor spinal networks could decode and process multiple stimuli in a complex manner.

Indeed, locomotor spinal networks can sum frequency of stimuli reaching the central pattern generator from multiple afferents (frequency-related summation), while each afferent input is individually filtered out if below a threshold value (intensity-related occlusion).

It should be mentioned that our *in vitro* model does not allow us to fully analyse the fine-tuning of motor control observed with kinematic

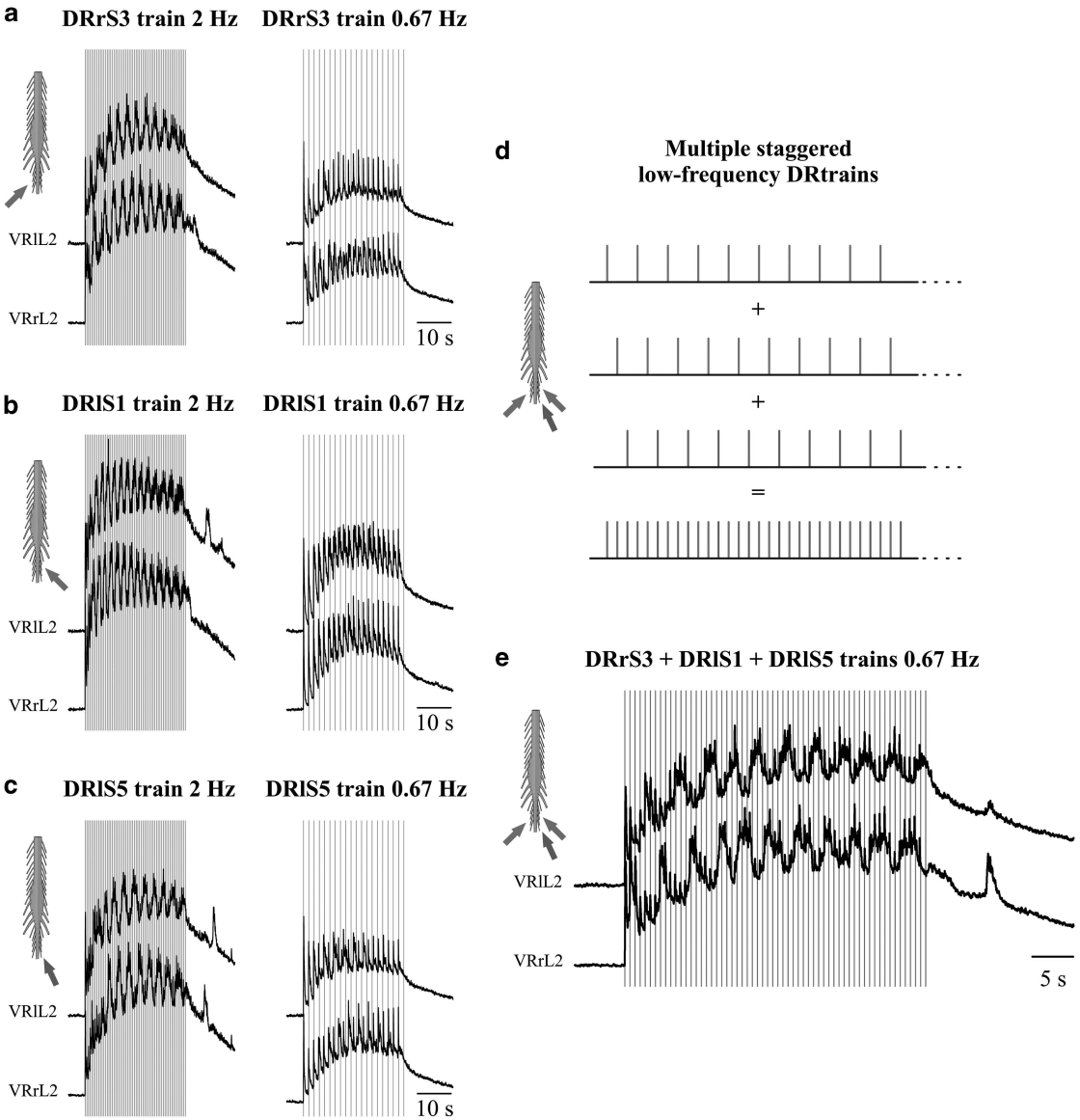

Figure 3 Low-frequency trains of stimuli applied to multiple DRs with staggered onsets elicit an episode of FL oscillations. (**a**) A train of 60 stimuli to DRrS3 induces a locomotor response when applied at 2 Hz (left; CCF = −0.654), but not when delivered with a lower frequency (0.67 Hz; right; CCF = 0.555), although with equal intensity (18 μA, 2 × threshold). In the same preparation, a similar trend is observed when trains at 2 and 0.67 Hz are serially delivered to DRIS1 (amplitude = 25 μA, 2 × threshold; (**b**) CCF = −0.500 and CCF = 0.870, respectively) or DRIS5 (amplitude = 25 μA, 2.5 × threshold; (**c**) CCF = −0.629 and CCF = 0.600, respectively). (**d**) Sketches how the stimulating protocol is prepared, by superimposing three trains of low frequency (0.67 Hz), each one applied to a distinct afferent of the same cord and with an onset staggered by 0.5 s from the previous train. In **e**, this protocol proves (same preparation as in **a**—**c**) to be able to activate an episode of FL (CCF = −0.608) comparable, as for number and regularity of cycles, to the ones evoked from single DR trains at 2 Hz when delivered separately. CCF, cross-correlation function; DRIL, left lumbar dorsal root; DRrS, right sacral dorsal root; DRIS, left sacral dorsal root; VRIL, left lumbar ventral root; VRrL, right lumbar ventral root.

analysis in walking animals. Nevertheless, our method has the important advantage of recording motor output of pure neuronal origin without any influence of either compensatory muscle activation or modulators of the peripheral circulatory stream.

Frequency of incoming inputs is more important than intensity

Although previous reports point out that also capsaicin-sensitive pain-related fibres are involved in the modulation of ongoing FL,[15] modelling studies have shown that DR electrical stimulation activates the locomotor pattern mainly due to a selective recruitment of multiple fibres carrying tactile and proprioceptive inputs. These fibres are characterized by a wide diameter and low excitation threshold, thus being unable to discriminate small variations in stimulus amplitude.[4] This characteristic can account for the inability of simultaneous stimuli of low amplitude to summate and generate a locomotor pattern. We, therefore, propose the existence of a gating system that filters the amplitude of afferent stimuli. Such a system is reminiscent of the relay neurons in the sacrococcygeal spinal cord that were previously suggested to drive lumbar rhythms.[10] On the other hand, previous studies have shown that stimulation frequency might sculpt circuit synapses through different plasticity mechanisms: modifying either the amount[16] or type[17] of released neurotransmitters, reversing the balance between excitation and inhibition,[18] or limiting negative-feedback pre-synaptic processes.[19] In addition, circuit

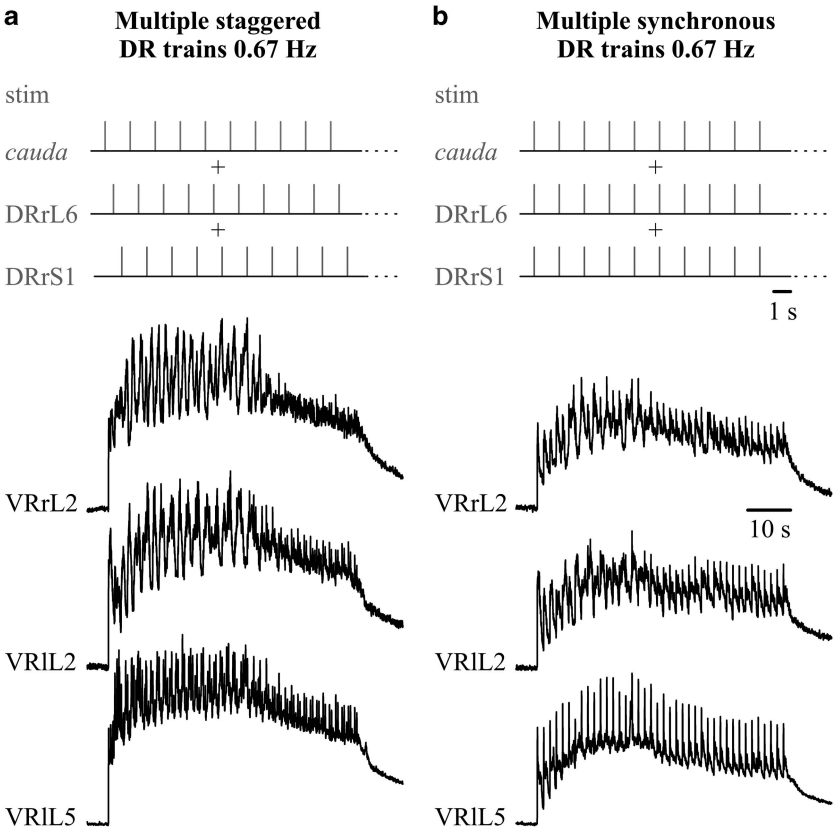

Figure 4 Low-frequency multi-site synchronous stimulation fails to induce FL. (**a**) A sixty-second protocol of multiple staggered trains of pulses applied at low frequency (0.67 Hz) to the cauda equina (amplitude = 30 μA, 1.5 × threshold), DRrS1 (amplitude = 15 μA, 1.5 × threshold) and DRrL6 induced an episode of FL (CCF = −0.539) that does not last beyond 38 s, whereas a depolarizing plateau with superimposed tonic activity replaces the locomotor-like cycles during the rest of the stimulation. When trains at 0.67 Hz are delivered synchronously to the three afferents, alternating cycles of FL are replaced by tonic responses time-locked with each of the train's stimuli (**b**, CCF = +0.136). It is noteworthy that the amplitude of the pulses is kept unvaried for each afferent during delivery of protocols in **a** and **b**. CCF, cross-correlation function; DRrL, right lumbar dorsal root; DRrS, right sacral dorsal root; VRlL, left lumbar ventral root; VRrL, right lumbar ventral root.

architecture can be flexibly reconfigured by distinct stimulation frequencies. Indeed, they may either recruit distinct types of interneurons[20] or add previously 'silent' frequency-dependent spinal pathways to the ongoing locomotor pattern.[21] Our data here reported may spur further studies on these findings also for the spinal locomotor networks.

Afferent stimuli modulate locomotor circuits

Interneuronal circuits embedded in locomotor networks of the mammalian spinal cord are known to span several lumbar segments.[9] Within these segments, many features of the rhythmic pattern are affected by inputs from the periphery.[14] One of our main findings is that within the *in vitro* neonatal rat spinal cord, inputs coming from multiple DRs converge onto the same locomotor circuits. This consideration is based on the observed phase-shift in the oscillatory rhythm of FL induced by stimulation of a distant DR, with the implication that the locomotor network is accessible also via inputs from anatomically different locations. To the best of our knowledge, no phase resetting has ever been reported during electrically induced FL *in vitro*.

Multiple-source inputs facilitate neuronal networks

Multiple-source stimulation is a concept with wide support in the field of neuromodulation, as it has been used to activate different types of neurons and pathways,[22] and to promote behaviours, viz. learning and associative plasticity.[23] Simultaneous electrical stimuli delivered to numerous spinal segments facilitate involuntary stepping movements and limb oscillation amplitude in non-injured human subjects, thus proving synergy among inputs converging onto locomotor circuits.[24]

In our experiments, electrical stimulation with staggered trains of low frequency was simultaneously applied to multiple DRs and sacrocaudal afferents. Although each train on its own was ineffective, their combination activated the locomotor program and the delay in latency at which each DR was stimulated proved to be essential to this effect. The responsiveness of locomotor networks to electrical stimuli from multiple DRs supports the concept that spatial and temporal addition of numerous afferent inputs is fundamental for activating spinal locomotor networks. This phenomenon is closely related to the role had by stochastic variability in the recruitment of neuronal networks, as previously described.[25]

There is further evidence in support of the concept that multiple types of afferent stimuli are required to activate the locomotor circuits in the ventral spinal cord. FL can be induced by stimulating a single DR or sacrocaudal afferent root, which contains several types of afferent fibres, each with their own conduction velocities.[26] In contrast, electrical stimulation of only a fraction of the fibres that reside in a nerve afferent failed to activate the locomotor pattern[27].

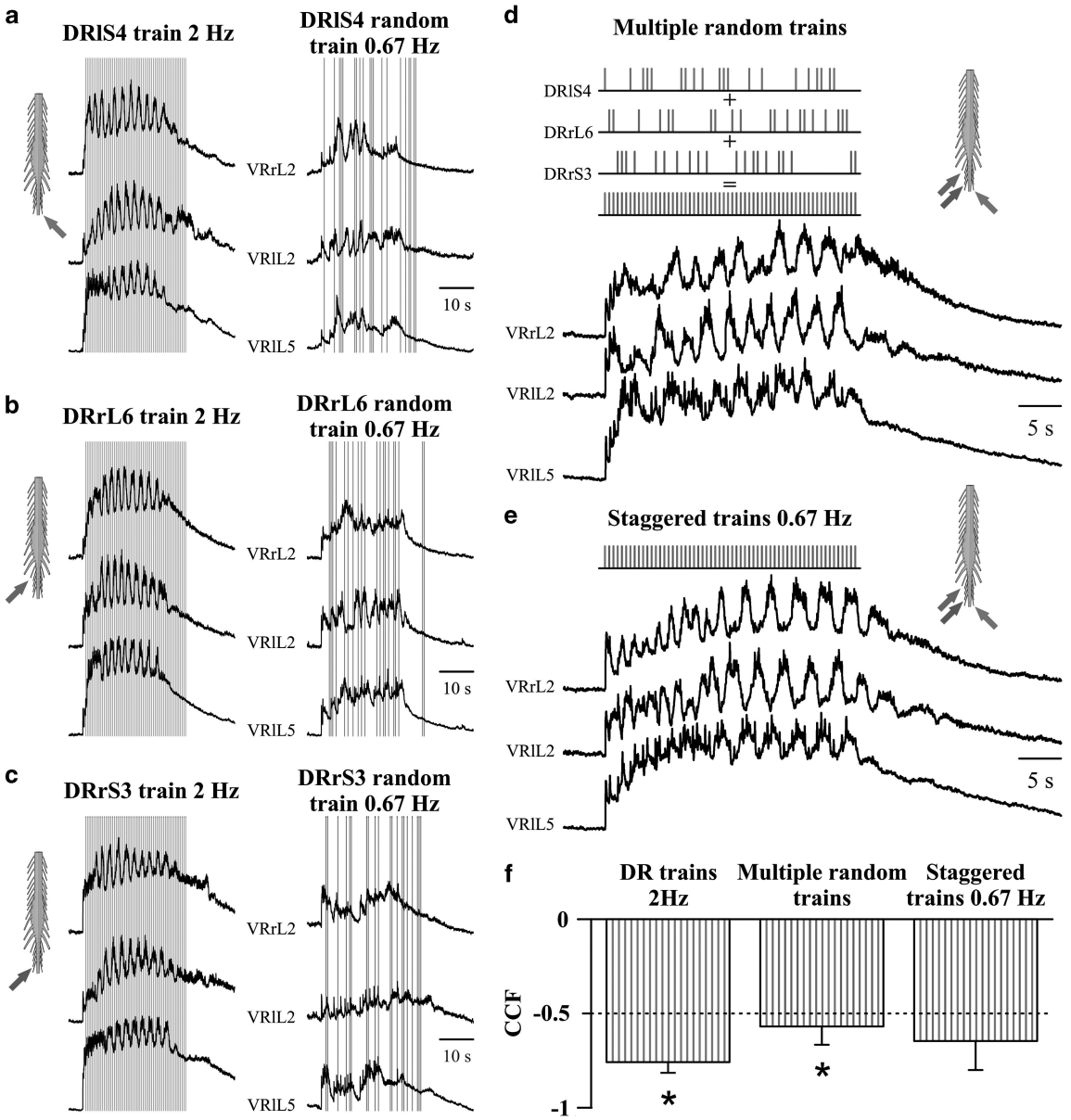

Figure 5 Low-frequency trains of pulses randomly delivered to three DRs induced FL. (**a**, Left) A 2-Hz train (intensity = 13 μA) applied to DRIS4 elicited a stable FL (CCF = −0.870). A new protocol (mean frequency of 0.67 Hz), designed by randomly selecting only one-third of pulses from the 2 Hz train, was delivered to the same DR without evoking any locomotor patterns ((**a**, right) CCF = −0.296)). (**b**, Left) The 2-Hz train delivered to DRrL6 (intensity = 7 μA) also induced an FL episode (CCF = −0.852), where the multiple random protocol failed to do so ((**b**, right) CCF = −0.347). (**c**, Left) FL (CCF = −0.761) was elicited by the 2-Hz train (intensity = 20 μA) to DRrS3 contrary to the random protocol applied to the same root ((**c**, right) CCF = 0.088). The three multiple random trains (mean frequency = 0.67 Hz) were now simultaneously applied to the three DRs, as graphically schematized in **d** (top), showing how the superimposition of single trains recomposed the overall 2 Hz frequency. This stimulating pattern evoked an episode of alternating cycles (CCF = −0.507), similar to multiple staggered trains at low frequency ((**e**) 0.67 Hz; CCF = −0.748). FL episodes evoked by the three protocols were compared in **f** as for phase coupling between the pair of homosegmental L2 VRs. All three protocols induced locomotor-like cycles (CCF < −0.5, see dotted line), although the 2-Hz train evoked a statistically stronger alternated coupling among oscillations than did multiple random trains (*Kruskal–Wallis one-way ANOVA followed by all pairwise multiple comparison with Dunn's method, $P = 0.011$, $n = 12, 4, 4$). CCF, cross-correlation function; DRrL, right lumbar dorsal root; DRrS, right sacral dorsal root; VRIL, left lumbar ventral root; VRrL, right lumbar ventral root.

CONCLUSIONS

A multi-site stimulating protocol with low-frequency trains, delivered with a controlled staggered onset, effectively activated the locomotor central pattern generator in the neonatal rat spinal cord *in vitro*. As the lumbosacral circuitry controlling locomotion in rats and humans has been considered strikingly similar,[28] our data cast light on the intrinsic logic adopted by spinal networks to integrate peripheral stimuli during locomotion and thereby propose new protocols of low-energy multi-site stimulation to improve rehabilitation and/or chronic pain neuromodulation. Moreover, advantages of the proposed stimulation protocol will extend to a reduced energetic demand that increases the life span of batteries in implantable stimulators, thereby increasing the interval between battery replacements. Finally, this protocol should reduce adverse effects, typically

associated with high-energy stimulation, for example, muscle fatigue and spasticity.[29,30]

DATA ARCHIVING

There were no data to deposit.

CONFLICT OF INTEREST

The authors declare no conflict of interest.

ACKNOWLEDGEMENTS

We are grateful to Dr Alessandra Fabbro and Professor Andrea Nistri for data discussion, John Fischetti for technical advice and Dr Elisa Ius for her excellent assistance in preparing the manuscript. We thank Mrs Giulia Bossolini for her generous support.

1 Harkema S, Gerasimenko Y, Hodes J, Burdick J, Angeli C, Chen Y *et al.* Effect of epidural stimulation of the lumbosacral spinal cord on voluntary movement, standing, and assisted stepping after motor complete paraplegia: a case study. *Lancet* 2011; **377**: 1938–1947.
2 Angeli CA, Edgerton VR, Gerasimenko YP, Harkema SJ. Altering spinal cord excitability enables voluntary movements after chronic complete paralysis in humans. *Brain* 2014; **137**: 1394–1409.
3 Minassian K, Persy I, Rattay F, Pinter MM, Kern H, Dimitrijevic MR. Human lumbar cord circuitries can be activated by extrinsic tonic input to generate locomotor-like activity. *Hum Mov Sci* 2007; **26**: 275–295.
4 Capogrosso M, Wenger N, Raspopovic S, Musienko P, Beauparlant J, Bassi Luciani L *et al.* A computational model for epidural electrical stimulation of spinal sensorimotor circuits. *J Neurosci* 2013; **33**: 19326–19340.
5 Meacham KW, Guo L, Deweerth SP, Hochman S. Selective stimulation of the spinal cord surface using a stretchable microelectrode array. *Front Neuroengineering* 2011; **4**: 5.
6 Gad P, Choe J, Nandra MS, Zhong H, Roy RR, Tai YC *et al.* Development of a multi-electrode array for spinal cord epidural stimulation to facilitate stepping and standing after a complete spinal cord injury in adult rats. *J Neuroeng Rehabil* 2013; **10**: 2.
7 Taccola G, Marchetti C, Nistri A. Effect of metabotropic glutamate receptor activity on rhythmic discharges of the neonatal rat spinal cord *in vitro*. *Exp Brain Res* 2003; **153**: 388–393.
8 Marchetti C, Beato M, Nistri A. Alternating rhythmic activity induced by dorsal root stimulation in the neonatal rat spinal cord *in vitro*. *J Physiol* 2001; **530**: 105–112.
9 Kjaerulff O, Kiehn O. Distribution of networks generating and coordinating locomotor activity in the neonatal rat spinal cord *in vitro*: a lesion study. *J Neurosci* 1996; **16**: 5777–5794.
10 Strauss I, Lev-Tov A. Neural pathways between sacrocaudal afferents and lumbar pattern generators in neonatal rats. *J Neurophysiol* 2003; **89**: 773–784.
11 Perreault MC, Angel MJ, Guertin P, McCrea DA. Effects of stimulation of hindlimb flexor group II afferents during fictive locomotion in the cat. *J Physiol* 1995; **487**: 211–220.
12 Taccola G, Mladinic M, Nistri A. Dynamics of early locomotor network dysfunction following a focal lesion in an *in vitro* model of spinal injury. *Eur J Neurosci* 2010; **31**: 60–78.
13 Lennard PR. Afferent perturbations during "monopodal" swimming movements in the turtle: phase-dependent cutaneous modulation and proprioceptive resetting of the locomotor rhythm. *J Neurosci* 1985; **5**: 1434–1445.
14 Pearson KG. Neural adaptation in the generation of rhythmic behavior. *Ann Rev Physiol* 2000; **62**: 723–753.
15 Mandadi S, Hong P, Tran MA, Braz JM, Colarusso P, Basbaum AI *et al.* Identification of multisegmental nociceptive afferents that modulate locomotor circuits in the neonatal mouse spinal cord. *J Comp Neurol* 2013; **521**: 2870–2887.
16 Elhamdani A, Palfrey HC, Artalejo CR. Quantal size is dependent on stimulation frequency and calcium entry in calf chromaffin cells. *Neuron* 2001; **31**: 819–830.
17 Liu X, Porteous R, d'Anglemont de Tassigny X, Colledge WH, Millar R, Petersen SL *et al.* Frequency-dependent recruitment of fast amino acid and slow neuropeptide neurotransmitter release controls gonadotropin-releasing hormone neuron excitability. *J Neurosci* 2011; **31**: 2421–2430.
18 Zhang TC, Janik JJ, Grill WM. Modeling effects of spinal cord stimulation on wide-dynamic range dorsal horn neurons: influence of stimulation frequency and GABAergic inhibition. *J Neurophysiol* 2014; **112**: 552–567.
19 Rancillac A, Barbara JG. Frequency-dependent recruitment of inhibition mediated by stellate cells in the rat cerebellar cortex. *J Neurosci Res* 2005; **80**: 414–423.
20 McLean DL, Masino MA, Koh IY, Lindquist WB, Fetcho JR. Continuous shifts in the active set of spinal interneurons during changes in locomotor speed. *Nat Neurosci* 2008; **11**: 1419–1429.
21 Jilge B, Minassian K, Rattay F, Dimitrijevic MR. Frequency-dependent selection of alternative spinal pathways with common periodic sensory input. *Biol Cybern* 2004; **91**: 359–376.
22 Bonifazi P, Ruaro ME, Torre V. Statistical properties of information processing in neuronal networks. *Eur J Neurosci* 2005; **22**: 2953–2964.
23 Harris CA, Passaro PA, Kemenes I, Kemenes G, O'Shea M. Sensory driven multi-neuronal activity and associative learning monitored in an intact CNS on a multielectrode array. *J Neurosci Methods* 2010; **186**: 171–178.
24 Gerasimenko YP, Gorodnichev R, Puhov A, Moshonkina T, Savochin A, Selionov VA *et al.* Initiation and modulation of locomotor circuitry output with multi-site transcutaneous electrical stimulation of the spinal cord in non-injured humans. *J Neurophysiol* 2014; **113**: 834–842.
25 Taccola G. The locomotor central pattern generator of the rat spinal cord *in vitro* is optimally activated by noisy dorsal root waveforms. *J Neurophysiol* 2011; **106**: 872–884.
26 Nagy I, Dray A, Urban L. Possible branching of myelinated primary afferent fibres in the dorsal root of the rat. *Brain Res* 1995; **703**: 223–226.
27 Viala G, Orsal D, Buser P. Cutaneous fiber groups involved in the inhibition of fictive locomotion in the rabbit. *Exp Brain Res* 1978; **33**: 257–267.
28 Gerasimenko Y, Gorodnichev R, Machueva E, Pivovarova E, Semyenov D, Savochin A *et al.* Novel and direct access to the human locomotor spinal circuitry. *J Neurosci* 2010; **30**: 3700–3708.
29 Binder-Macleod SA, Snyder-Mackler L. Muscle fatigue: clinical implications for fatigue assessment and neuromuscular electrical stimulation. *Phys Ther* 1993; **73**: 902–910.
30 Mela P, Veltink PH, Huijing PA. Excessive reflexes in spinal cord injury triggered by electrical stimulation. *Arch Physiol Biochem* 2001; **109**: 309–315.

Supplementary Information accompanies this paper on the Spinal Cord website (http://www.nature.com/sc)

Supplementary information

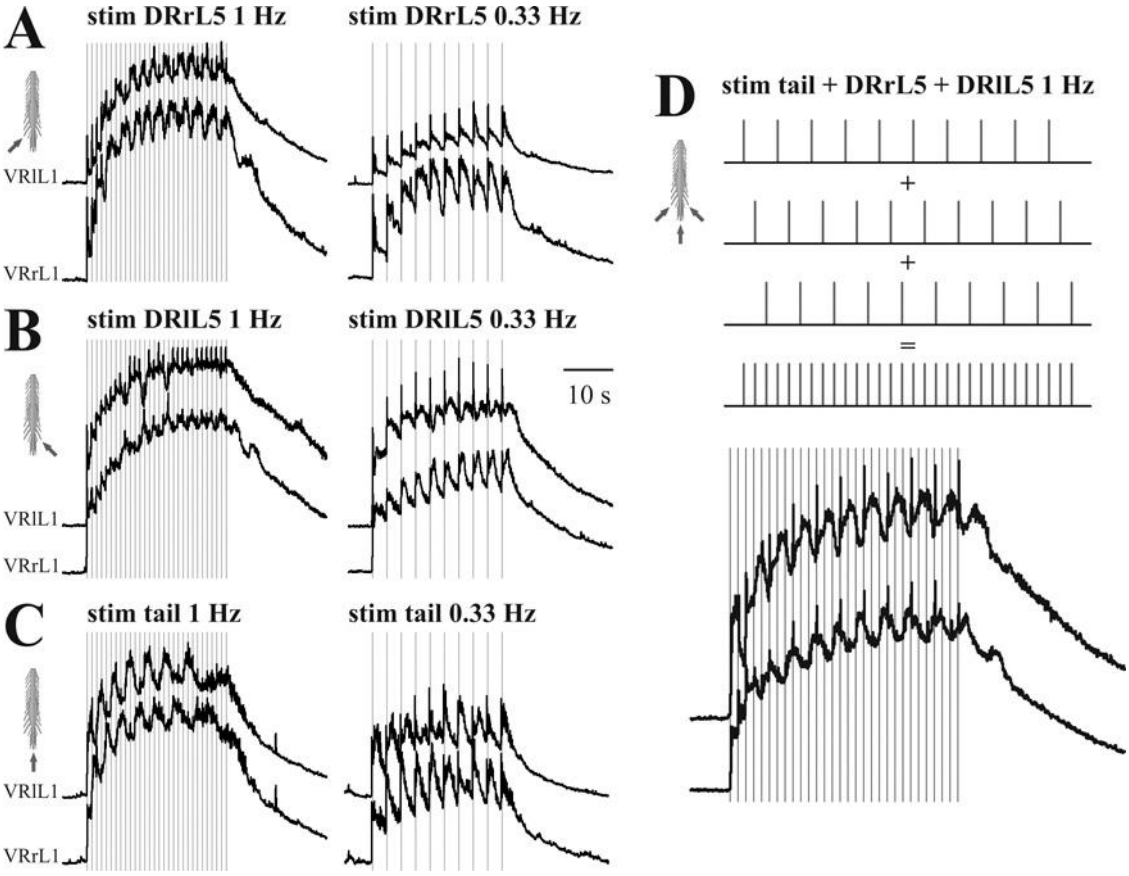

Figure S1. Intersegmental VR responses are not related to current leakage from closeby electrodes. *A, single pulses (intensity = 400 µA) delivered to DRrL6 evoke a reflex response from contralateral VR (peak = 0.32 mV) and, after a delay of 17.8 ms, from the close VRIS2 (peak = 0.16 mV). B, single pulses (intensity = 400 µA) delivered to DRrS2 evoked a reflex response from contralateral VR (peak = 0.30 mV) and, after a delay of 11.3 ms, from the close VRIL6 (peak = 0.15 mV). C, after complete transection at S1 level, the two spinal portions were kept close and DRIL6 was stimulated at the same intensity as in panel A and B, inducing a response of 0.37 mV from VRIL6 while disconnected VRIS2 did not elicit any response. D, similarly, after cutting at S1, stimulation of DRrS2 elicited a peak reflex response of 0.21 mV from VRIS2 and none from VRIL6. Note that artefacts of stimulation (downwards deflections at the beginning of each trace) are passively conducted through all recording electrodes, but they do not influence active intersegmental responses. Traces in the figure are averaged from at least 5 sweeps.*

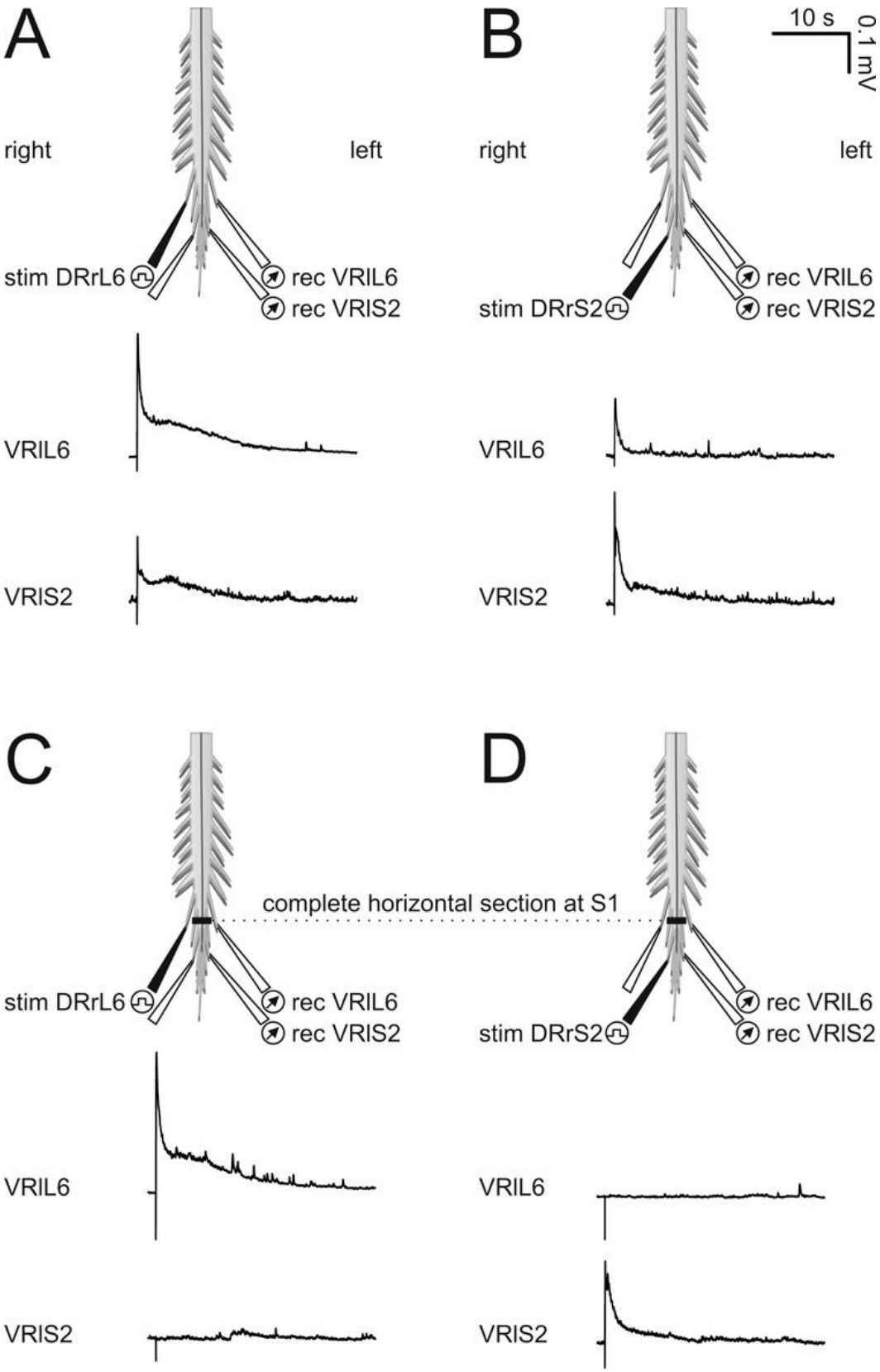

Figure S2. The slowest staggered protocol evoking FL is 0.33 Hz. *A-C right; DR trains at 1 Hz, individually applied to three DRs at once (rL5, intensity = 100 µA; lL5 intensity = 30 µA, and tail, intensity = 100 µA), evoked a cumulative depolarization (1.34 ± 0.06 mV) with*

superimposed 8 ± 3 oscillations (2.99 ± 0.51 s periodicity and 0.21 ± 0.08 CV period) alternated between homosegmental VRs (CCF= - 0.534 ± 0.100, n = 3). Contrariwise, when a 0.33 Hz train was individually delivered to a single DRs, a lower cumulative depolarization (0.66 ± 0.09 mV) was accompanied by reflex responses time-locked with each stimulus (A-C, left; CCF = 0.740 ± 0.282, n = 3). In D, multiple stimulation of the three DRs (as schematized above) at 0.33 Hz, with a staggered onset of 1 s for each DRs, depolarized VRs (1.40 mV) and induced an epoch of FL (11 FL cycles, CCF = -0.537).

Received: August 18, 2015 Revised: December 21, 2015 Accepted: December 29, 2015

(onlinelibrary.wiley.com) DOI: 10.1111/ner.12402

Two Distinct Stimulus Frequencies Delivered Simultaneously at Low Intensity Generate Robust Locomotor Patterns

Francesco Dose, MSc*†; Giuliano Taccola, PhD*†

Objectives: Explore the primary characteristics of afferent noisy stimuli, which optimally activate locomotor patterns at low intensity.

Materials and Methods: Intracellular and extracellular electrophysiological traces were derived from single motoneurons and from ventral roots, respectively. From these recordings, we obtained noisy stimulating protocols, delivered to a dorsal root (DR) of an isolated neonatal rat spinal cord, while recording fictive locomotion (FL) from ventral roots.

Results: We decreased complexity of efficient noisy stimulating protocols down to single cell spikes. Then, we identified four main components within the power spectrum of these signals and used them to construct a basic multifrequency protocol of rectangular impulses, able to induce FL. Further disassembling generated the minimum stimulation paradigm that activated FL, which consisted of a pair of 35 and 172 Hz frequency pulse trains, strongly effective at low intensity when delivered either jointly to one lumbosacral DR or as single simultaneous trains to two distinct DRs. This simplified pulse schedule always activated a locomotor rhythm, even when delivered for a very short time (500 ms). One prerequisite for the two-frequency protocol to activate FL at low intensity when applied to sacrocaudal afferents was the ability to induce ascending volleys of greater amplitude.

Conclusion: Multifrequency protocols can support future studies in defining the most effective characteristics for electrical stimulation to reactivate stepping following motor injury.

Keywords: Spinal cord, central pattern generators, fictive locomotion, train of pulses, frequency

Conflict of Interest: The authors reported no conflict of interest.

INTRODUCTION

In healthy individuals, rhythmic movements of lower limbs can be triggered by electrostimulation of the spinal cord (1–3). This phenomenon is thought to originate from the activation of interneuronal circuits, that constitute the locomotor central pattern generator (CPG), driving the rhythmic and alternated output of thoraco-lumbar motoneurons (4,5). Although, CPGs are believed to be an intrinsic motor program operating without external commands, it is clear that CPGs continuously receive and integrate afferent information from the periphery to refine the motor output according to demand. Direct electrical stimulation of the dorsal cord through epidural electrodes is actually proposed to mimic the role of afferent inputs. Furthermore, electrical stimulation has been exploited to reactivate the alternating movements of lower limbs in subjects with chronic, complete spinal lesion (6–8). The latter clinical results rely on protocols previously devised and developed (9) with *in vitro* experimental preparations that generate rhythmic patterns, alternating between flexor and extensor motor pools on either side of the spinal cord (fictive locomotion, FL; 4). In particular, FL can be evoked by stimulating dorsal root (DRs) with a train of stereotypic stimuli of a single frequency comprised within a small range (2–10 Hz; 10).

In the attempt to enhance the efficacy of electrical stimulation and to lower the side-effects potentially associated with the use of strong current (11,12), new paradigms using stimuli reconstructed from sampled motor outputs recorded from ventral roots (VRs) and endowed with intrinsic variability have been observed to generate longer locomotor episodes (noisy waves; 13–16). Nevertheless, translation of this approach to clinical use is limited by lack of suitable technology, as existing apparatus only deliver stereotyped impulses within a small frequency range (International Electrotechnical Commission directive 60601-2-10:2012). Conversely, the artificial addition of the sole noise to a stereotyped stimulating protocol did not elicit any locomotor pattern, as opposed to noisy biosignals (13). Thus, the benefits of noisy patterns must be ascribed to distinct characteristics within the noisy VR motor output. As certain frequencies can better

Address correspondence to: Dr. Giuliano Taccola, IMFR, Via Gervasutta 48, 33100 Udine, Italy. Email: taccola@sissa.it

* Neuroscience Area, International School for Advanced Studies (SISSA), Trieste, TS, Italy; and

† SPINAL (Spinal Person Injury Neurorehabilitation Applied Laboratory), Istituto di Medicina Fisica e Riabilitazione (IMFR), Udine, UD, Italy

For more information on author guidelines, an explanation of our peer review process, and conflict of interest informed consent policies, please go to http://www.wiley.com/WileyCDA/Section/id-301854.html

Sources of financial support: Authors did not receive any funding apart from institutions funds provided by SISSA (Trieste) and the Health Department ASS4 Medio Friuli (Udine).

Additional Supporting Information may be found in the online version of this article.

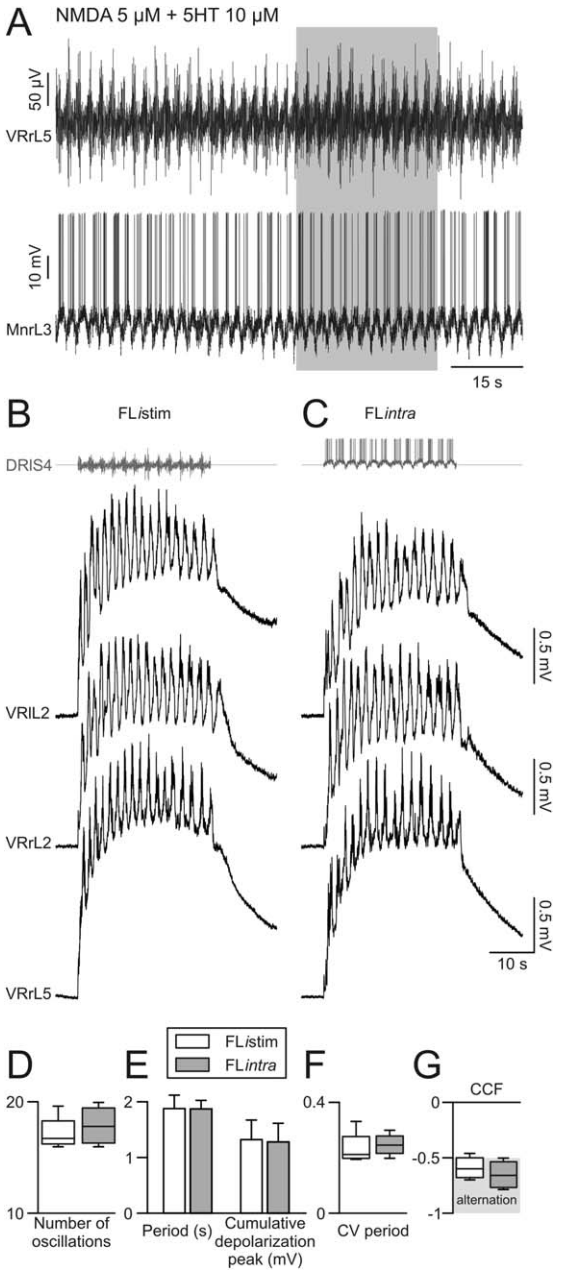

Figure 1. FL*i*stim and FL*intra* evoke a similar FL in the continuous presence of NMDA (5 μM) and serotonin (10 μM), an extracellular trace AC coupled from motor pools (VRrL5; A, top) and an intracellular trace in current clamp mode from single cell (MnrL3; A, bottom) are simultaneously recorded from the same spinal cord to design the stimulating protocols FL*i*stim and FL*intra*, respectively. FL*i*stim (B, left) and FL*intra* (B, right) are delivered (3 μA) to the DRlS4 of the same preparation. Both protocols evoke a similar FL episode, as for cumulative depolarization (0.98 mV FL*intra* vs. 1.15 mV FL*i*stim), duration (31.42 sec FL*intra* vs. 31.08 sec FL*i*stim), period (1.95 sec FL*intra* vs. 1.81 sec FL*i*stim), regularity (0.17 FL*intra* vs. 0.15 FL*i*stim) and number of cycles (17 FL*intra* vs. 18 FL*i*stim), alternating among homosegmental VRs, as confirmed by the negative values of cross correlogram analysis ($CCF_{homosegmental} = -0.71$ FL*intra* vs. -0.78 FL*i*stim). Graphs quantify the main features of FL episodes induced by the two protocols as for number of oscillations (D), period, and cumulative depolarization (E) CV period (F) and CCF values (G).

activate neuronal circuits (17,18), we hypothesized that locomotor spinal circuits can be selectively recruited when delivering pulses at distinct frequencies among the principal components of the spectrum discharge during FL. Such recordings were taken from a single motoneuron as, at single cell level, the signal resolution is undoubtedly higher while sharing the fundamental properties of the network FL (19). Subsequently, we tested the efficacy of such frequencies in a train of square impulses applied to DRs to activate the CPG. The aims of this study were to decode the complexity of noisy waves, and to identify the most advantageous characteristics of frequency and site stimulation to evoke FL episodes longer than hitherto available.

METHODS

To partially identify the mechanisms of electrostimulation able to activate the locomotor pattern at low intensities, we firstly isolated spinal cords from neonatal rats and recorded the motor output both from a VR and a motoneuron. These traces were then imported in a stimulator, as they were or after offline analysis, and either immediately delivered at varying settings to the same spinal cords or stored for other experiments. Statistical analysis was then performed to detect the most responsive protocols for inducing episodes of FL.

Ethical Approval

All procedures involving animals were accurately conducted in line with the guidelines provided by the Italian Animal Welfare act, following the European Union directive for animal experiments (86/609/EEC) and were approved by the Scuola Internazionale Superiore di Studi Avanzati (SISSA) ethics committee. Every effort was made to reduce the number of animals used and to minimize their suffering.

Isolation of Spinal Cords

Experiments were performed on 85 spinal cord preparations after isolation from Rattus norvegicus neonatal pups (P0–P3), as previously reported (20). Spinal cords were dissected from the midthoracic level to the cauda equina to extract the whole spinal cord. To keep the spinal cord viable for the duration of the experiments (around 8 hours) in a physiological environment, preparations were carefully mounted in a small recording chamber, continuously superfused (5 mL/min) at constant room temperature (22–24°C) with oxygenated (95% O_2; 5% CO_2) Krebs solution of the following composition (in mM): 113 NaCl, 4.5 KCl, 1 $MgCl_27H_2O$, 2 $CaCl_2$, 1 NaH_2PO_4, 25 $NaHCO_3$, and 11 glucose, pH 7.4.

Electrophysiological Recordings

Extracellular recordings were performed in DC mode (DP-304 differential amplifier, Warner Instruments, CT, USA) via tightly fitting monopolar suction electrodes. Borosilicate glass electrodes (Harvard Apparatus, MA, USA) contain an Ag–AgCl pellet and are filled with physiological solution. In particular, recordings were taken from left and right lumbar (L) 2 VRs, which mainly convey flexor motor-pool signals, and from left and right L5 VRs, principally expressing extensor commands (21). The alternation of discharges between flexor and extensor motor pools and between the left and right sides of the cord proves activation of the locomotor CPG and represents the distinctive characteristic of FL (22). In five experiments, to evaluate cord potentials that correspond to conduction of ascending afferent inputs induced by DR stimulation, a glass suction electrode was carefully placed onto the ventrolateral surface of the lumbar spinal cord at the level L6–S2. For intracellular recordings, antidromically identified lumbar (from L3 to L5) motoneurons (23) were impaled using borosilicate glass microelectrodes (Harvard Apparatus, MA, USA) filled with 3 M-KCl (30–60 MΩ resistance), in current-clamp

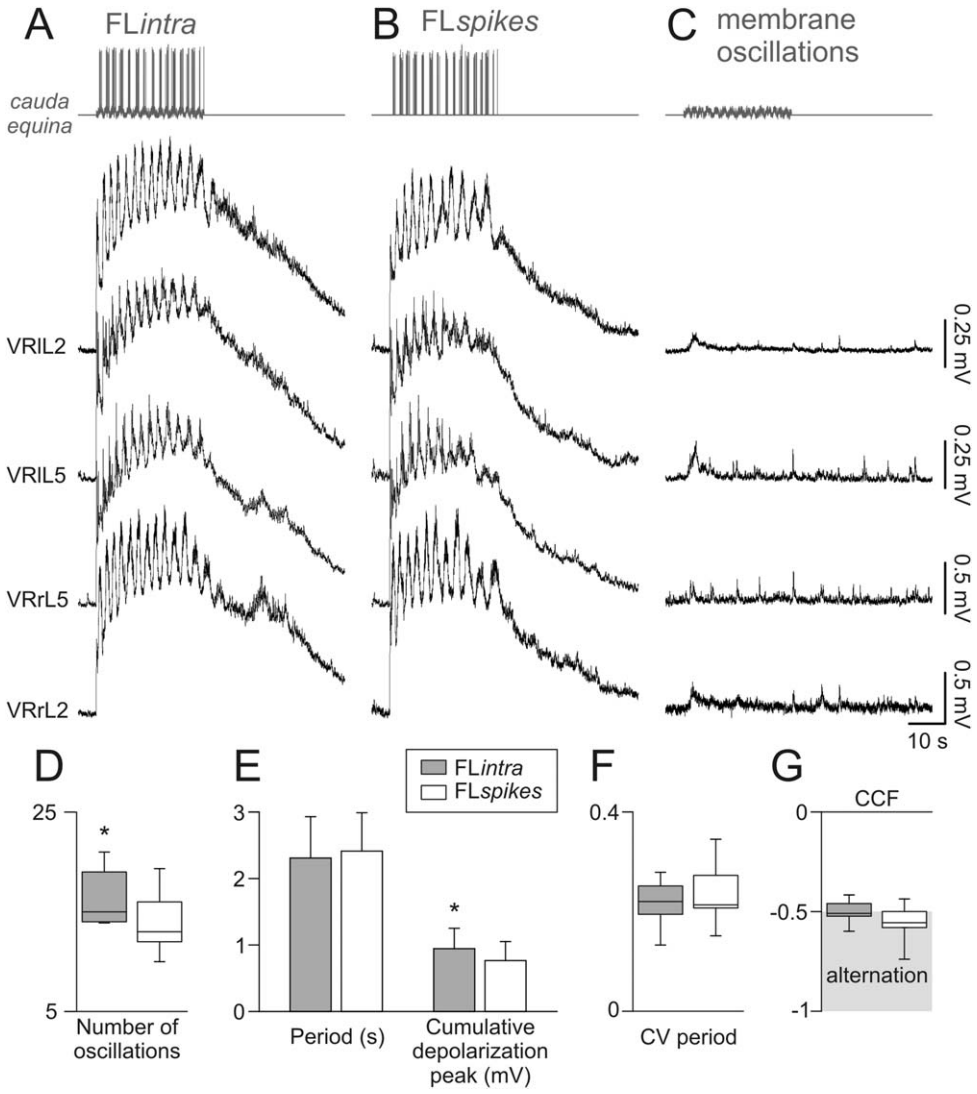

Figure 2. FL*spikes*, but not membrane oscillations, still induces locomotor-like cycles, albeit less numerous than FL*intra*. FL*intra* (A) and FL*spikes* (B) are delivered at the same intensity of stimulation (18 μA) to the same preparation. The two protocols induce a comparable cumulative depolarization (0.74 mV FL*intra* and 0.68 mV FLspikes) with superimposed a series of alternating oscillations (CCF VRs L2 −0.74 FL*intra* and −0.68 FL*spikes*) of similar number (14, FL*intra* and 11, FL*spikes*), period (2.59 s FL*intra* and 2.85 s FL*spikes*) and regularity (0.21 FL*intra* and 0.26 FL*spikes*). On the contrary, stimulation with membrane potential oscillations alone (C), at the same amplitude as that of the background oscillation in FL*intra*, fails to generate any alternating oscillations (CCF = 0.68). Averaged values in the graphs report the higher number of oscillations (D) and greater cumulative depolarization induced by FL*intra* (E), while FL oscillations maintain the same period (E), CV (F) and phase coupling in response to FL*intra* and FL*spikes* (*G*, * $t = -4815$, df = 8, $p = 0.001$, paired *t*-test, $n = 9$; *E*, * $p = 0.297$, Wilcoxon signed rank test, $n = 9$).

conditions (Axoclamp® 900A amplifier, Molecular Devices, LLC, CA, USA).

Electrical Stimulation

Single or repetitive square wave pulses were delivered in current mode to one or more DRs, using bipolar suction electrodes, to evoke single VR responses and cumulative depolarization (24). Stimulation required delivery at different current intensities (minimum = 0.6 μA, maximum = 21 μA, mean = 5.97 ± 4.82 μA; $n = 70$) to compensate experimental changes. For delivered noisy signals, intensity was reported as the difference between the maximum positive and the maximum negative amplitudes of waveforms (peak to peak). However, a comparable stimulation strength among different experiments was confirmed by precisely calculating stimulus amplitude in terms of threshold (Th), defined as the minimum intensity required to elicit a detectable response from the homologous VR (11.29 ± 4.47 μA; $n = 70$). On average, to optimally elicit FL, the lowest intensity of stimulation used in this study was 0.52 ± 0.32 times the Th ($n = 70$). To trace the most effective components of stimulation, we repeatedly applied different stimulating protocols, either noisy waveforms or trains of square pulses. First, Fictive Locomotion-*induced* stimulation (FL*i*stim) is a 30 sec or a 60 sec segment of chemically induced FL (NMDA 4–5 μM + 5HT 10 μM), extracellularly derived from a randomly selected VR. Traces were acquired in AC mode with a differential amplifier (DP-304, Warner Instruments, CT, USA; gain 1000, range 0.1–10,000 Hz), then digitalized at 10,000 Hz (Digidata® 1440, Molecular Devices, LLC, CA, USA) and finally offline reduced to the sampling rate of 500 Hz, through Clampfit® 10.3 software (Molecular Devices, LLC, CA, USA) (13,14,16). Segments of FL (30 sec) were also derived from a single motoneuron, through intracellular recordings in current clamp mode (Axoclamp® 900A amplifier,

Table 1. During FL at Different Speeds, Each Motoneuron Fires Around Four Main Spectrum Components.

Motoneurons	Period FL (s)	8 Hz	11 Hz	35 Hz	172 Hz
# 1	1.95	8.05	11.18	34.56	171.51
# 2	4.86	9.19	11.25	37.96	170.21
# 3	3.34	6.66	10.83	35.59	172.73
# 4	2.98	6.65	12.63	36.89	172.42
# 5	5.31	8.89	12.78	32.46	171.39
# 6	5.26	6.71	10.91	35.82	171.97
# 7	3.59	6.22	9.35	34.90	165.44
# 8	4.68	7.70	9.31	36.47	173.68
# 9	7.33	8.96	11.02	34.83	172.00
# 10	8.49	7.70	12.28	35.09	170.67
# 11	4.46	8.70	11.18	35.09	171.28
# 12	4.95	8.47	10.79	36.20	172.31
# 13	2.47	8.39	11.44	35.05	171.31
# 14	2.86	8.05	12.32	35.40	173.34
# 15	2.70	8.16	11.44	34.98	172.16
MEAN	4.35	7.90	11.25	35.42	171.49
SD ±	1.82	0.94	1.02	1.23	1.91

Molecular Devices, LLC, CA, USA), to define FL*intra* protocol. Traces were originally digitalized at 50,000 Hz (Digidata® 1440, Molecular Devices, LLC, CA) and then offline reduced to the final sampling rate of 5000 Hz, using Clampfit® 10.3 software (Molecular Devices, LLC, CA, USA). The trace consists of rhythmic membrane oscillations (around 25 mV) with an asynchronous discharge of action potentials (around 60 mV) at the peak of each cycle. Membrane potential oscillations were removed from FLintra using Clampfit® 10.3 software (Molecular Devices, LLC, CA, USA), the resulting FL*spikes* protocol maintained solely the barrage of action potentials at the original amplitude. Conversely, stimulation with sole oscillations of membrane potential was delivered at the same amplitude as that of the background oscillation in the FL*intra*.

Finally, multiple frequency protocols of rectangular pulses (duration = 0.1 ms) were obtained by superimposing single stereotyped trains through offline analysis (Clampfit® 10.3 software, Molecular Devices, LLC, CA, USA; Origin® 9.0 software, OriginLab Corporation, Northampton, MA, USA). The amplitude of multiple frequency protocols was maintained unvaried during protocol, by removing offline sporadic events of pulse summation with Origin® 9.0 software (OriginLab Corporation, Northampton, MA, USA). All protocols were exported (as an ASCII text file) to a programmable stimulator (STG 4002®; Multi Channel Systems, Reutlingen, Germany) and, then, applied to DRs.

In a subset of experiments, FL*i*stim protocol was modified through a Matlab (MathWorks®, Natick, MA, USA) code that filters selected frequencies values for varying bandwidths. The power spectrums for all stimulating patterns were obtained through Clampfit® 10.3 software (Molecular Devices, LLC, CA, USA).

Parameters of Spinal Network Activity

Episodes of FL were thoroughly analyzed in terms of number of oscillations, duration (calculated as the time interval between the first and the last cycle), periodicity (considered as the time between the onset of two consecutive cycles) and regularity, expressed by the period coefficient of variation (CV displayed as standard deviation [SD] mean^{-1}). Cumulative depolarization of the FL episode was always measured as the voltage difference between the onset of electrical stimulation and the value at plateau. The strength of coupling among pairs of VRs signals was rigorously defined by the cross-correlation function (CCF) analysis performed by Clampfit®

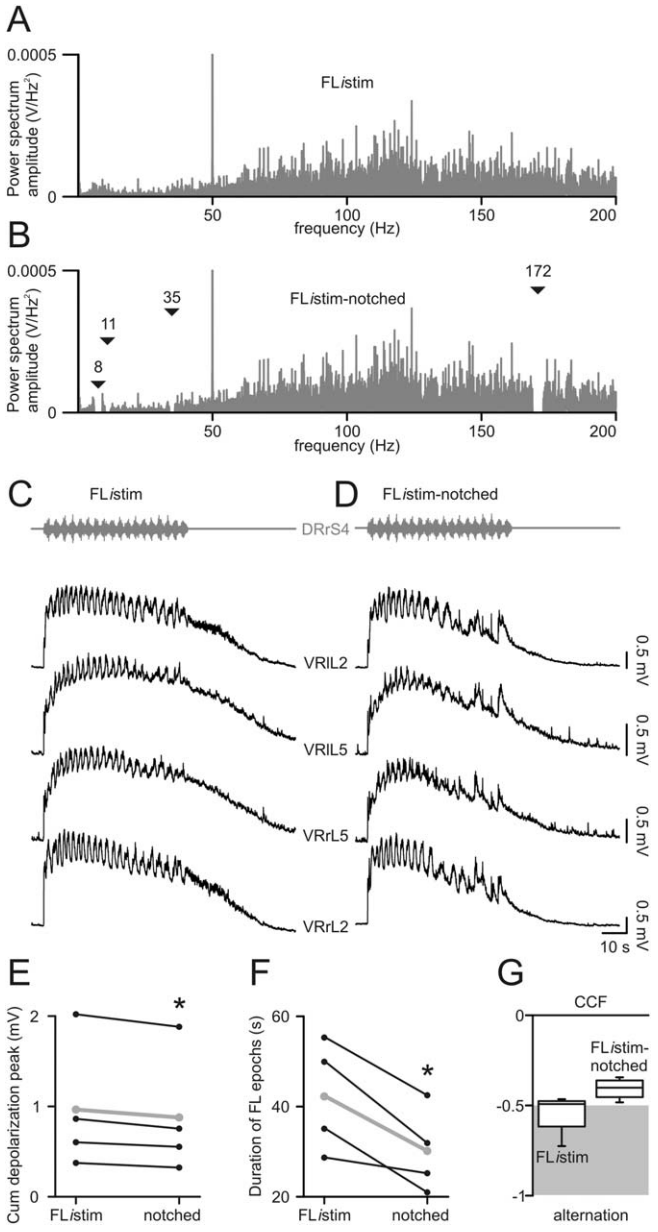

Figure 3. Deleting the four main components from FL*i*stim deteriorates FL episode. The four principal components found in motoneuron spectra are filtered out of the power spectrum of FL*i*stim (A) to define FL*i*stim-notched, whose spectrum is reported in B. Holes of different width centred around each notched frequency correspond to the SD value obtained by averaging the firing of the 15 motoneurons recorded. FL*i*stim (C) and FL*i*stim-notched (D) are then applied to the same preparation at the same intensity (2 μA). FL*i*stim induces a cumulative depolarization of 2.10 mV, with 23 alternating cycles (CCF = −0.72) of 2.60 sec period and 0.24 regularity. In parallel, FL*i*stim-notched evokes a cumulative depolarization of 1.96 mV, with a reduced number of oscillations (14) of the same period (2.56 sec) and regularity (0.25), and with a phase relation among homosegmental VRs of −0.48. FL*i*stim and FL*i*stim-notched are serially delivered in four experiments at an average intensity of 1.75 ± 0.29 μA. Pooled values (mean values in gray lines) are summarized for amplitude of cumulative depolarization (E) and duration of FL episodes (F), showing a significant reduction of FL after notching the FL*i*stim protocol (E, * t = 3959, df = 3, p = 0.029, paired t-test, n = 4; F, * t = 3,927, df = 3, p = 0.029, paired t-test, n = 4). In the whisker box in G is reported the CCF analysis for the pair of homosegmental L2 during FL elicited by the two protocols.

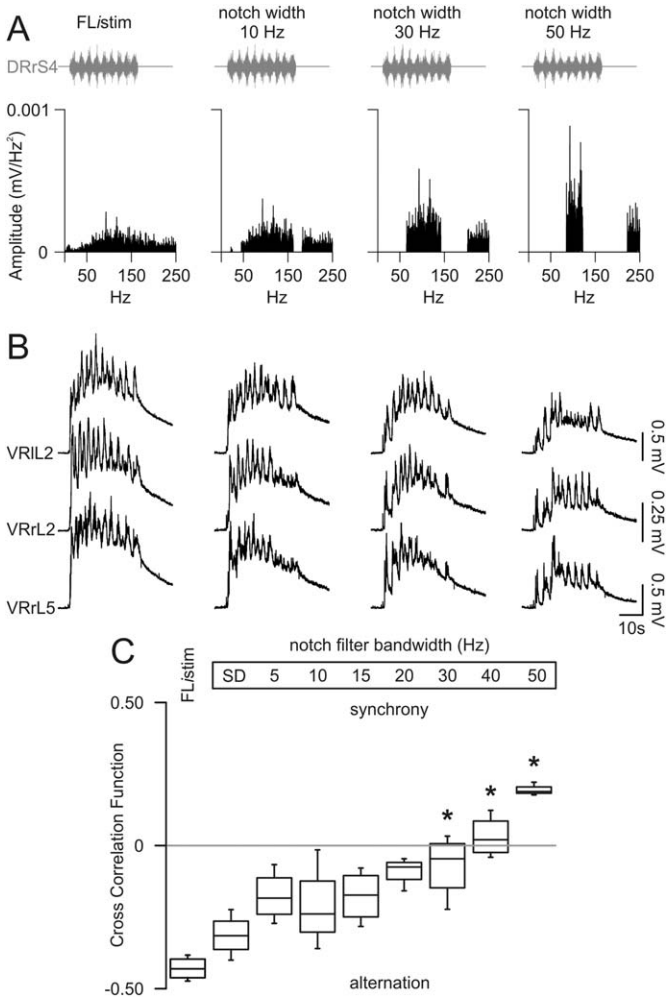

Figure 4. Broader width notching of FL*i*stim progressively worsens FL up to complete suppression. In A, left, FL*i*stim (duration = 30 sec, intensity = 0.3 × Th) induces an episode of FL (13 cycles and CCF = −0.45; B, left) that decays in correspondence to progressive notching of FL*i*stim with wider amplitude ranges (width = 10, 30, and 50 Hz; A). The notch filter for 10 Hz intervals decreases the number (10) and alternation of oscillations (CCF = −0.36; B, middle-left). FL*i*stim-notched for 30 Hz intervals further reduces number of oscillations and their alternating pattern (7 cycles, CCF = 0.03; B, middle-right). Finally, 50 Hz wide filtering completely suppresses FL, which is replaced by synchronous discharges (CCF = 0.18; B, right). Boxes in C show, for the same cords, how FL cycles are progressively replaced by uncorrelated discharges as the four principal components found in motoneuron spectra are filtered out of the power spectrum of FL*i*stim (C, * $F = 19.224$, df = 35, $p = 0.001$, Kruskall–Wallis ANOVA on ranks followed by multiple comparison vs. control with Dunn's method, $n = 4$). Note that SD reported in the bar indicates a FL*i*stim in which values of the four frequencies are notched in a bandpass interval corresponding to their standard deviation, as reported in Table 1.

10.3 software (Molecular Devices, LLC, CA, USA). A CCF greater than +0.5 indicates that two roots are synchronous, while a CCF smaller than −0.5 shows full alternation (13).

Statistical Analysis

Data were reported as mean ± SD values and the number of spinal cord preparations was indicated as *n*.

Statistics were performed using SigmaStat® 3.5 software (Systat Software, CA, USA). First, it was determined whether data approximated a normal curve, using a Kolmogorov-Smirnov normality test. Then, all parametric values were analyzed with Student's *t*-test (paired or unpaired) to compare two groups of data, or ANOVA for more than two groups.

For nonparametric values, Wilcoxon Signed-Rank test was used for two groups, or Kruskal–Wallis ANOVA on Ranks for more than two groups. As for multiple comparisons, posthoc tests were applied: Tukey's methods for parametric and Dunn's methods for nonparametric ANOVAs. Repeated measures within each sample of nonparametric data were performed with Friedman test.

Results were considered significant when $p < 0.05$.

RESULTS

Fictive Locomotion Recorded From a Single Motoneuron Can Be Used to Activate the Locomotor CPG

FL episodes extracellularly recorded from a VR and then delivered to a DR as a stimulating protocol (FL*i*stim) elicit a rhythmic locomotor pattern (13).

The mechanisms for the efficacy of this protocol remain elusive because records obtained from a complex motor pool contain a multitude of incompletely resolved signals (25). To simplify FL*i*stim stimulation, we, therefore, simultaneously acquired noisy waveform traces (30 sec) from an intracellularly recorded motoneuron in the lumbar motor pool.

A sample experiment is shown in Figure 1, in which the rhythmic patterns of FL evoked by NMDA and 5HT are simultaneously recorded at VR level (top trace) and at single motoneuron level (bottom). A segment of these records (see shaded area in Fig. 1A) was then used to reconstruct FL*i*stim, which elicited a very similar response whether the extra (Fig. 1B) or intracellular (Fig. 1C; the latter termed FLintra) signals were used at the same intensity (peak to peak). FL episodes evoked by either protocol were analogous for cumulative depolarization, duration, period, regularity, and number of alternating cycles. In four experiments FL*i*stim and FL*intra* were delivered at the same intensity (8.00 ± 3.91 μA; 0.60 ± 0.27 × Th) to the same DR. The average values are shown in the histograms in Figure 1D–F and indicate that FL*intra* activated locomotor patterns as efficiently as FL*i*stim.

Stimulation Mimicking Action Potential Firing of Single Motoneuron Elicits FL

Within an episode of FL sampled from a single motoneuron, we observed two main components. The first one was represented by membrane potential oscillations underlying the rhythmic signal originated from the CPG (26,27); the second component was the barrage of action potentials during each cycle (28,29). To define efficacy of the latter component, membrane potential oscillations were removed from FL*intra* through Clampfit® 10.3 software (Molecular Devices, LLC, CA), obtaining the FLspikes protocol, which only contained the barrage of action potentials, at original amplitude. Hence, FL*spikes* delivered to the same preparation and at the same intensity of stimulation as FL*intra* (0.26 × Th peak to peak) induced comparable cumulative depolarization with superimposed a series of alternating oscillations of analogous properties (Fig. 2A,B). Conversely, stimulation with membrane potential oscillations alone, delivered at the same amplitude as background oscillations in FL*intra* (Fig. 2C), only generated sporadic, synchronous oscillations.

Interestingly, an episode of FL appeared when amplitude of the sole membrane oscillations pattern was progressively increased, suggesting that input to motoneurons is as effective as the output of motoneurons (both FL*i*stim and FL*spikes*) in evoking locomotion (Supporting Information Fig. 1). Analysis of nine preparations shows

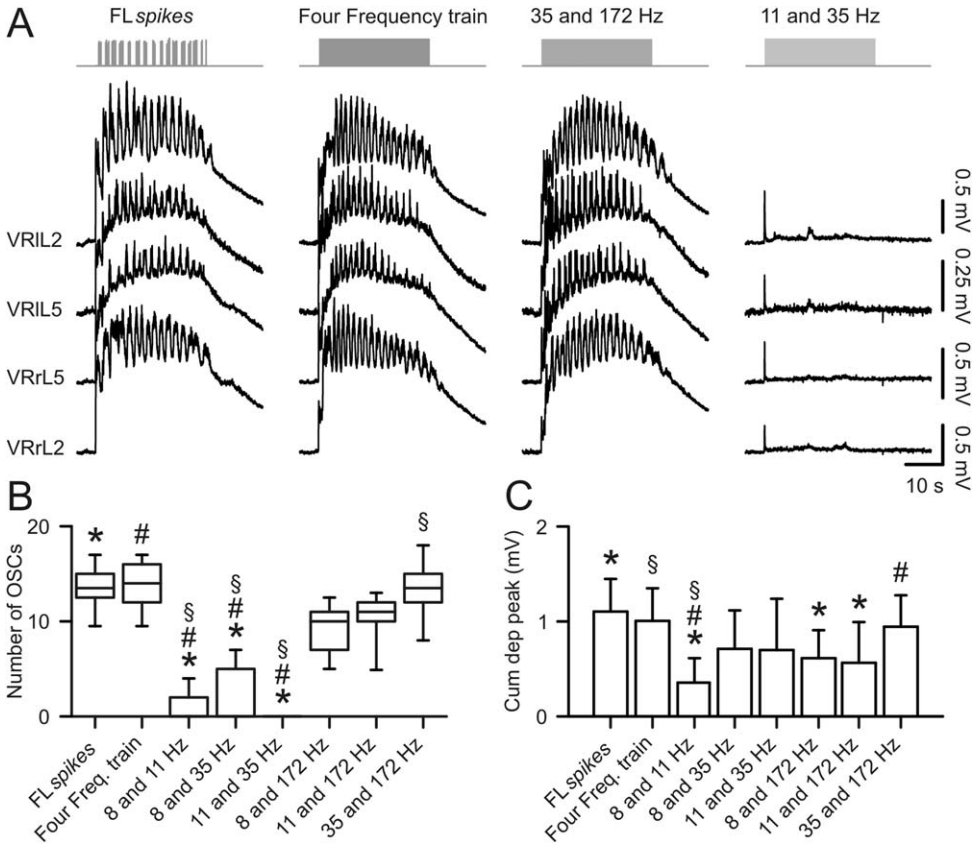

Figure 5. A train composed of the four frequencies or of a selected pair evokes FL cycles, on par with FL*spikes*. In the same preparation, delivery of Four Frequency train and FL*spikes* to DRrS3 at the same intensities of stimulation (3 μA; A, left and middle-left) induces a similar episode of FL, as for the mean number of oscillations (15, FL*spikes* and 17, Four Frequency train), period (1.92 s FL*spikes* and 1.64 sec Four Frequency train), regularity (0.16 FL*spikes* and 0.17 Four Frequency train), cumulative depolarization (1.12 mV FL*spikes* and 0.69 mV Four Frequency train), and phase correlation among pairs of homosegmental VRs L2 (−0.54 FL*spikes* and −0.64 Four Frequency train). A, middle-right, the pair 35 and 172 Hz evokes a FL similarly to the Four Frequency train, as for the mean number of oscillations (18), period (1.75 sec), CV (0.23), cumulative depolarization (1.23 mV), and phase correlation among pairs of homosegmental L2 VRs (CCF = −0.71). Conversely, another pair of frequencies (namely 11 and 35 Hz; A, left) does not evoke any cumulative depolarization superimposed by alternating oscillations, but only a first synchronous reflex response. In the same cords ($n = 11$), delivery at the same intensity (mean value 3.68 ± 1.79 μA) of other two-frequency trains, resulting from all possible permutations, is compared to FL*spikes* and Four frequency train. Average values are reported in B and C, as for number of oscillations and peak of cumulative depolarization, respectively, showing the supremacy of 35 and 172 Hz (B, Chi-square = 71,298, df = 7, $p < 0.001$, Friedman repeated measures ANOVA on Ranks followed by all pairwise multiple comparison with Dunn's test, $n = 11$; * 8 and 11 Hz, 8 and 35 Hz, 11 and 35 Hz vs. FL*spikes*; # 8 and 11 Hz, 8 and 35 Hz, 11 and 35 Hz vs. Four Frequency train; § 8 and 11 Hz, 8 and 35 Hz, 11 and 35 Hz vs. 35 and 172 Hz); (C, $F = 6.319$, df = 87, $p < 0.001$, one way repeated measures ANOVA followed by all pairwise multiple comparison with Tukey test, $n = 11$; * 8 and 11 Hz, 11 and 172 Hz, 8 and 172 Hz vs. FLspikes; # 8 and 11 Hz vs. Four Frequency train; § 8 and 11 Hz vs. 35 and 172 Hz).

that, compared with FL*spikes*, FL*intra* significantly increased the number of oscillations ($p = 0.008$, Wilcoxon signed rank test; Fig. 2D) and the size of cumulative depolarization ($t = -4815$, df = 8, $p = 0.001$, paired *t*-test; Fig. 2E right). FLs induced by the two protocols were not statistically different as for period or regularity of cycles ($t = 0.852$, df = 8, $p = 0.419$, paired *t*-test; $p = 0.426$, Wilcoxon signed rank test; Fig. 2E), or phase alternation ($p = 0.297$, Wilcoxon signed rank test; Fig. 2F). While the functional consequences of FL*intra* were only marginally stronger than FL*spikes*, the latter protocol represented a simpler stimulating protocol to activate the CPG at low intensity of stimulation.

Contribution of Frequency Domain to FL*spike*

We wondered whether activation of locomotor circuits arises from a preferential range of motoneuronal firing frequencies during FL. To explore this issue, different concentrations of NMDA (2–5 μM plus 5HT, 10 μM) were applied to induce FL which was intracellularly recorded from 15 single motoneurons (L3–L5; see example in Supporting Information Fig. 2A). Then, FL records were used to extract the action potentials (Supporting Information Fig. 2B) and to calculate their power spectrum (Supporting Information Fig. 2C). Despite variation in the oscillation period (2–8 sec), it was interesting to note that all motoneuron discharge profiles during FL contained four main frequencies (8, 11, 35, and 172 Hz; Table 1). Conversely, the first four components of traces taken under resting conditions did not correspond to any of the four main frequencies during FL. Indeed, the first four components at rest were 0.20 ± 0.18 Hz; 0.87 ± 0.70 Hz; 1.47 ± 0.95 Hz; 2.71 ± 1.51 Hz ($n = 15$).

Four Distinct Frequencies Are Crucial for the Efficacy of Noisy Waves

To confirm the hypothesis that the efficacy of noisy waves in inducing FL relied on four main frequencies of the firing profile of a single motoneuron, we eliminated these frequencies (8, 11, 35, and 172 Hz) from the FL*i*stim trace through a Matlab (Mathworks Inc, MA, USA) *ad hoc* code. This gave a protocol termed FL*i*stim-notched that lacked the four main frequencies as demonstrated by comparing its power spectrum with the one of the original FL*i*stim

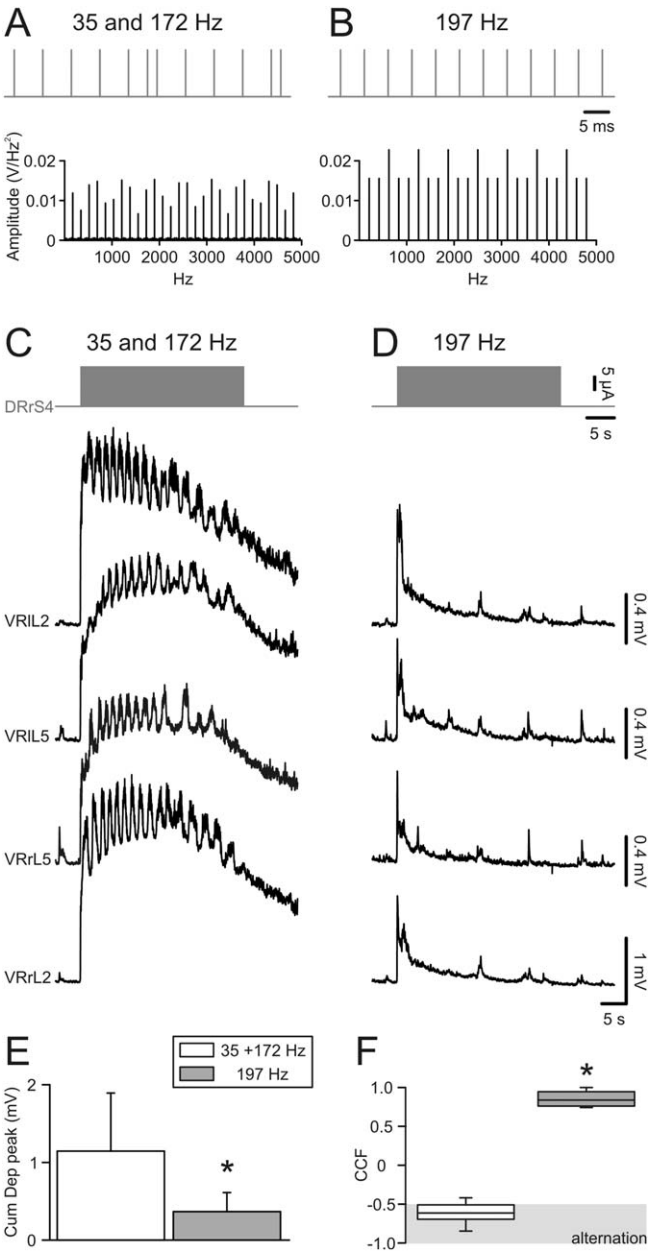

Figure 6. Induction of FL by 35 and 172 Hz train is not related to total number of pulses. The same number of pulses are delivered either as a two-frequency train (35 and 172 Hz, A) or as a stereotyped train (197 Hz, B). As reported in the power spectrum, 35 and 172 Hz protocol contains more components than 197 Hz. In C and D, the two protocols were serially delivered to the same preparation at the same intensity (14 μA). While 35 and 172 Hz evokes a cumulative depolarization (2.25 mV) and an episode of FL (17 cycles of 2.02 sec period and 0.25 regularity) with alternating oscillations (CCF VRL2 = −0.58), the stereotyped train at 197 Hz elicits a much lower depolarization (0.48 mV) with only few synchronous discharges (CCF = 0.78). Graphs report a significant reduction in cumulative depolarization (*E*) and loss of alternation (*F*) for 197 Hz (*E*, * $t = 3.328$, df = 6, $p = 0.016$, paired *t*-test, $n = 7$; F, * $p = 0.031$, Wilcoxon signed rank test, $n = 5$).

(Fig. 3A,B). Figure 3C,D illustrates how FL*i*stim and FL*i*stim-notched applied to the same preparation at the same low intensity (0.22 × Th, peak to peak) gave a similar cumulative depolarization with alternating cycles.

FL*i*stim and FL*i*stim-notched were serially delivered in four experiments at an average intensity of 0.19 ± 0.04 × Th. Pooled values are summarized in terms of amplitude of cumulative depolarization (Fig. 3E) and duration of FL episode (Fig. 3F). Statistical analysis indicated a significant reduction in depolarization induced by FL*i*stim-notched ($t = 3{,}959$, df = 3, $p = 0.029$, paired *t*-test) with a locomotor episode of lesser duration ($t = 3{,}927$, df = 3, $p = 0.029$, paired *t*-test). Furthermore, we tried to define quality of FL induced by the two protocols, using the CCF (Fig. 3G). Analysis reported that cycles evoked by FL*i*stim-notched are as alternated as the ones evoked by FL*i*stim ($p = 0.125$, Wilcoxon signed rank test). Although FL*i*stim-notched still evoked a FL when delivered at low intensity, the duration of FL episodes was significantly reduced, highlighting the importance of the four components identified.

Broadening the bandwidth of the notch filter around the frequencies of 8, 11, 35, and 172 Hz enabled us to find out their role in FL quality. In Figure 4A, FListim (duration = 30 sec) was delivered to the same preparation at constant intensity (0.3 × Th, peak to peak) but with progressively increasing the bandwidth (from 10 to 30 and then 50 Hz) of notch filter centered around each of the four principal frequencies identified.

The larger filtering was confirmed by gaps in the power spectrum (Fig. 4A, bottom row), which made stimulating traces less intrinsically variable and gradually reduced number and alternation of FL oscillations. Setting the notch filter for 10 Hz intervals only decreased the number and alternation of oscillations (Fig. 4B). The 30 Hz notch filtering (Fig. 4B middle-right) further reduced the number of oscillations, which became uncorrelated. Finally, FL*i*stim-notched for 50 Hz intervals abolished FL cycles and replaced them with synchronous discharges (Fig. 4B).

The same experiment was performed in five preparations, in which the different protocols were delivered at an average intensity of 0.18 ± 0.06 × Th. The progressive worsening of FL, up to its disappearance, is expressed by CCF values that are grouped around zero when stimulating with FListim using larger notching intervals (Fig. 4C).

Relative Role of the Four Main Frequencies in CPG Activation

Considering the four main discharge frequencies (8, 11, 35, and 172 Hz) during FL, we analysed their relative role in triggering the locomotor pattern. Thus, each frequency was used to create a single stereotyped train. The traces were then superimposed to design a train of rectangular stimuli comprising either all four of them (Four Frequency train; duration = 0.1 ms; Supplementary Fig. 2D) or pairs. In the same preparation, we could, therefore, compare the effects of the Four Frequency train and FL*spikes* at the same stimulation intensity (0.3 × Th, peak to peak; Fig. 5A, left and middle-left). The two protocols induced a similar episode of FL. Using pairs of the main frequencies demonstrated that 35 + 172 Hz evoked a FL similar to the one observed with four frequency train (Fig. 5A, middle-right). Conversely, 11 + 35 Hz frequencies (Fig. 5A right) induced just an initial synchronous reflex without cumulative depolarization or alternating oscillations.

The different protocols were serially delivered to 11 preparations at the same intensity of stimulation (mean value 0.35 ± 0.13 × Th). Pooled values for number of oscillations and peak of cumulative depolarization are reported in Figure 5B,C indicating the effectiveness of the various frequency combinations. In the four experiments in which bilateral L2 and L5 roots were simultaneously recorded, cross-correlation analysis showed an average for the homosegmental L2 CCF of −0.51 ± 0. 03 for FL*intra*, −0.70 ± 0.10 for Four Frequency train, −0.60 ± 0.10 for the train at 35 + 172 Hz, and 0.21 ± 0.66 for the train at 11 + 35 Hz, supporting the notion that

Table 2. Power Spectrum Magnitude and Number of Pulses of All Stimulating Protocols used in the Study.

Protocols	Power spectrum magnitude (RMS)	Number of stimulating pulses
FL*i*stim intra	3.18621	88
FL*i*stim membrane oscillation	0.07416	0
FL*i*stim only spikes	2.26191	88
DRtrain 4 frequencies	0.66271	6379
DRtrain 8 and 11 Hz	0.01646	567
DRtrain 8 and 35 Hz	0.05482	1265
DRtrain 11 and 35 Hz	0.06064	1281
DRtrain 11 and 172 Hz	0.49547	5237
DRtrain 8 and 172 Hz	0.48359	5149
DRtrain 35 and 172 Hz	0.59535	5915
DRtrain 70 and 150 Hz	0.34155	4285
DRtrain 8 Hz	0.00454	240
DRtrain 11 Hz	0.00732	330
DRtrain 35 Hz	0.04275	1034
DRtrain 172 Hz	0.45287	4918
DRtrain 197 Hz	0.60158	5915

the combination of 35 + 172 Hz was equi-effective as the FL*spikes* and Four Frequency train. Moreover, 35 + 172 Hz applied at low intensity (5 μA, 0.5 × Th) for a longer duration (>4 min) evoked a prolonged episode of FL that persists up to 106.36 sec with 37 alternating cycles (Supporting Information Fig. 3).

Finally, single trains at 8, 11, 35, or 172 Hz did not evoke any cumulative depolarization or any FL cycle ($n = 4$, data not shown) when delivered at the same intensity as FL*spikes* and Four Frequency train. In summary, the minimum variability required to activate the CPG was represented by two selected frequencies.

Efficacy of the 35 + 172 Hz Protocol Does Not Rely on Number of Impulses or Their Power

The efficacy of 35 and 172 Hz might arise from the greater power of the protocol and/or the higher number of single stimuli, compared with trains with other frequencies. To explore this issue, we delivered a 30-second train of stimuli at the single frequency of 197 Hz, containing the same number of impulses (5915) as the 35 + 172 Hz protocol (see Fig. 6A,B). Table 2 reports for all protocols used in the study the power spectrum magnitude, expressed as root mean square (RMS), and the number of peaks.

In experiments as the one shown in Figure 6C,D, the two protocols at 35 + 172 Hz and at 197 Hz were serially delivered to the same preparation at the same intensity of stimulation (0.56 × Th). The train 35 + 172 Hz evoked a cumulative depolarization and an episode of FL with alternating oscillations. On the contrary, the stereotyped train at 197 Hz only induced a weaker depolarizing response superimposed by only two synchronous discharges. The average values (Fig. 6E) show that the protocol 35 + 172 Hz evoked a significantly larger cumulative depolarization than the train at 197 Hz ($t = 3.328$, df = 6, $p = 0.016$, paired *t*-test, $n = 7$). Furthermore, CCF analysis for VRL2 confirms the presence of alternating FL oscillations only for the protocol at 35 + 172 Hz ($p = 0.031$, Wilcoxon signed rank test, $n = 5$; Fig. 6F). Thus, CPG activation did not depend on the number of impulses or power of the stimulating protocol, as it required a distinct frequency code.

Efficacy of 35 + 172 Hz Is Not Shared by Other Pairs of Frequencies

Provided the same number of pulses, 35 + 172 Hz protocol always activates the locomotor rhythm, as opposed to a stereotyped train. We wondered whether only the pair 35 and 172 Hz evoked FL or if also other pairs of frequencies within a comparable range (30–200 Hz) are equally effective. Thus, we randomly selected the pair 70 + 150 Hz as a stimulating pattern. 70 + 150 Hz and 35 + 172 Hz trains were serially delivered at the same amplitude to the same preparations and VRs responses were compared.

The protocol 35 + 172 Hz elicited a FL (Fig. 7A), while 70 + 150 Hz did not (Fig. 7B), but only evoked a small cumulative depolarization.

Mean values from six experiments confirmed that stimulation with 70 + 150 Hz, in comparison to 35 + 172 Hz at the same intensity (0.42 ± 0.16 × Th), produces only few sporadic oscillations (Fig. 7C; $p = 0.031$, Wilcoxon Signed Rank Test), a smaller cumulative depolarization (Fig. 7D; $t = 4.810$, df = 5, $p = 0.005$, paired *t*-test), but never elicits alternated locomotor-like cycles (Fig. 7E; $p = 0.031$, Wilcoxon Signed Rank Test). These results demonstrate that 35 + 172 Hz is the only train that contains a distinct frequency code able to selectively activate the CPG.

Multisite Stimulation to Trigger FL

A recent study has demonstrated robust afferent input convergence at the level of the CPG (30). Thus, we wondered whether stimulating one DR with the 35 Hz train and another one with the 172 Hz train could still efficiently trigger FL.

First, we delivered a train at 35 Hz to the lS4 root (intensity 0.5 × Th), inducing cumulative depolarization superimposed by uncorrelated discharges (Fig. 8A). Afterwards, we applied a train at 172 Hz to the contralateral DR (intensity 0.47 × Th), evoking only few synchronous cycles superimposed by a comparable cumulative depolarization (Fig. 8B). Finally, the two stereotyped trains were simultaneously delivered to the two DRs, inducing a locomotor response characterized by a wider cumulative depolarization and the presence of FL cycles (Fig. 8C). Even by swapping the DR for these trains, FL episodes were similar (Fig. 8D), suggesting integration of afferent stimuli into synergic activation of the CPG.

In a total of three preparations, stereotyped trains at 35 and 172 Hz were simultaneously delivered to two DRs at the same intensity

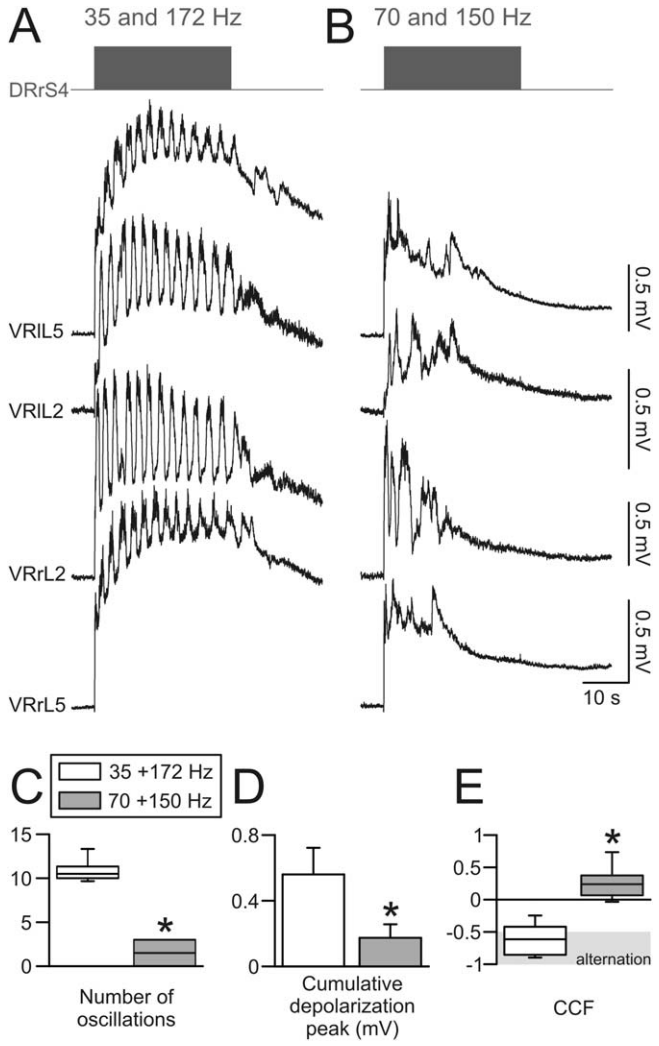

Figure 7. The efficacy of 35 and 172 Hz is not shown by other pairs of frequencies in the same domain. Two trains, 35 and 172; 70 and 150 Hz, were serially delivered to the DRlS4 at the same amplitude of stimulation (3.75 μA; 0.37 $\times$ Th). 35 and 172 Hz (A) elicited a cumulative depolarization (0.83 mV) with superimposed 13 oscillations of FL (CCF = -0.89), while 70 and 150 Hz (Fig. 7B) did not evoked any alternated patterns (CCF = 0.02) and only induced a small cumulative depolarization (0.25 mV). Graphs highlight that the 35 and 172 Hz (white bars) statistically elicited a higher number of locomotor cycles (C), a stronger cumulative depolarization (D) and fully alternating cycles (E) with respect to the 70 and 150 Hz protocol (gray bars; C, * $p = 0.031$ Wilcoxon signed rank test, $n = 6$; D, * $t = 4.810$, df = 5, $p = 0.005$, paired t-test, $n = 6$; E, * $p = 0.031$, Wilcoxon signed rank test, $n = 6$).

($0.58 \pm 0.19 \times$ Th), always activating a FL episode (mean number of oscillations = 11 ± 1; mean CCF = -0.62 ± 0.08), regardless of the topography of DRs to which we applied single trains (mean number of oscillations = 10 ± 2; mean CCF = -0.58 ± 0.03).

Effect of 35 + 172 Hz Stimulation on Ascending Inputs to the Spinal Cord

Electrically stimulated sacrocaudal afferents activate the lumbar CPG through ascending fibers in the ventrolateral funiculus (31). We wondered whether the 35 + 172 Hz protocol was the most effective paradigm to activate these fibers so that expression of FL had a strong contribution from preferential activity of afferents in addition to any intraspinal signal processing. Thus, we delivered to rS4 three stimulating trains (same low intensity = 0.6 $\times$ Th; Fig. 9A), that is, 35 + 172 Hz (yielding FL), 8 + 11 Hz (unable to produce FL) and a 197 Hz train containing the same number of impulses as 35 + 172 Hz. As illustrated in the example of Figure 9A, only the 35 + 172 Hz (top, left) depolarized VRs and induced alternating oscillations, whereas the 8 + 11 Hz (middle) and the 197 Hz (left) paradigms elicited weaker VR depolarization with synchronous discharges. At the same time we recorded (with AC coupling), from the ventro-lateral surface of the spinal cord, a response that corresponds to conduction of ascending inputs induced by caudal stimulation. Interestingly, these stimulation protocols induced ascending volleys, whose peak amplitude was larger for 35 + 172 Hz, compared to 8 + 11 Hz and 197 Hz (Fig. 9B, arrow) and was confirmed by pooled data from five experiments ($F = 8.931$, df = 14, $p = 0.009$, One way repeated measures ANOVA followed by all pairwise multiple comparison with Tukey test, $n = 5$).

The histograms in Figure 9C summarize five experiments and indicate a significant increase in the temporally integrated area during the first 500 ms for 35 + 172 Hz ($F = 9.788$, df = 14, $p = 0.007$, one way repeated measures ANOVA followed by all pairwise multiple comparison with Tukey test). This result suggests that, at low intensities of stimulation, a distinctive frequency protocol was the most efficient to recruit ascending signals in the first 500 ms to trigger FL.

To further test this hypothesis, the protocol at 35 + 172 Hz was applied to DRrS4 for only 500 ms at the intensity of 0.5 $\times$ Th and generated an episode of alternating oscillations (Fig. 9D). In five preparations, the 35 + 172 Hz paradigm delivered for just 500 ms (amplitude of $1.10 \pm 0.65 \times$ Th) induced a short episode of FL with an average of 5 ± 2 alternating cycles (average CCF = -0.67 ± 0.15).

35+ 172 Hz Has Direct Access to the CPG

Even when delivered for a very short time, the protocol 35 + 172 Hz elicits a FL when applied to sacrocaudal afferents. Electrical stimulation of sacrocaudal afferents allows an easier surgical access for neurorehabilitation purposes. However, stimulation of caudal afferents encounters one more level of complexity, due to at least one interneuron interposed between stimulus and CPG (31), potentially resulting in further filtering of the stimulus.

We wondered whether efficacy of 35 + 172 Hz protocol is related to afferent filtering or if it is a mere frequency-dependent response by the CPG. To address this issue, we directly stimulated the segments where the CPG is putatively located (4,5) and which are likely to have a more direct access to the specific rhythm generating neurons. Thus, we tested if 35 + 172 Hz evoked a FL when delivered to lumbar DRs, on par with noisy waveforms (13). As shown in Figure 10A,B, FL was equally evoked by the 35 + 172 Hz protocol when serially delivered at the same intensity to either DRrS4 and DRrL3. Mean value from four experiments confirms that the stimulating protocol ($0.56 \pm 0.20 \times$ Th) applied to either sacral or lumbar DR was equally effective in inducing comparable locomotor patterns, as the number of oscillations (Fig. 10C, $p = 0.125$, Wilcoxon Signed Rank Test), period (Fig. 10D, $t = -1494$, df = 3, $p = 0.232$, paired t-test), regularity (Fig. 10E, $p = 0.375$, Wilcoxon Signed Rank Test), and CCF (Fig. 10F, $p = 0.625$, Wilcoxon Signed Rank Test) did not differ between the two protocols.

DISCUSSION

This data are the first description of two principal stimulus frequencies that, when applied at very low intensity, even to distinct sites, can generate robust locomotor patterns. For neurorehabilitation purposes, optimizing the protocols of functional electrical

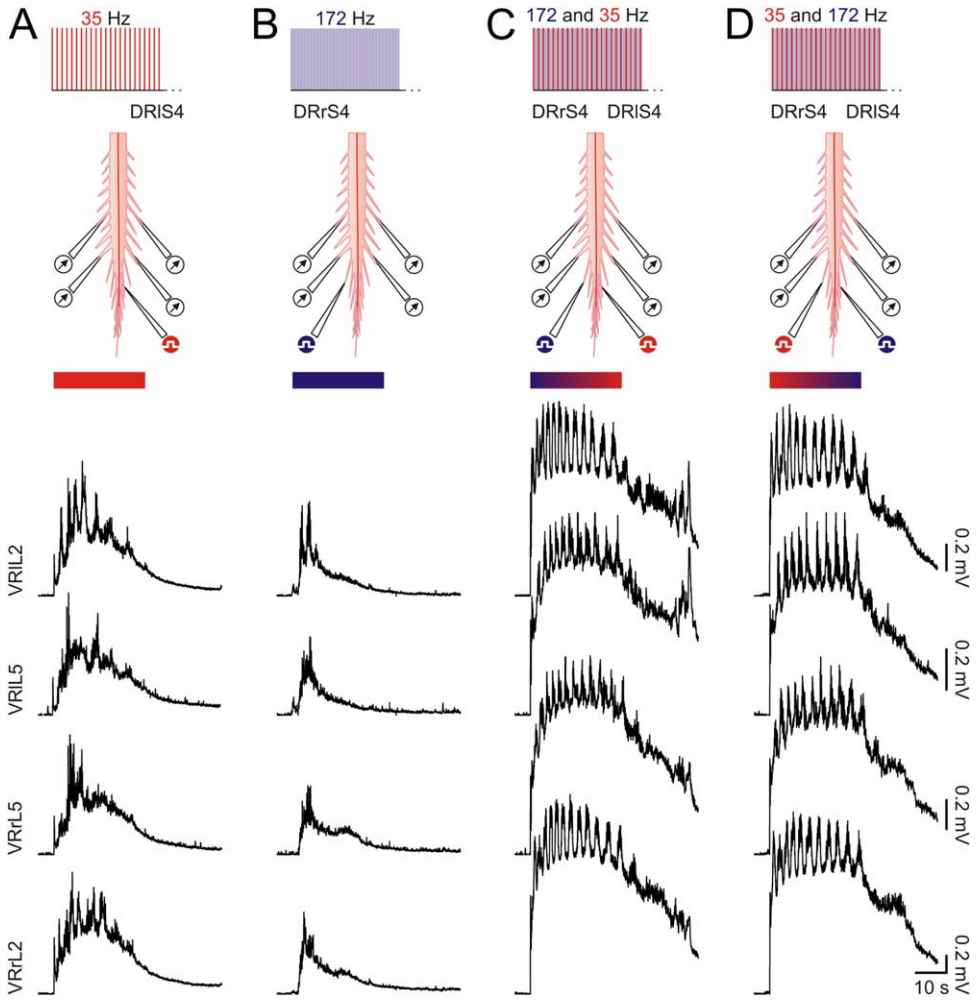

Figure 8. Multisite delivery of stereotyped trains at 35 and 172 Hz triggers FL. A train at 35 Hz (A), applied to lS4 with an intensity of 4 μA, induces a cumulative depolarization (0.54 mV) superimposed by uncorrelated discharges (CCF = 0.11). A train at 172 Hz (B) to the contralateral DR (intensity 2.8 μA; 0.47 × Th) evokes only few synchronous cycles (CCF = 0.52) superimposed on a comparable cumulative depolarization of 0.48 mV. Two stereotyped trains are simultaneously delivered to the two DRs, inducing a locomotor response characterized by a larger cumulative depolarization (1.51 mV) and more FL cycles (CCF = −0.64; C). Even by swapping DRs individually stimulated by trains, FL episodes remained similar (1.68 mV of cumulative depolarization with 12 alternating cycles of CCF = −0.60; D).

stimulation to regain standing and gait after SCI is a primary goal of current research to improve efficacy and decrease potential side effects associated with strong electrical pulses (11,12). Our laboratory has recently discovered that noisy waveforms recorded from VRs of animals or extracted from the EMG of walking humans (13–16), and applied to a single DR at low intensity, most effectively induce FL in the in vitro spinal cord. This study was, therefore, focused on understanding what protocols are most effective in activating the CPG using relatively weak afferent stimuli.

Locomotor CPG Activation Related to Low-Intensity Stimulation With Selected Frequencies

One unexpected outcome of the present investigation was the demonstration of four main components of the power spectrum present in the VR noise during FL. Hence; the relative contribution of a certain stimulus frequency was explored when applied in isolation or combination with the others. We first excluded that efficacy of multifrequency protocols depended on either the number of impulses or the integrated stimulus strength. Two of the principal frequencies, namely 35 and 172 Hz, fall into the domain that activates Aβ and Aγ fibers, which are mainly involved in conducting proprioceptive inputs (32), and may be expected to facilitate the activity of the locomotor CPG (33), a goal that has not escaped the attention of modern neurorehabilitation protocols (34). Nevertheless, stimulation with the high frequency train at 197 Hz, which should have strongly activated Aβ and Aγ afferents (32), did not trigger FL. Thus, preferential recruitment of certain fiber classes could not explain *per se* the present data.

We favor the hypothesis that selective activation of FL might come from the frequency-dependent responsiveness of discrete CPG elements. In the spinal cord, varying the frequency of epidural stimulation in man seamlessly induces different motor tasks (35), just like in hippocampal networks, where different frequencies evoke diverse motor behaviors (36). Recruitment of spinal network elements might occur both at pre- and post-synaptic level. We may surmise that primary afferents synapses might act as a band-pass filter of inputs from the periphery. Indeed, afferent stimulation within a discrete range of frequencies increases glutamate release from presynaptic terminals through either autoreceptors (37) or certain ionic conductances (38). These mechanisms contribute to trigger locomotor

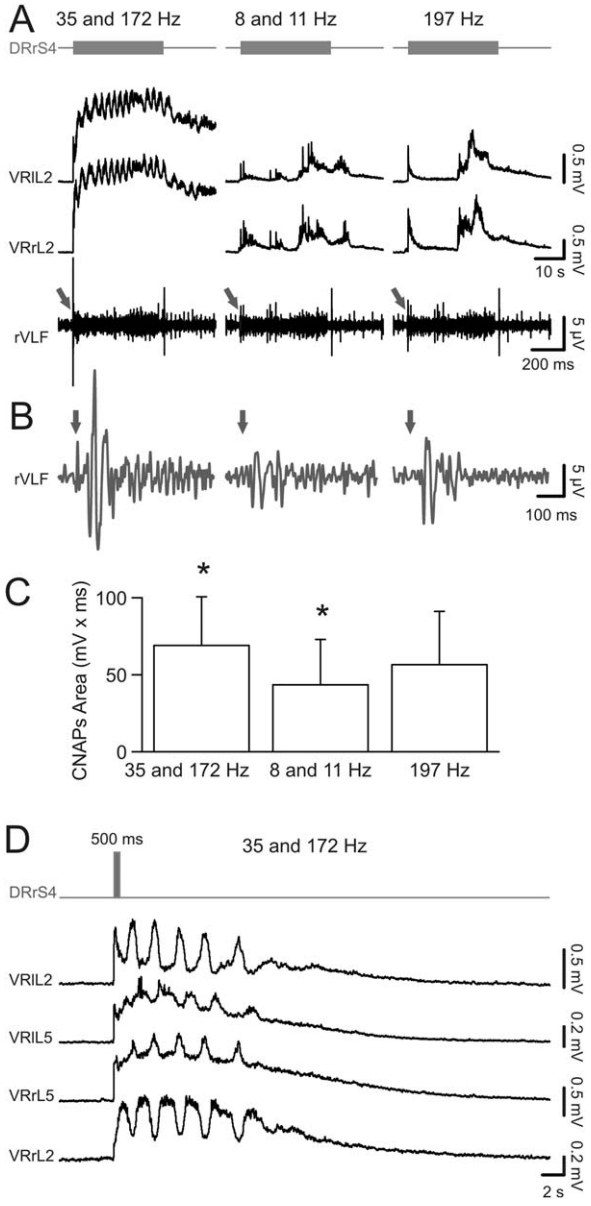

Figure 9. 35 and 172 Hz evokes a first ascending volley able to trigger FL cycles. Three stimulating trains are serially delivered at the same low intensity (6 μA; A). Out of the three protocols, only the pair of 35 and 172 Hz (A, left) induced an episode of 14 alternating oscillations (CCF = −0.51), with a cumulative depolarization of 2.06 mV. Both the 8 and 11 Hz pair (A, middle) and the train at 197 Hz (A, right) induce a weaker depolarization (0.21 mV for the train at 8 and 11 Hz and 0.55 mV for the train at 197 Hz), with only synchronous discharges (CCF = 0.63 for the train at 8 and 11 Hz and CCF = 0.76 for that at 197 Hz). In the same experiments, ascending volleys are induced by stimulation (arrows) of the ventro lateral funiculus and are extracellularly recorded through suction electrodes. In B, volleys in ventro lateral funiculus are reported from beginning of stimulation (arrow) at a greater time base scale, showing the highest response to 35 and 172 Hz, measured from peak to antipeak (166% of 8 and 11 Hz and 151% of 197 Hz). In C, pooled data for the first 500 ms highlights that 35 and 172 Hz generates a significantly higher area of compound neural action potentials (CNAPs) than the protocol at 8 and 11 Hz (* $F = 9.788$, df = 14, $p = 0.007$, one way repeated measures ANOVA followed by all pairwise multiple comparison with Tukey test, $n = 5$). In D, a short train at 35 and 172 Hz (duration = 500 ms; intensity = 2 μA) applied to the DRrS4 of a different cord only generates an episode of six alternating oscillations (CCF = −0.88). Note that the same train, applied for a longer time (30 sec) at the same intensity, elicits a longer FL episode (16 cycles, CCF = −0.87).

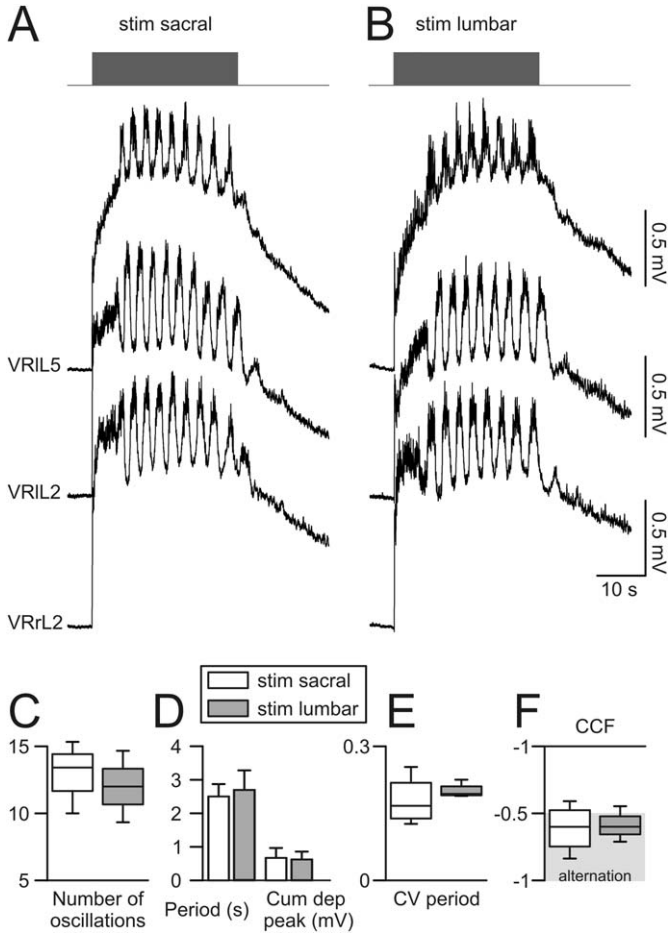

Figure 10. 35 and 172 Hz is equally effective on both sacral and lumbar afferents. The protocol 35 and 172 Hz is serially applied at the optimal intensity for inducing FL to DRrS4 (7.5 μA, 0.5 × Th) and DRrL2 (5 μA, 1 × Th) of the same spinal cord. Stimulation of a sacral (A) and a lumbar DR (B) evoke a similar FL episode, as for cumulative depolarization (1.11 mV sacral vs. 0.99 mV lumbar), duration (25.39 sec sacral vs. 28.31 sec lumbar), period (2.81 sec sacral vs. 3.13 sec lumbar), regularity (0.13 sacral vs. 0.18 lumbar), and number of cycles (10 sacral vs. 10 lumbar), which similarly alternate among homosegmental VRs, as confirmed by the negative values of cross-correlogram analysis ($CCF_{homosegmental} = -0.72$ sacral vs. −0.66 lumbar). Graphs quantify the main features of FL episodes evoked by the two stimulations as for number of oscillations (C), period, cumulative depolarization (D), CV period (E), and CCF values (F).

rhythmic patterns supported by persistent rise in network excitability maintained by the lingering increase in extracellular potassium (39).

Conversely, at postsynaptic level, intrinsic membrane properties might render some CPG interneurons responsive to distinct inputs within a narrow range of frequencies (40–42). Furthermore, high frequency stimulation might modulate the balance between excitation and inhibition, for instance by increasing adenosine release (43,44). Finally, also the recruitment of previously silent synapses might be involved in the efficacy of stimulating patterns (45).

Future studies are needed to clarify the relative contribution by pre- and post-synaptic effects to determine the particular frequency range effective for FL onset.

Common Characteristics of Firing From Different Motoneurons During FL

Spinal motoneurons show state-dependent changes in excitability during locomotion (46–48). Rhythmically active motoneurons selectively respond to inputs at preferred frequencies (42) with both

membrane oscillations consistent with a locomotor drive potential, and stable firing without frequency adaptation (mean rate 30 Hz; maximum 170–200 Hz; 48). The distinctive range of frequencies that characterizes motoneuron discharges during FL might be exploited to stimulate CPG with train impulses of low intensity.

In our study, during a stable FL, intracellular motoneuronal traces showed distinctive components unmodified by varying rhythmic frequencies. This result is in line with *in vivo* studies, in which motoneurons during locomotion generate coherent firing independent from walking speed (49). In this work, the same motoneuronal discharge frequencies were common among different preparations. This observation is in accordance with the notion that the firing frequency of motoneurons during FL represents a widespread task-specific behavior (46) and that the relative role of various inputs is kept constant regardless of individual variability (50).

FL records were consistently characterized by four main frequencies, which might be considered a remarkable state-dependent feature of locomotor activity. The same frequencies are contained in noisy waves, which optimally activate FL. Nevertheless, electronic filtering out of each one of these four frequencies did not strongly decrease the efficacy of noisy waves, unless wide band intervals were used. Thus, the four main frequencies are not absolute values as some scattering may be permissible.

Identifying Critical Stimulation Frequencies Was Useful to Apply Short Stimulation Protocols

Traditionally, an epoch of 10–30 sec stimulation of nerve afferents is used to induce an episode of fictive motor pattern (10,51,52). More efficient stimulating protocols would require lower intensities and a shorter application. Electrical stimulation with noisy waves optimally evokes FL with a minimum application of at least five seconds (13). This study indicated that a low-intensity stimulating protocol, composed of the sole frequencies of 35 + 172 Hz, activated FL even when applied for only 500 ms. To the best of our knowledge, this is the shortest train of electrical impulses to elicit a FL.

The stimulation of sacrocaudal afferents at 35 + 172 Hz evoked ascending inputs recorded from the ventro-lateral surface of the spinal cord. These signals were likely due to inputs travelling in the ventrolateral funiculus first reaching sacral relay neurons (51) and then lumbar segments, where locomotor CPG neurons are putatively located (53). Conversely, the protocol was optimally able to induce FL when applied to upper lumbar dorsal afferents with close and direct access to the CPG (4,5), suggesting that efficacy of 35 + 172 Hz is not related to the filtering by afferents, but it is a frequency-dependent response of the CPG.

Thus, the protocol at 35 and 172 Hz represents the simplest protocol that still preserves the advantages of noisy waves (13–16) and maximizes the benefits of afferent stimulation with variable inputs of weak strength (54,55). The selective efficacy of 35 + 172 Hz in inducing FL is not shared neither with a stereotyped train containing the same number of pulses nor with another train of two frequencies randomly selected in a comparable frequency domain. Interestingly, the stimulation protocol at low intensity remained effective even when the single frequencies of 35 and 172 Hz were applied to two different DRs converging onto the CPG (30).

New Perspectives for Deciphering the Functional Organization of the Locomotor CPG

The optimal induction of FL by the pair 35 + 172 Hz, when delivered to the spinal segments where specifically rhythm generating neurons are located, could suggest this protocol as a valuable experimental tool to selectively decode the functional organization of spinal networks and their integration of afferent inputs. To this purpose, experiments with the spinal cord from knock-out mice ablating certain interneuronal subtypes (5,56) could help identify the spinal neurons essential to trigger a FL in response to weak multifrequency stimulation. Although the study was performed on neonatal rats, preliminary tests showed that stimulating protocols at low intensity were likewise effective on spinal cords of neonatal mice. Optogenetic approaches (57,58) could adopt pulsing light stimuli at different frequencies, to identify the location of neurons selectively recruited by each protocol.

CONCLUSION

The results of this study might suggest a new strategy of electrical stimulation to recover standing posture and locomotion after a motor lesion. In view of statutory restrictions concerning the electromedical devices used for stimulation, the most feasible approach to translate the present main finding is to conjointly use two electromedical devices, each one set at 35 or 172 Hz output. Each train should be individually applied to one of two different afferents, to reconstitute the pair of effective frequencies at CPG level.

Acknowledgements

We are grateful to Prof. Andrea Nistri for data discussion and Dr. Elisa Lus for her excellent assistance in preparing the manuscript. I would like to thank Dr. Simon M. Danner, who kindly supported us in designing a software code to selectively filter stimulating protocols.

Authorship Statements

Francesco Dose and Giuliano Taccola conducted the experiments, analyzed the data, and revised the manuscript. Giuliano Taccola designed the study, drafted the manuscript, and prepared the figures. Both authors approved the final version of the manuscript.

How to Cite this Article:

Dose F., Taccola G. 2016. Two Distinct Stimulus Frequencies Delivered Simultaneously at Low Intensity Generate Robust Locomotor Patterns. Neuromodulation 2016; 19: 563–575

REFERENCES

1. Selionov VA, Ivanenko YP, Solopova IA, Gurfinkel VS. Tonic central and sensory stimuli facilitate involuntary air-stepping in humans. *J Neurophysiol* 2009;101:2847–2858.
2. Gerasimenko Y, Gorodnichev R, Machueva E et al. Novel and direct access to the human locomotor spinal circuitry. *J Neurosci* 2010;30:3700–3708.
3. Gerasimenko Y, Gorodnichev R, Puhov A et al. Initiation and modulation of locomotor circuitry output with multisite transcutaneous electrical stimulation of the spinal cord in noninjured humans. *J Neurophysiol* 2015;113:834–842.
4. Kiehn O. Locomotor circuits in the mammalian spinal cord. *Annu Rev Neurosci* 2006; 29:279–306.
5. Kiehn O. Development and functional organization of spinal locomotor circuits. *Curr Opin Neurobiol* 2011;21:100–109.
6. Minassian K, Persy I, Rattay F et al. Human lumbar cord circuitries can be activated by extrinsic tonic input to generate locomotor-like activity. *Hum Mov Sci* 2007;26: 275–295.
7. Harkema S, Gerasimenko Y, Hodes J et al. Effect of epidural stimulation of the lumbosacral spinal cord on voluntary movement, standing, and assisted stepping after motor complete paraplegia: a case study. *Lancet* 2011;377:1938–1947.

8. Angeli CA, Edgerton VR, Gerasimenko YP, Harkema SJ. Altering spinal cord excitability enables voluntary movements after chronic complete paralysis in humans. *Brain* 2014;137:1394–1409.
9. Wakabayashi T, Kuroda T. Effect of stimulation with impulse trains of various patterns, including adaptational type, on frog's nerve-muscle and spinal reflex preparations. *Tohoku J Exp Med* 1977;121:219–229.
10. Marchetti C, Beato M, Nistri A. Alternating rhythmic activity induced by dorsal root stimulation in the neonatal rat spinal cord in vitro. *J Physiol* 2001a;530:105–112.
11. Binder-Macleod SA, Snyder-Mackler L. Muscle fatigue: clinical implications for fatigue assessment and neuromuscular electrical stimulation. *Physical Therapy* 1993; 73:902–910.
12. Mela P, Veltink PH, Huijing PA. Excessive reflexes in spinal cord injury triggered by electrical stimulation. *Arch Physiol Biochem* 2001;109:309–315.
13. Taccola G. The locomotor central pattern generator of the rat spinal cord in vitro is optimally activated by noisy dorsal root waveforms. *J Neurophysiol* 2011;106:872–884.
14. Dose F, Taccola G. Coapplication of noisy patterned electrical stimuli and NMDA plus serotonin facilitates fictive locomotion in the rat spinal cord. *J Neurophysiol* 2012;108:2977–2990.
15. Dose F, Menosso R, Taccola G. Rat locomotor spinal circuits in vitro are activated by electrical stimulation with noisy waveforms sampled from human gait. *Physiol Rep* 2013;1:e00025.
16. Dose F, Zanon P, Coslovich T, Taccola G. Nanomolar oxytocin synergizes with weak electrical afferent stimulation to activate the locomotor CPG of the rat spinal cord in vitro. *PLoS One* 2014;9:e92967.
17. Weitz AJ, Fang Z, Lee HJ et al. Optogenetic fMRI reveals distinct, frequency-dependent networks recruited by dorsal and intermediate hippocampus stimulations. *Neuroimage* 2015;107:229–41.
18. Wójtowicz T, Mozrzymas JW. Diverse impact of neuronal activity at θ frequency on hippocampal long-term plasticity. *J Neurosci Res* 2015;93:1330–1344.
19. Soffe SR, Roberts A. Tonic and phasic synaptic input to spinal cord motoneurons during fictive locomotion in frog embryos. *J Neurophysiol* 1982;48:1279–1288.
20. Taccola G, Marchetti C, Nistri A. Effect of metabotropic glutamate receptor activity on rhythmic discharges of the neonatal rat spinal cord in vitro. *Exp Brain Res* 2003; 153:388–393.
21. Kiehn O, Kjaerulff O. Spatiotemporal characteristics of 5-HT and dopamine-induced rhythmic hindlimb activity in the in vitro neonatal rat. *J Neurophysiol* 1996;75:1472–1482.
22. Juvin L, Simmers J, Morin D. Locomotor rhythmogenesis in the isolated rat spinal cord: a phase-coupled set of symmetrical flexion extension oscillators. *J Physiol* 2007;583:115–128.
23. Fulton BP, Walton K. Electrophysiological properties of neonatal rat motoneurones studied in vitro. *J Physiol* 1986;370:651–678.
24. Barbieri M, Nistri A. Depression of windup of spinal neurons in the neonatal rat spinal cord in vitro by an NK3 tachykinin receptor antagonist. *J Neurophysiol* 2001;85: 1502–1511.
25. Navarro X, Krueger TB, Lago N, Micera S, Stieglitz T, Dario P. A critical review of interfaces with the peripheral nervous system for the control of neuroprostheses and hybrid bionic systems. *J Peripher Nerv Syst* 2005;10:229–258.
26. Wallén P, Grillner S. N-methyl-D-aspartate receptor-induced, inherent oscillatory activity in neurons active during fictive locomotion in the lamprey. *J Neurosci* 1987; 7:2745–2755.
27. Zhong G, Shevtsova NA, Rybak IA, Harris-Warrick RM. Neuronal activity in the isolated mouse spinal cord during spontaneous deletions in fictive locomotion: insights into locomotor central pattern generator organization. *J Physiol* 2012;590: 4735–4759.
28. Gabriel JP, Ausborn J, Ampatzis K, Mahmood R, Eklöf-Ljunggren E, El Manira A. Principles governing recruitment of motoneurons during swimming in zebrafish. *Nat Neurosci* 2011;14:93–99.
29. Meehan CF, Grondahl L, Nielsen JB, Hultborn H. Fictive locomotion in the adult decerebrate and spinal mouse in vivo. *J Physiol* 2012;590:289–300.
30. Dose F, Deumens R, Forget P, Taccola G. Staggered multi-site low frequency electrostimulation effectively induces locomotor patterns in the isolated rat spinal cord. *Spinal Cord* 2016;54:93–101.
31. Etlin A, Blivis D, Ben-Zwi M, Lev-Tov A. Long and short multifunicular projections of sacral neurons are activated by sensory input to produce locomotor activity in the absence of supraspinal control. *J Neurosci* 2010;30:10324–10336.
32. Koga K, Furue H, Rashid MH, Takaki A, Katafuchi T, Yoshimura M. Selective activation of primary afferent fibers evaluated by sine-wave electrical stimulation. *Mol Pain* 2005;1:13.
33. Van de Crommert HW, Mulder T, Duysens J. Neural control of locomotion: sensory control of the central pattern generator and its relation to treadmill training. *Gait Posture* 1998;7:251–263.
34. Van Hedel HJ, Dietz V. Rehabilitation of locomotion after spinal cord injury. *Restor Neurol Neurosci* 2010;28:123–134.
35. Dimitrijevic MR, Gerasimenko Y, Pinter MM. Evidence for a spinal central pattern generator in humans. *Ann NY Acad Sci* 1998;860:360–376.
36. La Corte G, Wei Y, Chernyy N, Gluckman BJ, Schiff SJ. Frequency dependence of behavioral modulation by hippocampal electrical stimulation. *J Neurophysiol* 2014; 111:470–480.
37. Tong CK, MacDermott AB. Synaptic GluN2A and GluN2B containing NMDA receptors within the superficial dorsal horn activated following primary afferent stimulation. *J Neurosci* 2014;34:10808–10820.
38. Cangiano L, Wallén P, Grillner S. Role of apamin-sensitive K(Ca) channels for reticulospinal synaptic transmission to motoneuron and for the afterhyperpolarization. *J Neurophysiol* 2002;88:289–299.
39. Marchetti C, Beato M, Nistri A. Evidence for increased extracellular K(+) as an important mechanism for dorsal root induced alternating rhythmic activity in the neonatal rat spinal cord in vitro. *Neurosci Lett* 2001b;304:77–80.
40. Llinás R, Yarom Y. Oscillatory properties of guinea-pig inferior olivary neurones and their pharmacological modulation: an in vitro study. *J Physiol* 1986;376: 163–182.
41. Lampl I, Yarom Y. Subthreshold oscillations and resonant behavior: two manifestations of the same mechanism. *Neuroscience* 1997;78:325–341.
42. Hutcheon B, Yarom Y. Resonance, oscillation and the intrinsic frequency preferences of neurons. *Trends Neurosci* 2000;23:216–222.
43. Bekar L, Libionka W, Tian GF et al. Adenosine is crucial for deep brain stimulation-mediated attenuation of tremor. *Nat Med* 2008;14:75–80.
44. Tawfik VL, Chang SY, Hitti FL et al. Deep brain stimulation results in local glutamate and adenosine release: investigation into the role of astrocytes. *Neurosurgery* 2010; 67:367–375.
45. Jilge B, Minassian K, Rattay F, Dimitrijevic MR. Frequency-dependent selection of alternative spinal pathways with common periodic sensory input. *Biol Cybern* 2004; 91:359–376.
46. Brownstone RM, Jordan LM, Kriellaars DJ, Noga BR, Shefchyk SJ. On the regulation of repetitive firing in lumbar motoneurones during fictive locomotion in the cat. *Exp Brain Res* 1992;90:441–455.
47. Krawitz S, Fedirchuk B, Dai Y, Jordan LM, McCrea DA. State-dependent hyperpolarization of voltage threshold enhances motoneurone excitability during fictive locomotion in the cat. *J Physiol* 2001;532:271–81.
48. MacDonell CW, Power KE, Chopek JW, Gardiner KR, Gardiner PF. Extensor motoneurone properties are altered immediately before and during fictive locomotion in the adult decerebrate rat. *J Physiol* 2015;593:2327–2342.
49. Severin FV, Shik ML & Orlovskiĭ G. Work of the muscles and single motor neurons during controlled locomotion. *Biofizika* 1967;12:660–668.
50. Norris BJ, Wenning A, Wright TM, Calabrese RL. Constancy and variability in the output of a central pattern generator. *J Neurosci* 2011;31:4663–4674.
51. Strauss I, Lev-Tov A. Neural pathways between sacrocaudal afferents and lumbar pattern generators in neonatal rats. *J Neurophysiol* 2003;89:773–784.
52. Juranek J, Currie SN. Electrically evoked fictive swimming in the low-spinal immobilized turtle. *J Neurophysiol* 2000;83:146–155.
53. Cherniak M, Etlin A, Strauss I, Anglister L, Lev-Tov A. The sacral networks and neural pathways used to elicit lumbar motor rhythm in the rodent spinal cord. *Front Neural Circuits* 2014;8:143.
54. Ziegler MD, Zhong H, Roy RR, Edgerton VR. Why variability facilitates spinal learning. *J Neurosci* 2010;30:10720–10726.
55. Shah PK, Gerasimenko Y, Shyu A et al. Variability in step training enhances locomotor recovery after a spinal cord injury. *Eur J Neurosci* 2012;36:2054–2062.
56. Gosgnach S. The role of genetically-defined interneurons in generating the mammalian locomotor rhythm. *Integr Comp Biol* 2011;51: 903–912.
57. Dougherty KJ, Zagoraiou L, Satoh D et al. Locomotor rhythm generation linked to the output of spinal shox2 excitatory interneurons. *Neuron* 2013;80: 920–33.
58. Hägglund M, Dougherty KJ, Borgius L, Itohara S, Iwasato T, Kiehn O. Optogenetic dissection reveals multiple rhythmogenic modules underlying locomotion. *Proc Natl Acad Sci USA* 2013;110:11589–11594.

Supplementary information

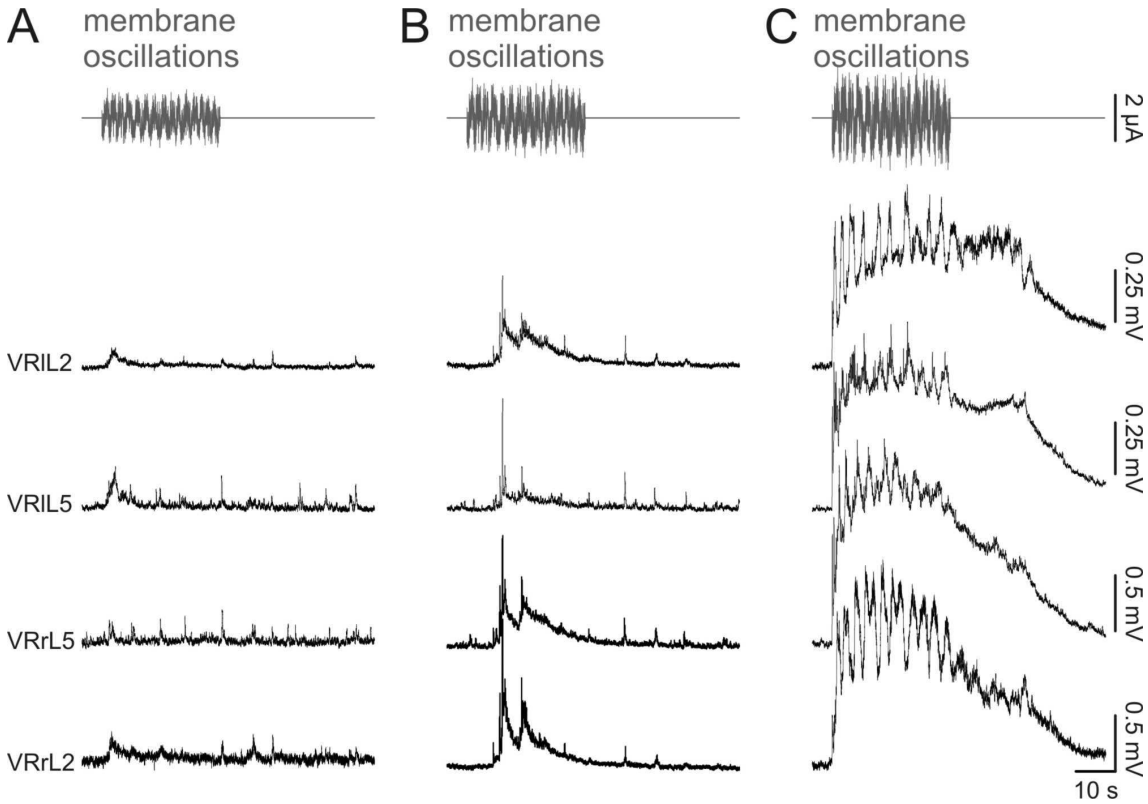

Figure S1. By increasing stimulus strength, membrane potential oscillations also effectively evoke locomotion. *The same stimulating pattern consisting of sole membrane oscillations is unable to generate FL when delivered at the amplitude of 2.6 µA (same trace of Fig. 2). When stimulus amplitude (peak to peak) is progressively increased to 3.5 µA (B) and finally to 4.6 µA, a burst of synchronous discharges was replaced by an episode of alternating cycles on VRs.*

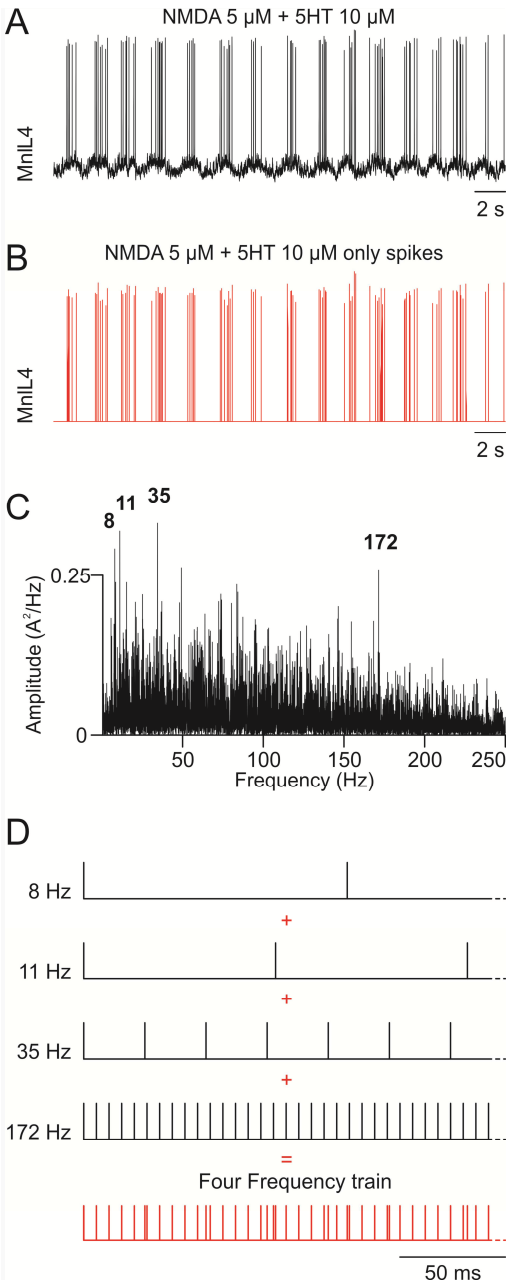

Figure S2. Power spectrum of FLspikes reveals four main frequency components. *Through off line analysis, membrane potential oscillations were removed from the original traces recorded from a single motoneuron (MnIL4; A) in order to design FLspikes (B). In C, the Fourier analysis of FLspikes identifies four main components in the low (8 and 11 Hz), intermediate (35 Hz) and high frequency ranges (172 Hz). The four single trains of pulses centered around the main components of the spectrum in C are superimposed to obtain the Four Frequency train protocol (D).*

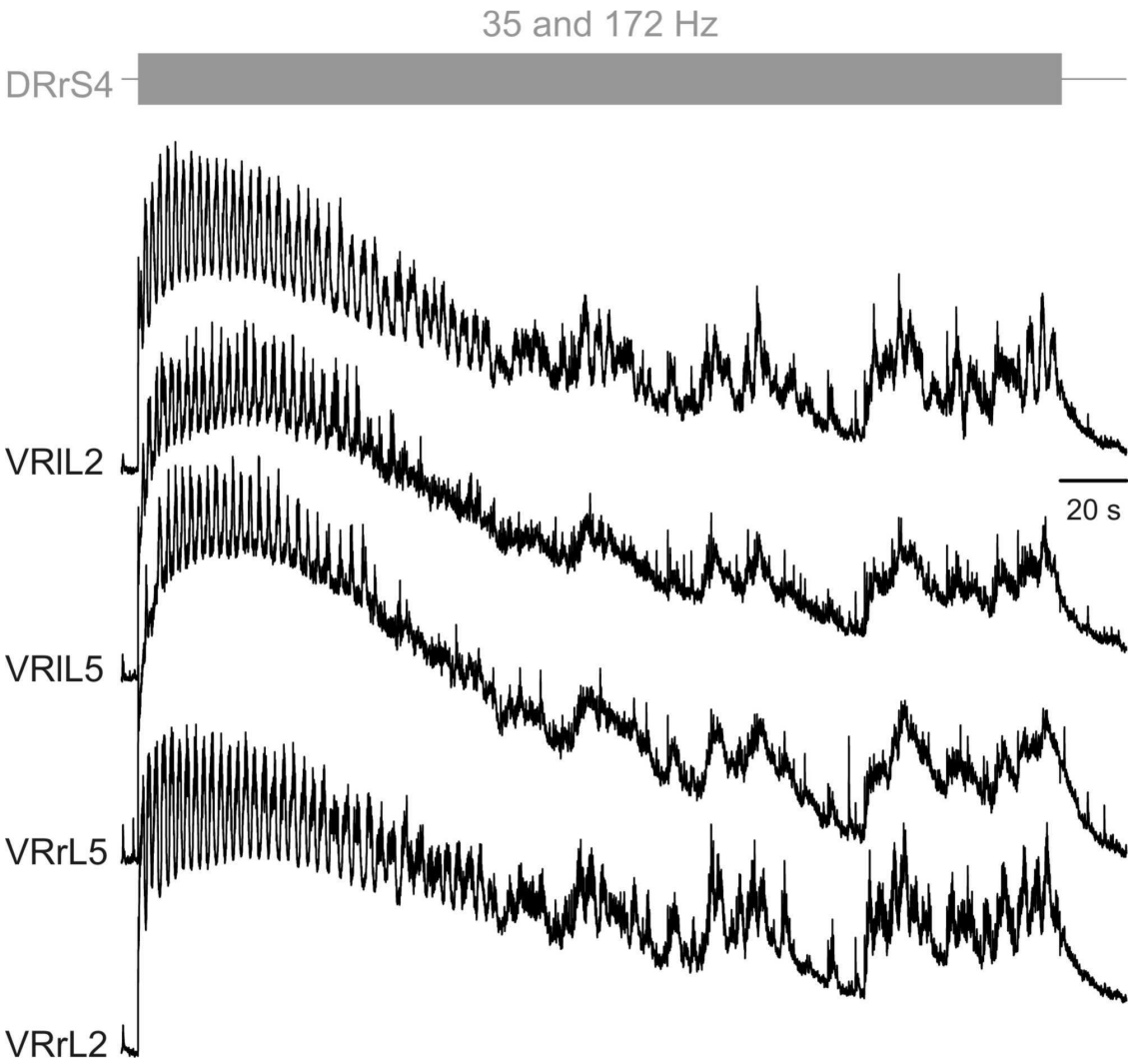

Figure S3. A longer stimulation with 35 and 172 Hz augments the number of FL cycles. *A 35 and 172 Hz train of longer duration (280 s) was delivered to DRrS4 at 5 µA (0.5 x Th). In response to stimulation, a long-lasting (106.36 s) episode of 37 FL cycles (period = 2.93 ± 0.59 s) appears at the top of cumulative depolarization (0.39 mV).*

Discussion

In the present thesis, I focus my attention on three main issues: 1) understanding the features that make electrical stimulation with sub-threshold noisy waves effective for activating locomotor patterns, 2) investigating how the noisy stimulating protocol can be facilitated by innovative pharmacological agents, and 3) exploring the effect of multi-site spinal cord stimulation.

As a first approach, I compared the appearance of locomotor-like patterns in response to different noisy stimulating waveforms. Since FL bursts recorded from VRs show a narrow range of the main periodicity (Juvin et al., 2007), I recorded the electrical activity from multiple muscles of adult volunteers during real locomotion and during the execution of several phasic and rhythmic motor tasks to obtain a wide palette of noisy protocols. I compared the number of locomotor-like cycles induced by intrinsically variable protocols and by the sinusoidal trajectories of the kinematic analysis acquired during the same sessions of locomotion. This demonstrates that only the noisy waveforms obtained from EMG recordings—not the smooth kinematic profiles—are able to induce an epoch of locomotor-like oscillations. This observation is reminiscent of the loss of the efficacy of fictive locomotor waveforms when they are progressively acquired at lower sampling frequency (Taccola, 2011).

Proprioceptive feedback from flexor and extensor muscles plays a crucial role during the gait cycle. Indeed, while extensor-muscle feedback is mainly involved in controlling the stance phase, avoiding swing initiation when the leg is loaded, afferent inputs from flexor muscles are important in facilitating the initiation of the

swing phase during walking (Lam and Pearson, 2002). Moreover, gait starts with the activation of a flexor muscle: namely, the tibialis anterior (TA) of the swinging limb (Crenna and Frigo 1991). However, in experiments performed for the current thesis project, episodes of FL were equally triggered regardless of the origin of stimulating EMG protocols. The same observation was obtained from noisy waveforms sampled *in vitro* from L2 or L5 VRs (Taccola et al., 2011) mainly convoying extensor and flexor commands (Kiehn and Kjerluff, 1996).

On the other hand, the noisy patterns acquired during standing or isometric muscle contraction are unable to elicit FL, thus indicating the importance of a low frequency phasic component in the noisy paradigms. Currently, the stimulation protocols that are employed *in vitro* to evoke an episode of FL are based on trains of square pulses delivered at 2Hz (Marchetti et al., 2001a; Juvin et al., 2007; Dunbar et al., 2010). This value is comparable to the stepping frequency in adult rats (1.3–4 Hz; Krizsan-Agbas et al., 2014; Bellardita and Kiehn, 2015), humans (1.30-2 Hz; Snaterse et al., 1985) and to the frequency of a chemically-induced FL in an *in vitro* spinal cord (1-5 Hz; Atsuta et al., 1990; Juvin et al., 2007).

EMG traces sampled from volunteers during the execution of different motor behaviours show scarce task specificity in inducing FL episodes. In fact, all stimulating patterns obtained from noisy and phasic EMGs that are characterized by a periodicity near that of the locomotor trials (1 Hz) were able to activate the *in vitro* CPGs.

From this first part of the study, it emerged that the sole noise is not *per se* sufficient to induce FL: a low-frequency component is also crucial, as already

considered by the canonical, stereotyped stimulation. To interpret the improvements provided by the innovative protocols studied in this thesis, an intriguing working hypothesis is formulated: that elements of the locomotor CPGs are selectively recruited by a distinct frequency code contained in the noisy waveforms among the many others frequencies that characterize their complex spectrum. Indeed, in other networks, it has been demonstrated that different types of neurons have distinct frequency preferences (Pike et al., 2000).

To verify whether a particular frequency content is involved, noisy waveforms were progressively filtered by reducing the number of original frequency components. Moreover, to further simplify the complex nature of noisy waveforms recorded from motor pools, intracellular recordings were collected from a single motoneuron. Indeed, at the level of a single motoneuron, the appearance of harmonics due to desynchronized firing among motoneurons in the same motor pools is minimized (Wever et al., 1937; Lambertz and Langhorst, 1998). In addition, by delivering the sole electrical oscillations of the motoneuronal membrane during FL, it is also possible to stimulate the locomotor CPG with its putative output.

All protocols of stimulation obtained from the electrical activity of a single motoneuron during FL are able to induce a long-lasting episode of FL when delivered at sub-threshold intensities. In other words, they are unable to induce a reflex response when applied to a DR as a single square pulse. Nevertheless, paradigms obtained from intracellular recordings are slightly less effective than protocols extracellularly derived from VRs and delivered to the same peak-to-peak amplitude. This indicates that the intrinsic variability of a single motoneuron firing is

not able to faithfully reproduce the noise recorded from the entire motor pool. Then, the small contribution of other sources of noise must be considered at the base of the satisfactory activation of the locomotor CPGs by noisy waveforms sampled from VRs or muscles.

Nonetheless, the power-spectrum analysis of the firing activity during FL from single motoneurons is useful to reveal four main characteristic frequencies. These frequencies are also identified *a posteriori* in the noisy waveforms recorded from VRs, which in fact become less effective when the same frequencies are selectively filtered out using an *ad hoc*, custom-made Matlab code. The four components are good candidates for the optimal activation of the locomotor CPG. Indeed, the four frequencies identified are able to activate an episode of FL when applied simultaneously as a multifrequency paradigm.

Different permutations were delivered to further simplify the multifrequency protocol and at the same time identify the most effective components among the four identified frequencies. This analysis shows that the best protocol is a train of square pulses that contain the following pair of frequencies: 35 and 172 Hz. This efficacy depends neither on the number of pulses applied nor on the energy of the protocol, as the random selection of a different pair of frequencies with an equal number of pulses and spectrum magnitudes triggered lower episodes of locomotor patterns.

Furthermore, the 35-172 Hz protocol is effective even when applied for only 500ms, making it the shortest stimulating protocol currently available to induce FL

(Juranek and Currie, 2000; Marchetti et al., 2001a; Strauss and Lev-Tov, 2003; Taccola, 2011).

Studies conducted in other districts of the CNS highlight the importance of 35 or 172 Hz when individually applied; so far, however, they have never been delivered simultaneously. For instance, in the ponto-cerebellum, stimulation around 40 Hz selectively activates the auditory region (Pastor et al., 2002; Pastor et al., 2008) while, stimulation of the vagus nerve in the frequency range of 130-180 Hz is more effective for inhibiting seizure episodes (Jiao et al., 2016).

Despite improvement in eliciting locomotor patterns of longer duration and with a shorter and weaker protocol than the canonical electrical stimulation of DRs, the effect of noisy stimulation remains transient as opposed to the stable FL induced by neurochemicals. Also, the electrical stimulation with a stereotyped train of pulses is able to induce only transient episodes of locomotor-like patterns (Lev-Tov and Pinco, 1992; Marchetti et al., 2001a). Thus, to prolong the activation of locomotor spinal circuits, specific pharmacological agents acting on spinal networks were explored (Cote et al., 2003; Guertin, 2004b; Gerasimenko et al., 2007). To this purpose, in the current project, the modulatory effects of oxytocin on locomotor networks and its effect on motoneuronal membrane and synaptic spinal transmission were investigated. Oxytocin has previously been demonstrated to modulate spinal networks (Pearson et al., 2003; Barrière et al., 2005). This effect is reminiscent of the neuromodulator role of other neuropeptides (Marchetti and Nistri, 2001c). In the current thesis, the modulatory effects of oxytocin were ascribed to pre-motoneuronal networks as pointed out by intracellular recordings

performed from single motoneuron in the presence of blockers of the action potential-mediated transmission (Marchetti et al., 2003). As for the mechanism of action of oxytocin, the experimental part of this thesis, in which isolated spinal cord was treated overnight with the inhibitor of the tryptophan hydroxylase, p-chlorophenylalanine (PCPA, 10 mM; Branchereau et al., 2002), demonstrates that oxytocin facilitates the endogenous release of 5HT. An original contribution of this study is the discovery that a nanomolar concentration of oxytocin (1nM) improves the electrical stimulation with noisy waveforms by facilitating FL even at weaker intensity. Interestingly, the oxytocin did not have, at the same nanomolar concentration, any significant action on reflexes, thus indicating that a more complex spinal network is recruited by the neuropeptide.

As already stated, the fact that FL elicited by optimal noisy waveform protocols can be further improved by neurochemicals suggests the importance of a combined approach to activate locomotor patterns (Guertin and Hounsgaard, 1998; Gerasimenko et al., 2007; Courtine et al., 2009; Gad et al., 2013).

However, even in the presence of the best neurochemicals explored so far, the electrical stimulation of a DR evokes a number of FL cycles that remain dramatically lower than the one elicited through the direct activation of spinal circuits by the un-physiological bath-application of neurochemicals to the entire cord. This indicates that further aspects have to be considered to improve the effect of the current electrical paradigms. Among them, I considered the potential existence of a spinal-gating mechanism responsible for filtering trains of stereotyped input persistently delivered (Weinberg, 2013). In this context, sub-

threshold paradigms as the noisy waves would prevent blockage of charge conduction along dorsal fibres. Although recordings from isolated DR (unpublished observation), do not show any block in conducting afferent volleys, a fatiguing effect of continuous electrical stimulation on primary afferents cannot be excluded (Lee and O'Donovan, 1991). Indeed, FL episodes can be elicited in the long term only when an adequate pause (3-5 min) is interposed between two consecutive protocols (Dose and Taccola, 2012; Dingu et al., 2016). Accounting for this limitation, a potential way to increase the efficiency of electrical stimulation is to swap among multiple DRs during the stimulation. Nevertheless, it must be confirmed that multiple pulses applied to different DRs converge on the same locomotor network. Indeed, while it has been shown that electrical stimulation of a DR resets the locomotor-like patterns generated by neurochemicals (Sqalli-Houssaini et al., 1993; Iizuka et al., 1997; Dose and Taccola, 2012), it has not yet been demonstrated that single pulses applied to a different DR perturb rhythmic patterns elicited by the repetitive stimulation of another DR.

The experimental part of this thesis indicates that afferent inputs coming from multiple DRs converge to generate locomotor rhythm, thus opening the possibility to decompose the most effective stimulating protocol to multiple sites. Accordingly, the optimal multifrequency protocol (35-172 Hz) was separately delivered with a multi-site approach to two different DRs without losing efficacy.

Comparison between noisy waveform protocols and stereotyped trains of rectangular pulses.

Many parameters of the trains of stereotyped rectangular pulses (DRtrain) were varied without significant impact on the duration of FL episodes (Lev-Tov et al., 2000; Marchetti et al., 2001a; Whelan et al., 2000; Delvolvé et al., 2001; Strauss and Lev-Tov., 2003). The intensity of stimulation was explored in the range of 1.5 to 3 times the threshold, while the pulse frequency ranged from 1 Hz to 10 Hz. The duration of each pulse was changed from 0.1 ms to 4 ms (Lev-Tov et al., 2000; Marchetti et al., 2001a; Whelan et al., 2000; Delvolvé et al., 2001; Strauss and Lev-Tov., 2003), and single pulses were delivered monophasically (Marchetti et al., 2001a) or biphasically (Joucla et al., 2016).

Although only a few studies have highlighted the benefits of variations in the stimulus shape (McIntyre and Grill, 2002; Hofmann et al., 2011), the vast majority of stimulation protocols used in research and in clinics deliver stereotyped trains of pulses. However, some studies have developed stimulation techniques that are based on the use of signals sampled from biological sources (Rolston et al., 2010; Hebb et al., 2014; Wenger et al., 2016) to provide more natural information to finely tune neuronal networks.

A unique protocol of stimulation that consists of noisy electrical oscillations sampled from a motor nerve during the pharmacological activation of the locomotor CPG *in vitro* (FL*i*stim) has been proposed to elicit longer episodes of locomotor-like patterns (Taccola, 2011). Though the mechanism of an intrinsically variable paradigms pattern has to be fully clarified, a hypothesis comes from the possibility that some interneurons crucial for the expression of the locomotor program are

selectively activated by discrete frequencies. For instance, Renshaw cells, which in mice are responsible for the expression of FL episodes elicited by the electrical stimulation of a VR (Wenner et al., 1998), activate different receptors on postsynaptic targets according to the frequency of stimulation (Lamotte d'Incamps and Ascher, 2008). From this point of view, a stimulus with very complex frequency spectrum, such as FL*i*stim, can embrace all possible candidates.

An additional explanation might consider changes in transmitter release from afferent terminals in response to distinct frequencies of stimulation (Tong and MacDermott, 2014). Possibly, the ensemble of frequencies contained in FL*i*stim would determine a profile of transmitter release on the elements constituting the CPGs that differ from the one induced by stereotyped trains (Eliot et al., 1994; Tawfik et al., 2010). To this reference, the amount of glutamate released from primary afferent synapses is modulated by the frequency of inputs that travel along axons (Sluka et al., 2004; Tong and MacDermott, 2014).

Furthermore, it must be considered that noisy and stereotyped stimulating protocols may recruit different set of afferent fibres according to their strength of stimulation (Koga et al., 2005).

According to a finalistic interpretation, it can be speculated that the best afferent stimulation is one that mimics the phasic and noisy nature of the sensory feedback that rhythmically reaches the spinal cord during locomotion. Although noisy waves sampled from VRs do not represent the physiological feedback, it has been demonstrated by recording from DRG in cats walking on a treadmill that the afferent feedback during locomotion pairs with the pattern simultaneously derived from VRs (Loeb et al., 1977).

Moreover, during locomotion, afferent feedback generated from periphery as a consequence of the continuous alternate movement of the lower limbs interacts with the locomotor CPGs and helps to modulate both the timing and magnitude of the locomotor pattern (Pearson et al., 1998; Pearson et al., 2003; Grillner and Jessell, 2009). Indeed, in isolated spinal cords with hind limbs attached, the pharmacologically-induced FL is abolished by complete dorsal rhizotomy (Acevedo and Diaz, 2013). These observations suggest that the noisy nature of the afferent feedback and other asynchronous patterns agree with the intrinsic logic of the locomotor CPGs in processing peripheral input for the expression and control of the locomotor program.

Noise makes stimulating patterns more effective to elicit FL.

An important property of the innovative stimulating protocols introduced in this thesis is constituted by their "noisy" content. The noise is a key component of a wide range of biological systems (Hubbard et al., 1967; Faisal et al., 2008). At the level of a single neuron, it appears as random fluctuations of membrane potential (Jacobson et al., 2005). The nervous system is permeated by noise from the perception of sensory signals to the generation of motor responses. Neurons are influenced by noise arising from both intrinsic and extrinsic sources.

For instance, ionic channels show variations in the conductance driven by thermal fluctuations (Steinmetz et al., 2000). Furthermore, electrical noise, such as channel noise, which refers to the probabilistic gating of voltage-dependent ion channels (White et al., 2000; Steinmetz et al., 2000; van Rossum et al., 2003), induces

membrane-potential fluctuations even in the absence of synaptic inputs. Nevertheless, synaptic activity also generates noise (Destexhe et al., 2001). Spontaneous miniature postsynaptic currents (mPSCs) contribute to synaptic noise (Faisal et al., 2008), as they derive from the quantal release of the neurotransmitter, which in turn follows a probabilistic, Gaussian distribution (Katz and Miledi, 1962). Another source of noise derives from a common property shared by neurons that generates action potentials: spike-frequency adaptation (SFA). It consists in a decline in the neuronal firing rate in response to a constant and prolonged stimulus. At the base of SFA are variations in ionic intracellular concentrations that activate hyperpolarizing conductances (Peron and Gabbiani, 2009).

In spinal motoneurons, SFA is a fundamental property that modulates repetitive firing. It seems that the mechanism underlying SFA in motoneurons is mainly mediated by the slow inactivation of Na^+-channels (Miles et al., 2005). However, it is more likely that SFA in spinal motoneurons is ensured by several channels that act together. To this regard, the pharmacological blockade of a set of channels will result in an enhanced contribution of the others (Powers et al., 1999).

In nonlinear systems such as several sensory systems, noisy basal fluctuations provide substantial improvements in detecting weak periodic signals according to a phenomenon called stochastic resonance (SR; Douglass et al., 1993; McDonnell and Abbott, 2009). Already at the level of a single mechanoreceptor, external noise is relevant for sensing small periodic signals in the environment (Ivey et al., 1998). SR phenomenon has also been reported in sensory neurons (Douglass et al.,

1993) and in the neuromotor system (Martínez et al., 2007). For instance, the sensitivity of muscle spindle receptors to weak limb movement can be increased by introducing noise through the tendon of the parent muscle (Cordo et al., 1996).

The concept of SR has been applied to the contribution of intrinsic variability in increasing the performance of non-linear neuronal networks (Rabinovich and Abarbanel, 1998). Here the addition of noise enhances synchronization among different coupled oscillators (Lindner et al., 1996) that in turn increase the coherence of the spiking response of neurons, improving in this way the ability to respond to weak stimuli (Liu et al., 1999).

Moreover, SR has been hypothesized as a mechanism for neuronal synchronization of different brain areas (Kitajo et al., 2003) and hippocampal neurons (Stacey and Durand, 2001).

SR has also found some interesting applications in clinical research. Transcranial stimulation with random electrical oscillation is able to increase the excitability of cortical neurons (Terney et al., 2008). Interestingly, the latter effect is reported only when the full frequency spectrum is employed (from 0.1 to 640 Hz) (Terney et al., 2008). This evidence strengthens the hypothesis that the effectiveness of noisy stimulating waves resides in the inherent variability of the signal and that through stochastic resonance recruits spinal neuronal networks.

Conjoint pharmacological and electrical stimulation facilitates FL.

A promising approach in rehabilitation for the recovery of function after SCI is the modulation towards the physiological state of the spinal cord circuitry (Lavrov et al., 2006; Gerasimenko et al., 2007; Courtine et al., 2007; Lavrov et al., 2008; Gerasimenko et al., 2009).

A SCI induces complex biochemical changes that result in both direct mechanical injury and secondary pathophysiological mechanisms caused by the initial trauma (Rowland et al., 2008). In particular, following a SCI, the descending transport of neurotrasmitters synthetized in supraspinal centres is interrupted, causing a significant reorganization of the sensorimotor pathways caudally to the lesion (Nacimiento et al., 1995).

For this reason, input to the spinal cord is interpreted differently from the intact condition. For instance, after a SCI, the excitability of CPGs is changed, leaving some synapses hyperexcitable and others hypoexcitable (Calancie et al., 1993; Edgerton et al., 2001).

The exogenous application of pharmacological agents can restore the physiological biochemical environment of the injured spinal cord. In particular, the low dosage of the 5HT receptor agonist, quipazine (Gerasimenko et al., 2007), the dopamine precursor, L-DOPA (Guertin, 2004b), or the alpha-2 agonists, clonidine (Côté et al., 2003), have been shown to facilitate locomotion in spinalized animals (Rossignol and Barbeau, 1993). When administered during spinal stepping in cats, 5HT exerts a facilitatory effect by increasing the step length and the EMG amplitude of hind-limb extensors and flexors muscles (Barbeau and Rossignol, 1990). However, on

spinalized mice, the treatment with quipazine alone is not sufficient to enhance stepping ability, highlighting the need of multiple strategies (Fong et al., 2005). It has been suggested that 5HT binds to receptors located in the dorsal horn of the lumbosacral spinal cord (Liu et al., 2002), thereby facilitating the primary afferent-synaptic responses onto dorsal horn neurons (Lopez-Garcia JA, 1998). Therefore, 5HT seems to favour interneuronal dorsal pathways related to proprioceptive and cutaneous inputs (Fong et al., 2005). However, its action on the dorsal network is far from exclusive, as 5HT cooperates with NMDA by inducing FL from the sole ventral hemicord (Taccola and Nistri, 2006).

Pharmacological and electrical stimulation may conjointly facilitate the recruitment of CPGs (Fong et al., 2009), thereby modulating the physiological state of the spinal cord toward one that can more readily generate locomotion (Chau et al., 1998b; Gerasimenko et al., 2007; Edgerton et al., 2008; Courtine et al., 2009; Van den Brand et al., 2012).

As a good translation of this principle, the combined application of buspirone, a partial agonist of $5HT_{1A}$ receptors, with transcutaneous electrical stimulation facilitates stepping in individuals with complete motor paralysis (Gerasimenko et al., 2015). Analogously, weak FL*i*stim delivered in the presence of sub-threshold concentrations of NMDA and 5HT cooperates in facilitating the appearance of FL rhythm (Dose and Taccola, 2012). Nevertheless, the vast majority of the molecules explored so far are not suitable for human systemic pharmacotherapy due to a general excitation of the central nervous system and other peripheral targets.

A new drug combination has been recently shown to produce robust hind-limb stepping with weight-bearing capabilities in SCI persons (Guertin et al., 2010), and it appears to be quite safe for human use (Guertin and Brochu, 2009; Guertin et al 2011). However, this drug combination has not been used conjointly with electrical stimulation; thus, further investigations are warranted.

In this thesis, oxytocin is chosen as a neuropeptide of interest because it has been previously shown to modulate chemically-induced locomotor patterns (Pearson et al., 2003; Barrière et al., 2005) and because it has been safely employed in several clinical trials for the treatment of multiple disorders of the CNS (Gimpl and Fahrenholz, 2001).

I discovered that oxytocin facilitates neuronal rhythmic activity and the emergence of FL episodes in response to weak noisy waveforms. This effect, however, occurs in a very narrow range of concentrations. This is probably due to the selective localization of its receptors on discrete neuronal elements (Liu et al., 2003; Chini and Manning, 2007) and to the fact that, at higher doses, it might exert a reflex depressant action (Wilson et al., 2009), thereby negatively affecting the transmission of inputs to CPGs.

When I applied it at low concentrations during conjoint stimulation with weak FL*i*stim, oxytocin induced the appearance of FL episodes; at high concentrations, however, this result is not observed. Low-dose oxytocin and weak electrical stimulation show to synergize, since the effect produced by their conjoint application is greater than the sum of their single effects. Indeed, the synchronous pattern evoked from VRs that stimulate weak noisy waveforms is converted into a

locomotor-like pattern when the two treatments are co-applied. On the contrary, neither increasing the strength of stimulation nor higher concentrations of oxytocin are able to reinstate FL.

Since afferent fibres do not express oxytocin receptors (Moreno-Lo´pez et al., 2013), the facilitation exerted by oxytocin on the sub-threshold electrical stimulation probably depends on a discrete distribution of its receptors on specific neuronal elements that are capable of selectively contributing to the expression of FL (Schoenen et al., 1985; Liu et al., 2003; Chini and Manning, 2007). Oxytocin receptors have been shown to modulate 5HT release (Eaton et al., 2012; Marazziti et al., 2012), which in turn acts on different receptor subtypes (Barnes and Sharp, 1999), thereby producing different cellular responses (Garraway and Hochman, 2001). Thus, oxytocin action depends on where and how the endogenous 5HT is liberated.

Relevance of stimulation frequency to the activation of the locomotor CPG.

The cartoon below illustrates a wiring diagram that may explain the findings of the multi-site stimulation collected in the present thesis. According to this model, two levels of filter for afferent inputs exist: the first for amplitude and the second for frequency. Moreover, DRs do not directly innervate locomotor spinal networks, but rather use an afferent relay that consists of multiple functional units in parallel. Through this relay, inputs from three distinct DRs along the lumbosacral spinal cord require specific characteristics to ultimately activate the locomotor CPGs.

Simultaneous sub-threshold amplitude pulses of the three DRs cannot be summed to transmit an activating signal to CPGs. In contrast, multi-level pulses of sub-threshold frequency and supra-threshold amplitude can be summed to reach the threshold frequency and activate CPGs when they are given in a staggered way. Note that here the threshold values are considered as those that can activate CPGs without any direct relation with the threshold intensity for eliciting a reflex response from motoneurons.

Such a model could represent the basic structure for the integration of afferent inputs by the locomotor CPGs, as revealed by the data of the present thesis. The afferent relay in our wiring diagram is reminiscent of the relay neurons in the sacrococcygeal spinal cord, previously proposed to drive lumbar rhythms (Strauss and Lev-Tov, 2003).

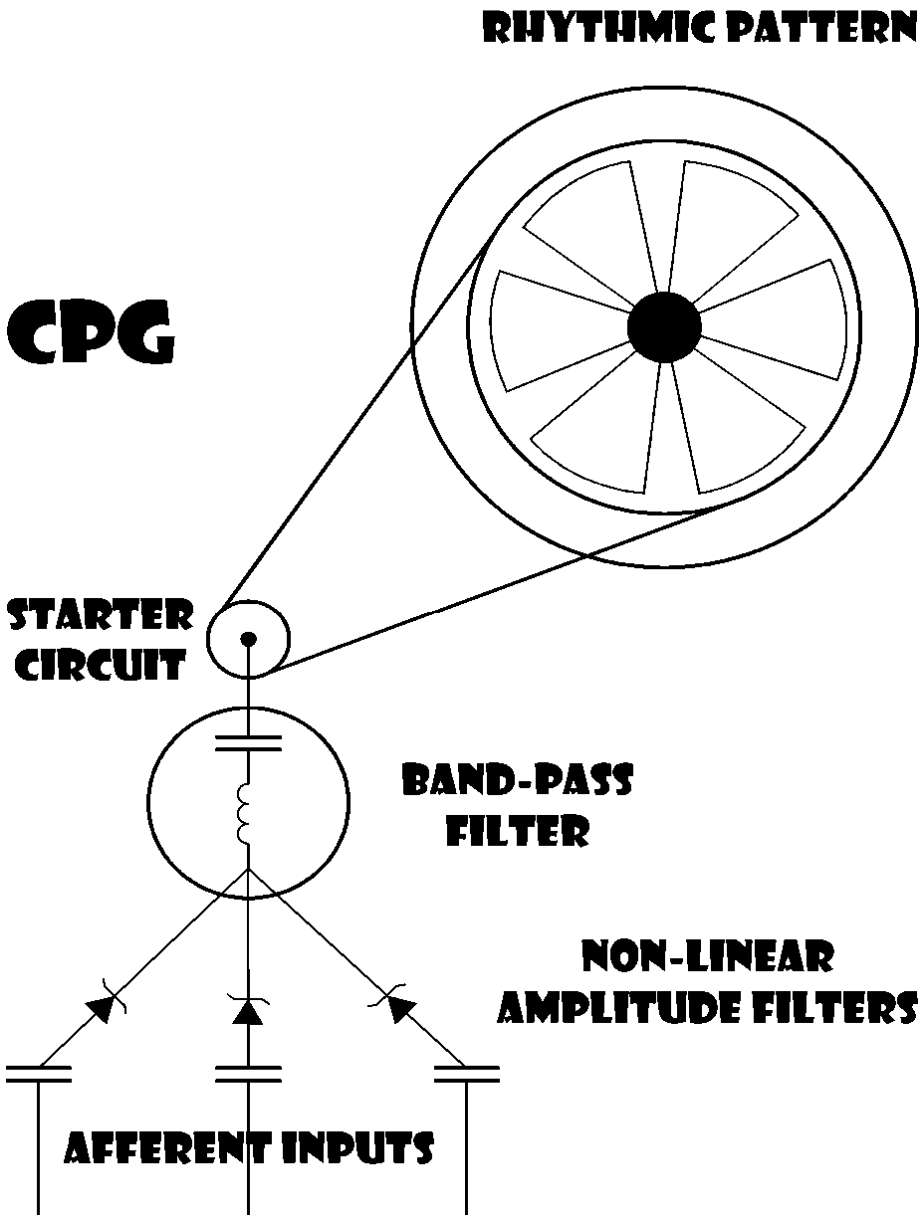

Figure 8. A wiring diagram providing a rational, schematic explanation for the effect of multi-site electrical stimulation. *Three afferent synapses that correspond to capacitors in electronics (indicated with electronic symbol) are depicted at the bottom. In this particular investigation, only three inputs are used; but a convergence of many more peripheral afferents may be considered in an* in vivo *situation. The synapses of these afferents process the amplitude of the inputs in a non-linear manner (as indicated by the Zener diode symbol). These signals can only pass the synapse if they reach a certain intensity threshold. According to this concept, multiple, simultaneous 2 Hz trains, each of sub-threshold amplitude, will not lead to an activation of the locomotor pattern. This*

may, then, be interpreted as a first amplitude-dependent processing of signals prior to any relevance for stimulation frequency. Next in our diagram is a downstream relay, which acts as a frequency filter and is indicated as an electronic symbol for band-pass filter (inductance plus an in-series capacitor). This part of the circuit is responsible for selecting a discrete range of input frequencies. At the level of the band-pass filter, multiple afferent trains may converge and, as long as each of these is at suprathreshold amplitude, temporal summation may occur to recompose the frequency threshold. According to this concept, a staggering of sub-threshold frequency stimuli adds up to a frequency that can pass through the band-pass filter. Through the band-pass filter, signals are passed on to a starter circuit that drives the ignition of the rhythmic locomotor pattern. The existence of a starter circuit driven by afferent inputs can explain why, experimentally, only few cycles of FL are induced by electrical stimulation of a DR while the direct activation of FL by chemicals is characterized by a stable and prolonged locomotor pattern (maintained for as long as chemicals remain present). It is important to note that, although this simple wiring diagram may be considered for stereotyped trains (i.e., only one stimulation frequency at a time), inputs of a more variable nature (e.g., noisy waveforms) may exploit the presence of the non-linear synapse (capacitor) downstream of the inductance of the band-pass filter. Herein, multiple stimulation frequencies passing the inductance of the band-pass filter add up at the non-linear synapse (capacitor) of the band-pass filter.

Conclusion

From the results collected in this thesis, noisy waveforms result in a more efficient protocol than the canonical, stereotyped trains for activating the locomotor central-pattern generators in the spinal cord. Unfortunately, with the technology currently available, it is not feasible to use these variable signals for the stimulation of the spinal cord in a clinical setting.

Disassembling the complexity of the noisy waves makes it possible to apply them in clinical electrostimulators.

An approach that may improve the neurorehabilitation for motor recovery after spinal injury is the simultaneous delivery of two stereotyped trains of pulses, each set at distinct values and applied to different sites. Due to the lower intensity required, this method makes it possible to reduce the energetic demand of implantable stimulator and reduce the adverse effects.

Finally, the conjoined application of innovative and safe neuromodulators seems to be crucial for the yield of the electrical stimulation.

Bibliography

Acevedo JM, Díaz-Ríos M. (2013) Removing sensory input disrupts spinal locomotor activity in the early postnatal period. J Comp Physiol A Neuroethol Sens Neural Behav Physiol 199(12):1105-16.

Agnati LF, Fuxe K. (2000) Volume transmission as a key feature of information handling in the central nervous system possible new interpretative value of the Turing's B-type machine. Prog Brain Res 125:3-19.

Ahn AN, Furrow E, Biewener AA. (2004) Walking and running in the red legged running frog, Kassina maculata. J Exp Biol 207(Pt 3):399-410.

Alexander RM. (1989) Optimization and gaits in the locomotion of vertebrates. Physiol Rev 69(4):1199-227.

Angeli CA, Edgerton VR, Gerasimenko YP, Harkema SJ. (2014) Altering spinal cord excitability enables voluntary movements after chronic complete paralysis in humans. Brain 137(Pt 5):1394-409.

Atsuta Y, Garcia-Rill E, Skinner RD. (1990) Characteristics of electrically induced locomotion in rat in vitro brain stem-spinal cord preparation. J Neurophysiol 64(3):727-35.

Barbeau H, Rossignol S. (1987) Recovery of locomotion after chronic spinalization in the adult cat. Brain Res 412(1):84-95.

Barbeau H, Rossignol S. (1990) The effects of serotonergic drugs on the locomotor pattern and on cutaneous reflexes of the adult chronic spinal cat. Brain Res 23;514(1):55-67.

Barnes NM, Sharp T. (1999) A review of central 5-HT receptors and their function. Neuropharmacology 38:1083–1152.

Barolat-Romana G, Myklebust JB, Hemmy DC, Myklebust B, Wenninger W. (1985) Immediate effects of spinal cord stimulation in spinal spasticity. J Neurosurg 62(4):558-62.

Barrière G, Bertrand S, Cazalets JR. (2005) Peptidergic neuromodulation of the lumbar locomotor network in the neonatal rat spinal cord. Peptides 26(2):277-86.

Beato M, Bracci E, Nistri A. (1997) Contribution of NMDA and non-NMDA glutamate receptors to locomotor pattern generation in the neonatal rat spinal cord. Proc Biol Sci 264(1383):877-84.

Beato M, Nistri A. (1999) Interaction between disinhibited bursting and fictive locomotor patterns in the rat isolated spinal cord. J Neurophysiol 82(5):2029-38.

Bellardita C, Kiehn O. (2015) Phenotypic characterization of speed-associated gait changes in mice reveals modular organization oflocomotor networks. Curr Biol 25(11):1426-36.

Beloozerova IN, Zelenin PV, Popova LB, Orlovsky GN, Grillner S, Deliagina TG. (2003) Postural control in the rabbit maintaining balance on the tilting platform. J Neurophysiol 90(6):3783-93.

Berg RW, Alaburda A, Hounsgaard J. (2007) Balanced inhibition and excitation drive spike activity in spinal half-centers. Science 315(5810):390-3.

Bertrand SS, Cazalets JR. (2013) Activity-dependent synaptic plasticity and metaplasticity in spinal motor networks. Curr Pharm Des 19(24):4498-508.

Bizzi E, Mussa-Ivaldi FA, Giszter S. (1991) Computations underlying the execution of movement: a biological perspective. Science 253(5017):287-91.

Boulenguez P, Vinay L. (2009) Strategies to restore motor functions after spinal cord injury. Curr Opin Neurobiol 19(6):587-600.

Bracci E, Ballerini L, Nistri A. (1996a) Spontaneous rhythmic bursts induced by pharmacological block of inhibition in lumbar motoneurons of the neonatal rat spinal cord. J Neurophysiol 75(2):640-7.

Bracci E, Ballerini L, Nistri A. (1996b) Localization of rhythmogenic networks responsible for spontaneous bursts induced by strychnine and bicuculline in the rat isolated spinal cord. J Neurosci 16(21):7063-76.

Bracci E, Beato M, Nistri A. (1998) Extracellular K+ induces locomotor-like patterns in the rat spinal cord in vitro: comparison with NMDA or 5-HT induced activity. J Neurophysiol. 79(5):2643-52.

Branchereau P, Chapron J, Meyrand P. (2002) Descending 5-hydroxytryptamine raphe inputs repress the expression of serotonergic neurons and slow the maturation of inhibitory systems in mouse embryonic spinal cord. J Neurosci 22:2598–2606.

Broggi G, Servello D, Dones I, Carbone G. (1994) Italian multicentric study on pain treatment with epidural spinal cordstimulation. Stereotact Funct Neurosurg 62(1-4):273-8.

Brownstone RM, Wilson JM. (2008) Strategies for delineating spinal locomotor rhythm-generating networks and the possible role of Hb9 interneurones in rhythmogenesis. Brain Res Rev 57(1):64-76.

Büschges A, Akay T, Gabriel JP, Schmidt J. (2008) Organizing network action for locomotion: insights from studying insect walking. Brain Res Rev 57(1):162-71.

Butt SJ, Kiehn O. (2003) Functional identification of interneurons responsible for left-right coordination of hindlimbs in mammals. Neuron 38(6):953-63.

Calancie B, Broton JG, Klose KJ, Traad M, Difini J, Ayyar DR. (1993) Evidence that alterations in presynaptic inhibition contribute to segmental hypo- and hyperexcitability after spinal cord injury in man. Electroencephalogr Clin Neurophysiol 89(3):177-86.

Carrascal L, Nieto-Gonzalez JL, Cameron WE, Torres B, Nunez-Abades PA. (2005) Changes during the postnatal development in physiological and anatomical characteristics of rat motoneurons studied in vitro. Brain Res Brain Res Rev 49(2):377-87.

Cavagna GA, Saibene FP, Margaria R. (1963) External work in walking. *J Appl Physiol.* 18, 1-9.

Cavagna GA, Saibene FP, Margaria R. (1964) Mechanical work in running. J Appl Physiol 19:249-56.

Cavagna GA, Heglund NC, Taylor CR. (1977) Mechanical work in terrestrial locomotion: two basic mechanisms for minimizing energy expenditure. Am J Physiol 233(5):R243-61.

Cazalets JR, Sqalli-Houssaini Y, Clarac F. (1992) Activation of the central pattern generators for locomotion by serotonin and excitatory amino acids in neonatal rat. J Physiol 455:187-204.

Cazalets JR, Bertrand S, Sqalli-Houssaini Y, Clarac F. (1998) GABAergic control of spinal locomotor networks in the neonatal rat. Ann N Y Acad Sci 860:168-80.

Cazalets JR, Bertrand S. (2000) Coupling between lumbar and sacral motor networks in the neonatal rat spinal cord. Eur J Neurosci 12(8):2993-3002.

Chau C, Barbeau H, Rossignol S. (1998b)Effects of intrathecal α_1- and α_2-noradrenergic agonists and norepinephrine on locomotion in chronic spinal cats. J Neurophysiol 79: 2941–2963.

Chini B, Manning M. (2007) Agonist selectivity in the oxytocin/vasopressin receptor family: new insights and challenges. Biochem Soc Trans 35: 737–741.

Christie KJ, Whelan PJ. (2005) Monoaminergic establishment of rostrocaudal gradients of rhythmicity in the neonatal mouse spinal cord. J Neurophysiol 94(2):1554-64.

Clarac F, Vinay L, Cazalets JR, Fady JC, Jamon M. (1998) Role of gravity in the development of posture and locomotion in the neonatal rat. Brain Res Brain Res Rev 28(1-2):35-43.

Clarac F, Brocard F, Vinay L. (2004) The maturation of locomotor networks. Prog Brain Res 143:57-66.

Conway BA, Hultborn H, Kiehn O. (1987) Proprioceptive input resets central locomotor rhythm in the spinal cat. Exp Brain Res 68(3):643-56.

Cordo P, Inglis JT, Verschueren S, Collins JJ, Merfeld DM, Rosenblum S, Buckley S, Moss F. (1996) Noise in human muscle spindles. Nature 383(6603):769-70.

Côté MP, Ménard A, Gossard JP. (2003) Spinal cats on the treadmill: changes in load pathways. J Neurosci 23(7):2789-96.

Courtine G, Roy RR, Hodgson J, McKay H, Raven J, Zhong H, Yang H, Tuszynski MH, Edgerton VR. (2005) Kinematic and EMG determinants in quadrupedal locomotion of a non-human primate (Rhesus). J Neurophysiol 93(6):3127-45.

Courtine G, Gerasimenko Y, Van den Brand R, Yew A, Musienko P, Zhong H, Song B, Ao Y, Ichiyama RM,Lavrov I, Roy RR, Sofroniew MV, Edgerton VR. (2009) Transformation of nonfunctional spinal circuits into functional states after the loss of brain input. Nat Neurosci 12(10):1333-42.

Cowley KC, Schmidt BJ. (1997) Regional distribution of the locomotor pattern-generating network in the neonatal rat spinal cord. J Neurophysiol 77(1):247-59.

Crenna P, Frigo C. (1991) A motor program for the initiation of forward oriented movements in humans. J Physiol 437:635-53.

Crone SA, Quinlan KA, Zagoraiou L, Droho S, Restrepo CE, Lundfald L, Endo T, Setlak J, Jessell TM, Kiehn O, Sharma K. (2008) Genetic ablation of V2a ipsilateral interneurons disrupts left-right locomotor coordination in mammalian spinal cord. Neuron 60(1):70-83.

Dale N, Gilday D. (1996) Regulation of rhythmic movements by purinergic neurotransmitters in frog embryos. Nature 383(6597):259-63.

Deliagina TG, Orlovsky GN. (2002) Comparative neurobiology of postural control. Curr Opin Neurobiol 12(6):652-7.

Deliagina TG, Zelenin PV, Beloozerova IN, Orlovsky GN. (2007) Nervous mechanisms controlling body posture. Physiol Behav 92(1-2):148-54.

Deliagina TG, Beloozerova IN, Zelenin PV, Orlovsky GN. (2008) Spinal and supraspinal postural networks. Brain Res Rev 57(1):212-21.

Delvolvé I, Gabbay H, Lev-Tov A. (2001) The motor output and behavior produced by rhythmogenic sacrocaudal networks in spinal cords of neonatal rats. J Neurophysiol 85(5):2100-10.

Destexhe A, Rudolph M, Fellous JM, Sejnowski TJ. Fluctuating synaptic conductances recreate in vivo-like activity in neocortical neurons. Neuroscience 107(1):13-24.

Devivo MJ. (2012) Epidemiology of traumatic spinal cord injury: trends and future implications. Spinal Cord 50(5):365-72.

Dickinson MH, Farley CT, Full RJ, Koehl MA, Kram R, Lehman S. (2000) How animals move: an integrative view. Science 288(5463):100-6.

Dietz V, Harkema SJ. (2004) Locomotor activity in spinal cord-injured persons. J Appl Physiol 96(5):1954-60.

Dimitrijevic MR, Gerasimenko Y, Pinter MM. (1998a) Evidence for a spinal central pattern generator in humans. Ann N Y Acad Sci 860:360-76.

Dingu N, Deumens R, Taccola G. (2016) Electrical Stimulation Able to Trigger Locomotor Spinal Circuits Also Induces Dorsal Horn Activity. Neuromodulation 19(1):38-46.

Dominici N, Ivanenko YP, Cappellini G, d'Avella A, Mondì V, Cicchese M, Fabiano A, Silei T, Di Paolo A, Giannini C, Poppele RE, Lacquaniti F. (2011) Locomotor primitives in newborn babies and their development. Science 334(6058):997-9.

Dose F, Taccola G. (2012) Coapplication of noisy patterned electrical stimuli and NMDA plus serotonin facilitates fictive locomotion in the rat spinal cord. J Neurophysiol 108(11):2977-90.

Dose F, Menosso R, Taccola G. (2013) Rat locomotor spinal circuits in vitro are activated by electrical stimulation with noisy waveforms sampled from human gait. Physiol Rep 1(2):e00025.

Dose F, Zanon P, Coslovich T, Taccola G. (2014) Nanomolar oxytocin synergizes with weak electrical afferent stimulation to activate the locomotor CpG of the rat spinal cord in vitro. PLoS One 9(3):e92967.

Dose F, Deumens R, Forget P, Taccola G. (2016) Staggered multi-site low-frequency electrostimulation effectively induces locomotor patterns in the isolated rat spinal cord. Spinal Cord 54(2):93-101.

Dose F, Taccola G. (2016) Two distinct stimulus frequencies delivered simultaneously at low intensity generate robust locomotor patterns. Neuromodulation 19(6):563-75.

Douglass JK, Wilkens L, Pantazelou E, Moss F. (1993) Noise enhancement of information transfer in crayfish mechanoreceptors by stochastic resonance. Nature 365(6444):337-40.

Dunbar MJ, Tran MA, Whelan PJ. (2010) Endogenous extracellular serotonin modulates the spinal locomotor network of the neonatal mouse. J Physiol 588(Pt 1):139-56.

Eaton JL, Roache L, Nguyen KN, Cushing BS, Troyer E, et al. (2012) Organizational effects of oxytocin on serotonin innervation. Dev Psychobiol 54:92–97.

Edgerton VR, Leon RD, Harkema SJ, Hodgson JA, London N, Reinkensmeyer DJ, Roy RR, Talmadge RJ, Tillakaratne NJ, Timoszyk W, Tobin A. (2001) Retraining the injured spinal cord. J Physiol 533(Pt 1):15-22.

Edgerton VR, Tillakaratne NJ, Bigbee AJ, de Leon RD, Roy RR. (2004) Plasticity of the spinal neural circuitry after injury. Annu Rev Neurosci 27:145-67.

Edgerton VR, Kim SJ, Ichiyama RM, Gerasimenko YP, Roy RR. (2006) Rehabilitative therapies after spinal cord injury. J Neurotrauma 23(3-4):560-70.

Edgerton VR, Courtine G, Gerasimenko YP, Lavrov I, Ichiyama RM, Fong AJ, Cai LL, Otoshi CK, Tillakaratne NJ, Burdick JW, Roy RR. (2008) Training locomotor networks. Brain Res Rev 57(1):241-54.

Edgerton VR, Harkema S (2011) Epidural stimulation of the spinal cord in spinal cord injury: current status and future challenges. Expert Rev Neurother 11(10):1351-3.

Eklöf-Ljunggren E, Haupt S, Ausborn J, Dehnisch I, Uhlén P, Higashijima S, El Manira A. (2012) Origin of excitation underlying locomotion in the spinal circuit of zebrafish. Proc Natl Acad Sci U S A 109(14):5511-6.

Eliot LS, Kandel ER, Hawkins RD. (1994) Modulation of spontaneous transmitter release during depression and posttetanic potentiation of Aplysia sensory-motor neuron synapses isolated in culture. J Neurosci 14(5 Pt 2):3280-92.

Etlin A, Finkel E, Mor Y, O'Donovan MJ, Anglister L, Lev-Tov A. (2013) Characterization of sacral interneurons that mediate activation of locomotor pattern generators by sacrocaudal afferent input. J Neurosci 33(2):734-47.

Fady JC, Jamon M, Clarac F. (1998) Early olfactory-induced rhythmic limb activity in the newborn rat. Dev. Brain Res108 (1), pp. 111–123.

Faisal AA, Selen LP, Wolpert DM. (2008) Noise in the nervous system. Nat Rev Neurosci 9(4):292-303.

Farley CT, Ko TC. (1997) Mechanics of locomotion in lizards. J Exp Biol 200(Pt 16):2177-88.

Fong AJ, Cai LL, Otoshi CK, Reinkensmeyer DJ, Burdick JW, Roy RR, Edgerton VR. (2005) Spinal cord-transected mice learn to step in response to quipazine treatment and robotic training. J Neurosci 25(50):11738-47.

Fong AJ, Roy RR, Ichiyama RM, Lavrov I, Courtine G, Gerasimenko Y, Tai YC, Burdick J, Edgerton VR. (2009) Recovery of control of posture and locomotion after a spinal cord injury: solutions staring us in the face. Prog Brain Res 175:393-418.

Forssberg H, Grillner S, and Halbertsma J. (1980a) The locomotion of the low spinal cat. I. Coordination within a hindlimb. Acta Physiol Scand 108: 269–281.

Forssberg H, Grillner S, Halbertsma J, and Rossignol S. (1980b) The locomotion of the low spinal cat. II. Interlimb coordination. Acta Physiol Scand 108: 283–295.

Frigon A, Rossignol S. (2006) Experiments and models of sensorimotor interactions during locomotion. Biol Cybern 95(6):607-27.

Frolich LM, Biewener AA. (1992) Kinematic and electromyographyc analysis of the functional role of the body axis during terrestrial and aquatic locomotion in the salamander ambystoma tigrinum. J exp Biol 162, 107-130.

Fuxe K, Dahlström A, Höistad M, Marcellino D, Jansson A, Rivera A, Diaz-Cabiale Z, Jacobsen K, Tinner-Staines B, Hagman B, Leo G, Staines W, Guidolin D, Kehr J, Genedani S, Belluardo N, Agnati LF. (2007) From the Golgi-Cajal mapping to the transmitter-based characterization of the

neuronal networks leading to two modes of brain communication: wiring and volume transmission. Brain Res Rev 55(1):17-54.

Fuxe K, Dahlström AB, Jonsson G, Marcellino D, Guescini M, Dam M, Manger P, Agnati L. (2010) The discovery of central monoamine neurons gave volume transmission to the wired brain. Prog Neurobiol 90(2):82-100.

Gabell A, Nayak US. (1984) The effect of age on variability in gait. J Gerontol 39(6):662-6.

Gad P, Lavrov I, Shah P, Zhong H, Roy RR, Edgerton VR, Gerasimenko Y. (2013) Neuromodulation of motor-evoked potentials during stepping in spinal rats. J Neurophysiol 110(6):1311-22.

Garraway SM, Hochman S. (2001) Pharmacological characterization of serotonin receptor subtypes modulating primary afferent input to deep dorsal horn neurons in the neonatal rat. Br J Pharmacol 132: 1789–1798.

Gerasimenko YP, Bogacheva IN, Shcherbakova NA, Makarovskii AN. (2001) Bioelectric activity of spinal cord in patients with vertebrospinal pathologies. Bull Exp Biol Med 132(5):1106-9.

Gerasimenko YP, Avelev VD, Nikitin OA, Lavrov IA. (2003) Initiation of locomotor activity in spinal cats by epidural stimulation of the spinal cord. Neurosci Behav Physiol 33(3):247-54.

Gerasimenko YP, Ichiyama RM, Lavrov IA, Courtine G, Cai L, Zhong H, Roy RR, Edgerton VR. (2007) Epidural spinal cord stimulation plus quipazine administration enable stepping in complete spinal adult rats. J Neurophysiol 98(5):2525-36.

Gerasimenko Y, Roy RR, Edgerton VR. (2008) Epidural stimulation: comparison of the spinal circuits that generate and control locomotion in rats, cats and humans. Exp Neurol 209(2):417-25.

Gerasimenko Y, Musienko P, Bogacheva I, Moshonkina T, Savochin A, Lavrov I, Roy RR, Edgerton VR. (2009) Propriospinal bypass of the serotonergic system that can facilitate stepping. J Neurosci 29(17):5681-9.

Gerasimenko Y, Gorodnichev R, Moshonkina T, Sayenko D, Gad P, Reggie Edgerton V. (2015) Transcutaneous electrical spinal-cord stimulation in humans. Ann Phys Rehabil Med 58(4):225-31.

Gimpl G, Fahrenholz F. (2001) The oxytocin receptor system: structure, function, and regulation. Physiol Rev 81: 629–683.

Giszter SF, McIntyre Bizzi JE. (1989) Kinematic strategies and sensorimotor transformations in the wiping movements of frogs. J Neurophysiol 62(3):750-67.

Giuliani CA, Smith JL. (1987) Stepping behaviors in chronic spinal cats with one hindlimb deafferented. J Neurosci 7(8):2537-46.

Gorassini MA, Prochazka A, Hiebert GW, Gauthier MJ. (1994) Corrective responses to loss of ground support during walking. I. Intact cats. J Neurophysiol 71(2):603-10.

Gordon IT, Whelan PJ. (2006) Deciphering the organization and modulation of spinal locomotor central pattern generators. J Exp Biol 209(Pt 11):2007-14.

Gosgnach S, Lanuza GM, Butt SJ, Saueressig H, Zhang Y, Velasquez T, Riethmacher D, Callaway EM, Kiehn O, Goulding M. (2006) V1 spinal neurons regulate the speed of vertebrate locomotor outputs. Nature 440(7081):215-9.

Gosgnach S. (2011) The role of genetically-defined interneurons in generating the mammalian locomotor rhythm. Integr Comp Biol 51(6):903-12.

Goslow GE Jr, Seeherman HJ, Taylor CR, McCutchin MN, Heglund NC. (1981) Electrical activity and relative length changes of dog limb muscles as a function of speed and gait. J Exp Biol 94:15-42.

Graham Brown T. (1911) The intrinsic factors in the act of progression in the mammal. Proc R Soc B 84:308–319.

Graham Brown T. (1914) On the nature of the fundamental activity of the nervous centres; together with an analysis of the conditioning of rhythmic activity in progression, and a theory of the evolution of function in the nervous system.J Physiol. 48, 18–46.

Grillner S, Rossignol S. (1978) On the initiation of the swing phase of locomotion in chronic spinal cats. Brain Res 146: 269–277.

Grillner S, Zangger P. (1979) On the central generation of locomotion in the low spinal cat. Exp Brain Res 34(2):241-61.

Grillner S, Zangger P. (1984) The effect of dorsal root transection on the efferent motor pattern in the cat's hindlimb during locomotion. Acta Physiol Scand 120(3):393-405.

Grillner S, Ekeberg, El Manira A, Lansner A, Parker D, Tegnér J, Wallén P. (1998a) Intrinsic function of a neuronal network a vertebrate central pattern generator. Brain Res Brain Res Rev 26(2-3):184-97.

Grillner S, Parker D, el Manira A. (1998b) Vertebrate locomotion--a lamprey perspective. Ann N Y Acad Sci 860:1-18.

Grillner S. (2006) Neuronal networks in motion from ion channels to behaviour. An R Acad Nac Med 123(2):297-8.

Grillner S, Jessell TM. (2009) Measured motion: searching for simplicity in spinal locomotor networks. Curr Opin Neurobiol. 19(6):572-86.

Grillner S. (2011) Neuroscience. Human locomotor circuits conform. Science 334(6058):912-3.

Grillner S, El Manira A (2015) The intrinsic operation of the networks that make us locomote. Curr Opin Neurobiol 31:244-9.

Guertin PA, Hounsgaard J. (1998) Chemical and electrical stimulation induce rhythmic motor activity in an in vitro preparation of the spinal cord from adult turtles. Neurosci Lett 245(1):5-8.

Guertin PA. (2004b) Synergistic activation of the central pattern generator for locomotion by l-beta-3,4-dihydroxyphenylalanine and quipazine in adult paraplegic mice. Neurosci Lett 358(2):71-4.

Guertin PA, Brochu C. (2009) Preliminary evidence of safety following administration of L-DOPA and buspirone in an incomplete monoplegic patient. Spinal Cord 47(1):91-2.

Guertin PA, Ung RV, Rouleau P. (2010) Oral administration of a tri-therapy for central pattern generator activation in paraplegic mice: proof-of-concept of efficacy. Biotechnol J 5(4):421-6.0

Guertin PA, Ung RV, Rouleau P, Steuer I. (2011) Effects on locomotion, muscle, bone, and blood induced by a combination therapy eliciting weight-bearing stepping in non assisted spinal cord-transected mice. Neurorehabil Neural Repair 25(3):234-42.

Hägglund M, Dougherty KJ, Borgius L, Itohara S, Iwasato T, Kiehn O. (2013) Optogenetic dissection reveals multiple rhythmogenic modules underlying locomotion. Proc Natl Acad Sci U S A 110(28):11589-94.

Hardingham GE, Bading H. (2010) Synaptic versus extrasynaptic NMDA receptor signalling: implications for neurodegenerative disorders. Nat Rev Neurosci 11(10):682-96.

Harkema S, Gerasimenko Y, Hodes J, Burdick J, Angeli C, Chen Y, Ferreira C, Willhite A, Rejc E, Grossman RG, Edgerton VR. (2011) Effect of epidural stimulation of the lumbosacral spinal cord on voluntary movement, standing, and assisted stepping after motor complete paraplegia: a case study. Lancet 377(9781):1938-47.

Harkey HL, White EA, Tibbs RE Jr, Haines DE. (2003) A clinician's view of spinal cord injury. Anat Rec B New Anat 271(1):41-8.

Harris-Warrick RM, Cohen AH. (1985) Serotonin modulates the central pattern generator for locomotion in the isolated lamprey spinal cord. J Exp Biol 116:27-46.

Harris-Warrick RM, Flamm RE. (1987) Multiple mechanisms of bursting in a conditional bursting neuron. J Neurosci 7(7):2113-28.

Harris-Warrick RM. (2010) General principles of rhythmogenesis in central pattern generator networks. Prog Brain Res187:213-22.

Hart CB, Giszter SF. (2004) Modular premotor drives and unit bursts as primitives for frog motor behaviors. J Neurosci 24(22):5269-82.

Harvey PJ, Li X, Li Y, Bennett DJ. (2006) 5-HT2 receptor activation facilitates a persistent sodium current and repetitive firing in spinal motoneurons of rats with and without chronic spinal cord injury. J Neurophysiol 96(3):1158-70.

Hausdorff JM. (2005) Gait variability: methods, modeling and meaning. J Neuroengineering Rehabil 2:19.

Hebb AO, Zhang JJ, Mahoor MH, Tsiokos C, Matlack C, Chizeck HJ, Pouratian N. (2014) Creating the feedback loop: closed-loop neurostimulation. Neurosurg Clin N Am 25(1):187-204.

Heglund NC, Cavagna GA, Taylor CR. (1982) Energetics and mechanics of terrestrial locomotion. III. Energy changes of the centre of mass as a function of speed and body size in birds and mammals. J Exp Biol 97:41-56.

Hill R, Matsushima T, Schotland J, Grillner S. (1992) Apamin blocks the slow AHP in lamprey and delays termination of locomotor bursts. Neuroreport 3(10):943-5.

Hofmann L, Ebert M, Tass PA, Hauptmann C. (2011) Modified pulse shapes for effective neural stimulation. Front Neuroeng 4:9.

Hofstoetter US, McKay WB, Tansey KE, Mayr W, Kern H, Minassian K. (2014) Modification of spasticity by transcutaneous spinal cord stimulation in individuals with incomplete spinal cord injury. J Spinal Cord Med 37(2):202-11.

Hofstoetter US, Krenn M, Danner SM, Hofer C, Kern H, McKay WB, Mayr W, Minassian K. (2015) Augmentation of Voluntary Locomotor Activity by Transcutaneous Spinal Cord Stimulation in Motor-Incomplete Spinal Cord-Injured Individuals. Artif Organs 39(10):E176-86.

Hubbard JI, Stenhouse D, Eccles RM. (1967) Origin of synaptic noise, Science 157(3786):330-1.

Hulsebosch CE. (2002) Recent advances in pathophysiology and treatment of spinal cord injury. Adv Physiol Educ 26(1-4):238-55.

Ichiyama RM, Gerasimenko YP, Zhong H, Roy RR, Edgerton VR. (2005) Hindlimb stepping movements in complete spinal rats induced by epidural spinal cord stimulation. Neurosci Lett 383(3):339-44.

Iizuka M, Kiehn O, Kudo N. (1997) Development in neonatal rats of the sensory resetting of the locomotor rhythm induced by NMDA and 5-HT. Exp Brain Res 114(2):193-204.

Iizuka M, Nishimaru H, Kudo N. (1998) Development of the spatial pattern of 5-HT-induced locomotor rhythm in the lumbar spinal cord of rat fetuses in vitro. Neurosci Res 31(2):107-11.

Ivanenko YP, Dominici N, Cappellini G, Dan B, Cheron G, Lacquaniti F. (2004) Development of pendulum mechanism and kinematic coordination from the first unsupported steps in toddlers. J Exp Biol 207(Pt 21):3797-810.

Ivey C, Apkarian AV, Chialvo DR. (1998) Noise induced tuning curve changes in mechanoreceptors. J Neurophysiol 79(4):1879-90.

Iwahara T, Atsuta Y, Garcia-Rill E, Skinner RD. (1992) Spinal cord stimulation-induced locomotion in the adult cat. Brain Res Bull 28(1):99-105.

Jacobson GA, Diba K, Yaron-Jakoubovitch A, Oz Y, Koch C, Segev I, Yarom Y. (2005) Subthreshold voltage noise of rat neocortical pyramidal neurones. J Physiol 564(Pt 1):145-60.

Jessell TM (2000) Neuronal specification in the spinal cord: inductive signals and transcriptional codes. Nat Rev Genet 1(1):20-9

Jiao J, Harreby KR, Sevcencu C, Jensen W. (2016) Optimal Vagus nerve stimulation frequency for Suppression of Spike-and-Wave Seizures in Rats. Artif Organs 40(6):E120-7.

Joucla S, Ambroise M, Levi T, Lafon T, Chauvet P, Saïghi S, Bornat Y, Lewis N, Renaud S, Yvert B. (2016) Generation of Locomotor-Like Activity in the Isolated Rat Spinal Cord Using Intraspinal Electrical Microstimulation Driven by a Digital Neuromorphic CPG. Front Neurosci 10:67.

Juranek J, Currie SN. (2000) Electrically evoked fictive swimming in the low-spinal immobilized turtle. J Neurophysiol 83:146–155.

Juvin L, Simmers J, Morin D. (2007) Locomotor rhythmogenesis in the isolated rat spinal cord: a phase-coupled set of symmetrical flexion extension oscillators. J Physiol 583(Pt 1):115-28.

Kangrga I, Randic M. (1990) Tachykinins and calcitonin gene-related peptide enhance release of endogenous glutamate and aspartate from the rat spinal dorsal horn slice. J Neurosci 10(6):2026-38.

Katz B, Miledi R. (1963) A study of spontaneous miniature potentials in spinal motoneurones. J Physiol 168:389-422.

Katz PS. (1995) Intrinsic and extrinsic neuromodulation of motor circuits. Curr. Opin. Neurobiol.5:799–808.

Katz PS, Frost WN. (1996) Intrinsic neuromodulation: altering neuronal circuits from within. Trends Neurosci 19(2):54-61.

Kazennikov OV, Shik ML, Yakovleva GV. (1983) Stepping movements induced by stimulation of the dorsolateral column of the spinal cord in the cat. *Byull Éksp Biol Med* 96, 8-10.

Kiehn O, Sillar KT, Kjaerulff O, McDearmid JR. (1999a) Effects of noradrenaline on locomotor rhythm-generating networks in the isolated neonatal rat spinal cord. J Neurophysiol 82(2):741-6.

Kiehn O, Butt SJ. (2003) Physiological, anatomical and genetic identification of CPG neurons in the developing mammalian spinal cord. Prog Neurobiol 70(4):347-61.

Kiehn O. (2006) Locomotor circuits in the mammalian spinal cord. Annu Rev Neurosci 29:279-306.

Kitajo K, Nozaki D, Ward LM, Yamamoto Y. (2003) Behavioral stochastic resonance within the human brain. Phys Rev Lett 90(21):218103.

Kjaerulff O, Kiehn O (1994) Localization of the central pattern generator for hindlimb locomotion in the neonatal rat. A lesion study. Soc Neurosci Abstr 20:1757.

Kjaerulff O, Kiehn O. (1996) Distribution of networks generating and coordinating locomotor activity in the neonatal rat spinal cord in vitro: a lesion study. J Neurosci 16(18):5777-94.

Koga K, Furue H, Rashid MH, Takaki A, Katafuchi T, Yoshimura M. (2005) Selective activation of primary afferent fibers evaluated by sine-wave electrical stimulation. Mol Pain 1:13.

Kremer E, Lev-Tov A. (1997) Localization of the spinal network associated with generation of hindlimb locomotion in the neonatal rat and organization of its transverse coupling system. J Neurophysiol 77(3):1155-70.

Kriellaars DJ, Brownstone RM, Noga BR, Jordan LM. (1994) Mechanical entrainment of fictive locomotion in the decerebrate cat. J Neurophysiol 71(6):2074-86.

Krizsan-Agbas D, Winter MK, Eggimann LS, Meriwether J, Berman NE, Smith PG, McCarson KE. (2014) Gait analysis at multiple speeds reveals differential functional and structural outcomes in response to gradedspinal cord injury. J Neurotrauma 31(9):846-56.

Kudo N, Yamada T. (1987) N-methyl-D,L-aspartate-induced locomotor activity in a spinal cord-hindlimb muscles preparation of the newborn rat studied in vitro. Neurosci Lett 75(1):43-8.

Kuo AD, Donelan JM. (2010) Dynamic principles of gait and their clinical implications. Phys Ther 90(2):157-74.

Kyriakatos A, El Manira A. (2007) Long-term plasticity of the spinal locomotor circuitry mediated by endocannabinoid and nitric oxide signaling. J Neurosci 27(46):12664-74.

Kyriakatos A, Molinari M, Mahmood R, Grillner S, Sillar KT, El Manira A. (2009) Nitric oxide potentiation of locomotor activity in the spinal cord of the lamprey. J Neurosci. 29(42):13283-91.

Kyriakatos A, Mahmood R, Ausborn J, Porres CP, Büschges A, El Manira A. (2011) Initiation of locomotion in adult zebrafish. J Neurosci 31(23):8422-31.

Lacquaniti F, Grasso R, Zago M. (1999) Motor Patterns in Walking. News Physiol Sci 14:168-174.

Lafreniere-Roula M, McCrea DA. (2005) Deletions of rhythmic motoneuron activity during fictive locomotion and scratch provide clues to the organization of the mammalian central pattern generator. J Neurophysiol 94(2):1120-32.

Lam T, Pearson KG. (2002) The role of proprioceptive feedback in the regulation and adaptation of locomotor activity. Adv Exp Med Biol 508:343-55.

Lambertz M, Langhorst P. (1998) Simultaneous changes of rhythmic organization in brainstem neurons, respiration, cardiovascular system and EEG between 0.05 Hz and 0.5 Hz. J Auton Nerv Syst 68(1-2):58-77.

Lamotte d'Incamps B, AscherP (2008) Four excitatory postsynaptic ionotropic receptors coactivated at the motoneuron-Renshaw cell synapse. J Neurosci 28:14121–14131.

Lang P. (1997) The treatment of chronic pain by epidural spinal cord stimulation--a 15 year follow up; present status. Axone 18(4):71-3.

Lanuza GM, Gosgnach S, Pierani A, Jessell TM, Goulding M. (2004) Genetic identification of spinal interneurons that coordinate left-right locomotor activity necessary for walking movements. Neuron 42(3):375-86.

Lavrov I, Gerasimenko YP, Ichiyama RM, Courtine G, Zhong H, Roy RR, Edgerton VR. (2006) Plasticity of spinal cord reflexes after a complete transection in adult rats: relationship to stepping ability. J Neurophysiol 96(4):1699-710.

Lavrov I, Dy CJ, Fong AJ, Gerasimenko Y, Courtine G, Zhong H, Roy RR, Edgerton VR. (2008) Epidural stimulation induced modulation of spinal locomotor networks in adult spinal rats. J Neurosci 28(23):6022-9.

Lee MT, O'Donovan MJ. (1991) Organization of hindlimb muscle afferent projections to lumbosacral motoneurons in the chick embryo. J Neurosci 11(8):2564-73.

Legrand JC, Darbon P, Streit J. (2004) Contributions of NMDA receptors to network recruitment and rhythm generation in spinal cord cultures. Eur J Neurosci 19(3):521-32.

Lennard PR. (1985) Afferent perturbations during "monopodal" swimming movements in the turtle: phase-dependent cutaneous modulation and proprioceptive resetting of the locomotor rhythm. J Neurosci 5(6):1434-45.

Leong SK, Shieh JY, Wong WC (1984) Localizing spinal cord-projecting neurons in adult albino rats. J Comp Neurol 228:1–17.

Lev-Tov A, Pinco M. (1992) In vitro studies of prolonged synaptic depression in the neonatal rat spinal cord. J Physiol 447:149-69.

Lev-Tov A, Delvolvé I, Kremer E. (2000) Sacrocaudal afferents induce rhythmic efferent bursting in isolated spinal cords of neonatal rats. J Neurophysiol 83(2):888-94.

Lev-Tov A, Etlin A, Blivis D. (2010) Sensory-induced activation of pattern generators in the absence of supraspinal control. Ann N Y Acad Sci 1198:54-62.

Li X, Murray K, Harvey PJ, Ballou EW, Bennett DJ. (2007) Serotonin facilitates a persistent calcium current in motoneurons of rats with and without chronic spinal cord injury. J Neurophysiol 97: 1236–1246.

Lindner JF, Meadows BK, Ditto WL, Inchiosa ME, Bulsara AR. (1996) Scaling laws for spatiotemporal synchronization and array enhanced stochastic resonance. Phys Rev E Stat Phys Plasmas Fluids Relat Interdiscip Topics 53(3):2081-2086.

Liu F, Wang J F, Wang W. (1999) Frequency sensitivity in weak signal detection. Phys Rev E 59:3453-3460.

Liu J, Jordan LM. (2005) Stimulation of the parapyramidal region of the neonatal rat brain stem produces locomotor-like activity involving spinal 5-HT7 and 5-HT2A receptors. J Neurophysiol 94(2):1392-404.

Liu X, Tribollet E, Ogier R, Barberis C, Raggenbass M. (2003) Presence of functional vasopressin receptors in spinal ventral horn neurons of young rats: a morphological and electrophysiological study. Eur J Neurosci 17: 1833–1846.

Liu ZY, Zhuang DB, Lunderberg T, Yu LC. (2002) Involvement of 5-hydroxytryptamine(1A) receptors in the descending anti-nociceptive pathway from periaqueductal gray to the spinal dorsal horn in intact rats, rats with nerve injury and rats with inflammation. Neuroscience 112(2):399-407.

Loeb GE, Bak MJ, Duysens J. (1977) Long-term unit recording from somatosensory neurons in the spinal ganglia of the freely walking cat. Science197(4309):1192-4.

Lopez-Garcia JA. (1998) Serotonergic modulation of the responses to excitatory amino acids of rat dorsal horn neurons in vitro: implications for somatosensory transmission. Eur J Neurosci 10(4):1341-9.

Lundfald L, Restrepo CE, Butt SJ, Peng CY, Droho S, Endo T, Zeilhofer HU, Sharma K, Kiehn O. (2007) Phenotype of V2-derived interneurons and their relationship to the axon guidance molecule EphA4 in the developing mouse spinal cord. Eur J Neurosci 26(11):2989-3002.

Madriaga MA, McPhee LC, Chersa T, Christie KJ, Whelan PJ. (2004) Modulation of locomotor activity by multiple 5-HT and dopaminergic receptor subtypes in the neonatal mouse spinal cord. J Neurophysiol 92(3):1566-76.

Marazziti D, Baroni S, Giannaccini G, Betti L, Massimetti G, Carmassi C, Catena-Dell'Osso M. (2012) A link between oxytocin and serotonin in humans: supporting evidence from peripheral markers. Eur Neuropsychopharmacol 22: 578–583.

Marchetti C, Beato M, Nistri A. (2001a) Alternating rhythmic activity induced by dorsal root stimulation in the neonatal rat spinal cord in vitro. J Physiol. 530(Pt 1):105-12.

Marchetti C, Beato M, Nistri A. (2001b) Evidence for increased extracellular K(+) as an important mechanism for dorsal root induced alternating rhythmic activity in the neonatal rat spinal cord in vitro. Neurosci Lett 304(1-2):77-80.

Marchetti C, Nistri A. (2001c) Neuronal bursting induced by NK3 receptor activation in the neonatal rat spinal cord in vitro. J Neurophysiol 86(6):2939-50.

Marchetti C, Taccola G, Nistri A. (2003) Distinct subtypes of group I metabotropic glutamate receptors on rat spinal neurons mediate complex facilitatory and inhibitory effects. Eur J Neurosci 18(7):1873-83.

Marder E, Bucher D. (2001) Central pattern generators and the control of rhythmic movements. Curr Biol 11(23):R986-96.

Martínez L, Pérez T, Mirasso CR, Manjarrez E. (2007) Stochastic resonance in the motor system: Effects of noise on the monosynaptic reflex pathway of the cat spinal cord. J Neurophysiol 97:4007–4016.

McDonnell MD, Abbott D. (2009) What is stochastic resonance? Definitions, misconceptions, debates, and its relevance to biology. PLoS Comput Biol 5(5):e1000348.

McIntyre CC, Grill WM. (2002) Extracellular stimulation of central neurons: influence of stimulus waveform and frequency on neuronal output. J Neurophysiol 88(4):1592-604.

Miles GB, Dai Y, Brownstone RM. (2005) Mechanisms underlying the early phase of spike frequency adaptation in mouse spinal motoneurones. J Physiol 566(Pt 2):519-32.

Miles GB, Sillar KT. (2011) Neuromodulation of vertebrate locomotor control networks. Physiology 26(6):393-411.

Minassian K, Persy I, Rattay F, Pinter MM, Kern H, Dimitrijevic MR. (2007) Human lumbar cord circuitries can be activated by extrinsic tonic input to generate locomotor-like activity. Hum Mov Sci 26(2):275-95.

Minassian K, Hofstoetter U, Tansey K, Mayr W. (2012) Neuromodulation of lower limb motor control in restorative neurology. Clin Neurol Neurosurg 114(5):489-97.

Moreno-Duarte I, Morse LR, Alam M, Bikson M, Zafonte R, Fregni F. (2014) Targeted therapies using electrical and magnetic neural stimulation for the treatment of chronic pain in spinal cord injury. Neuroimage 85 Pt 3:1003-13.

Moreno-Lo´pez Y, Martı´nez-Lorenzana G, Conde´s-Lara M, Rojas-Piloni G. (2013) Identification of oxytocin receptor in the dorsal horn and nociceptive dorsal root ganglion neurons. Neuropeptides 47: 117–123.

Murray KC, Nakae A, Stephens MJ, Rank M, D'Amico J, Harvey PJ, Li X, Harris RL, Ballou EW, Anelli R, Heckman CJ, Mashimo T, Vavrek R, Sanelli L, Gorassini MA, Bennett DJ, Fouad K. (2010) Recovery of motoneuron and locomotor function after spinal cord injury depends on constitutive activity in 5-HT2C receptors. Nat Med 16(6):694-700.

Musienko PE, Zelenin PV, Orlovsky GN, Deliagina TG. (2010) Facilitation of Postural Limb Reflexes With Epidural Stimulation in Spinal Rabbits J Neurophysiol 103(2): 1080–1092.

Musienko PE, Courtine G, Tibbs JE, Kilimnik V, Savochin A, Garfinkel A, Roy RR, Edgerton VR, Gerasimenko Y. (2012) Somatosensory control of balance during locomotion in decerebrated cat. J Neurophysiol 107(8):2072-82.

Mussa-Ivaldi FA, Giszter SF. (1992) Vector field approximation: a computational paradigm for motor control and learning. Biol Cybern 67(6):491-500.

Mussa-Ivaldi FA. (1999) Modular features of motor control and learning. Curr Opin Neurobiol 9(6):713-7.

Nacimiento W, Sappok T, Brook GA, Tóth L, Schoen SW, Noth J, Kreutzberg GW. (1995) Structural changes of anterior horn neurons and their synaptic input caudal to a low thoracic spinal cordhemisection in the adult rat: a light and electron microscopic study. Acta Neuropathol 90(6):552-64.

Nakayama K, Nishimaru H, Iizuka M, Ozaki S, Kudo N. (1999) Rostrocaudal progression in the development of periodic spontaneous activity in fetal rat spinal motor circuits in vitro. J Neurophysiol 81:2592–2595.

Nakayama K, Nishimaru H, Kudo N. (2004) Rhythmic motor activity in thin transverse slice preparations of the fetal rat spinal cord. J Neurophysiol 92(1):648-52.

Nishimaru H, Kudo N. (2000) Formation of the central pattern generator for locomotion in the rat and mouse. Brain Res Bull 53(5):661-9.

Nistri A, Ostroumov K, Sharifullina E, Taccola G. (2006) Tuning and playing a motor rhythm: how metabotropic glutamate receptors orchestrate generation of motor patterns in the mammalian central nervous system. J Physiol 572(Pt 2):323-34.

O'Donovan MJ, Chub N, Wenner P. (1998) Mechanisms of spontaneous activity in developing spinal networks. J Neurobiol 37:131–145.

Pastor MA, Artieda J, Arbizu J, Marti-Climent JM, Peñuelas I, Masdeu JC. (2002) Activation of human cerebral and cerebellar cortex by auditory stimulation at 40 Hz. J Neurosci 22(23):10501-6.

Pastor MA, Vidaurre C, Fernández-Seara MA, Villanueva A, Friston KJ. (2008) Frequency-specific coupling in the cortico-cerebellar auditory system. J Neurophysiol 100(4):1699-705.

Pearlstein E, Ben Mabrouk F, Pflieger JF, Vinay L. (2005) Serotonin refines the locomotor-related alternations in the in vitro neonatal rat spinal cord. Eur J Neurosci 21(5):1338-46.

Pearson KG, Rossignol S. (1991) Fictive motor patterns in chronic spinal cats. J Neurophysiol 66(6):1874-87.

Pearson KG, Misiaszek JE, Fouad K. (1998) Enhancement and resetting of locomotor activity by muscle afferents. Ann N Y Acad Sci 860:203-15.

Pearson KG, Misiaszek JE, Hulliger M. (2003) Chemical ablation of sensory afferents in the walking system of the cat abolishes the capacity for functional recovery after peripheral nerve lesions. Exp Brain Res 150(1):50-60.

Peckham PH, Knutson JS. (2005) Functional electrical stimulation for neuromuscular applications. Annu Rev Biomed Eng 7:327-60.

Peron SP, Gabbiani F. (2009) Role of spike-frequency adaptation in shaping neuronal response to dynamic stimuli. Biol Cybern 100(6):505-20.

Perreault MC, Angel MJ, Guertin P, McCrea DA. (1995) Effects of stimulation of hindlimb flexor group II afferents during fictive locomotion in the cat. J Physiol 487(1):211-20.

Perrier JF, Alaburda A, Hounsgaard J. (2003) 5-HT1A receptors increase excitability of spinal motoneurons by inhibiting a TASK-1-like K^+ current in the adult turtle. J Physiol 548(Pt 2):485-92.

Perry J, Burnfield JM. (2010) Gait Analysis: Normal and Pathological Function. J Sports Sci Med 9(2): 353.

Petralia RS, Wang YX, Hua F, Yi Z, Zhou A, Ge L, Stephenson FA, Wenthold RJ. (2010) Organization of NMDA receptors at extrasynaptic locations. Neuroscience 167(1):68-87.

Pflieger JF, Clarac F, Vinay L. (2002) Picrotoxin and bicuculline have different effects on lumbar spinal networks and motoneurons in the neonatal rat. Brain Res 935(1-2):81-6.

Pike FG, Goddard RS, Suckling JM, Ganter P, Kasthuri N, Paulsen O. (2000) Distinct frequency preferences of different types of rat hippocampal neurones in response to oscillatory inputcurrents. J Physiol 529 Pt 1:205-13.

Powers RK, Sawczuk A, Musick JR, Binder MD. (1999) Multiple mechanisms of spike-frequency adaptation in motoneurones. J Physiol Paris 93(1-2):101-14.

Rabinovich MI, Abarbanel HD. (1998) The role of chaos in neural systems. Neuroscience 87(1):5-14.

Rolston JD, Gross RE, Potter SM. (2010) Closed-loop, open-source electrophysiology. Front Neurosci 4:31.

Rossignol S, Barbeau H. (1993) Pharmacology of locomotion: an account of studies in spinal cats and spinal cord injured subjects. J Am Paraplegia Soc 16(4):190-6.

Rossignol S, Dubuc R, Gossard JP. (2006) Dynamic Sensorimotor Interactions in Locomotion. Physiological Revews 1, 89-154.

Rouleau P, Guertin PA. (2011) Traumatic and nontraumatic spinal-cord-injured patients in Quebec, Canada. Part 3: pharmacological characteristics. Spinal Cord 49(2):186-95.

Rowland JW, Hawryluk GW, Kwon B, Fehlings MG. (2008) Current status of acute spinal cord injury pathophysiology and emerging therapies: promise on the horizon. Neurosurg Focus 25(5):E2.

Saulino M. (2014) Spinal cord injury pain. Phys Med Rehabil Clin N Am 25(2):397-410.

Sayenko DG, Atkinson DA, Floyd TC, Gorodnichev RM, Moshonkina TR, Harkema SJ, Edgerton VR, Gerasimenko YP. (2015) Effects of paired transcutaneous electrical stimulation delivered at single and dual sites over lumbosacral spinal cord. Neurosci Lett 609:229-34.

Schoenen J, Lotstra F, Vierendeels G, Reznik M, Vanderhaeghen JJ. (1985) Substance P, enkephalins, somatostatin, cholecystokinin, oxytocin, and vasopressin in human spinal cord. Neurology 35: 881–890.

Schwindt PC, Crill WE. (1981) Voltage clamp study of cat spinal motoneurons during strychnine-induced seizures. Brain Res 204(1):226-30.

Selverston AI, Moulins M. (1985) Oscillatory neural networks. Annu Rev Physiol 47:29-48.

Shah PK, Sureddi S, Alam M, Zhong H, Roy RR, Edgerton VR, Gerasimenko Y (2016) Unique Spatiotemporal Neuromodulation of the Lumbosacral Circuitry Shapes Locomotor Success after Spinal Cord Injury. J Neurotrauma Doi: 10.1089/neu.2015.4256.

Shealy CN, Mortimer JT, Reswick JB. (1967) Electrical inhibition of pain by stimulation of the dorsal columns: preliminary clinical report. Anesth Analg 46(4):489-91.

Sherrington CS. (1910a) Remarks on the reflex mechanism of the step. Brain 33: 1–25.

Sherrington CS. (1910b) Flexion-reflex of the limb, crossed extension-reflex, and reflex stepping and standing. J Physiol 40(1-2):28-121.

Sjölund BH. (2002) Pain and rehabilitation after spinal cord injury: the case of sensory spasticity Brain Res Brain Res Rev 40(1-3):250-6.

Sluka KA, Vance CG, Lisi TL. (2005) High-frequency, but not low-frequency, transcutaneous electrical nerve stimulation reduces aspartate andglutamate release in the spinal cord dorsal horn. J Neurochem 95(6):1794-801.

Smith JC, Feldman JL, Schmidt BJ. (1988) Neural mechanisms generating locomotion studied in mammalian brain stem-spinal cord in vitro. FASEB J 2(7):2283-8.

Snaterse M, Ton R, Kuo AD, Donelan JM. (1985) Distinct fast and slow processes contribute to the selection of preferred step frequency during human walking. J Appl Physiol 110(6):1682-90.

Sqalli-Houssaini Y, Cazalets JR, Clarac F. (1993) Oscillatory properties of the central pattern generator for locomotion in neonatal rats. J Neurophysiol 70(2):803-13.

Stacey WC, Durand DM. (2001) Synaptic noise improves detection of subthreshold signals in hippocampal CA1 neurons. J Neurophysiol 86(3):1104-12.

Steinmetz PN, Manwani A, Koch C, London M, Segev I. (2000) Subthreshold voltage noise due to channel fluctuations in active neuronal membranes. J Comput Neurosci 9(2):133-48.

Strauss I, Lev-Tov A. (2003) Neural pathways between sacrocaudal afferents and lumbar pattern generators in neonatal rats. J Neurophysiol 89(2):773-84.

Streit J. (1993) Regular oscillations of synaptic activity in spinal networks in vitro. J Neurophysiol 70(3):871-8.

Swanson LW, McKellar S. (1979) The distribution of oxytocin- and neurophysin-stained fibers in the spinal cord of the rat and monkey. J Comp Neurol 188(1):87-106.

Taccola G, Nistri A. (2006) Oscillatory circuits underlying locomotor networks in the rat spinal cord. Crit Rev Neurobiol 18(1-2):25-36.

Taccola G, Margaryan G, Mladinic M, Nistri A (2008) Kainate and metabolic perturbation mimicking spinal injury differentially contribute to early damage of locomotor networks in the in vitro neonatal rat spinal cord. Neuroscience 155(2):538-55.

Taccola G, Mladinic M, Nistri A. (2010) Dynamics of early locomotor network dysfunction following a focal lesion in an in vitro model of spinal injury. Eur J Neurosci 31(1):60-78.

Taccola G. (2011) The locomotor central pattern generator of the rat spinal cord in vitro is optimally activated by noisy dorsal root waveforms. J Neurophysiol 106(2):872-84.

Takakusaki K, Chiba R, Nozu T, Okumura T. (2016) Brainstem control of locomotion and muscle tone with special reference to the role of the mesopontine tegmentum and medullary reticulospinal systems. J Neural Transm 123(7):695-729.

Tator CH, Minassian K, Mushahwar VK. (2012) Spinal cord stimulation: therapeutic benefits and movement generation after spinal cord injury. Handb Clin Neurol 109:283-96.

Tawfik VL, Chang SY, Hitti FL et al. (2010) Deep brain stimulation results in local glutamate and adenosine release: investigation into the role of astrocytes. Neurosurgery 67:367–375.

Terney D, Chaieb L, Moliadze V, Antal A, Paulus W. (2008) Increasing human brain excitability by transcranial high-frequency random noise stimulation. J Neurosci 28(52):14147-55.

Terrier P, Schutz Y. (2003) Variability of gait patterns during unconstrained walking assessed by satellite positioning (GPS). Eur J Appl Physiol 90(5-6):554-61.

Tong CK, MacDermott AB. (2014) Synaptic GluN2A and GluN2B contining NMDA receptors within the superficial dorsal horn activated followingprimary afferent stimulation. J Neurosci. 34(33):10808-20.

Van den Brand R, Heutschi J, Barraud Q, DiGiovanna J, Bartholdi K, Huerlimann M, Friedli L, Vollenweider I,Moraud EM, Duis S, Dominici N, Micera S, Musienko P, Courtine G. (2012) Restoring voluntary control of locomotion after paralyzing spinal cord injury. Science 336(6085):1182-5.

Van Rossum MC, O'Brien BJ, Smith RG. (2003) Effects of noise on the spike timing precision of retinal ganglion cells. J Neurophysiol 89(5):2406-19.

Viala D, Viala G, Jordan M. (1991) Interneurones of the lumbar cord related to spontaneous locomotor activity in the rabbit. I. Rhythmically active interneurones. Exp Brain Res 84(1):177-86.

Vinay L., Brocard F., Pflieger J., Simeoni-Alias J., Clarac F. (2000). Perinatal development of lumbar motoneurons and their inputs in the rat. Brain Res Bull 53(5):635-47.

Vinay L, Brocard F, Clarac F, Norreel JC., Pearlstein E, Pflieger JF. (2002). Development of posture and locomotion: an interplay of endogenously generated activities and neurotrophic actions by descending pathways. Brain Res. Brain Res. Rev 40(1-3):118-29.

Vogelstein RJ, Tenore F, Etienne-Cummings R, Lewis MA, Cohen AH. (2006) Dynamic control of the central pattern generator for locomotion. Biol Cybern 95(6):555-66.

Weinberg SH. (2013) High-frequency stimulation of excitable cells and networks. PLoS One 8(11):e81402.

Wenger N, Moraud EM, Gandar J, Musienko P, Capogrosso M, Baud L, Le Goff CG, Barraud Q, Pavlova N, Dominici N, Minev IR, Asboth L, Hirsch A, Duis S, Kreider J, Mortera A,Haverbeck O, Kraus S, Schmitz F, DiGiovanna J, Van den Brand R, Bloch J, Detemple P, Lacour SP, Bézard E, Micera S, Courtine G. (2016) Spatiotemporal neuromodulation therapies engaging muscle synergies improve motor control after spinal cord injury. Nat Med 22(2):138-45.

Wenner P, Matise MP, Joyner A, O'Donovan MJ. (1998) Physiological and molecular characterization of interneurons in the developing spinal cord. Ann N Y Acad Sci 860:425-7.

Wever E; Bray C. (1937) The Perception of Low Tones and the Resonance-Volley Theory. The Journal of Psychology: Interdisciplinary and Applied. 3(1): 101–114.

Whelan PJ, Bonnot A, O'Donovan MJ (2000) Properties of rhythmic activity generated by the isolated spinal cord of the neonatal mouse. J Neurophysiol 84:2821–2833.

White JA, Rubinstein JT, Kay AR. (2000) Channel noise in neurons. Trends Neurosci 23(3):131-7.

Wilson LA, Wayman CP, Jackson VM. (2009) Neuropeptide modulation of a lumbar spinal reflex: potential implications for female sexual function. J Sex Med 6(4):947-57.

Young W. (2015) Electrical stimulation and motor recovery. Cell Transplant 24(3):429-46.

Zajac FE, Neptune RR, Kautz SA. (2002) Biomechanics and muscle coordination of human walking. Part I: introduction to concepts, power transfer,dynamics and simulations. Gait Posture 16(3):215-32.

Zajac FE, Neptune RR, Kautz SA. (2003) Biomechanics and muscle coordination of human walking: part II: lessons from dynamical simulations andclinical implications. Gait Posture17(1):1-17.

Zelenin PV, Grillner S, Orlovsky GN, Deliagina TG. (2003) The pattern of motor coordination underlying the roll in the lamprey. J Exp Biol 206(Pt 15):2557-66.

Zhang Y, Narayan S, Geiman E, Lanuza GM, Velasquez T, Shanks B, Akay T, Dyck J, Pearson K, Gosgnach S, Fan CM, Goulding M. (2008) V3 spinal neurons establish a robust and balanced locomotor rhythm during walking. Neuron 60(1):84-96.

List of Abbreviations

5HT	5-hydroxytryptamine
APV	d-(-)-2-amino-5-phosphonopentanoic acid
ATP	Adenosine triphosphate
CINs	Commissural interneurons
CNQX	6-cyano-7-nitroquinoxaline-2,3-dione
CNS	Central nervous system
COM	Center of mass
CPGs	Central Pattern Generators
DOFs	Degrees of freedom
DRG	Dorsal root ganglion
DRs	Dorsal Roots
EMG	Electromyographic
ES	Embryonic stem cells
FES	Functional electrical stimulation
FL	Fictive locomotion
FL*i*stim	Fictive locomotion *induced* stimulation
GABA	γ-aminobutyric acid
Glu	Glutamate
Gly	Glycine
GTOs	Golgi tendon organs
L	Lumbar

L-DOPA	L-3,4-dihydroxyphenylalanine
mPSCs	Miniature postsynaptic currents
NMDA	N-methyl-D-aspartate
NO	Nitric oxide
NSCISC	National Spinal Cord Injury Statistical Center
PCPA	p-chlorophenilalanine
PF	Pattern formation
PICs	Persistent inward currents
PSD	Postsynaptic density zone
PVN	Paraventricular hypothalamic nucleus
ReaL*i*stim	Real Locomotion-*induced* stimulation
RG	Rhythm generator
sAHP	Slow afterhyperpolarization
SCI	Spinal cord injury
SFA	Spike frequency adaptation
SR	Stochastic resonance
TA	Tibialis anterior
TTX	Tetrodotoxin
VF	Ventral f*uniculus*
VRs	Ventral roots

Acknowledgements

I am grateful to various people who have been journeying with me in these recent years in which I have been working on this thesis.

I would like to express the deepest gratitude to my supervisor Dr. Giuliano Taccola for his full support, expert guidance, understanding and encouragement throughout my study and research. I am also extremely thankful to Prof. Andrea Nistri for sharing his experience and knowledge through a very constructive criticism for the completion of this project.

My deepest aprecciation also extends to Rita Turissini and John Fischetti.

A special thank goes to Nejada Dingu, Rosmary Blanco, Vladimir Rancic, Giulia Bernardon for their help and encouragement which made my stay and studies more enjoyable during my PhD. Moreover, I would like to thank also all the other people I met during the years spent in the SPINAL Lab.

I do owe a great sense of gratitude to all of my friends for they continuous moral support and co-operation. Nicol Perissutti, Stefania Grosso, Elisa Pitton, Sabrina Gigante, Stefania Del ponte, Sara Pitton, Giorgia Damiani, Francesco Corso, Marco Terranova. I would not have been able to complete this thesis without their continuous support.

I am also grateful to Luisa and Sandra for all those amazing dinners and their support through delicious dishes.

Last but not least I would like to thank my parents Paolo and Marina and my grandmother Maria Pia for their moral and material assistance.

THE FUTURE IS UNWRITTEN.